NUMERICAL SOLUTIONS OF WEATHER DERIVATIVES AND OTHER INCOMPLETE MARKET PROBLEMS

A dissertation submitted to the University of Manchester
for the degree of Doctor of Philosophy
in the Faculty of Engineering and Physical Sciences

2012

By
Edwin Kwaku Broni-Mensah
School of Mathematics

Contents

List of Tables

List of Figures

Abstract

The valuation of weather derivatives is complex since the underlying temperature process has no negotiable price. This thesis introduces a selection of models for the valuation of weather derivative contracts, governed by a stochastic underlying temperature process.

We then present a new weather pricing model, which is used to determine the fair hedging price of a weather derivative under the assumptions of *mean self-financing*. This model is then extended to incorporate a compensation (or market price of risk) awarded to investors who hold undiversifiable risks. This results in the derivation of a non-linear two-dimensional PDE, for which the numerical evaluation cannot be performed using standard finite-difference techniques.

The numerical techniques applied in this thesis are based on a broad range of lattice based schemes, including enhancements to finite-differences, quadrature methods and binomial trees. Furthermore simulations of temperature processes are undertaken that involves the development of Monte Carlo based methods.

Declaration

No portion of the work referred to in this dissertation has been submitted in support of an application for another degree or qualification of this or any other university or other institute of learning.

Copyright

i. The author of this thesis (including any appendices and/or schedules to this thesis) owns certain copyright or related rights in it (the "Copyright") and s/he has given The University of Manchester certain rights to use such Copyright, including for administrative purposes.

ii. Copies of this thesis, either in full or in extracts and whether in hard or electronic copy, may be made only in accordance with the Copyright, Designs and Patents Act 1988 (as amended) and regulations issued under it or, where appropriate, in accordance with licensing agreements which the University has from time to time. This page must form part of any such copies made.

iii. The ownership of certain Copyright, patents, designs, trade marks and other intellectual property (the "Intellectual Property") and any reproductions of copyright works in the thesis, for example graphs and tables ("Reproductions"), which may be described in this thesis, may not be owned by the author and may be owned by third parties. Such Intellectual Property and Reproductions cannot and must not be made available for use without the prior written permission of the owner(s) of the relevant Intellectual Property and/or Reproductions.

iv. Further information on the conditions under which disclosure, publication and commercialisation of this thesis, the Copyright and any Intellectual Property and/or Reproductions described in it may take place is available in the University IP Policy (see `http://www.campus.manchester.ac.uk/medialibrary/policies/intellectual-property.pdf`), in any relevant Thesis restriction declarations deposited in the University Library, The University Library's regulations (see `http://www.manchester.ac.uk/`

`library/aboutus/regulations`) and in The University's policy on presentation of Theses

Acknowledgements

My time as a PhD student has certainly been a wonderful experience. Leaving my job in a global investment bank to return to complete academic research was one of the best decisions I have made. I would like to thank my supervisors Professor Peter Duck and Professor David Newton for their unwavering support, and most of for all the patience they showed me, especially, during my final year. Dr Andrew Hazel helped me in innumerable ways during my studies at The University of Manchester.

A special thank you goes to my friends and colleagues. Paul Johnson for imparting his knowledge and spending countless hours with me discussing various financial topics; Sebastian Law for introducing me to the Financial Mathematics PhD group when I was considering what area of research to pursue, and also for being my outlet for talking about economics, entrepreneurship, and U.S TV shows; Dong Mei-Wang for being so supportive and knowing how to life my spirits.

The completion of this work would would not have been possible without the love and support given to me by my wonderful parents and siblings. This thesis is dedicated to them.

Dedication

To my awesome Mum, Dad, sister and two brothers.

Chapter 1

Introduction

The beginning is the most important part of the work.

Plato

For millennia people have tried to forecast the weather. According to Lynch (2008), the earliest attempts began in 650 BC as the Babylonians used cloud formation patterns and astrology to make weather predications. Modern day weather forecasting is attributed to Francis Beaufort and Robert Fitzroy, who were ridiculed for their work. The development of this area accelerated with the developments of computers leading to the creation of numerical weather prediction that was first proposed by Vilhelm Bjerknes and later developed by British mathematician Lewis Fry Richardson in 1922 (Richardson, 2007).

The models that arise in numerical weather prediction are mathematical equations that closely resembles the physics and dynamics of the atmosphere. These sophisticated models are nonlinear, which makes them impossible to solve analytically and therefore they require supercomputing power to solve. An understanding of how weather behaves has become crucial to the financial performance of numerous industries (Dutton, 2002). As discussed in chapter 2, various industries, e.g. utility companies, are reliant on weather forecasts to anticipate demand and therefore company profits. In order to protect themselves during periods of unfavourable weather conditions, companies may attempt to enter into financial contracts to minimise their exposure to weather risk. This has given rise to new

forms of financial instruments that are based on the changes in weather. However, in the trading of these new instruments the use of sophisticated weather forecasting models are not relevant for two reasons. Firstly, the level of sophistication required to model climate restricts the application to within meteorological centres. Secondly, and more importantly, the majority of weather-based contracts are traded long before the start date of the contract, and long before any meaningful forecasts have been published by climate centres (Bellini, 2005). For example, a utilities company wishing to protect against warm conditions in the winter months may purchase weather protection in the preceding spring. Instead, simpler models based on an understanding of seasonal behaviour are used. A discussion of these simplified models is presented in chapter 4.

As company cash reserves are placed under enormous strain due to the credit crunch (that began in 2007), companies require techniques to value weather-based contracts to avoid further losses due to adverse weather conditions. This is the focus of this thesis. The follow section outlines the discussions of each chapter.

1.1 Thesis aims and structure

This thesis proposes a new model using incomplete market theory and techniques from actuarial sciences to produce a PDE suitable for valuing weather derivatives. Chapter 2 serves as a basic introduction to the background of the weather derivatives market and its uses. The specifications of weather derivatives are outlined and the relevant formulae and notation for subsequent chapters are introduced. The goal of chapter 3 is to provide an introduction to the financial and mathematical concepts and techniques that are used for the later research in chapters 5 to 7. A short overview of incomplete market models (such as illiquid options with stochastic volatility) is presented.

Chapter 4 focuses on the existing temperature models that have been proposed in the literature. The chapter begins by examining the properties of temperature and the various models that have been introduced to capture its behaviour. These models are not as comprehensive (as they omit some of the physical properties) as those traditionally used in meteorological forecasting, but do provide an adequate

model of behaviour (see the comprehensive work of Kalnay, 2003, for model examples). Clarifications between the differences in modelling the temperature or the index are provided and the advantages and disadvantages of each approach are discussed. Since later chapters involve the numerical evaluation of weather derivatives, current numerical techniques are also explored in chapter 4.

Chapter 5 applies techniques from chapter 3 to propose a new model for valuing an option where the underlying cannot be hedged completely. From this model, a two-dimensional PDE that values a weather derivative is derived. The hedged portfolio is created using a suitably correlated asset and we assume that the hedging portfolio is *mean self-financing* (details are found in §5.2.3). The underlying assumptions used in our model are discussed, with particular interest in the conditions under which the PDE is suitable for use and the important hedging strategy needed to derive the derivative's price is given. Finally, necessary estimates of parameters governing the temperature are calculated for use in subsequent chapters.

Numerical evaluation of the two-dimensional PDE is performed in chapter 6. Here, an analysis of our derived weather PDE is presented and the difficulties in numerically solving it are discussed. A review of the existing numerical techniques used to overcome these difficulties is conducted, and then an improved numerical procedure is introduced to solve our PDE. This procedure has by applied in a financial mathematical setting in Harris (2003), d'Halluin, Forsyth, and Labahn (2006) and more recently in the valuation of a mine in Evatt, Johnson, Duck, and Howell (2010a) and Evatt, Johnson, Duck, Howell, and Moriarty (2010b). We utilise the numerical procedure but derive some new bounds for the grid spacing to suppress introduced errors from interpolation.

In chapter 7, the newly proposed model in chapter 5 is extended. The extension relaxes the assumption of allowing the portfolio to be mean self-financing and instead assumes that the holder of the option will be compensated for taking on risk that cannot be diversified. Various choices exist for the mathematical definition of how the compensation should be assessed, and we briefly highlight a few, then one is selected. This is then an incomplete market problem since the choices of how compensation should be given will vary between investors. Therefore there is no longer one suitable price for the derivative. The impact of the correlation coefficient ρ between the temperature process and the chosen imperfectly correlated

asset is examined towards the end of the chapter. Depending on the option to be valued, the PDE may become non-linear. For example, the PDE is non-linear when the option payoff has a sign-alternating delta.

In an attempt to remove the presence of spurious oscillations often experienced in lattice-based schemes (see figure 6.6(d) in §6.4 for example), an improved numerical scheme is proposed in chapter 8. It is shown to lead to superior convergence over other lattice methods. We begin by introducing an improved numerical scheme that leads to superior convergence over traditional lattice-based schemes. Based on the motivation to value weather derivative contracts on multiple locations, a discussion of the difficulties in using existing approaches applied in this thesis is presented, and subsequently we propose and develop a generic methodology for overcoming them. The approach can readily be applied to a broad class of numerical schemes to improve convergence, including, but not limited to, binomial trees, quadrature and finite-difference schemes. The methodology enables extrapolation techniques to be employed on non-monotonic data sets, and is equally applicable to pricing options with early exercise features, and produces significant improvements in accuracy.

Chapter 9 concludes this thesis by summarising the results and providing several directions for future research.

Chapter 2

Introducing Weather Derivatives

> *A bank is a place where they lend you an umbrella in fair weather and ask for it back when it begins to rain.*
>
> **Robert Frost**

In 1996, the US energy sector began the process of deregulation in the hope of providing reliable services to consumers at reasonable prices. The deregulation was imposed to allow competition, giving consumers a choice of electricity and/or natural gas suppliers. As a result, companies within this sector had to increase their knowledge and skill in trading financial instruments in order to remain competitive and profitable. The drive for energy sector participants to remain competitive led to the urgent reassessment of business risk exposure. One crucial, and sometimes overlooked, aspect of business-risk was how weather changes affected demand (volumetric risk), and thus company profits. An ability to mitigate weather risk was attractive not for its money making ability, but as an instrument for hedging purposes to stabilise cash-flow. Prior to this, the effects of unpredictable seasonal weather patterns had been absorbed and managed within a regulated and monopoly environment, whereby institutions could simply pass on the burden to the customer without consequence.

At the time of energy deregulation, the overall management of weather risk was extremely problematic for companies. To reduce their exposure, four possible approaches were available (Myers, 2009):

- **Diversification** - Consider a company whose sales are reliant on one type of weather, for example snowfall. They could aim to diversify their product range in order to reduce their overall exposure. For example, a manufacturer of snowmobiles could also produce jet skis, or a ski resort might install a heated pool for summer guests. However, this approach merely offsets losses, and does not eliminate them, and would also be expensive to implement.

- **Commodity Futures** - Commodities futures and forward contracts could aid in protecting end-users against unfavourable weather conditions. Take, for example a farmer who is concerned about strong industry crop yield. Weather conditions conducive to crop growth would increase total crop yield and lead to reduction in the value of his crop, due to the imbalance between supply and demand. For protection, the farmer may enter a futures or forward contract on his crop to secure a guaranteed price for his stock. However, selling crop ahead of harvest creates some extra risk, namely if the physical crop is smaller than the amount presold.

- **Insurance** - Catastrophic weather-related insurance has been available for many years to protect the holder from losses incurred from, say, a hurricane or flood. Using these instruments for hedging against unusual (non-catastrophic) weather conditions, for example a hot period in the winter that reduces the demand for heating in homes, is ineffective because a loss in profits cannot necessarily be classified as a weather-induced loss (Jewson, Brix, and Ziehmann, 2005). Furthermore, a company may find it difficult to prove to the insurance company that the loss of earnings was solely due to adverse weather conditions.

- **Contract Contingencies** - A company may decide to pass on the impact of weather fluctuations to customers by raising prices (Jewson et al., 2005). Construction companies often include weather contingencies in contracts, which specify that in the event of frost that would prevent work from progressing, the buyer must take on the extra cost for the added time required to complete the project. This is an effective method in times of economic growth. However, its effectiveness diminishes in an economy slowing down because of heavy competition.

As noted by Schiller, Seidler, and Wimmer (2008), the preferred method to manage weather risk, prior to the energy deregulation, was through purchasing of weather insurance from private financial institutions. However, these insurance contracts would only protect against catastrophic events, but due to deregulation, a number of companies developed a need to manage non-catastrophic events such as warm or cold temperature periods, rainy or dry periods, sunny periods, etc.

As commercial companies attempted to understand their exposure to climate, academics began to stress the impact that climate change (or more specifically weather fluctuations) was having on global economies. A study by the US Department of Commerce (see Dutton, 2002) concluded that up to a third of the US Gross Domestic Product (approximately $3.8 trillion) was exposed to weather risks. Additionally, Dutton (2002) stated that around 15% of the industrialised economy was affected by daily weather. In 2001, the UK Met Office conducted a survey examining the impact of weather on British industry, and found that 95% of respondents admitted to a 10% loss in profits due to adverse climate effects (Met-Office, 2001). In the United States, several institutions attributed the increased levels of unpredictable climate conditions to global warming, an idea supported by the results obtained by the U.S National Oceanic and Atmospheric Administration, which highlighted lower precipitation and higher temperature on average over the United States.

Unpredictable weather conditions can have dramatic impacts on companies. Dutton (2002) highlighted a few particular cases of such affected companies in his review of the weather service industry. He reported that 2001 fourth quarter electricity sales by First-Energy were down $122 million on the previous year, due to milder winter conditions. Similarly, another energy company, Dominion, reported a $47 million decrease in earnings in 2001 because of unfavourable weather conditions. As management within a company may wish to mitigate weather fluctuations to maintain performance/sales and in turn ensure their bonuses (which may also not be in the interest of diversified investors, who may have already accounted for the weather risk), together with deregulation of the energy and utility industries, helps to explain the impetus for the creation of a new asset class: *weather derivatives*.

2.0.1 Anatomy of a Weather Derivative

A weather derivative is a contract with a future settlement contingent on a specified weather variable. Generally, a weather derivative is defined by (Jewson et al., 2005):

- A weather variable, such as temperature, rainfall, snowfall;
- a reference weather station that measures the weather variable;
- a measurement period, given by a starting date t_1 and finishing date t_2;
- an index that governs how the weather variable is aggregated over the measurement period;
- a payoff function indicating how cash-flows are calculated, containing key attributes such as contract structure (for example defining it as a *call, put, swap*, etc.), the strike level, tick size (the payout amount per unit above/below the strike), and a maximum payout (usually referred to as a cap);
- and possibly a premium, which is awarded to the seller if the derivative is an option. Additionally, an insurance premium may often be added to provide compensation for the sellers inability to completely hedge their position.

A distinguishing feature of a weather derivative contract is that it has no negotiable underlying index, as for example, temperature has no traded value in the market. Also, contracts are not created on the instantaneous weather variable, but rather on some accumulated average or total, which we discuss in §2.2. The existence of a traded underlying variable usually forms the basis of a traditional derivatives contract. The absence of a tradable underlying presents many problems, which we examine in chapters 4 - 6.

2.1 History and Development of Weather Derivatives

It is an old cliché that the British are obsessed with the weather, yet it was in the United States where the modern weather risk-trading market was born. The commencement date of the weather derivatives market is not clear, with Nicholls (2004), Jewson et al. (2005) and Hamisultane (2006) alluding to its inception in 1996, whilst others, such as Garman, Blanco, and Erickson (2000), Harris (2003) and Bellini (2005), suggest 1997 as the first year. According to Nicholls (2004), Aqulia Energy, a subsidiary of UtiliCorp United, pioneered the use of weather derivatives by constructing the first deal in July/August 1996. Aqulia Energy entered into a transaction with Consolidated Edison Co to offset the risk of power sales decline due to a cool August period (Nicholls, 2004). In 1997, a weather derivatives transaction between Koch Industries and Enron Corporation, the infamous energy company that later imploded in an accounting scandal, was the first publicised deal of its kind, which indicates why it is often regarded as the first weather derivatives transaction. The contract was based on a temperature index for Milwaukee, Wisconsin. The index was an accumulated quantity of temperature by a given formula (various types are defined in details in §2.2). The contract was structured such that Enron would pay Koch $\$10,000$ for every degree the temperature fell below a specified value during the winter of 1997-1998, while Koch would pay Enron $\$10,000$ for every degree above the specified value. This type of deal is commonly referred to as a swap contract, whereby two counter-parties agree to exchange cash flows in the future in some prearranged manner (see §2.3.1, and refer to Hull, 2006, for further details).

Leading the way in establishing the weather-risk market were Enron, Koch and Swiss Re. Although the energy and utilities industries pushed for the development of weather derivatives, the economic fortunes of several enterprises within the agriculture, retail, entertainment and tourism sectors are also subject to the mercy of mother nature and equally required a financial instrument to reduce their sensitivity to weather changes. This resulted in contract variants of the original deals being created for, among others, a brewery, a sports-drink company, a golf resort and a fertiliser maker. These took the form of options and futures linked to a specific and measurable weather property, such as rainfall. Market participants

recognised weather derivatives as suitable instruments to hedge weather exposure in their core energy assets and as a form of risk management.

Of the non-energy specific sectors, the application of weather derivatives has been most prominent within the agriculture sector and has been examined in the literature in depth by Geman (2005) and Turvey (2008). In the energy sector weather derivatives are used to hedge volumetric risk, whereas in the agriculture sector weather derivatives are used to protect against production yield risk.

2.1.1 The effect of El Niño

The weather derivatives market grew significantly during the warm Midwest and Northwest El Niño-Southern Oscillation (commonly referred to as El Niño) in the winter of 1997-1998. In general terms, El Niño is a periodic change in the atmosphere and ocean of the tropical Pacific region, causing weather changes in large parts of the world, especially in countries situated around the equator, namely certain parts of Africa, Indian Ocean, South America and Australia. Although the effects of El Niño in the United States were weaker than those experienced in other regions (according to Jewson et al., 2005), it still led to higher temperatures over most of the northern United States and an increase in rainfall in the southern and coastal regions of the United States. These changes in weather were significant enough to act as a catalyst in growing the weather derivatives market as companies sought to protect themselves from declines in earnings due to unfavourable weather conditions. The impact of El Niño stimulated the demand for companies seeking warm-side winter protection, by purchasing weather derivatives. Contracts were primarily traded in an over-the-counter (OTC) market (Jewson et al., 2005).

In September 1999, weather derivatives were standardised on the Chicago Mercantile Exchange (CME) through the creation of the electronic platform Globex (Hamisultane, 2008). This was the first exchange where standardised weather contracts could be traded and Hamisultane (2008) cites this as one of the main drivers for the growth in market participation and trade volume. The reason for this increase in trading activity was that exchanged-based transactions provided investors with the most reliable price for a given contract, and eliminated credit

risk (the risk that the other counter-party may default) through the establishment and use of the clearing house. Additionally, market makers specialising in trading weather derivatives viewed the exchange as creating a liquid weather-risk market that is crucial to quick transfer of risk. The platform initially listed contracts for ten cities in US: Atlanta, Chicago, Cincinnati, Dallas, Des Moines, Las Vegas, New York, Philadelphia, Portland and Tucson, which were chosen based on population size, the locations' seasonal temperature variability, and the level of trades in the over-the-counter market. By 2003, European contracts began to trade on the CME, and were quickly followed by the introduction of contracts on the Japanese cities Osaka and Tokyo. Today, the CME Group has weather derivative contracts on 24 cities in the United States, ten in European, six in Canada, three in Australia and three in Japan (Myers, 2009; Matthews, 2009).

Following in the footsteps of the CME, the London International Financial Futures and Options Exchange (LIFFE) in conjunction with two information technology companies, Intelligent Financial Systems (IFS) and World-wide Intellectual Resources Exchange (WIRE Limited) created the first London-based weather exchange with the release of the website I-WeX.com on 23rd December 2001. The exchange promised to be an on-line marketplace where market-makers, buyers and sellers came together to construct and trade weather contracts on European cities through an over-the-counter auction system (Hamisultane, 2008). Additionally, it provided bulletin boards and news, on-line pricing models and weather data services (Mehta, 2000). The first trade on this exchange was by Accord Energy Limited and Aquila Risk Management, where five lots were traded for January 2002 contracts where temperature data were observed at London Heathrow. The exchange failed to deliver on its promises, and due to insufficient turnover and significant structural issues, LIFFE suspended the trading of weather derivatives contracts in 2004 (Jewson et al., 2005).

Market makers and market participants offered the weather-derivative market a greater depth and breadth. Brockett, Wang, and Yang (2005) explained that these rapid developments contributed to the market widening to include a variety of sectors, including agriculture, construction, retail, transportation, tourism and entertainment[1]. These developments are now bringing the weather-derivative market to the attention of brokers, banks and other financial institutions.

[1]According to the Weather Risk Management Association www.wrma.org/risk_history.html

2.1.2 Market Size

A Price Waterhouse Coopers (PwC) survey conducted over twelve months in 2003-2004 found that the weather-risk market size[2] stood at \$4.7bn (£3.2bn), and by 2006 this had increased to \$45bn (£30bn). However, according to the survey, by 2007 a contrasting story was being told as the market size had more than halved to \$19bn (£13bn). The Weather Risk Management Association (WRMA), the industry body that represents the weather risk management business, attributes the decline to a quieter hurricane season in 2007 in contrast to the occurrence of the costly Hurricane Katrina in the equivalent season of 2005.

Year	Summer	Winter	Total
2000-2001	1126	1633	2759
2001-2002	868	3069	3937
2002-2003	2412	2105	4517
2003-2004	1175	1987	3162
2004-2005	1928	2129	4057
2005-2006	1036	1144	2180
2006-2007	372	402	774
2007-2008	163	268	431

Table 2.1: A breakdown of the number of OTC contracts (of various structures) traded during the winter and summer months, as reported by survey participants (excluding CME trades). Source: PwC/WRMA.

	2006-2007 (%)	2007-2008 (%)
Heating degree days	20	29
Cooling degree days	5	4
Other temperature	62	37
Non-temperature contracts	13	30

Table 2.2: Over-the-counter trades by types. Source PwC/WRMA

The most recent annual survey, over the period April 2008 to March 2009, conducted by PwC for the Weather Risk Management Association reported that the trading volumes were down 39%, with notional values [3] falling 53% (Village, 2008). Observe from table 2.1 that winter-based weather contracts are more

[2]This represents the potential payout on weather derivatives contracts written globally in 12 months

[3]The total value of a leverage position's asset. For example, one S&P 500 Index futures contract obligates the buyer to 250 units of the S&P 500 index. If the index is trading at \$1,000, then the single futures contract is similar to investing \$250,000(250 × \$1,000). Therefore, \$250,000 is the notional value underlying the futures contract.

Year	Notional Value ($m)
2000-2001	2517
2001-2002	4339
2002-2003	4188
2003-2004	4710
2004-2005	9698
2005-2006	45244
2006-2007	19193
2007-2008	32008

Table 2.3: Notional value of all weather risk contracts. Source: PwC/WRMA

frequently traded than their summer variants and, furthermore, table 2.2 shows that almost 30% of the trades performed in the over-the-counter market were on heating degrees days (we formally define heating degree-days in §2.2.1). The current notional value of the market stands at $15.1bn, making it the lowest since 2004 (see table 2.3). Volumes have not grown as expected, partly because weather derivatives contracts are primarily used for hedging purposes (Dutton, 2002; Jewson et al., 2005), where the hedgers are primarily concerned with protection for their specific situations and, hence, deal directly with counterparties in the OTC market. Myers (2009) points to the turmoil in the financial markets and general economic contraction (often referred to as the credit crunch) that erupted from the 2007 sub-prime mortgage crisis, as the reason for the depressed volumes. Earnings shortfalls caused by weather conditions were not easy to mitigate because of the enormous strain the credit crunch has had on companies' cash reserves and/or bank credit makes it more difficult for companies to invest the required capital to invest in projects/assets which offset the losses due to unfavourable weather conditions.

Outside of the academic literature, Morrison (2009) (who is a natural advocate and provider of weather derivative products), indicates that market observers remain optimistic despite the recent volume decline, because they believe that the weather-risk market will benefit as the administration of President Barack Obama of the United States has placed significant emphasis on the use of wind power and other renewable energy solutions, all of which are heavily dependent on weather conditions. The WRMA president holds a similar view (STORM, 2009):

> The rising use of renewable energy - solar, wind and hydro - will spur more interest in employing weather risk management tools. Most renewable sources are tied to the weather and we are seeing increased interest from developers, operators and financiers in mitigating their weather exposure by using risk management tools.

Morrison suggests that although companies' cash reserves are strained, the weather derivatives market will grow as companies find that the recession forces them to assess the vulnerability to weather conditions since they may not be able to withstand further hits from abnormal weather patterns. This view is shared by another provider of weather derivative related products, the CEO of Galileo [4], Malinow (Morrison, 2009):

> With weather derivatives you have a whole slew of end users who will have to de-risk going forward to gain access to new capital. You are going to see people making more effective use of these products.

Being able to dramatically reduce earnings volatility in times of economic uncertainty is one of the major advantages that a company manager may see in purchasing weather derivatives. However, it must be noted that from the perspective of a diversified investor, the weather risk can be absorbed by shorting the company's stock and hence protecting themselves from downward risk.

As market participation from the United States declines, there is reason to remain optimistic about the future of this market, given increased participation from Asia and Europe Hamisultane (2006). A possible reason for this growth may be due to the introduction of a variety of ways in which the accumulated index (based on a weather variable) is calculated, and therefore market participants who operate in a climate that differs from the United States may now find a use for these contracts. We next consider a selection of the more popular types of indices.

[4] Galileo Weather Risk Management was formed in 2005 and writes tailored financial weather-related risk management products

2.2 Common underlying

There is a vast array of observable weather attributes, ranging from average daily temperatures to more obscure attributes such as sunshine hours. Even though there appear to be numerous types of observable weather effects on which a derivative could be created, table 2.2 indicates that temperature is more often used as an underlying. For example, in 2007-2008, 70% of all weather derivatives contracts traded were based on temperature as the underlyer. Table 2.4 reports the link between weather and financial risk from the perspective of a company manager, and suggest that across various industries temperature movement is strong component of financial performance. Also extremely cold temperatures, which result in snowfall, are of major concern to these industries. According to Tigler and Butte (2001), the dominant use of temperature derivatives arises because

1. it is relatively easy to quantify across a spectrum of industries, unlike other weather variables e.g. rainfall, which is highly spatially dependent.

2. high-quality data and sufficiently long historical records sets are available for numerous locations around the world,

3. the impact of temperature on a particular industry is easy to quantify, e.g. cold summers having a direct hit on sales of ice cream, which allows for forecast models to be created.

With the majority of traded weather contracts currently being written on temperature, we shall constrain our analysis primarily to derivatives where temperature represents the underlying weather variable in one form or another although it is worth noting that rainfall options are studied by Odening, Musshoff, and Xu (2007), in the context of wheat production levels. Turvey has published several papers within the weather derivatives literature, covering the use of these derivatives for specific events risk in agriculture (Turvey, 2001), examining the role of famine-indexed weather derivatives in Chantarat, Turvey, Mude, and Barrett (2008). More recently Turvey (2008) develops formulae for valuing coupon rates on weather-linked bonds and the interest rates on weather-linked mortgages and lines of credit.

Risk Holder	Weather Type	Risk
Energy Industry	Temperature	Lower sales during warm winters or cool summers
Energy Consumers	Temperature	Higher heating/cooling costs during cold winters and hot summers
Beverage Producers	Temperature	Lower sales during cool summers
Building Material Companies	Temperature/Snowfall	Lower sales during severe winters (construction sites shut down)
Construction Companies	Temperature/Snowfall	Delays in meeting schedules during periods of poor weather
Ski Resorts	Snowfall	Lower revenue during winters with below-average snowfall
Agricultural Industry	Temperature/Snowfall	Significant crop losses due to extreme temperatures or rainfall
Municipal Governments	Snowfall	Higher snow removal costs during winters with above-average snowfall
Road Salt Companies	Snowfall	Lower revenues during low snowfall winters
Hydro-electric power generation	Precipitation	Lower revenue during periods of drought

Table 2.4: Illustrative links between weather and financial Risk. Source: Climetrix, Risk Management Solutions Inc. http://www.climetrix.com.

With this in mind, we introduce the most commonly used measurements of temperature in the weather derivative market.

2.2.1 Degree-Day Indices

Meteorologists define a *degree-day* as the difference between a reference temperature and the average temperature on a given day. In this thesis, we take a day to be measured from midnight until the following midnight. The average[5] temperature $X(t)$ on day t is defined as (Geman, 2005; Jewson et al., 2005)

$$X(t) \equiv \frac{X_{max}(t) + X_{min}(t)}{2}, \tag{2.1}$$

where $X_{max}(t)$ and $X_{min}(t)$ denote the maximum and minimum temperature on day t, respectively. It is helpful to view the reference temperature as a barrier level, which we denote as $X_{ref}(t)$. Work in the weather derivatives literature often assumes this barrier to be constant and it is typically set to the temperature level for when heat furnaces are switched on/off. Therefore, we drop the time-dependency and write it simply as X_{ref}. The barrier is typically specified as 18.33°C (Cao, Li, and Wei, 2003; Jewson et al., 2005), since converting from measurements in Fahrenheit, ($X_{ref} = 65$°F) produces a decimal value for the barrier. Jewson et al. further mention that in all other countries where temperature is measured in Celsius it is usually taken as 18°C, and we adopt this value for X_{ref} throughout this thesis. Describing the reference temperature as a barrier strengthens the comparison of valuing a weather option with that of valuing a barrier option. We use this observation later in chapter 6 to aid in solving various weather options.

Degree-day indices come in two types: heating degree-days (HDD) and cooling degree-days (CDD). We provide an outline of these and their uses below.

[5]This is not a true average as we are taking extreme values of the temperature as opposed to observing all temperature movements and then taking the mean temperature. Unlike the true average, this average is locally horizontal as a variable, making jumps only at a countable number of occasions on which X jumps outside its previous range X_{min} to X_{max}. The author notes that statistically this approach has drawbacks and will prevent it from being useful in a PDE framework.

The Heating Degree-Day index

A *heating degree-day* is a measure of how cold the day was. In other words it provides information on the number of degrees that the observed average temperature, on day t, was below the barrier X_{ref},

$$(X_{ref} - X(t))^+. \tag{2.2}$$

When $X(t) > X_{ref}$, it implies that little fuel or electricity is consumed for the purpose of providing heating because the temperature is sufficiently warm. If $X(t) < X_{ref}$ then it is assumed that heating will be required. This quantity (2.2) is accumulated over a given time period T, and is known as the *heating degree-day index*. This may be defined as

$$I_H(t) = \sum_{i=0}^{j(t)} (X_{ref} - X(t_i))^+. \tag{2.3}$$

where t_i are the observation days and $j(t)$ is the largest integer such that $t_{j(t)} < t$. It is possible to represent the above quantity (2.3) in continuous time. We do this by redefining $X(t)$ such that it denotes the temperature observed at midday on day t. Previously, $X(t)$ was defined only in discrete time but is now treated as an Itô variable in continuous time such that the continuous form of equation (2.3) becomes:

$$I_H(t) = \int_0^t (X_{ref} - X(s))^+ \mathrm{d}s, \tag{2.4}$$

and by applying Itô's lemma (to $O(\mathrm{d}t)$) becomes

$$\mathrm{d}I_H(t) = (X_{ref} - X(t))^+ \mathrm{d}t. \tag{2.5}$$

Using a continuous description of the index is attractive because we can then observe this quantity at any time during the day. In (2.3) the subscript notation is used to denote that the index is defined for a *heating degree-day index* (from now on referred to as HDD).

A possible temperature path is simulated to illustrate graphically how the index may accumulate. Such a situation is shown in figure 2.1, which uses the stochastic differential equation suggested by Alaton et al. (2002) (see §4.1.4) to simulate a

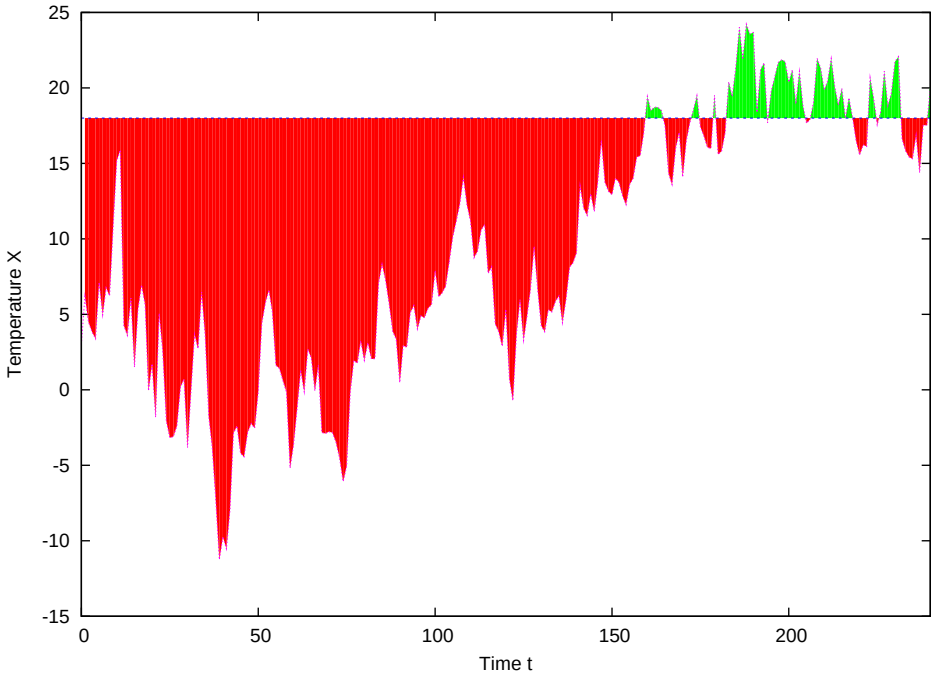

Figure 2.1: A simulated temperature path using the Monte Carlo method showing the area above and below the barrier. The start date is from January 1st (day 0). The temperature is measured in Celsius and 'Time' is the real calendar time measured in days. We use an Ornstein-Uhlenbeck SDE of the form given in (3.5) to simulate the temperature paths in this figure. Parameters for the SDE are given by estimates determine in chapter 5
.

temperature path using the Monte Carlo method. The red shaded region in this figure indicates the area between temperature and the barrier (here $X_{ref} = 18$), and the value of area is the quantity (2.4). The start date (day 0) of the simulated temperature is January 1st. It is evident that that during the winter months there will be a large number of heating degree-days, and fewer, or none during summer. In most countries, during the winter, the temperature rarely exceeds the 18°C barrier, which implies that the $\mathrm{d}I_H(t)$ on each day t will be positive.

The Cooling Degree-Day index

Conversely, a *cooling degree-day* is a measure of how warm a given day has been. It captures how many degrees the observed average temperature was above the

barrier, and is calculated as follows:

$$(X(t) - X_{ref})^+. \tag{2.6}$$

This quantity is effectively a measure of the energy demand for cooling on a given day t. As was the case for a heating degree-day index, the cooling degree-day index accumulates (2.6) until time T, and is given by

$$I_C(t) = \sum_{i=0}^{j(t)} (X(t_i) - X_{ref})^+, \tag{2.7}$$

and for the same reasons as stated in the above section, we define the continuous form as

$$I_C(t) = \int_0^t (X(t) - X_{ref})^+ \mathrm{d}s, \tag{2.8}$$

where

$$\mathrm{d}I_C(t) = (X(t) - X_{ref})^+ \mathrm{d}t. \tag{2.9}$$

Since (2.8) captures how hot a time period has been, cooling degree-day indices (hereafter CDD) are typically used during the summer months. This is further emphasised through figure 2.1, where the small green shaded region only has value during the summer months. Typically, weather conditions in most of the traded locations may rise above 18°C during summer, but often will drop below that level in summer. This differs from the winter months where the temperature is seen generally to be consistently below the barrier and, hence, the CDD has zero value. It is then evident that temperature movements during the winter and summer seasons are not symmetrical about the barrier level. The CDD index is rarely traded in Europe and Japan, because in these regions summer temperatures are typically not high enough to place significant demand for cooling. Therefore, the CDD index would have zero value.

It has been reported by Cao et al. (2003) and Jewson et al. (2005) that use of a CDD index is most relevant to the US electricity market and to a lesser extent the gas market, for the simple reason that part of the demand for electricity is driven by people's need for cooling. Jewson et al. (2005) also suggest that CDDs are becoming of more interest to participants in the gas market because more electricity is now being generated from natural gas.

The popularity of degree-days indices arises as they closely track the extent to which consumers use their heating systems and/or air conditioners. Geman (2005) shows the high correlation between HDD and gas and power use in the United States; Cao et al. (2003) shows the that consumption of gas is highly correlated with changes in temperature (they report $R^2 = 0.9416$). Because weather conditions and patterns concerning temperature and related industries across Europe and Asia behave differently from the United States, specifically that temperature fluctuations are not as significant, other indices are used in these locations.

2.2.2 Average of Average Temperature Indices

Often, there is a desire to understand the average temperature during a given time period. For this purpose, the *average of average temperature index* (AAT) is used. This is calculated by averaging across all the daily average temperature, $X(t)$, values over the time period, i.e.,

$$I_A(t) = \frac{1}{t}\int_0^t X(s)\mathrm{d}s. \tag{2.10}$$

The above is perhaps a more intuitive measure of temperature variability than degree-day measurements, though for that reason it is less relevant to the discontinuous payoffs of US CDD weather derivatives. It is also a more informative measure of the behaviour of the weather itself. However in practice it is not possible to observe temperature continuously, in a legally verifiable way, therefore a discrete representation of the above equation is more useful for defining contracts.

The average of average temperature indices are mainly used in Japan, but seldom used in United States or Europe. Derivative contracts whose underlying is an AAT can be regarded as Asian options. We discuss the significance of this in Chapter 6

2.2.3 Cumulative Average Temperature Indices

Northern European summer temperatures differ vastly from those observed in the United States, by the fact that the temperature does not often exceed the

typically-used reference temperature which is set at 18°C - set at this level as the market is dominated by agents from the energy markets in the United States - so the use of CDD based contracts in Europe is rare (table 2.2 highlights the low percentage of traded CDD contracts). This is supported by the fact that the CME contracts provides no CDD based contracts on European locations (see Matthews, 2009). Instead, the cumulative average temperature (CAT) index is used and is defined as the summation of daily average temperature over the contract period (Jewson et al., 2005):

$$I_{CAT}(t) = \int_0^t X(s)\mathrm{d}s. \tag{2.11}$$

2.2.4 Event indices

Occasionally, companies may be interested in monitoring the number of days over a given period that some particular weather event occurs, e.g. the temperature exceeds some temperature threshold. These are known as *critical day indices*. Alternatively, a contract can be created which measures the period over which a particular event occurs and will pay out once the length of time is above a given threshold. Contracts written on these indices may be regarded as Parisian, or in some instances Par-Asian, options (for precise definitions of both Parisian and Par-Asian options we refer the interested reader to Hull, 2006). Jewson et al. (2005) explain that because of the specific nature of these indices, transactions are typically between hedgers and speculators. An example of such a transaction could be to provide insurance for construction workers in the event that frost occurs. The contract might be dependent on the number of *frost days* from November to March. The event is triggered if on a working day [6] the temperature at 7am was below -3.5°C, or at 10am was below -1.5°C, or the temperatures between 7am and 10am was both below -0.5°C.

2.3 Product Overview

As with all new markets, the OTC arena drove the initial volume in weather derivatives trading. Activity in the OTC weather market has lessened due to

[6] This would only include weekdays and exclude public holidays which fell on a weekend

the standardisation and reduction in credit risk offered by exchanges, such as the CME (Hamisultane, 2008). The standardisations of contract specifications are outlined below, and where necessary we mention the economic purposes for further illustration.

2.3.1 Swaps

One of the first traded weather derivatives was constructed as a swap contract. As previously stated in §2.1, a swap contract is an agreement to exchange cash flows in the future, according to a prearranged formula (Hull, 2006). These exchanges of cash flows occur at predefined stages over the lifetime of the contract. Exchange-traded weather swap contracts involve daily cash settlement as the index fluctuates, while OTC traded swap contracts are cash settled only at maturity. At initiation, both counter-parties agree to pay each other according to the weather conditions over a pre-agreed period, at some future date, with (rarely) any premiums being exchanged at initiation (Jewson et al., 2005). However the level of risk taken by the two counter-parties involved in the transaction is often different, and so the strike level is set at a value where the expected pay-off at maturity is close to zero, but offset slightly in favour of the counter-party taking on more risk. The market, therefore, prices costless swaps prior to trading by appropriately determining the strike level - and explains why weather swaps contracts that are traded on an exchange are quoted by their respective strike level.

Swaps as forwards

$$P(I_H(T),T) = \begin{cases} tick \cdot (L_1 - K), & \text{if } I_H(T) < L_1 \\ tick \cdot (I_H(T) - K), & \text{if } L_1 < I_H(T) < L_2 \\ tick \cdot (L_2 - K), & \text{if } I_H(T) > L_2 \end{cases} \tag{2.12}$$

where $I_H(T)$ is the value of the HDD index at maturity, $tick$ is used to translate the quantity $(I_H(T) - K)$ into monetary terms, K is the strike level, and L_1 and L_2 denote the level at which a limit to the payoff is applied. When the index is below L_1, the maximum amount the buyer of the swap contract will have to pay the other counterparty is $tick \cdot (L_1 - K)$. In the instance when the index is above

L_2, the maximum amount the buyer will receive is $tick \cdot (L_2 - K)$. This contract has the economic benefit of protecting against a high HDD index values. The downside of such a contract is that the buyer must pay the seller for low values of the settlement index. Figure 2.2(a) provides an illustration of the payoff just described.

Exchange based weather swaps

The CME offers the trading of swaps as futures contracts based on the CME Degree Day Index. According to the CME (2011), these contracts are often uncapped and have maturity dates which last for weeks, months or a season[7]. Weather future contracts are available on the CME Globex platform, and come in the following forms:

1. U.S. Weekly, Monthly and Season Weather Futures using either the HDD or CDD temperature settlement index
2. European Monthly and Seasonal Weather Futures using either HDD or CATs temperature settlement index
3. Asia-Pacific Monthly and Seasonal Weather Futures based on temperature
4. Canadian Monthly and Seasonal Weather Futures based on HDD, CDD or CATs temperature indices

Additionally, non-temperature based contracts are offered:

1. Frost Day Monthly and Seasonal Futures
2. Snowfall and Seasonal Snowfall Futures
3. Hurricane Seasonal, Seasonal Maximum and Event based Futures. These contracts are based on the Carvill Hurricane Index [8], which is is an index that describes the potential for damage from an Atlantic hurricane.

[7]Traditionally, a season lasts 3 months, where winter begins in November, spring in February, summer in May, and autumn in August

[8]The maximum sustained wind speed of a hurricane and the radius to the hurricane force winds are used to calculate the CHI. The CME uses the values 74 mph and 60 miles for the maximum sustained wind speed and radius of hurricane force winds respectively. The variable CHI is used as the basis for trading hurricane futures and options on the CME.

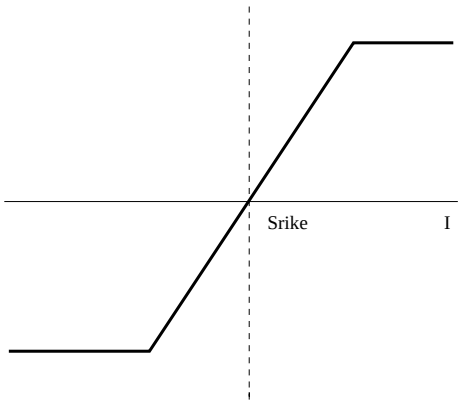

(a) Swap payoff

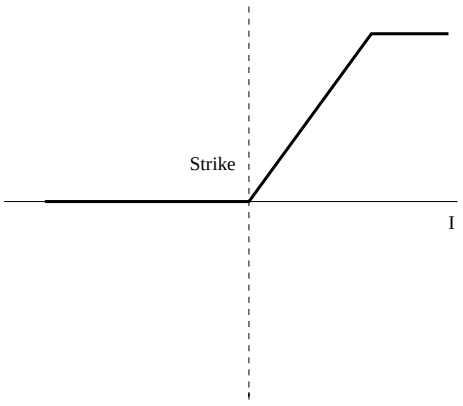

(b) Call payoff

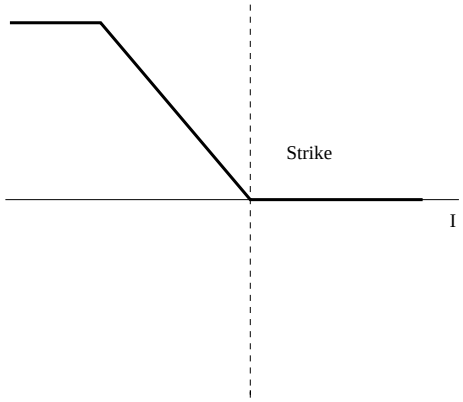

(c) Put payoff

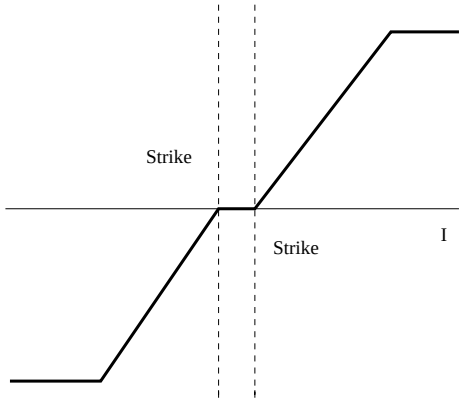

(d) Collar payoff

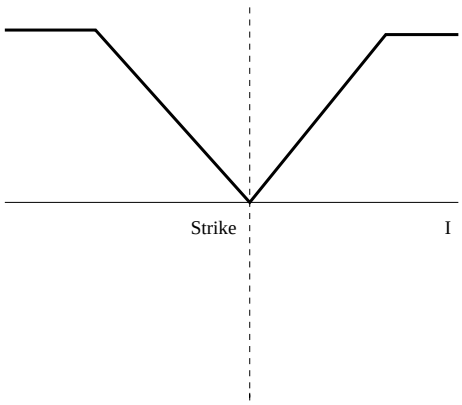

(e) Straddle payoff

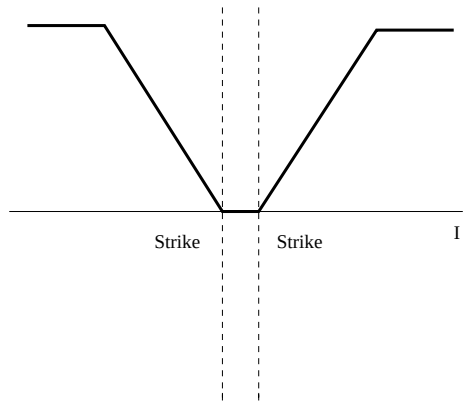

(f) Strangle payoff

Figure 2.2: The payoff functions for the various weather derivative contracts. The solid represents the payoff, and the dotted lines denote the strike level(s).

Additionally, the exchange provides options on these futures:

1. The HDD/CDD Index futures are agreements to buy or sell the value of the HDD/CDD Index at a specific future date.
2. The size of the unit trading shall be 20 British pounds times the respective HDD/CDD index.
3. Weather futures are cash-settled daily at 15:15 Central American Time (CT), unless the exchange closes early, and therefore are daily mark-to-market, based upon the index.

2.3.2 Options

The temperature index call (put) option gives the holder the right, but not obligation, to own (short) one index at a given strike level. Unlike the equities market, where an option may have several different strikes, in weather-based contracts the strike is typically set at the historical expected index value or one standard deviation above or below the expected index depending on if the contract is being bought or sold, or is a call or put option (Jewson et al., 2005). These contracts' maximum payoffs are usually capped at a level which is either two standard deviations or the most extreme historical value of the weather index. Most contracts traded in the OTC market impose a limit on the financial gains or losses, but the weather contracts specified on the CME have no such restriction. At the time of writing, weather option contracts are only of European style.

Unlike swap contracts, where both parties are exposed to making an unpredictable, but in capped contracts, potentially bounded payment at the end of every reset date or marked to market like futures, the downside for the holder of an option is limited to the value of the option, the so-called premium. This benefit justifies why it has been estimated that around 80% of weather derivatives are structured as options (Bellini, 2005). Taking the example of a capped HDD put option, its payoff is given by

$$P(I_H(T), T) = \begin{cases} tick \cdot (K - L), & \text{if } I_H(T) < L \\ tick \cdot (K - I_H(T))^+, & \text{otherwise} \end{cases} \tag{2.13}$$

and the capped call option is defined as

$$C(I_H(T), T) = \begin{cases} tick \cdot (I_H(T) - K)^+, & \text{if } I_H(T) < L \\ tick \cdot (L - K), & \text{otherwise} \end{cases} \tag{2.14}$$

where *tick* and K are as defined in (2.12), and the maximum payout is set when the index value equals L. Let us consider a call option. The holder of this option receives money if the index value is greater than the strike level. If the value of the index exceeds L, the holder's payout is limited to $tick \cdot (L - K)^+$. When the index is lower than the strike level no money is gained. The buyer's profit is simply the payment from the seller, which is discounted to account for time value of money, minus the initial premium value.

A wide range of different option structures, such as collars, straddles, strangles, etc., are used by counter-parties in the weather market depending on their requirements. Figure 2.2 illustrates the payoffs from the different option types.

2.3.3 Basket options

The contract types so far have only considered the case where the derivative is dependent on the temperature observed at one location. Suppose an investor is affected by weather conditions across multiple cities. Rather than purchasing individual contracts on each location it would be cost-effective (in terms of transaction costs) to purchase a single basket option, which depends on all the necessary locations. In chapter 8, we examine basket options in the more general case of options with multiple underlying assets, and investigate the application of existing techniques often used to solve these problems. Later in chapter 8, we offer an improvement on current numerical schemes through the development of a generic methodology that can be utilised to value weather derivatives with multiple underlying indices, or a variety of financial derivatives.

2.3.4 Weather Bonds

In addition to swaps and option-style derivative contracts, the growth of weather derivatives has seen the re-emergence of risk management for events caused by

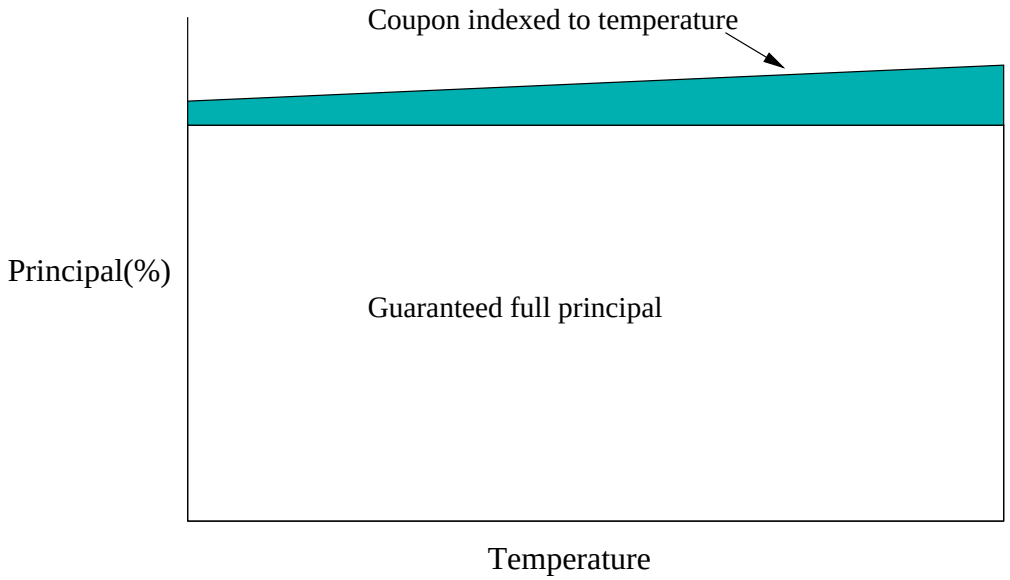

Figure 2.3: Payout of a tranche with the principal guaranteed and temperature-indexed coupon risk.

nature. Securities based on observable individual natural events, which are unaffected by trading, were constructed and traded on the Chicago Board of Trade (CBOT) until 2000, when they were delisted (Poncet and Vaugirard, 2001). After their relegation from the CBOT, investment bankers began structuring these products as insurance-linked bonds. These new products give corporations the opportunity to hedge risks associated to nature, by means of tailor-made assets. Furthermore, insurance and reinsurance companies can utilise such products to share their business risk with other market participants. Poncet and Vaugirard (2001) highlight an example of such a situation of companies sharing risk when, in 1999, Goldman Sachs offered insurance bonds to protect the reinsurance company Gerling Global Re from high-level catastrophe losses from earthquakes in Japan. Gerling Global Re sold these bonds and had to pay a coupon of 450 basis points above the six-month London InterBank Offered Rate (LIBOR); however the investor's principal was at risk. The rise of structured weather products is not limited to the risk management of catastrophic events. Corporations are often equally concerned with non-catastrophic weather events and have created structured commodity-linked bonds to manage their exposure to these events. The bond coupon payments are linked to some weather variable and pay out according to how much the variable deviates from some norm. For example, a weather bond structure may include a series of tranches whose returns are linked

to temperature (either degree-days or average temperature). Particular tranches guarantee partial or full return of the principal, and have a coupon that would be indexed to the temperature at a prescribed set of locations. Figure 2.3 illustrates this, where the tranche guarantees the full return of principal, and has a warm winter coupon, such that higher temperatures in winter imply higher tranche yield. Due to the specific nature of more structured products, their liquidity is limited (Dischel and Observer, 2002). The first bond-type weather derivative was developed by Koch Energy Trading (now Energy-Koch) in 1997. The contract was a multi-tranche, multi-year bond structure. Cash-flows were linked to the performance of 28 weather derivatives contracts at 19 US locations. Dischel and Observer (2002) correctly state that the complex nature of these contract has led to them being infrequently traded. They report that Enron also experienced this when they tried to create a simpler contract, but still investors complained about pricing issues and consequently the contract was never issued.

2.4 Summary

The introduction of weather derivatives has provided investors with a method to mitigate daily weather fluctuations and to remain competitive within today's economy. With market analysts (such as Myers, 2009) believing the weather derivatives market is to expand further, the valuation of such contracts has become hugely important.

As mentioned briefly toward the end of §2.0.1, since temperature (or any weather variable) cannot be explicitly traded, the use of well-known pricing methodologies, such as the analysis performed by Black and Scholes (1973) and Merton (1973), cannot be applied since a risk-free portfolio cannot be constructed. According to Schiller et al. (2008), the absence of a consensus pricing model has limited investors' appetite for trading these contracts. Much of the existing work in the literature assumes that the weather derivatives market is liquid and therefore is able to construct hedging strategies appropriately. Jewson et al. (2005), in particular, take this approach and assume that the weather futures contract is sufficiently traded to allow for the derivation of a suitable partial differential equation (PDE) in the Black-Scholes & Merton framework.

More work is required to develop the various methods currently in the literature. The job of financial engineers is to adopt a unified approach, similar to the way Black-Scholes & Merton revolutionised the equity derivatives market. In the next chapter, we introduce the financial and mathematical concepts and techniques that are used throughout this thesis.

Chapter 3

Preliminaries

A successful man is one who can lay a firm foundation with the bricks others have thrown at him.

David Brinkley

This chapter considers the concepts and techniques used for pricing financial derivatives. This is by no means an exhaustive review of the financial derivatives literature, but acts as the minimal requirements for understanding the material in this thesis.

3.1 Stochastic differential equations

Stochastic differential equations (SDEs) litter the finance literature and are used to describe various random phenomena. The SDEs consist of a Newtonian (deterministic) component related to an incremental change in time, $\mathrm{d}t$, and a Brownian increment $\mathrm{d}W_t$. In the general case of a continuous random process S_t, its evolution can be described by

$$\mathrm{d}S_t = S_0 + \int_0^t \mu(S_t, u)\mathrm{d}u + \int_0^t \sigma(S_t, u)\mathrm{d}W_t, \tag{3.1}$$

where S_0 is the starting point, $\int_0^t \mathrm{d}u$ is a Riemann integral, and $\int_0^t \mathrm{d}W_t$ is an Itô integral. In the limit of the integral, as $\mathrm{d}t \to 0$, we can express (3.1) as

$$\mathrm{d}S_t = \mu(S_t, t)\mathrm{d}t + \sigma(S_t, t)\mathrm{d}W_t. \tag{3.2}$$

The terms $\mu(S_t, t)$ and $\sigma(S_t, t)$ pertain to the drift and volatility of the process S and can take various forms. In this thesis, arithmetic Brownian motion (ABM) is used extensively. This is defined as

$$\mathrm{d}S_t = \mu\mathrm{d}t + \sigma\mathrm{d}W_t, \tag{3.3}$$

where μ and σ denote the constant drift and volatility of S respectively. Another form is geometric Brownian motion (GBM)

$$\mathrm{d}S_t = \mu S_t\mathrm{d}t + \sigma S_t\mathrm{d}W_t, \tag{3.4}$$

which takes account of the proportional variations of the process, and where μ and σ denote the constant drift and volatility of S respectively. Lastly, and importantly in the studying of weather dynamics, an Ornstein-Uhlenbeck (OU) processes is considered and is given by

$$\mathrm{d}S_t = \kappa(\mu - X_t)\mathrm{d}t + \sigma\mathrm{d}W_t, \tag{3.5}$$

In equation (3.5), μ is the mean value, σ the degree of variability about this mean, κ is the rate at which any deviations dissipate and revert back towards the mean μ. Note that the parameters in the above equations can be constant, dependent on a stated variable(s), or even stochastic, and we consider each of these cases in this work.

Using an OU description (3.5) prevents inappropriately large values from being reached, in contrast with ABM or GBM models. The properties of this process make it attractive in modelling various financial quantities such as interest rates (see Vasicek, 1977), currency exchange rates and commodity prices (Geman, 2005). Moreover, OU processes have been shown to capture sufficiently the behaviour of weather variables and we discuss their application in chapter 4.

3.2 Fundamentals of financial derivatives

Much of the research described in this thesis depends on several financial principles and we begin by providing a summary of the mathematical and financial tools and concepts used to value financial derivatives, drawing particular attention to cases where the market is incomplete. The interested reader should explore works such as Neftci (2000) for an accessible read on stochastic calculus, both books by Wilmott, Howison, and Dewynne(1995, 2000) are excellent for an account of the standard PDE valuation techniques.

3.2.1 Self-financing portfolio

An appropriate starting point for discussing financial concepts, and one of the most fundamental aspects of financial derivatives pricing is that of having a *self-financing portfolio*. This property is used throughout the financial mathematical literature. Generally, a portfolio is said to be self-financing if there is no exogenous infusion or withdrawal of money, such that all future purchases of new assets are financed by the sales of older ones. Following Björk (2009) we define the portfolio process as

$$\Pi(t) = \sum_{i=1}^{t} h_i(t) S_i(t), \tag{3.6}$$

where $h_i(t)$ represents the number of units held in each i asset at time t, and $S_i(t)$ the price of the ith asset at time t. A portfolio that adheres to a strategy given by $h(t) = (h_1(t), \ldots, h_n(t))$ is self-financing if the following condition holds for all time t

$$\mathrm{d}\Pi(t) = \sum_{i=1}^{n} h_i(t) \mathrm{d}S_i(t) \tag{3.7}$$

where $\mathrm{d}S_i(t)$ is the change in the price of the ith asset at time t. This means that the portfolio's value is not altered by changing the number of units held in the asset i but, rather, by the change in the ith asset. Note that the sign of h_i indicates whether the asset was bought (when positive) or short sold (when negative), though there are cases whereby a constraint is imposed which may force h_i to adopt a particular sign. An example is when no short selling of risky assets is imposed. Such a situation was experienced in 2008 when the Financial

Service Authority (FSA) banned the short selling of 34 particular financial stocks in the UK; this was later lifted in January 2009 (details can be found in FSA, 2009). Therefore, where short selling is not permitted the value of h_i in (3.6) is non-negative.

Operating a self-financing strategy is one of the key principles, along with the principles of no-arbitrage and delta-hedging, in deriving the much celebrated Black-Scholes-Merton PDE (see either Black and Scholes, 1973; Wilmott et al., 1995, for example).

3.2.2 Arbitrage principle

It is often said that there "is no such thing as a free lunch" and this underpins the essence of *no-arbitrage*. By using the no-arbitrage argument it is possible to uniquely determine a financial derivative's price, irrespective of our views of how asset prices evolve. This is the great revolution that has spurred much of the research in mathematical finance (Joshi, 2003).

Where arbitrage is possible, this implies that one can make money at zero cost. Recall the definition for the portfolio's total value Π as given in equation (3.6). A self-financing strategy $h(t)$ is called an arbitrage if either of the following hold for some fixed time t (Glasserman, 2004):

1. if $\Pi(0) < 0$ and then $\mathbb{P}(\Pi(t) \geq 0) = 1$;
2. if $\Pi(0) = 0$, with $\mathbb{P}(\Pi(t) \geq 0) = 1$ and $\mathbb{P}(\Pi(t) > 0) > 0$,

where $\mathbb{P}$ is the real-world probability. This first statement says that if the portfolio holding has a negative value at inception it will finish with positive value with probability 1. Statement 2 suggests that following a strategy denoted by both the number of physical quantities $h(t)$ and the set of asset prices S will turn a zero net investment into non-negative final wealth with positive probability. In other words, an arbitrage portfolio is one that has zero setup cost, has non-negative value in the future, and may be of positive value in the future. Though arbitrage opportunities may exist in the market, this generally occurs over short time intervals because the relative mis-pricing will be corrected by the pressures of supply and demand in the market. This is closely related to the concept of

market efficiency, which roughly states that there is no such thing as a 'good' buy; that the value of the asset is its market value (for a explanation and illustrations of this concept see Wilmott et al., 1995; Joshi, 2003).

3.2.3 Delta hedging

Delta hedging is the removal of risk from a portfolio. Suppose that we have a self-financing portfolio Π containing the derivative V and short Δ of the underlying S,

$$\Pi = V - \Delta S. \tag{3.8}$$

where the underlying S follows GBM (3.4). The hedging property simply states that the stochastic movement in the derivative's value over a small time increment $\mathrm{d}t$ is offset by the movement from the negative quantity held in the asset.

It was shown by Black and Scholes (1973) that by setting $\Delta = \frac{\partial V}{\partial S}$ the risk from the portfolio (3.8) is removed, and so to prelude arbitrage the portfolio must grow at the risk-free rate, i.e.

$$\mathrm{d}\Pi = r\Pi \mathrm{d}t. \tag{3.9}$$

This resulted in the Black and Scholes and Merton (BSM) PDE that afforded both Scholes and Merton a Nobel prize in 1997.

$$\frac{\partial V}{\partial t} + \frac{1}{2}\sigma^2 S^2 \frac{\partial^2 V}{\partial S^2} + rS\frac{\partial V}{\partial S} - rV = 0. \tag{3.10}$$

An obvious assumption is that we must be able to continuously re-hedge the portfolio to ensure that it remains risk-free. However, in reality continuous hedging is impossible and so discrete hedging is used. Continuous delta-hedging may also be inappropriate if there are associated costs with buying or selling the underlying asset. This was first studied by Leland (1985), who showed that re-hedging continuously would result in infinite total transaction costs. To circumvent this, he suggests that re-hedging is done at discrete-time intervals, and subsequently he derives a similar PDE to that of BSM, though this PDE is *non-linear* and contains an extra term:

$$\frac{\partial V}{\partial t} + \frac{1}{2}\sigma^2 S^2 \frac{\partial^2 V}{\partial S^2} - \alpha\sigma S^2 \sqrt{\frac{2}{\pi \delta t}} \left| \frac{\partial^2 V}{\partial S^2} \right| + rS\frac{\partial V}{\partial S} - rV = 0. \tag{3.11}$$

Note that δt is the time-interval between re-hedges and is not assumed to tend to zero. In the above equation, α is a scaling constant defined by an investor which describes their view on the impact transaction costs have on their investments, and $\Gamma = \frac{\partial^2 V}{\partial S^2}$ is the second derivative of the option with respect to the asset. As the effect of transaction costs differs between investors (for example, the larger the book the less significant the transactions costs are), so too does the specification of α, which implies that the valuation model may no longer produce unique option prices. In equation (3.11), gamma, Γ, is a measure of how sensitive the delta-hedge is to changes in the asset price. In the BSM case, it indicates how much we need to re-hedge in order to maintain a risk-free position; however here $\left|\frac{\partial^2 V}{\partial S^2}\right|$ in (3.11) expresses the degree of mis-hedging due to δt not being infinitesimally small. More details on the significance of mis-hedging in incomplete markets are discussed in §3.2.6.

An interesting point in the derivation of Leland's PDE is that the portfolio is no longer risk-free. The important assumption here is that the hedge portfolio has an *expected* return that is equal to the risk-free rate, i.e.

$$\mathbb{E}[\delta\Pi] = r\Pi\delta t, \tag{3.12}$$

where $\delta\Pi$ and δt denote a small (but not infinitesimally small) change in the portfolio holding and time respectively. This approach of considering the expectation of a portfolio is considered in the derivation of our weather derivative PDE in chapter 5. The full derivation of an option valuation model including transaction costs can be found in Leland (1985) or outlined in Wilmott et al. (1995).

3.2.4 Market completeness

When a market has as many independent tradable assets as there are sources of randomness it is said to be *complete*. This is to say that any derivative may be perfectly replicated by the (risky and riskless) assets within the market (Joshi, 2003). As the payoff can be replicated through the construction of a self-financing portfolio (typically using a riskless asset and the underlying), the portfolio set-up cost is taken as the unique arbitrage-free price of the derivative.

If the number of sources of randomness exceeds the number of tradable instruments, then perfect replication is no longer possible. Here, the market is referred to as an *incomplete* one. This further implies that the sources of randomness are not hedgable, resulting in risk remaining in the portfolio. In fact, all markets are somewhat incomplete as many of the underlying assumptions underpinning pricing models do not hold in reality.

The underlying quantities of a weather-based security, such as temperature or rainfall, are not traded and, additionally, weather derivatives themselves are not traded with enough liquidity for constructing a delta-hedged portfolio. Hence there exists no self-financing replicating portfolio that is equivalent to the value of the contingent claim. Yet, replicating portfolios are not completely irrelevant as through them we can infer bounds on option prices.

3.2.5 Market price of risk

Given that risk cannot be completely eliminated in an incomplete market we must infer the monetary value per unit risk for the source of randomness, which is referred to as the *market price of risk*. In other words, the risk exposure is expressed in monetary terms. If we assume that the underlying process, S_t, follows GBM (3.4), we typically denote λ as

$$\lambda = \frac{\mu(S_t, t) - r}{\sigma(S_t, t)}. \tag{3.13}$$

where $\mu(S_t, t)$ and $\sigma(S_t, t)$ represent the drift and volatility of S at time t. The financial interpretation of the equation above is that it describes the excess return above the risk-free rate r per unit of volatility that we expect to receive in return for holding a risky asset S. In the spirit of pricing a weather derivative, this parameter is the market price of risk of temperature. Hull (2006) provides a helpful description of (3.13), by firstly rewriting (3.13) as

$$\lambda\sigma(S_t, t) = \mu(S_t, t) - r, \tag{3.14}$$

and stating that the left-hand side (LHS) of (3.14) is multiplying the quantity of temperature risk by the associated price of that risk. The RHS is the expected level of return in excess of the risk-free interest rate that is required to compensate

for this risk.

An excellent and elegant interpretation of this unknown function λ is provided by Wilmott et al. (1995). The explanation is set in the context of an incomplete market problem by valuing a derivative on a (non-traded) stochastic interest-rate, r_t, given by

$$\mathrm{d}r_t = \mu(r_t, t)\mathrm{d}t + \sigma(r_t, t)\mathrm{d}W. \tag{3.15}$$

By following an appropriate hedging strategy[1] the one-factor bond price V satisfies the following PDE

$$\frac{\partial V}{\partial t} + \Big(\mu(r_t, t) - \sigma(r_t, t)\lambda(r_t, t)\Big)\frac{\partial V}{\partial r} + \frac{1}{2}\sigma^2(r_t, t)\frac{\partial^2 V}{\partial r^2} - r_t V = 0, \tag{3.16}$$

where $\lambda(r_t, t)$ denotes the market price of interest rate risk. Next, consider holding a *naked* bond position, i.e. hold just the bond and do not attempt to hedge this position, $\Pi = V$. Using Itô's lemma, the variation of the the bond is simply

$$\mathrm{d}V = \left(\frac{\partial V}{\partial t} + \mu(r_t, t)\frac{\partial V}{\partial r} + \frac{1}{2}\sigma^2(r_t, t)\frac{\partial^2 V}{\partial r^2}\right)\mathrm{d}t + \sigma(r_t, t)\frac{\partial V}{\partial r}\mathrm{d}W. \tag{3.17}$$

Clearly this portfolio is not riskless, due to the presence of $\mathrm{d}W$. Now, rearrange equation (3.16) so that

$$\frac{\partial V}{\partial t} + \mu(r_t, t)\frac{\partial V}{\partial r} + \frac{1}{2}\sigma^2(r_t, t)\frac{\partial^2 V}{\partial r^2} = r_t V + \sigma(r_t, t)\lambda(r_t, t)\frac{\partial V}{\partial r}. \tag{3.18}$$

Substituting (3.18) into (3.17) and rearranging leads to

$$\mathrm{d}V - r_t V\mathrm{d}t = \sigma(r_t, t)\frac{\partial V}{\partial r}(\lambda(r_t, t)\mathrm{d}t + \mathrm{d}W_t). \tag{3.19}$$

In this form, it is clear that the LHS is the change in overall wealth from holding the bond, as $\mathrm{d}V$ is the change in bond investment, and $rV\mathrm{d}t$ is the cost of borrowing the money to finance this bond purchase (hence the negative sign). The RHS may be interpreted as the excess return above the risk-free rate that is awarded for accepting risk. Therefore, for each unit of extra risk, $\sigma(r_t, t)$, the portfolio gains (in expectation) an extra profit $\lambda\mathrm{d}t$.

[1] Holding a portfolio containing two bonds, with different maturity dates, such that $\mathrm{d}\Pi = V_1(r_t, t : T_1) - \Delta V_2(r_t, t; T_2)$, where $T_1 < T_2$.

When dealing with a traded asset, it is possible to construct a hedge that will remove risk $\mathrm{d}W$, making the investors indifferent to risk (often known as *risk-neutral*). In other words, the rate of return on the asset is equal to the risk-free rate, i.e. $\mu = r$, which leads to $\lambda = \frac{\mu - r}{\sigma} = 0$. We are then left with a standard Black-Scholes type PDE. In the case where the asset is not traded, the market price of risk denotes the compensation the investor expects for taking on non-diversifiable risk. The exact amount of compensation varies depending on an investor's attitude towards risk and, as stated by Joshi (2003) and Ibáñez (2005), λ may no longer be unique. Calibration is used to infer the value of λ, and limited investigations have been conducted by Alaton et al. (2002) and Bellini (2005) in the context of weather derivatives pricing. However, limited datasets used by the previously mentioned works restrict the usefulness of the derived value of λ. In chapter 7 we make no attempt to use real-world market prices to determine λ, but do investigate its impact on pricing by choosing a range of different values.

Alternatively, ideas from expectation theory can be applied to provide further insights. Introduce P to represent the total wealth created from holding the naked bond. So, write the LHS of (3.19) as

$$\mathrm{d}P(t) = \mathrm{d}V - rV\mathrm{d}t. \tag{3.20}$$

Thus,

$$\mathrm{d}P(t) = \sigma\frac{\partial V}{\partial r}\mathrm{d}W_t + \sigma\lambda\frac{\partial V}{\partial r}\mathrm{d}t. \tag{3.21}$$

Then write this in the stochastic integral form as in (3.1), to obtain

$$P(t) = P_0 + \int_0^t \sigma\frac{\partial V}{\partial r}\mathrm{d}W_t + \int_0^t \sigma\lambda\frac{\partial V}{\partial r}\mathrm{d}u, \tag{3.22}$$

with $P_0 = 0$. Now taking expectations (under real-world measure $\mathbb{P}$), and using the definition from Itô's integral means that

$$\mathbb{E}^{\mathbb{P}}\left[\int_0^t \sigma\frac{\partial V}{\partial r}\mathrm{d}W\right] = 0, \tag{3.23}$$

then leads to

$$\mathbb{E}^{\mathbb{P}}[P(t)] = \mathbb{E}^{\mathbb{P}}\left[\int_0^t \sigma\lambda\frac{\partial V}{\partial r}\mathrm{d}u\right]. \tag{3.24}$$

When $\lambda = 0$, this implies no compensation is provided for risk taking and therefore the expected profit is given by

$$\mathbb{E}^{\mathbb{P}}[P(t)] = 0. \tag{3.25}$$

However, for $\lambda > 0$ the expected profit is now non-zero as the investor is being compensated for the risk under-taken

$$\mathbb{E}^{\mathbb{P}}[P(t)] = \mathbb{E}^{\mathbb{P}}\left[\int_0^t \sigma\lambda\frac{\partial V}{\partial r}\mathrm{d}u\right] > 0. \tag{3.26}$$

3.2.6 The Hedging Error and Pricing Bounds

As stated in §3.2.3 in our discussion on delta hedging, in an incomplete market attempts using a given trading strategy $h(t)$ to hedge the derivative $V(t)$ with a portfolio holding $\Pi(t)$ cannot totally eliminate risk. This hedging error $Y(t)$ is then given by

$$Y(t) = \Pi(t) - V(t). \tag{3.27}$$

To remain arbitrage-free, the hedging error $Y(t)$ can be neither strictly positive nor strictly negative, otherwise, if $Y(t)$ were strictly positive, an investor could implement the trading strategy h that gains $\Pi(t)$ and then short the derivative, making a riskless profit of $\Pi(T) - V(T)$. Notice that if $Y(t)$ is always positive, we say that the portfolio Π dominates the option price $V^-(t)$, implying that its value is always at least larger than the derivative's payoff. Similarly when $Y(t) < 0$, the hedging portfolio is bounded above by $V^+(t)$, which leads to the following inequality

$$V^-(t) < \Pi(t) < V^+(t). \tag{3.28}$$

In the case where perfect hedging is possible, the value of the portfolio is equal to the value of the derivative.

3.3 Utility theory

This section does not attempt to summarise the area of utility theory, but is included since this is an alternative approach used in the literature to solve incomplete market problems. The theory arose as the solution to the St. Petersburg[2] paradox which was first stated by Nicolas Bernoulli in 1713. It was his cousin Daniel Bernoulli who provided the resolution which involved the explicit introduction of a utility function, and expected utility hypothesis, and the notion of diminishing marginal utility of money. A full discussion of the problem can be found in Durand (1957) and Samuelson (1977).

The main idea behind the use of utility theory is beautifully expressed by Daniel Bernoulli:

> The determination of the value of an item must not be based on the price, but rather on the utility it yields...There is no doubt that a gain of one thousand ducats is more significant to the pauper than to a rich man though both gain the same amount.

The basic idea of utility theory is that every level of wealth has a level of utility to the holder of that wealth. Writing the wealth as w and the utility as u we have $u = u(w)$. The function $u(w)$ describes one person's (or organisation's) risk preferences. Decisions are then made on the basis of the expected utility, where expectations are calculated over all possible values of w. If the probabilities of different levels of wealth lead to one decision having a higher expected utility than another, then it is to be preferred. If the expected utilities are the same, then we are indifferent.

There are a number of properties that utility functions are usually required to have to give a reasonable representation of real attitudes to risk (Jewson et al., 2005):

[2]The paradox poses the question of 'what is the fair price to enter a game, where you win 2^{k-1} dollars if the coin is tossed k times until the first tail appears?' The paradox lies in the fact that the expected value payoff is

$$\mathbb{E} = \sum_{k=1}^{\infty} \frac{1}{2} = \infty.$$

So a player should pay any amount since in the long run he can win a very large payout.

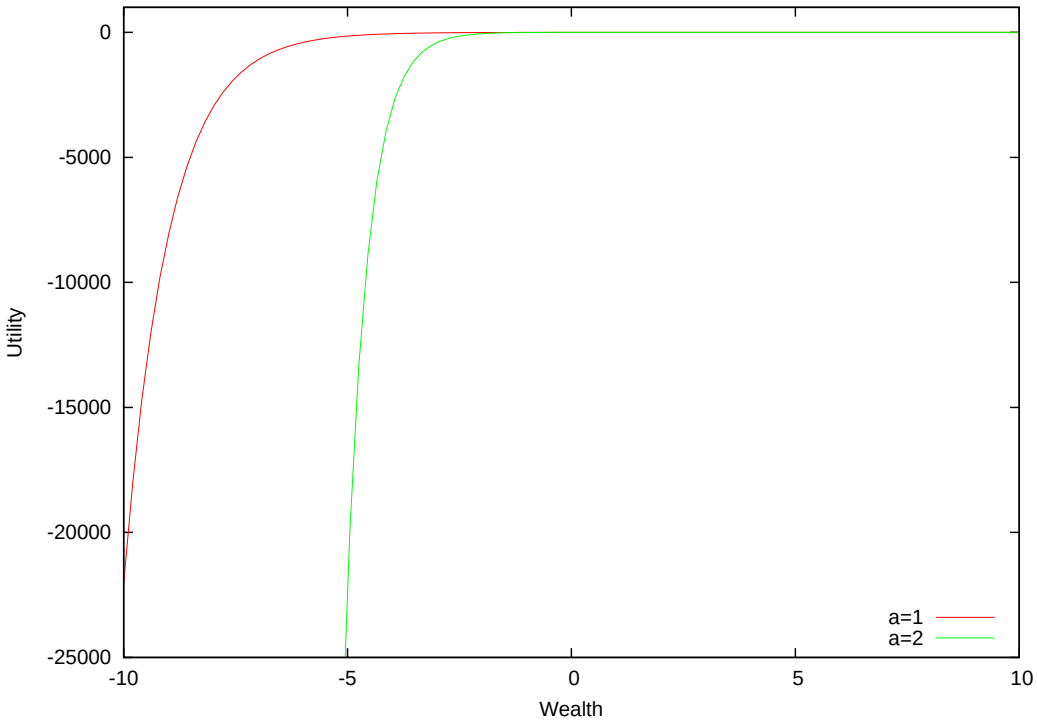

Figure 3.1: A depiction of the utility function (3.29), which could be used to describe someone's impression on how increases in wealth will improve utility. Two examples are show here for different levels of risk-aversion. A more risk averse investor's utility function is denoted by the green line (where $a = 2$), while the less risk averse person has utility represented by the red line ($a = 1$).

1. Wealth preference: more wealth is always better. An investor never believes that they have so much wealth that getting more would not be at least a little bit desirable. Therefore the first derivative $\frac{\mathrm{d}u}{\mathrm{d}w} > 0$.

2. Risk aversion: the marginal utility of wealth decreases as wealth increases, therefore the utility function is concave. To see why this is, consider someone who already has a million pounds, obtaining one more pound is almost meaningless. Hence $\frac{\mathrm{d}^2u}{\mathrm{d}w^2} > 0$.

The popular definition of the utility function with these properties is the so-called *exponential utility* function

$$u(w) = 1 - e^{-aw}, \tag{3.29}$$

where a is a positive parameter and measures the risk-aversion. Figure 3.1 shows this utility function for two different risk-aversion levels, 1 and 2. It clearly shows that the increase of utility diminishes the wealthier the person becomes. Utility

functions of this form have been discussed in valuing executive stock options by Henderson (2005), as even though the executive can invest in options and stocks in the market, he is restricted to investing in own-company stocks which leaves him subject to firm-specific risk. Other such forms exist, such as the power utility function. Henderson (2002) uses both power and exponential utility functions to compute the hedging strategy and price of an option on nontraded assets. Cao and Wei (2000) consider using utility theory in pricing weather derivative contracts. Given that each investor's view on risk differs, there will not be a unique utility function to describe the market and therefore this leads to varying determinations of price depending on risk appetite. Moreover, practitioners are unaware of the exact shape of their utility function and it is not an instructive approach, in that an answer is obtained but how that price arises is difficult to determine (Otaka and Kawaguchi, 2002).

3.4 Quadratic Hedging

Delta hedging strategies (3.2.3) are often used in a complete market setting. However, the idea of hedging used in such strategies is to minimise one's exposure to risk, whereas in the derivation of the BSM, the objective was to eliminate the variance of the portfolio: making it risk-free. This, in summary, is known as a form of *quadratic hedging* where the size of risk is constrained. This approach is classified into *variance-minimising hedging* and *risk-minimising hedging*.

3.4.1 Variance-minimising hedging

Variance-minimising hedging was first developed by Schweizer (1996). This approach involves minimising the tracking error of a self-financing portfolio (see (3.6)), against the terminal value of a derivative. Let $V(t)$ model the value of a derivative and follow the same notation from §3.2.1, such that the trading gain induced by following trading strategy $h(t)$ is denoted $\Pi(t)$. Assuming constant interest rate r, the total loss at $t = T$ to a hedger is therefore given as

$$V(T) - \Pi(T) - ce^{rT}, \tag{3.30}$$

with initial capital c invested. As an example, if we consider the specific case of hedging in the *mean-variance* sense, this amounts to solving the optimisation problem

$$\text{minimise} \quad \mathbb{E}\Big[(V(T) - \Pi(T) - ce^{rT})^2\Big] \quad \text{over all strategies} \quad h, \tag{3.31}$$

and has been studied by Pham, Rheinländer, and Schweizer (1998).

3.4.2 Risk-minimisation

In risk-minimising hedging, which is introduced by Föllmer and Sondermann (1985), funds are allowed to be injected or withdrawn from the portfolio in order that the cash flow movements in the underlying instrument and contingent claims are approximately equal. The ability to inject or withdraw funds violates the self-financing property (3.7). The amount of capital invested or withdrawn is denoted by a cost process $C(t)$. Consider a European call option V, with strike K and payoff $V(T) = (X(T) - K)^+$. Here, we assume that $X(T)$ is the observed value of a non-traded quantity at expiry. The accumulated gain Π is

$$\Pi(t) = \int_0^T h(t)\mathrm{d}X(t), \tag{3.32}$$

and we can define an associated cumulative cost process $C(t)$ such that

$$C(t) = V(t) - \Pi(t). \tag{3.33}$$

When performing risk-minimising hedging, the problem is to minimise the remaining risk. The exact element of risk to minimise is varied and Schäl (1994) specifies the following measures of risk for the accumulated cost:

(i) the local conditional risk $\mathbb{E}[(C(t+1) - C(t))^2]$,

(ii) the conditional remaining risk $\mathbb{E}[(C(T) - C(t))^2]$,

(iii) the total risk $\mathbb{E}[(C(T) - C(0))^2]$.

Using (i) amounts to minimising the risk between incremental time-steps. This is equivalent to the case in the BSM world, where Δ is chosen so that $Var[\mathrm{d}\Pi] = 0$.

The second statement (ii) implies that the remaining risk from T to t is minimised. This actually means that we assume that at time t one no longer cares about the past and only considers the total future risk. Another way to look at this, is that even if we have lost money in time before t we are simply trying to suppress the damage going forward. Lastly, statement (iii) attempts to reduce the risk by investing a sufficient amount upfront such that $Var[C(T) - C(t)] = 0$.

3.5 An example: Illiquid option with stochastic volatility

To see how the ideas from the above sections can be utilised, we next provide a derivation for the valuation of an option whose asset's volatility is stochastic, and for which the option itself is not liquidly traded.

It can be argued that volatility in practice varies stochastically (Hull, 2006). The incorporation of stochastic volatility in asset processes originates from Hull and White (1987). Assuming that the asset S_t follows GBM, whose variance σ_t is a stochastic mean-reverting process, such that

$$\begin{aligned} \mathrm{d}S_t &= \mu S_t \mathrm{d}t + \sqrt{\sigma_t} S_t \mathrm{d}Z_t, & (3.34) \\ \mathrm{d}\sigma_t &= \kappa(\theta_\sigma - \sigma_t)\mathrm{d}t + \nu \sigma_t^\alpha \mathrm{d}W_t^*. & (3.35) \end{aligned}$$

The drift term of the asset S_t is given by μ and is assumed constant. For the stochastic volatility term the mean reversion rate is κ, θ_σ denotes the reversion level and ν is the volatility of volatility. The two Wiener processes $\mathrm{d}Z_t$ and $\mathrm{d}W_t^*$ are correlated, such that

$$\mathrm{d}Z_t \mathrm{d}W_t^* = \rho \mathrm{d}t. \tag{3.36}$$

where ρ measures the correlation and

$$\mathrm{d}W_t^* = \rho \mathrm{d}Z_t + \sqrt{1-\rho^2}\mathrm{d}W_t. \tag{3.37}$$

Here $\mathrm{d}W_t$ and $\mathrm{d}Z_t$ are two orthogonal Brownian motions, so that $\mathbb{E}(\mathrm{d}W_t \mathrm{d}Z_t) = 0$. Pricing an option on an asset with stochastic volatility introduces another source of uncertainty, yet it is still a complete market problem since it is possible to create

a hedging portfolio (an outline can be found in Joshi, 2003). This additional source of risk can also be diversified provided that we allow ourselves to trade in a second option, for hedging purposes. Essentially we hedge the option with the underlying (as usual) and a second option in such a way that both the Delta and Vega (the sensitivity of the portfolio value to volatility (Joshi, 2003)), of the portfolio are both zero. This is known as *Vega-hedging*. A complete derivation of the associated PDE can be found in the excellent book *The concepts and practice of mathematical finance* by Joshi, 2003.

Market completeness breaks down if we assume that the option market is illiquid so it is not possible to trade in the second option, as doing so may be extremely costly. In this setting we face an incomplete market problem where the volatility risk cannot be Vega hedged. Consider that $C(S, \sigma, t)$ is an option dependent an asset S_t with stochastic volatility σ_t, which follow the dynamics given by (3.34), but with a volatility structure as defined in Heston (1993) (i.e. $\alpha = 1/2$ in (3.35)):

$$\mathrm{d}\sigma_t = \kappa(\theta_\sigma - \sigma_t)\mathrm{d}t + \nu\sqrt{\sigma_t}\mathrm{d}W_t^*. \tag{3.38}$$

This model permits negative volatilities since as the volatility approaches zero, the volatility of volatility becomes large. From Itô's lemma, the change in the option $C(S, \sigma, t)$ is given by

$$\mathrm{d}C = \frac{\partial C}{\partial t}\mathrm{d}t + \frac{\partial C}{\partial S}\mathrm{d}S_t + \frac{\partial C}{\partial \sigma}\mathrm{d}\sigma_t + \frac{1}{2}\frac{\partial^2 C}{\partial \sigma^2}\mathrm{d}\sigma_t^2 + \frac{\partial^2 C}{\partial S \partial \sigma}\mathrm{d}S_t\mathrm{d}\sigma_t + \frac{1}{2}\frac{\partial^2 C}{\partial S^2}\mathrm{d}S_t^2. \tag{3.39}$$

Substituting (3.34) and (3.38) into the equation above and simplifying gives

$$\begin{aligned}\mathrm{d}C &= \left(\frac{\partial C}{\partial t} + \mu S_t\frac{\partial C}{\partial S} + \kappa(\theta_\sigma - \sigma_t)\frac{\partial C}{\partial \sigma_t} + \frac{1}{2}\nu^2\sigma_t\frac{\partial^2 C}{\partial \sigma^2} + \nu\sqrt{\sigma_t}S_t\rho\frac{\partial^2 C}{\partial S\partial\sigma} + \frac{1}{2}\sigma_t S_t^2\frac{\partial^2 C}{\partial S^2}\right)\mathrm{d}t \\ &+ \sqrt{\sigma_t}S_t\frac{\partial C}{\partial S}\mathrm{d}Z_t + \nu\sqrt{\sigma_t}\frac{\partial C}{\partial \sigma}(\rho\mathrm{d}Z_t + \sqrt{1-\rho^2}\mathrm{d}W_t).\end{aligned} \tag{3.40}$$

Inspired by Ibáñez (2005), a portfolio can be constructed such that

$$\Pi = C - \Delta S \tag{3.41}$$

with instantaneous variation

$$\mathrm{d}\Pi = \mathrm{d}C - \Delta\mathrm{d}S. \tag{3.42}$$

Various strategies are available to hedge this portfolio. Ibáñez (2005) showed that the source of randomness associated with the asset S can be removed by setting Δ as

$$\Delta = \frac{\partial C}{\partial S} + \frac{\nu\rho\frac{\partial C}{\partial \sigma}}{S}. \tag{3.43}$$

However, the risk introduced by the volatility persists, and is referred to as the residual risk:

$$\nu\sqrt{\sigma_t}\frac{\partial C}{\partial \sigma}\sqrt{1-\rho^2}\mathrm{d}W_t. \tag{3.44}$$

The question is: how does one price and hedge this random payoff? Numerous techniques exist, and we noted the use of utility functions in §3.3. Another technique is capturing the market price of risk. Møller (2001) mentions how premiums are typically added for unhedgable risk, because the option writer should be compensated for not being able to diversify their risk. The chosen approach of Windcliff, Wang, Forsyth, and Vetzal (2007), and Ibáñez (2005) is to state that during each time interval the portfolio should earn a premium at a rate proportional to its instantaneous standard deviation. Using our notation, this is

$$\mathbb{E}[\mathrm{d}\Pi] = r\Pi\mathrm{d}t + \lambda\sqrt{\frac{Var[\mathrm{d}\Pi]}{\mathrm{d}t}}\mathrm{d}t. \tag{3.45}$$

Take the option variation (3.40), (3.42) and (3.43) and substitute into (3.45). This yields

$$\mathbb{E}[\mathrm{d}\Pi] = r\Pi\mathrm{d}t + \nu\sqrt{\sigma_t}\left|\frac{\partial C}{\partial \sigma}\right|\sqrt{1-\rho^2}. \tag{3.46}$$

The same approach of observing the expectation of portfolio growth was adopted by Leland (1985) (which we demonstrated in §3.2.3), and this description of being compensated per unit of risk is consistent with the definition of the market price of risk (3.19).

3.6 Summary

This chapter has presented the essential mathematical tools and concepts that are used throughout this thesis. The principles of *mean-self financing* has been introduced and also how pricing equations may be derived for options on illiquid assets is illustrated. This has been included since weather derivatives contracts are illiquid and operate in an incomplete market.

The next chapter provides an extensive overview of the current state of models and numerical approaches that have been proposed within the weather derivatives literature.

Chapter 4

Weather derivatives' models and pricing approaches

The trouble with weather forecasting is that it's right too often for us to ignore it and wrong too often for us to rely on it.

Patrick Young

This chapter completes the framework necessary to value derivatives whose underlying is temperature. Detailed descriptions of the fundamental models are provided, and a discussion of their respective strengths and weaknesses is included. Popular pricing approaches for the valuation of weather derivatives are then presented, namely *burn analysis*, *index modelling* and *daily simulation* (Jewson et al., 2005). This chapter forms the foundation for valuation of weather-based contingent claims that will be used throughout the thesis.

4.1 Temperature models

Modelling of temperature can be split into two classes:

1. modelling the distribution of the weather settlement index
2. modelling the true weather process and using it to construct the index distribution.

This is further broken down by Jewson et al. (2005) into finding a statistical model for one of the following:

- measured values of a daily temperature, $X(t)$;
- measurement of an average daily temperature, which we defined previously as
$$X(t) \equiv \frac{X_{max}(t) + X_{min}(t)}{2}; \tag{2.1}$$
this approach also requires us to model $X_{max}(t)$ and $X_{min}(t)$;
- the daily movements of the underlying weather index, see §4.2;
- the distribution of the final weather settlement index, which we examine in §4.3.3.

Each approach has its merits and has been applied in the valuation of weather-based contracts. In the following sections we explore these models for the underlying variable.

As mentioned in §2.1.2, contracts on temperature are the most frequently traded and so we choose to focus our analysis on temperature derivatives. The modelling of this weather variable has been widely discussed and previous work may be split into two groups: stochastic differential equations which model the dynamics, and another group which utilise time series. In the following section, we review various temperature models found in the weather derivatives literature.

4.1.1 Stochastic differential temperature models

Temperature dynamics can be characterised by four components (Alaton et al., 2002):

1. Seasonality;
2. Existence of long-term trends;
3. Randomness;
4. Mean reversion.

Temperature exhibits seasonal patterns and often reverts to a mean whose value is dependent on the time of year. Additionally, we observe that temperature does not grow/fall indefinitely. A well defined model should incorporate these characteristics. An appropriate choice would be an OU process of the form (3.5), and consequently much of the weather derivatives literature generally specifies the change in the temperature X as (see Dischel, 1998a; Dornier and Queruel, 2000; Alaton et al., 2002; Jewson et al., 2005, for example)

$$\mathrm{d}X_t = \kappa(t)\left[\theta(t) - X_t\right]\mathrm{d}t + \sigma(t)\mathrm{d}W_t. \tag{4.1}$$

The parameter $\kappa(t)$ is the speed the temperature reverts to its seasonal mean $\theta(t)$, and the volatility of temperature variations is expressed by $\sigma(t)$ and is assumed to be a deterministic function. Here it is assumed that the drift and standard deviation are functions of time t, but this need not be precisely the case. Since temperature exhibits seasonal patterns, the model reverts to a time-dependent mean level $\theta(t)$. The forms of $\theta(t)$, $\sigma(t)$ and $\kappa(t)$ are determined from analysis of historical temperatures (see §5.4).

4.1.2 Dischel (1998a) two parameter model

The most basic temperature model used to value weather contracts is the two parameter model presented by Dischel (1998a), where the temperature follows an OU process of the form (4.1), and the speed of mean-reversion κ is assumed constant. Furthermore, rather than using the seasonal mean $\theta(t)$, Dischel (1998a) suggests that the temperature on any given day is expected to revert back to the historical average temperature experienced on that day in the past. More precisely, for example, the historical average temperature of January 1st is computed by taking the average of all the recorded values on January 1st for each year in the sample set. The daily historical average temperature is denoted by $\bar{X}_t$:

$$\bar{X}_t = \frac{1}{N}\sum_{yr}^{N} X_{yr,t} \tag{4.2}$$

where $X_{yr,t}$ denotes the historical temperature taken from the yrth year from the sample set, on date t. Here $yr = 1, 2, \ldots, Y$ and Y is the total number of years in the sample. The number of years of data used to compute the average (here

denoted N) was not stated in Dischel (1998a), but since weather trends are slow-moving, averaging using all available data in the sample could be appropriate (hence $N = Y$). This gives rise to following temperature model,

$$\mathrm{d}X_t = \kappa \left[\bar{X}_t - X_t\right] \mathrm{d}t + \sigma(t)\zeta_1 \mathrm{d}W_{1,t} + \sigma(t)\zeta_2 \mathrm{d}W_{2,t} \tag{4.3}$$

where $W_{1,t}$ and $W_{1,t}$ are two Wiener processes, where the former drives the temperatures X_t and latter is alleged by (Bellini, 2005) to capture the high auto-correlation between consecutive days of temperature. The distribution of the random variables $\mathrm{d}W_1$ and $\mathrm{d}W_2$ in (4.3) are taken as normal, but in Dischel (1998b) this assumption is relaxed by approximating the distribution using historical data. The factors ζ_1 and ζ_2 are scaling quantities.

4.1.3 Dornier and Querel

Dornier and Queruel (2000) criticise Dischel (1998a) approach of using the daily historical average, $\hat{X}_t$, in-place of a seasonality term, $\theta(t)$. They show that Dischel (1998a) SDE model produces a process that in the long run does not revert to the required seasonal mean (this is also shown by Moreno, 2000). In other words, the expected value of the process is not equal to the seasonal mean. The mean-reverting component of (4.4) will make X_t approach $\theta(t)$, however, as X_t begins to tend toward the seasonal mean value, the value of $\theta(t)$ has already changed and so X_t should be approaching a different value. Therefore, to ensure that X_t tends to $\theta(t)$ in the long run (i.e. $\mathbb{E}[X_t] = \theta(t)$), we must account for the seasonal variation $\mathrm{d}\theta(t)$. This led Dornier and Queruel (2000) to propose an SDE process:

$$\mathrm{d}X_t \;=\; \mathrm{d}\theta(t) + \kappa(t)\left[\theta(t) - X_t\right]\mathrm{d}t + \sigma \mathrm{d}W_t, \tag{4.4}$$

where the volatility of temperature, σ, is assumed constant, and the seasonal mean is expressed as a deterministic function with a sine wave:

$$\theta(t) = A + Bt + C\sin(\omega t + \phi) \tag{4.5}$$

with $\omega = 2\pi/365$. The linear term $A + Bt$ in (4.5) captures the phenomena of global warming and/or urbanisation of cities [1], and C denotes the amplitude

[1] Dischel and Observer (2002) highlight the presence of a warming trend in the temperature.

of the sine-function and expresses half the difference in temperature between a typical winter and summer day. From inspecting figure 4.1, it is apparent that the maximum and minimum temperatures do not occur precisely on the 1st January and 1st July respectively; therefore, Dischel and Observer (2002) introduce a phase angle ϕ (i.e a shift) to capture correctly the seasonal mean. The term $\mathrm{d}\theta(t)$ in (4.4) expresses the seasonal variation and is included to ensure that the process tends to the seasonal mean in the long run (see A.2).

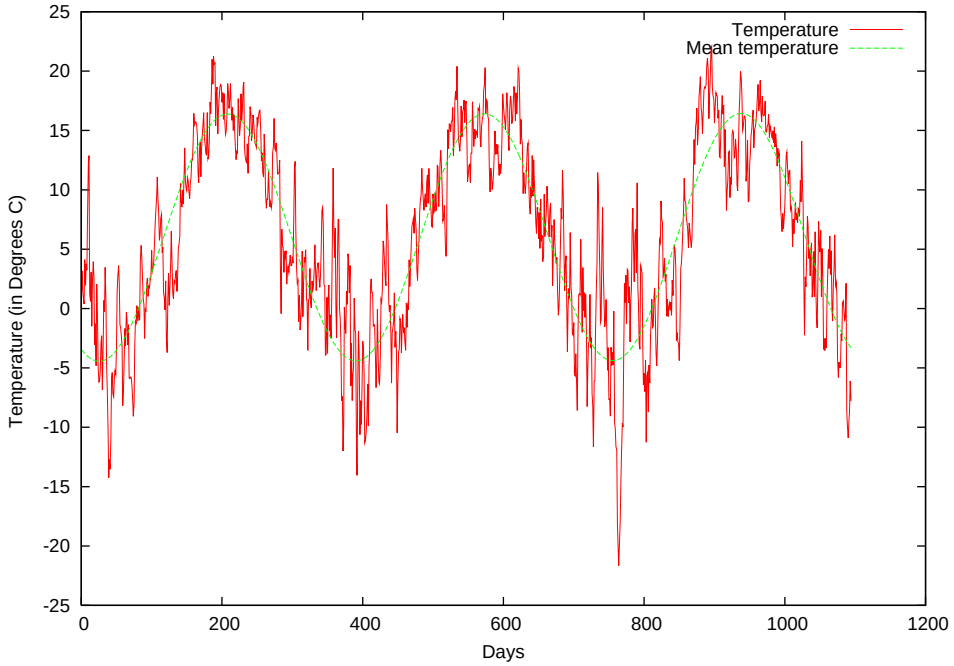

Figure 4.1: A comparison of the estimated seasonal mean as defined by (4.5) and the actual temperature data observed at London Heathrow from 1996 to 1999. Here the x-axis starts from January 1st 1996 (day 0).

4.1.4 Alaton et al. (2002) enhanced model

Alaton et al. (2002) extended the models of Dischel (1998a,1998b) and Dornier and Queruel (2000). Alaton et al. (2002) use the same temperature SDE process as given by equations (4.4) and (4.5), but model the monthly variation in the

variance of temperature, as a piecewise constant function:

$$\sigma(t) \quad = \quad \begin{cases} \sigma(1) & \text{during January} \\ \sigma(2) & \text{during February} \\ \vdots & \\ \sigma(12) & \text{during December} \end{cases}, \tag{4.6}$$

This change in specification of the volatility was observed when Alaton et al. (2002) considered 40 years of daily average temperature data at Bromma airport, Stockholm. Alaton et al. (2002) observed that the quadratic variation (see Appendix A.1 for definition) σ^2 of the temperature in the dataset is nearly constant over each month, though it varies for different months in a year.

Similar to Dornier and Queruel (2000), Alaton et al. (2002) argue that choosing a Wiener process as the driving noise in the SDE (4.4) is appropriate since temperature differences are close to being normally distributed. Alaton et al. (2002) however, admit that "the probability of getting small differences in the daily mean temperature will be slightly underestimated." To observe this, a histogram of the daily temperature differences in London Heathrow is computed using the online statistic software of Wessa (2010). In figure 4.2 the shapes of the computed histogram is compared with a normal distribution. Qualitatively, the figure suggests that the normal distribution underestimates the probability of small differences in temperature. A Q-Q plot of the quantiles of the observed daily differences in the temperature data versus the theoretical quantiles from a normal distribution is presented in figure 4.3 in order to graphically measure the goodness of fit. The solid straight line represents the theoretical quantile values if the data was perfectly normally distributed. The figure shows that the observed data falls approximately along the theoretical line, but there is evidences of departure from normality since it does not fall on the line for each quantile. To quantitatively test for normality we use the Jarque-Bera test (Ruppert, 2010). This test compares the estimated skewness and kurtosis the values expected under normality, which are 0 and 3 respectively. The test statistic is given as

$$JB = \frac{n}{6}\left(Sk^2 + \frac{(Kur-3)^2}{4}\right), \tag{4.7}$$

where Sk and Kur represent the skewness and kurtosis respectively. From the

Parameter	Estimated Value	Standard Deviation
Mean	0.0066	0.02611
Standard deviation	1.9602	0.01846
Skewness	-0.7476	N/A
Kurtosis	53.2510	N/A
Jarque-Bera	109.16	N/A

Table 4.1: The characteristics of the distribution of the daily temperature differences observed at London Heathrow between 1995 to 2010. It reports the mean, standard deviation, skewness, kurtosis, and the Jarque-Bera statistic. Here we omit stating the confidence intervals as they are not central to the argument.

value of the test statistic reported in table 4.1 it is evident that the sample is not precisely normally distributed since JB is not zero. This is mainly due to the large kurtosis value of the daily temperature differences distribution. Our findings are consistent with Alaton et al. (2002).

However, although the observed temperature differences at London Heathrow are not precisely normally distributed we simplify our modelling specifications by using a standard Wiener process as it allows mathematical tractability. The assumption of normality is very much dependent on the dataset. For example, Benth and Šaltytė-Benth (2005) note that in several Norwegian locations, the use of non-normal models should be preferred (more details are provided in §4.1.7).

Minor extension to Alaton et al. (2002) model

Schiller et al. (2008) propose a minor extension to the Alaton et al. (2002) model, by suggesting that the seasonality trend is generally stronger in the winter than in summer. This gives rise to the following altered seasonal component:

$$\theta(t) = A + Bt + C\sin(\omega t + \phi) + Dt\cos(\omega t + \phi), \tag{4.8}$$

where A, B, C, ω and ϕ are the same as defined in (4.5), and $Dt\cos(\omega t + \phi)$ captures the additional seasonality trend that is greater in the winter.

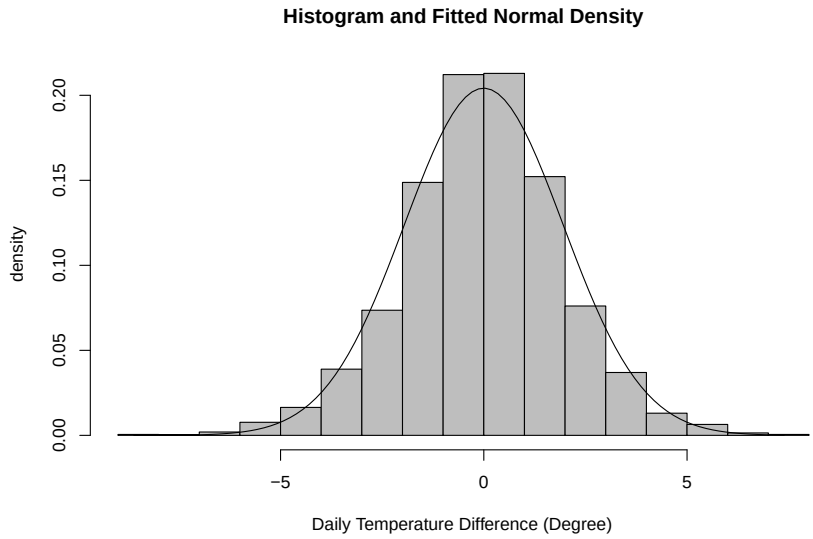

Figure 4.2: The figure plots the histogram of the differences of the daily average temperature using the data from London Heathrow from 1995 to 2010. The solid line represents the density curve of a theoretical normal random variable with mean and standard deviation estimated from the time series. The supporting statistics can be seen in table B.1 and the mean and standard deviation is given in table Appendix 4.1.

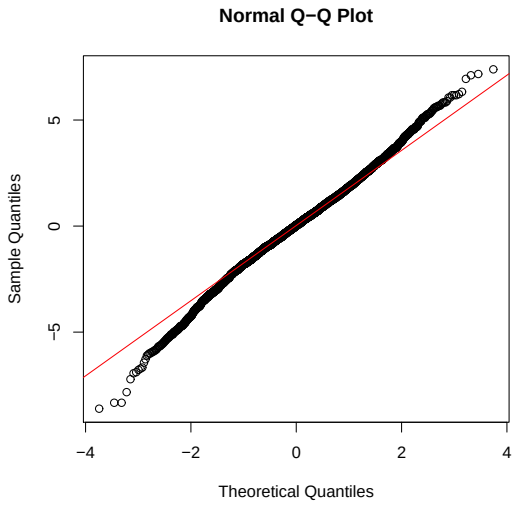

Figure 4.3: The figure displays a QQ-plot of the quantile of the observed temperature at London Heathrow versus theoretical quantiles from a normal distribution.

4.1.5 Benth and Benth (2007) model

Motivated by empirical results, Benth and Benth (2007) suggest using a truncated Fourier series to express both the seasonality component $\theta(t)$ and the daily volatility of temperature variation $\sigma(t)$. The processes are given by

$$\mathrm{d}X_t = \mathrm{d}\theta(t) + \kappa\left[\theta(t) - X_t\right]\mathrm{d}t + \sigma(t)\mathrm{d}W_t. \tag{4.9}$$

and

$$\theta(t) = A + Bt \quad + \quad \sum_{i=1}^{I_1} A_i \sin\left(\omega i t + \phi\right) + \sum_{j=1}^{J_1} B_j \cos\left(\omega j t + \phi\right), \tag{4.10}$$

$$\sigma^2(t) \quad = \quad C + \sum_{i=1}^{I_2} C_i \sin\left(\omega j t\right) + \sum_{j=1}^{J_2} D_j \cos\left(\omega j t\right). \tag{4.11}$$

The meanings of the parameters, A, B, ω, and ϕ that appear in equations (4.9) - (4.11) are identical to those described in Alaton et al. (2002) model (see §4.1.3, equation (4.5)).

The Benth and Benth (2007) model differs from Dischel (1998a) and Alaton et al. (2002) since volatility is specified as being time-varying and also seasonal. Using historical temperature observations from Stockholm, from 1961 to 2004, they fit the seasonal component $\theta(t)$ to the data using the method of least squares. Benth and Benth state that it is sufficient to capture the seasonality of the temperature and its variance by setting $I_1 = 1, J_1 = 1, I_2 = 4$ and $J_2 = 4$.

4.1.6 Mraoua (2009) two factor model

The two factor model of Mraoua (2009) is a natural extension of previous models, and attempts to more closely fit historical temperature. This is achieved by modelling the volatility as a stochastic process, σ_t, rather than a (piecewise) constant $\sigma(t)$ as used by Alaton et al. (2002), or as a time-varying quantity (for example Benth and Benth, 2007). This gives the model for temperature evolution

as

$$\mathrm{d}X_t = \mathrm{d}\theta(t) + \kappa\left[\theta(t) - X_t\right]\mathrm{d}t + \sigma_t \mathrm{d}W_t. \tag{4.12}$$

$$\mathrm{d}\sigma_t = \kappa_\sigma\big(\alpha - \sigma_t\big)\mathrm{d}t + \gamma \mathrm{d}W, \tag{4.13}$$

where κ_σ is constant and is the speed of reversion, α is the constant mean volatility value and γ expresses the variance of the volatility and is taken as constant. The parameters κ_σ and γ are estimated from 44 years of daily historical temperature data from Casablanca-Anfa meteorological station in Morocco. The validity of the Mraoua (2009) stochastic volatility model was tested on temperature data during 2004, with satisfactory results claimed (comparing the forecasts to the actual observed temperature).

4.1.7 Fractional Brownian motion model

Brody, Syroka, and Zervos (2002) discourage the use of standard Brownian motion as the driving noise of temperature evolution. They observe, from empirical studies, that temperature dynamics exhibits long-range temporal dependencies, which means that the present weather condition is influenced significantly by recent weather conditions. After examining UK data from 1772 to 1999, Brody et al. (2002) found clear signs of fractional behaviour in temperature fluctuations and suggested substituting the standard Brownian motion with a fractional Brownian motion (FBM) $W^H(t)$. Regular Brownian motion increments are independent, whereas FBM increments are dependent. The dependence between increments means that if there is an increasing pattern in the previous time, then it is likely that the current step will also be increasing. A FBM is characterised by the Hurst exponent $H \in (0, 1)$ (see Hurst, 1951), which determines the sign and the extent of correlation. Depending on the value of H different types of process are obtained:

1. for $\frac{1}{2} < H < 1$ the process has a long memory;
2. for $0 < H < \frac{1}{2}$ the process is said to be 'antipersistent';
3. for $H = \frac{1}{2}$ the process has short memory (this represents a standard linear Brownian motion).

The specified model is then given by

$$\begin{aligned} \mathrm{d}X_t &= \mathrm{d}\theta(t) + \kappa(t)\left[\theta(t) - X_t\right]\mathrm{d}t + \sigma(t)\mathrm{d}W_t^H, && (4.14)\\ \sigma(t) &= A + C\sin\left(\omega t + \phi\right). && (4.15) \end{aligned}$$

where again the parameters A, B, C, ω and ϕ are as defined in (4.5). Brody et al. (2002) assume that volatility is time-varying and seasonal and take the speed of mean-reversion as time-dependent. Discussions of implementation are omitted, however. Further details of FBM and the new calculus used to analyse it can be found in the classic work of Mandelbrot and Van Ness (1968) and in Duncan, Hu, and Pasik-Duncan (2000).

4.2 A stochastic model for weather indices

As weather derivative payoffs are usually explicitly described in terms of the weather accumulation index, a few authors have chosen to model directly the evolution of the index of temperature rather than modelling the seasonal behaviour of temperature itself. It can be safe to ignore seasonality if the index is being observed over short time horizons, say of less than three months. Notably, Davis (2001) and later Turvey (2005) both model the total accumulated weather index (in other words the total value the index has reached over a certain time period m) as a GBM process I_t^m satisfying

$$\mathrm{d}I_t^m = \mu I_t^m \mathrm{d}t + \sigma I_t^m \mathrm{d}W, \tag{4.16}$$

where μ is the drift and σ the standard deviation of the cumulative index. Here the superscript m specifies the time length over which the index is accumulated, for example, if we are concerned with modelling a 3-month HDD index then $m = 3$ (so $m = 0, 1, 2, \ldots, 12$). The solution of the SDE (4.16) is (Neftci, 2000)

$$I_T^m = I_0^m exp\left(\left(\mu - \frac{1}{2}\sigma^2\right)T + \sigma W_T\right). \tag{4.17}$$

Here, I_0^m refers to the total index value that has been obtained after the daily index values have been accumulated after m month(s) have past, I_1^m is the accumulated index value obtained over the same time period m but one year later,

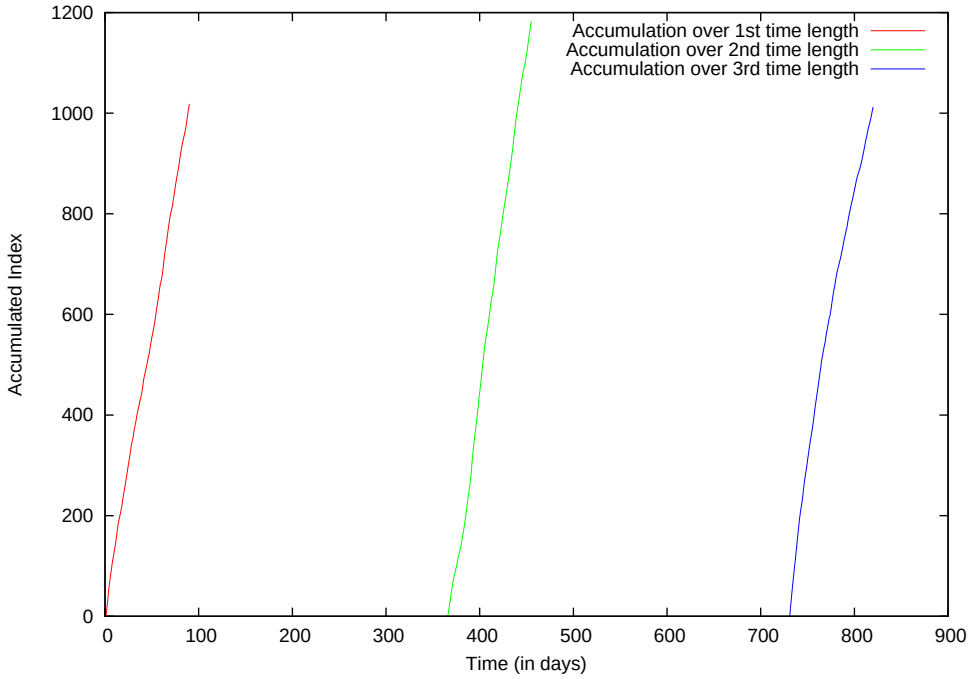

Figure 4.4: An illustration of the accumulated index HDD process over a 3-month time period. The top point of each line represents the values $I(0)$, $I(1)$, $I(2)$. It is these values which are assumed to be log-normally distributed as indicated by (4.17).

and so on.

To illustrate this clearly, over a period of three consecutive years, the London Heathrow temperature data are used to compute the accumulated HDD index value over a three month period, staring from January 1st 1996. The growth of each index is plotted in figure 4.4, where the highest points on the red, green and blue lines represents the accumulated index value of I_0^3, I_1^3, I_2^3 respectively. In modelling the index itself we are more concerned with the index value at the end of the accumulation period, since we are mostly interested in the distribution of the index at the exercise (maturity) time of the derivative, at time m. However, as Davis (2001) rightly states, it would be incorrect to model the whole process $I(t)$, from time 0 to T, as following a GBM because at all times t when the temperature is above X_{ref} the HDD increment is zero, which can certainly not be modelled as Brownian. Our new model, proposed in chapter 5, seems superior to the Davis (2001) approach in that it can directly model, and numerically solve under, the discontinuities intrinsic to the HDD process.

Turvey (2005) uses a similar model to (4.16), but assumes $\sigma(t)$ is time-dependent, and then continues to develop a valuation framework. To account for the tradeless nature of the temperature index, Turvey extends the SDE (4.16) to include the market price of risk of the weather index, as also carried out by Alaton et al. (2002). This modified process becomes

$$\mathrm{d}I_t^m = (\mu - \lambda\sigma(t))I_t^m\mathrm{d}t + \sigma(t)I_t^m\mathrm{d}W, \tag{4.18}$$

where λ is the market price of weather risk of (3.13), and $\lambda\sigma(t)$ is the associated risk premium. Turvey argues that $\lambda = 0$, since weather events are not correlated with the market portfolio that consists of a weighted sum of every asset in the market. By this hypothesis the market price of weather risk is absent or unimportant, which Cao and Wei (2000) appear to corroborate by empirical studies. However if a substantial market price of weather risk does exist, disregarding its impact could severely distort pricing, as was shown computed by Härdle and López Cabrera (2009) and Cao and Wei (2004) and extended by Bellini (2005). Only empirical evidence can test the hypothesis that weather risks are indeed large and undiversifiable. This question is outside the scope of this thesis, but within this thesis we compute in chapter 7 the effect on prices of the market price of weather risk, when its value is assumed to be non-zero.

4.3 Valuation methods

Given the various models outlined to describe the changes in temperature, we next review the current selection of valuation techniques often used to price weather derivatives. Discussions of the methods are provided and so too are numerical results that are then used to benchmark the two proposed models in chapters 5 and 7.

4.3.1 Burn analysis

Burn analysis is often used in the actuarial sciences and presumes that past results can be used to determine future outcomes. Burn analysis examines how the weather derivative would have performed (i.e. its payoff) in previous years,

and then takes an discounted average of these payoffs as the option's value. The simplicity of this method has made it very appealing to practitioners. Suppose we have 100 years of historical temperature data and we wish to determine the fair strike for a swap contract. The fair strike value of a swap contract is the one that gives an expected swap payoff of zero. This will occur when the strike level is equal to the expected weather index value. This is shown with an example below. Consider an uncapped swap with payoff

$$V(I,T) = tick \cdot (I - K), \tag{4.19}$$

where I is the value of a specified index at maturity time, T, K is the strike level, and $tick$ represents the cash value of one value movement in the sum $(I - K)$. Additionally, we assume that the contract is valued under the risk-free rate, r. The fair strike value satisfies

$$\mathbb{E}\big[V(I,T)\big] = 0, \tag{4.20}$$

where on substituting the equation of the payoff (4.19) into (4.20), gives

$$\begin{aligned} \mathbb{E}\left[tick \cdot (I - K)\right] &= 0, \\ tick \cdot (\mathbb{E}[I] - K) &= 0, \\ \text{and so} \quad \mathbb{E}[I] &= K. \end{aligned} \tag{4.21}$$

Additionally,

$$\begin{aligned} \mathrm{Var}[V(I,T)] &= \mathbb{E}[V^2(I,T)] - \mathbb{E}[V(I,T)]^2, \\ &= \mathbb{E}[tick^2 \cdot (K^2 - 2KI + I^2)] - tick^2 \cdot (K - \mathbb{E}[I])^2, \\ &= tick^2 \cdot (\mathbb{E}[I^2] - \mathbb{E}[I]^2), \\ &= tick^2 \cdot \mathrm{Var}[I], \end{aligned} \tag{4.22}$$

and, therefore, the standard deviation of the payoff distribution is simply the tick multiplied by the standard deviation of the index distribution:

$$\sigma_{payoff} = tick \cdot \sigma_I. \tag{4.23}$$

The procedure is more complicated for capped swaps when the maximum payouts

for the two counterparties are not equal, i.e,

$$V(I,T) = \begin{cases} tick \cdot (L_1 - K), & \text{if } I_H(T) < L_1 \\ tick \cdot (I_H(T) - K), & \text{if } L_1 < I_H(T) < L_2 \\ tick \cdot (L_2 - K), & \text{if } I_H(T) > L_2 \end{cases}, \tag{4.24}$$

where $I_H(T)$ is value of the HDD index at maturity, *tick* is used to translate the quantity $(I_H(T) - K)$ into monetary terms, K is the strike level, and L_1 and L_2 denote the level at which a limit to the payoff is applied. As the swap structure is not symmetrical we seek to determine the value of the strike K that satisfies the equation

$$H(K) = 0, \tag{4.25}$$

with H denoting the expected payoff from a swap contract. Equation (4.25) can be solved iteratively using a gradient-descent type numerical method such as Newton's method (see Press, Teukolsky, and Vetterling, 2002, for a description and implementation of the method). For simplicity, the interval bisecting method, as suggested in Jewson et al. (2005), is employed, and works as follows:

1. Set $K = \mathbb{E}[I]$.
2. Calculate the value of $H(K)$.
3. If the value of $H(K)$ is not within a given tolerance of zero, then evaluate $H(K + \delta K)$ and $H(K - \delta K)$.
4. Update K to the value yielding the smaller of the two quantities $H(K+\delta K)$ and $H(K - \delta K)$.
5. Repeat from steps 2 - 4 until $H(K)$ is within a specified tolerance.
6. Take this value of K as the fair strike price.

In practice, steps must be taken prior to calculating the expected index (or payoff) to ensure that the historical temperature data being used is suitable. In the next section these steps are outlined.

Removing the seasonality trend

To start with, before calculating the expectation of the index value, it is important to remove any data trends found in either the underlying temperature data or the index values (Jewson et al., 2005). Trends may exist in weather data for a variety of reasons, namely

1. Predictable climate variability;
2. Urbanisation;
3. Anthropogenic climate change;
4. Predictable internal climate variability;
5. Variability in solar forcing.

Jewson et al. (2005) states that in practice, the preferred approach is to remove the trend found in the weather index data rather than the daily temperature. This is because it is difficult to distinguish between the trend of daily temperature and the seasonality that daily temperature exhibits, during a given year. Furthermore, detrending daily temperatures requires that we define the trends of the mean, the variability, the correlation structure, the extremes, whereas focusing on just weather index values, we only need to capture the trend in the mean.

Various techniques can be utilised to capture the trend. Some of the most common ways to model this are by linear, piecewise linear, quadratic, exponential, moving average and LOESS forms. To choose the appropriate model, and also how many years of data to use, it is common practice within the meteorological industry to perform *backtesting*. Using backtesting, experiments are conducted using various time-scales in the length of historical data and fitting different regression models, in order to determine the optimal choice of the number of years of historical weather data and the type of trend assumed.

Here we provide an outline of the well known least squares method (see Press et al., 2002, for more precise details) to determine a line of best fit, which is then used to remove the trend. To begin, we define y_i as the value of the weather settlement index obtained from the linear regression approximation, and assume that

the dependent variable y_i can be expressed by a linear combination of parameters. In a simple linear regression model with N data points with one independent variable and two unknown parameters α and β, we have

$$y_i = r_i + \epsilon_i, \qquad i = 1, \ldots, N \tag{4.26}$$

where $r_i = \alpha + \beta x_i$, i.e. model is assumed to follow a linear trend, x_i denotes the year the weather settlement was measured and takes the values $x = 1, 2, \ldots, N$, and ϵ_i is the measurement error. It is assumed that the error is an independent random quantity that is normally distributed with expectation zero. The subscript i denotes the ith year, and the constant N denotes the number of historical years of data used. The unknown parameters α and β are then estimated from the dataset via the method of linear least squares (sometimes referred to as ordinary least squares). The method finds estimates for α and β such that the the sum of the squared errors (SSE) (the distances between the observed data and those predicted by the linear approximation squared) is minimised (see Press et al., 2002, for further details),

$$SSE = \min_{\{\alpha,\beta\}} \left(\sum_{i=1}^{N} \epsilon_i^2 \right). \tag{4.27}$$

$$y_i^{'} = y_i - \hat{\beta} x_i \tag{4.28}$$

Size of historical dataset

Rather than backtesting to determine how many years of historical data should be used, Jewson et al. (2005) suggest computing the mean and standard deviation on successively bigger portions of the data set. For example, collect t years of temperature data and calculate the standard deviation and mean of this dataset, then compare the mean and standard deviation of a larger dataset consisting of $t + 1$ years. By continuing this process, a graph can be plotted showing the sensitivity to the mean and standard deviation of the index as a function of years of historical data. When the sensitivities are low, the parameter values of $\hat{\alpha}$ and $\hat{\beta}$ are taken as the estimates of α and β. From conducting empirical studies, Jewson and Brix (2004) suggest as a rule of thumb that when fewer than 10 years of historical temperature data are considered, it is best to apply no detrending

since weather trends arise over long time-scales.

4.3.2 Numerical results

This section applies burn analysis method, as used by practitioners, to price a weather swap and option for the specific case where the underlying temperature index is based on weather conditions at London Heathrow. To price these weather derivatives, the gathering of historical climate data is vital.

The weather data used throughout this thesis are obtained from Weather Underground[2]. Temperature observations for London Heathrow starting from January 1st 1995 to May 12th 2010 [3] are used. The data consists of observations on the daily maximum and minimum and average temperature that are measured in Fahrenheit degrees. The average temperature in the dataset is computed using equation (2.1).The chosen length of data is suitable as it exceeds the 10 year data minimum requirement that was suggested by Jewson and Brix (2004). Herein we refer to this dataset using the naming convention *RTD* (to mean Real Temperature Data). The RTD can be found in Appendix B.2. The daily average temperature against time is plotted in figure 4.5. Table 4.2 contains the summary statistics for the daily temperature data. This shows a high value for the standard deviation of temperature that suggests weather is subject to broad oscillations over time. More data is spread out to the left, which implies that colder than normal weather is more likely since the skewness is negative (see table 4.2).

To use this dataset, the temperature readings are converted from Fahrenheit into degrees Celsius. Then any errors in the data are addressed. Typically this would consist of checking for

- **Missing data** - Dunis and Karalis (2003) propose that missing data are filled by taking the same daily temperature observed in the previous year. This method was used by Bellini (2005), however, we reject this naïve approach (as named by Dunis and Karalis, 2003) and instead favour the use

[2]Weather Underground delivers the most reliable, accurate weather information possible. They monitor conditions and forecasts for locations across the world. Website link: http://www.wunderground.com/

[3]This data set consists of 5599 observations.

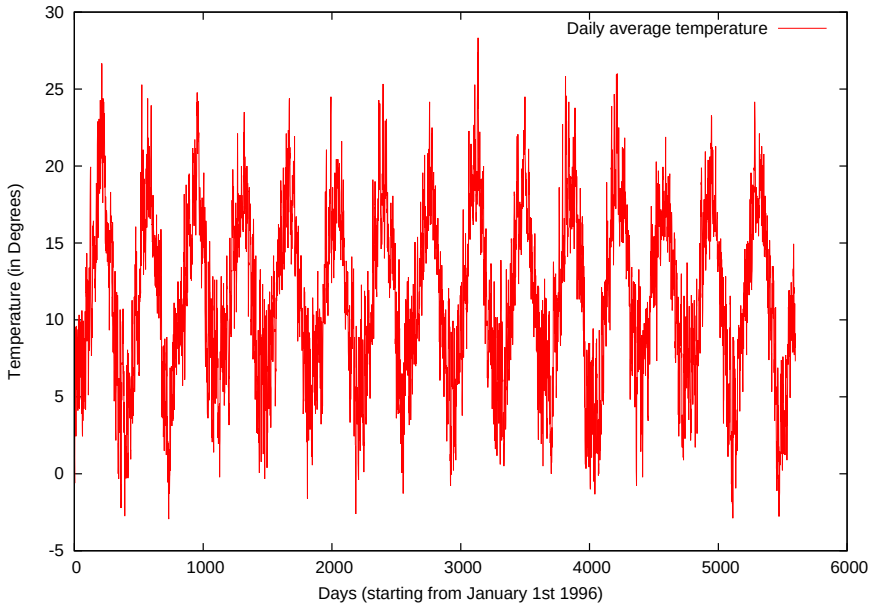

Figure 4.5: This figure plots the daily temperature against the day measured at London Heathrow starting from January 1st 1996 to May 12th 2010.

Parameter	Estimated Value
Mean	0.0066
Standard deviation	5.5809
Skewness	-1.8512
Kurtosis	2279.895
Jarque-Bera	98.6365

Table 4.2: The summary statistics for the distribution of the daily temperature observed at London Heathrow between 1995 to 2010. It reports the mean, standard deviation, skewness, kurtosis, and the Jarque-Bera statistic. The moments in the table are the central moments.

of linear interpolation, since it more accurately predicts the correct temperature, given the seasonal patterns of that year.

- **Consistency** - Checks that the daily minimum temperature is less than the daily maximum temperature, and, if required, substitute its value using spatial interpolation again.

- **Unrealistic data** - Finally, if large (unrealistic) jumps are present in the data, suitable adjustments are made; our chosen data sample has no jumps.

In the *RTD*, 7 pieces of data were missing and we used linear interpolation to determine the temperature value for those days. As the RTD is only comprised of

average temperature, consistency was already ensured. Given that RTD sample spanned over 15 years, we choose to remove the 4 leap year data points since any resulting bias is small, and their removal eases computation.

Pricing a costless weather swap contract

Using the historical data, as specified by *RTD*, we apply the burn analysis method to determine the fair strike K of a costless uncapped swap contract, with a HDD index I_H based on observations over three months (from 1st January to 31st March) at London Heathrow. The payoff is expressed as

$$V(I_H, T) = tick * (I_H - K), \tag{4.29}$$

where *tick* is used to convert the quantity $(I_H - K)$ into monetary terms. In the following section $tick = £5000$.

To begin, the HDD index is calculated for the three months from January to March in each year using

$$I_H(t) = \sum_{t=1}^{T} (X_{ref} - X(t))^+. \tag{2.3}$$

where the barrier temperature X_{ref} is set at 18°C. The results of the yearly HDD index values are shown in column 2 of table 4.4. The table shows a small cooling trend in the temperature, but can be confirm through regression analysis, whereby linear model is fitted to historical data. If $\hat{\beta}$ is distinguishable from zero then there is a trend. Performing the regression analysis produces estimates of (A.17) and (A.18), as shown in table 4.3. The value of $\hat{\beta}$ is positive and is relatively small when compared to the sizes of the accumulated HDD indices, and therefore, indicates that there is only a minor upward trend in the HDD index over this 15 year period. This is to be expected since significant climate changes often occur over longer time scales. The large and negative value of $\hat{\alpha}$ denotes the intercept of the regression line. Table 4.3 also includes the standard error and the t-statistic of each estimate. A t-statistic is a measure of the departure of an estimated parameter from its notional value and its standard error. This is

defined mathematically as

$$\text{t-statistic} = \frac{\hat{\beta} - \beta_0}{s.e(\hat{\beta})}, \tag{4.30}$$

where $\beta_0 = 0$ since we are using the t-statistic to test the significance of a regressor[4], $s.e(\hat{\beta})$ is the standard error of the estimator of the parameter. The estimated parameters are then used to produce detrended index values by using equation (4.28) produces the detrended index values shown in table 4.4, and also illustrated in figure 4.6.

Parameter	Estimate	Standard Error	t-statistic	$\Pr(>\|t\|)$
$\hat{\alpha}$	-7393.877	11209.100	-0.660	0.520
$\hat{\beta}$	4.213	5.598	0.7525	0.464

Table 4.3: The summary statistics obtained after fitting the linear trend (4.26) to RTD using the statistical program R to perform the method of least squares. The parameter values are presented, along with their respective standard error and t-statistic. $\Pr(>|t|)$ denotes the probability. The degrees of freedom is 14. The t-distribution is used due to the small sample set.

Next, the estimated expected index can be calculated by

$$\mathbb{E}[I_H] = \frac{\sum_{i=1}^{N} (I_H)_i'}{N} + \hat{\beta} N, \tag{4.31}$$

where $\hat{\beta}$ is the constant value specified in table 4.3. The values for the mean and standard deviation of the HDD index are presented in table 4.5. Therefore, from equation (4.21) it follows that the swap fair strike is $K = 1042.48$. As required, the calculated sample mean using the data in table 4.4 is given as zero.

Adjusting the strike level in an incomplete market

Trading the uncapped swap contract at the expected strike level of $K = 1074.07$ would not occur in practice, as mentioned by Møller (2001). Instead, the strike level is shifted away from the derived fair strike level in favour of the investor that is taking on more risk, or more specifically the one who holds the unhedgable risk. Adjusting the strike, is referred to in the actuarial literature as *risk loading*.

[4]When testing hypothesis, β_0 may be non-zero.

Year	HDD Index	Detrended HDD Index $(I_H)_i^{'} = (I_H)_i - \hat{\beta}x_i$	Swap Payoff $V(I,T) = tick * (I - K)$
1995	1024.56	1020.34	-89609.37
1996	1196.11	1187.69	768168.40
1997	1020.5	1007.86	-109887.15
1998	929.06	912.2	-567109.38
1999	982.81	961.74	-298359.38
2000	979.83	954.56	-313220.49
2001	1113.83	1084.34	356779.51
2002	909.28	875.57	-665998.26
2003	1047.33	1009.42	24279.51
2004	1027.28	985.15	-75998.26
2005	1014.56	968.21	-139609.38
2006	1212.17	1161.61	848446.18
2007	924.67	869.9	-589053.82
2008	961.22	902.24	-406276.04
2009	1115.06	1051.86	362890.63
2010	1221.39	1153.98	894557.29

Table 4.4: The historical HDD index over a 3 month period that starts on January 1st, for each year from 1996 to 2010. The third column shows the detrended historical HDD index values over the same periods. The strike level is $K = 1042.48$ and $tick = £5000$.

Statistic	Value
mean	1042.48
standard deviation	101.71

Table 4.5: The mean and standard deviation of the weather settlement index. The values are computed using RTD.

A market maker who is issuing the swap contract will set the strike level below the expected payoff as this would increase his payoff. We can think of this example as a client approaching the market maker, wishing to obtain a fixed level K while the market maker is to accept the floating level I. Continuing with the swap example from the beginning of §4.3.2, the strike level K is adjusted by the market maker such that (Jewson et al., 2005)

$$\hat{K} = K - \lambda R = \mathbb{E}[I] - \lambda R, \tag{4.32}$$

where λ is the risk loading factor, R is the risk measure we choose to model and $\hat{K}$ denotes the altered strike level. The risk measure can be modelled in different

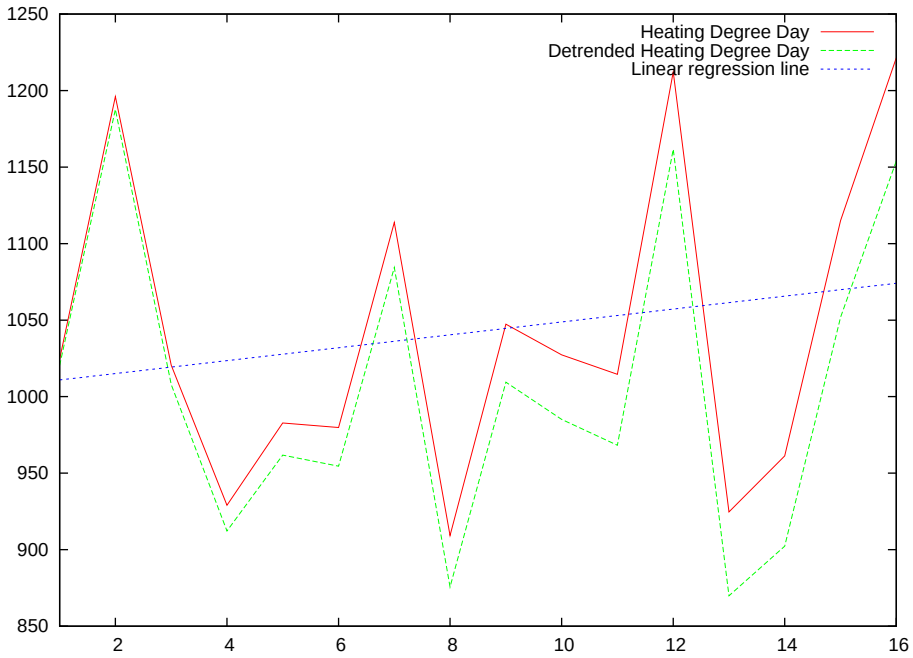

Figure 4.6: 15 years of historical index values using dataset RTD. The dashed green line shows the result after detrended the index. The regression line is represented by the dashed blue.

ways, but Gatzert, Schmeiser, and Toplek (2007), Windcliff et al. (2007) and Brix, Jewson, and Ziehmann (2002) suggest that it is often represented as the expectation, standard deviation or variance of the payoff. For consistency with the definition of the market price of risk (3.13), we only consider the case where R is the standard deviation of the index (i.e. $R = \sigma_I$), since this is comparable to the manner in which we defined the market price of risk in §3.2.5.

The expected payoff of the swap with strike $\hat{K}$ is given by the following

$$\begin{aligned} \mathbb{E}[P(I,T)] &= \mathbb{E}[tick \cdot (I - \hat{K})] && (4.33) \\ \mathbb{E}[P(I,T)] &= tick \cdot (\mathbb{E}[I] + \lambda\sigma_I - \mathbb{E}[I]) \\ &= tick \cdot \lambda\sigma_I. && (4.34) \end{aligned}$$

This is to say that the expected payoff for the speculator is a fraction of the standard deviation of the index distribution multiplied by the *tick*. It is clear that if no compensation (i.e. $\lambda = 0$) is provided for holding extra risk, then the expected payoff is zero. As a consequence of shifting the strike level, if we were to simulate the payoff of the market maker who sets the strike level at $\hat{K}$ many

Parameters	Value
λ	0.2
σ_I	101.71
$K = \mathbb{E}[I_H] - \lambda\sigma_I$	1011.96
T	90 days
$tick$	£5,000
$L_{£}$	£1,000,000

Table 4.6: Parameters for the capped put option written on a 3-month HDD index at London Heathrow. The time period of the contract is from 1st January to 31st March, i.e. $T = 90$ days, which is the same time period that the accumulated HDD index is calculated. The strike level is set at 20% of the standard deviation below the expected HDD index, i.e. $K = 1011.96$

times, it would show him making a profit on average, whilst the buyer would be losing money in most cases.

If we consider the case where the market maker sets $\lambda = 0.3$, then the adjusted strike becomes $\hat{K} = 1042.48$ HDDs. This consequently dramatically effects the expected payoff of the market maker, rising from zero to £152,567.14 in profit. The higher the risk loading factor, the larger the spread between the selling (bid) and buying (ask) strike level.

Pricing a weather option

As much of the work in this thesis is around the valuation of option contracts, a capped put option V on a 3-month HDD index based on London Heathrow is valued. The contract details can be found in table 4.6. The option's payoff is given by

$$V(I,T) = \min(tick \cdot \max(K - (I_H(T))^{'}), L_{£}). \tag{4.35}$$

Valuing an option using burn analysis is similar to valuing a swap, but instead of computing the expectation of the historical index, the historical payoffs of the option are calculated. The obtained payoffs of each year i with accumulated index I_H are presented in the fourth column of table 4.7. We present the option payoffs for each year in figure 4.7. The expected payoff is then computed and this is taken as the value of the capped put option. Importantly, we stress the use of the expectation here. Usually, one must define an appropriate measure under which

Year	HDD Index	Detrended HDD Index $(I_H)_i^{'} = (I_H)_i - \hat{\beta} x_i$	3-month Option Payoff $\min\left(tick \cdot \max(K - (I_H)^{'}, 0), L_{£}\right)$
1995	1024.56	1020.34	0
1996	1196.11	1187.69	0
1997	1020.5	1007.86	20,493
1998	929.06	912.2	498,780
1999	982.81	961.74	251,094
2000	979.83	954.56	287,019
2001	1113.83	1084.34	0
2002	909.28	875.57	681,926
2003	1047.33	1009.42	12,712
2004	1027.28	985.15	134,054
2005	1014.56	968.21	218,730
2006	1212.17	1161.61	0
2007	924.67	869.9	710,303
2008	961.22	902.24	548,590
2009	1115.06	1051.86	0
2010	1221.39	1153.98	0

Table 4.7: The historical performance of a 3 month HDD put option measured at London Heathrow from January 1st, for each year from 1996 to 2010. The third column shows the detrended historical HDD index values over the same periods. The strike level is $K = 1042.48$ and $tick = £5000$.

to take the expectation (either real-world $\mathbb{P}$ or risk-neutral $\mathbb{Q}$) to avoid arbitrage opportunities. In the case of equity options, where the underlying is traded, the option price is made up of the cost of hedging and the distribution of the payoffs. This price is the arbitrage price and is generally different from the price that would be charged if no such dynamic hedging were to be undertaken. However, because temperature itself is tradeless, one cannot form a parallel between temperature and equities. Therefore, the option premium is formally calculated by

$$V(I,t) = \frac{\sum_{i=0}^{N} V^H(I_i, T_i)}{N}, \tag{4.36}$$

where V^H is the historical payoff of the option during the equivalent time period T_i. Using (4.36), the historical expected payoff of our specified option is $£201,231$ and the standard deviation is $£216,273$. Therefore the *fair premium* to be charged is $V = £201,231$; however, as mentioned in §4.3.2 this value is very rarely used. As a fictitious example, a market maker who adds 20% (i.e. $\lambda = 0.2$) of the standard deviation might offer the following bid and ask prices

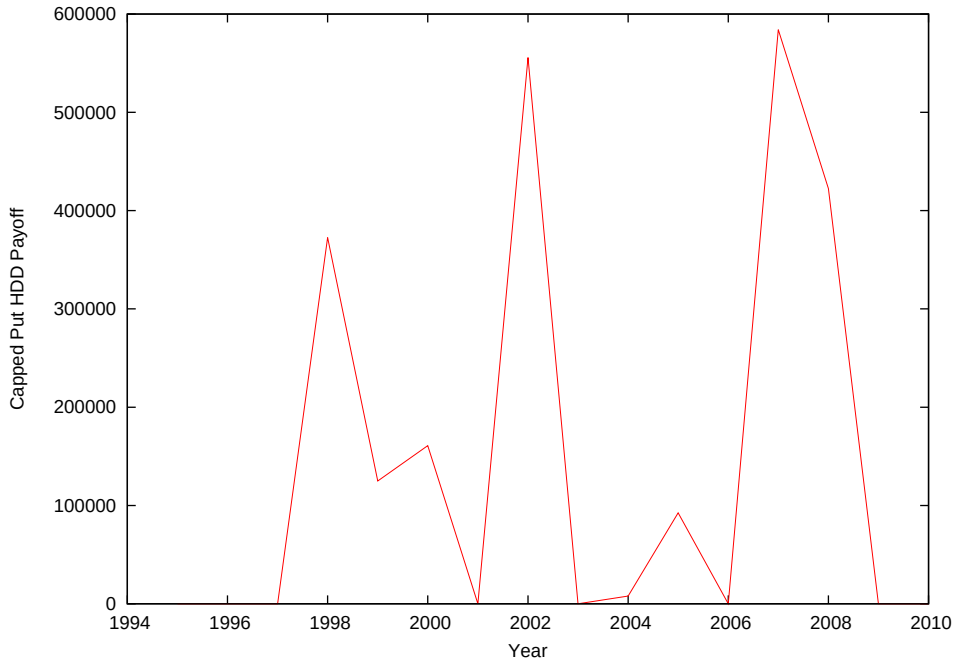

Figure 4.7: The historical payoff of a capped call option.

respectively:

$$\begin{aligned} V_{buy} &= V - \lambda\sigma_{payoff} = £157,977. \\ V_{sell} &= V + \lambda\sigma_{payoff} = £242,486, \end{aligned}$$

which creates a large bid/ask spread. Jewson et al. (2005) reports that large spreads are common in the weather derivatives market due to the high levels of risk in trading them. Additionally, because of the asymmetry of option payoffs, a market maker will favour buying options rather than selling them, since selling increases the risk of making a large pay out whereas only the initial premium is at risk when purchasing options. Therefore, from the principles of supply and demand, the market buying price will be further skewed away from the *fair strike* than the selling price.

Summary of the method

To summarise, the simplicity of the burn analysis methodology is one of the reasons it has been used by practitioners. However, the main limitation is that temperature forecasts are not incorporated as burn analysis assumes that future

seasons can resemble past seasons in a sample set. Relying on historical information in this way means that we may not be able to account for extreme events, e.g. El Niño, if the historical sample set did not include examples of such extreme events. The lack of clarity regarding the most appropriate number of years of historical data to be used in the analysis also presents issues. Jewson et al. (2005) and Bellini (2005) state that in many cases the historical simulations tend to overestimate prices, especially in instances where the set of temperature data is small.

4.3.3 Index modelling

The idea behind using *index modelling* to derive the value of a weather derivative is similar to that of burn analysis, as both methods are based on the analysis of historical weather index values. As with burn analysis, the academic basis for index modelling is tenuous. Due to the similarities between these methods, we choose to only briefly outline their differences and indicate the circumstances where one method is favoured over the other. For numerical examples of the method in practice, Jewson et al. (2005) is useful.

Index modelling attempts to fit a continuous distribution to the historical weather index values. To fit the distribution, various parameters must be estimated. This can be performed using either the *method of moments* or the *method of maximum likelihood*. The latter approach is preferred in the literature as along with determining the estimated parameters it is also possible to derive the uncertainty in these estimates.

Turvey (2005) and Harris (2003), both take the weather index as being normally distributed. Here, the hypothesis that the cumulative HDD index for the contract are normally distributed is tested by performing a Jarque-Bera test at the 5% significance level. At this level, the results from table 5.7 do not provide sufficient evidence to reject the hypothesis. This is because the $p - value(= 0.5602)$ is not less than 0.05. Given that a limited set of historical weather data is available a plot of the histogram indicates that the fit of the cumulative HDD at London Heathrow to normal distribution is poor. This is seen from the histogram that is compared with the normal distribution in figure 4.8

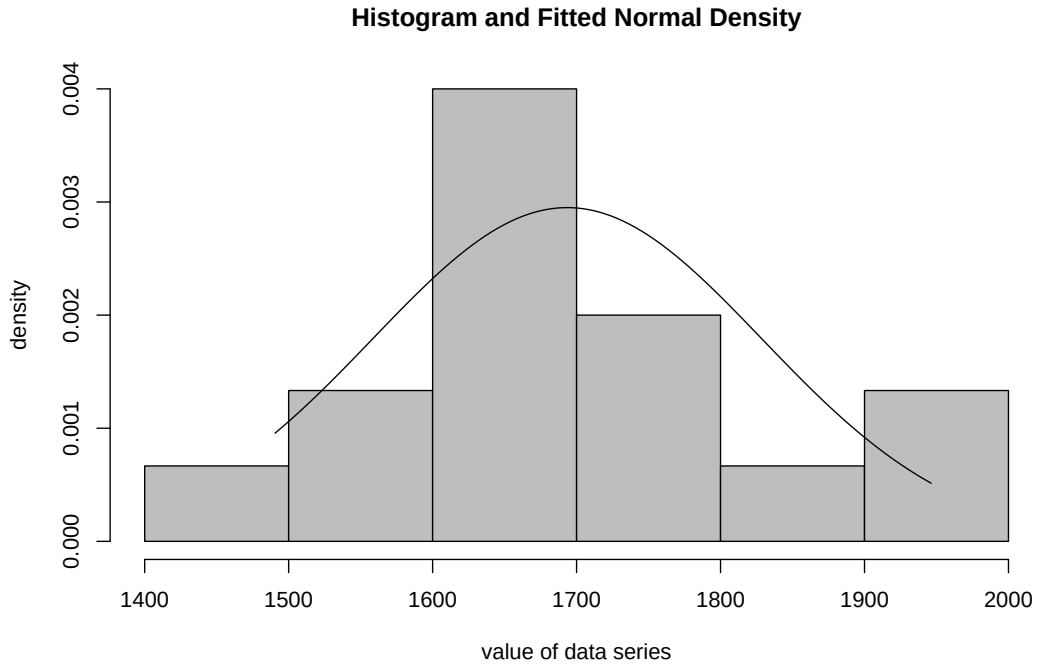

Figure 4.8: A comparison of a fitted normal density and a histogram of the historical index values.

Statistic	Value
p-value	0.5602
Jarque-Bera	1.159
Mean of HDD	1713.44
Std of HDD	135.6

Table 4.8: A summary of results from Jarque-Bera test of normality for the cumulative HDD index. The table shows the p-value, the mean of the proposed RTD cumulative HDD index and its standard deviation (denoted Std in the table). These values were computed using 5474 observations.

Using their own temperature data, Harris (2003), Turvey (2005) and Jewson et al. (2005) suggest that a normal distribution can in special cases be chosen to model the total index values, and specifies the instances where it is appropriate:

1. when modelling winter season HDD and CAT indices, and summer season CDD and CAT indices;
2. when considering monthly contracts based on CAT and HDD indices, it is only appropriate to model the indices in months January, February and March by a normal distribution;
3. for CAT indices based on individual summer months;
4. when modelling the month of July in a CDD based monthly contract;

As we previously discussed in §4.2, the reason why these authors state that a normal distribution can only be assumed in these limited cases, is due to the fact that the probability of the temperature breaching the barrier X_{ref} is higher in certain months. If the barrier is breach then the contribution to, for example a HDD index, would be zero and thus it is no longer valid to model the process as being normally distributed. Therefore, pricing a 1-month HDD index option may lead to mis-pricing as during that month the temperature may surpass 18 °C. However, using index modelling does provide an advantage over the burn analysis method described in §4.3.1 because extreme outcomes can be modelled since the smooth estimated distribution extends into the tails beyond the information provided by the historical data.

4.4 Summary

This chapter has surveyed the existing temperature models proposed in the weather derivatives literature and outlined the reasoning behind their creation. We have priced both swaps and option using the method of burn analysis and will compare these prices with the ones obtained from our newly developed models in the following chapters. As we have seen in this chapter, adjusting prices to account for the undiversifiable risk that an investor is exposed to in the weather derivatives market creates large price differences between the fair strike level or

option premium and the level/price chosen by the market maker. Therefore it is important to ask if the market price of risk is a significant factor when valuing these instruments and, if so, to what extent.

Chapter 5

A new weather derivative pricing model

To raise new questions, new possibilities, to regard old problems from a new angle, requires creative imagination and marks real advance in science.

Albert Einstein

Typically, option valuation is dependent on the underlying quantity being used to hedge the option's position. This is used so that movements in the derivative are balanced by the change of some multiple of the underlying, such that the portfolio can be assumed risk-free. In these instances, unique prices can be derived by following Black and Scholes-type analysis (see 3.2.3), with the key assumptions of their approach being that the portfolio can be delta-hedged continuously and that the underlying is available for trading. Alternatively, we could consider the use of the Feynman-Kač formula (5.1), below, which establishes a link between SDEs and PDEs, such that given a stochastic process and final condition (the payoff function, $V(X_T, T)$) we can derive an appropriate PDE by considering

$$V(x,t) = \mathbb{E}\left[\exp^{-\int_t^T r(u)\mathrm{d}u} V(X_T, T)|X_t = x\right]. \tag{5.1}$$

where X_t is an Itô process of the form (3.1), and then initial condition for X_t is $X_0 = x$. By using the Feynman-Kač formula, a hedging strategy can be derived if the implicit change of measure is specified. This is both a strength and weakness

of the method. On one hand we can effectively determine a value for an option on the given stochastic process, however it is not clear how this price is justified or how the risk can be managed. The technique has been used in almost all areas of finance and we make special reference to the work carried out by Law (2009) when valuing complex commodity derivatives, and by Evatt et al. (2010b) in the pricing of a mine. In deriving a mine valuation model, Evatt et al. (2010b) argue that the drift parameter that appears in the PDE should be set at the risk-free rate when hedging is possible. This is of course reliant on the standard hedging arguments presented by Black and Scholes, in which the portfolio becomes risk-free in a complete market. However, as Evatt et al. (2010b) point out, this cannot be done in cases where perfect hedging is not possible because the market is incomplete.

The emergence of innovative financial products that attempt to securitise risk has led researchers to question the validity of pricing methods based on standard hedging arguments (see Black and Scholes, 1973). This is because the underlying instrument may not be available for trading. For example, to price an interest-rate derivative it is not possible to construct a hedged position such that $\Pi_t = V_1(r_t, t) - \Delta r_t$ since the stochastic interest-rate r_t is not a tradable asset. Vasicek (1977) suggests that a hedged portfolio can be constructed if an interest-rate derivative $V_1(r_t, t : T_1)$ is hedged with another interest-rate derivative $V_2(r_t, t : T_2)$ on the same underlying r_t that expires at a later time $T_2 > T_1$. This gives a portfolio position of

$$\Pi_t = V_1(r_t, t : T_1) - \Delta V_2(r_t, t : T_2). \tag{5.2}$$

However, this approach is often not possible when the derivative does not possess sufficient liquidity, and hence it is not possible to maintain a delta-hedged position. In this case, it is generally useful and practical to make use of a correlated asset[1]. If the underlying processes of the option and the correlated asset behave identically, then complete elimination of the risk is possible. However, it is much more common for them to be imperfectly correlated. Consider the example as detailed in Hull (2006) of an airline that is concerned about the future price of jet fuel. As jet fuel futures contracts are illiquid[2], Hull (2006) states that in

[1]This could be an equity, commodity, index, or simply an observed process.

[2]Jet fuel futures contracts recently started traded on the Chicago Mercantile Exchange (CME). Gulf Coast jet fuel calendar swap futures give market participants the opportunity to

practice it is appropriate to utilise heating oil futures contracts as the hedging instrument. This is because price movements in jet fuel are strongly correlated to the price fluctuations in heating oil futures. This strategy of hedging using futures contracts from different markets is known as *cross hedging*. This only works if there is significant correlation between the prices of the spot and futures contracts. Another example, taken from Davis (2001), of where an imperfectly correlated asset is used in place of the hedging instrument is when a trader wishes to hedge a book of equity options. When there are associated transaction costs in trading the underlying equities, it is often not possible to hedge with each of the individual equities as transaction costs rapidly increase. Instead, the trader observes that the correlation between the basket of equities and the index futures is indeed very high, and so hedges with the index. Now, because only one contract (the index futures contract) needs to be re-hedged, the associated transaction costs would be several magnitudes lower.

The pricing of weather derivatives is an incomplete market problem. In general, determining the value of a contingent claim in an incomplete market is non-trivial, and generally leads to pricing concepts based on probability or utility theory. Heston (1993) and Sircar and Papanicolaou (1999) study the problem of pricing derivatives when volatility is itself a random process, and view this as an incomplete market problem for which pricing bands are derived. An approach developed by Cochrane and Saa-Requejo (2000), leads to very tight bounds on option values in an incomplete market by finding strategies that have a bounded market price of risk (or Sharpe ratio), and assumes that investors want 'good-deals' in a market. Another approach, and one that is considered in this thesis, is to assume that the value of a derivative can be made up of the cost of constructing a partially hedged portfolio plus some risk-premium; this approach is also considered by Ibáñez (2005).

First attempts to value weather derivatives assumed that the market was complete. Harris (2003), following McIntyre and Doherty (1999), assume that the cumulative number of HDD's is a normally distributed variable with mean m

target their risk management coverage for jet fuel traded on the Gulf Coast, the most liquid physical jet fuel market.

and standard deviation σ, with probability density function

$$f(x) = \frac{1}{\sigma\sqrt{2\pi}} e^{-\frac{(x-m)^2}{2\sigma^2}}. \tag{5.3}$$

where parameter μ is the mean and σ^2 is the variance. McIntyre and Doherty (1999) arrive at a simple analytical model similar to the Black and Scholes (1973) formula for option pricing, where the value of an HDD call option is

$$C = (m - K)N\left(\frac{m-K}{\sigma}\right) + \sigma^2 f(K), \tag{5.4}$$

where K is the strike level, $N(.)$ is the cumulative standard normal distribution. A similar result is also derived by Harris (2003) for an HDD put option.

We find however, that limited research has been undertaken to value weather derivatives from an incomplete markets perspective. The papers that have considered this are Cao and Wei (2000) who propose and implement an equilibrium valuation framework, Platen and West (2004) use the growth optimal portfolio (which they define as a world stock index) as a benchmark in order to value a weather derivative, Davis (2001) approaches valuation from the angle of marginal utility, and Brockett et al. (2005) also price the contract in an incomplete market framework. These works focus primarily on the use of utility functions (see §3.3) and therefore have limited practical use, though, Platen and West (2004) is an exception to this list, as they adopt an approach more closely linked with actuarial pricing.

In this chapter we firstly consider the use of an imperfectly correlated instrument that can be used as a substitute for temperature. We then introduce the fundamental state variables, and construct a suitable hedging argument which minimises the risk in the portfolio. Subsequently, a two-dimensional PDE for a weather option is formulated, and we complete the specification of the problem by prescribing the necessary boundary and terminal conditions. We conclude the chapter by calculating estimates of the temperature model parameters that are required before actually pricing any temperature derivatives.

5.1 Imperfectly correlated instruments

Climate[3] conditions, as stated by Cao and Wei (2004), greatly affect short-term demand and long-term supply of energy. Geman (2005) and Zanotti, Gabbi, and Laboratore (2003) showed that both electricity load and gas consumption are significantly correlated with temperature. Electricity load is thought to be largely dependent on weather conditions (specifically temperature) that Pirrong and Jermakyan (2008) take the underlying power spot price to be dependent on weather rather than on load when formulating their electricity derivative PDE. Cao and Wei (2004) also showed this strong relationship, and observed that the maximum power load is at its lowest when the average daily temperature is around 18°C, and increases as temperature moves away from this level; this reiterates why most temperature derivative indices use $X_{ref} = 18°\text{C}$ (see §2.2.1).

Natural gas consumption is also highly dependent on monthly average temperature and Cao and Wei (2004), again, demonstrate this by taking the monthly average temperature for the US state of Illinois and regressing it against the monthly delivery of natural gas. The results from Cao and Wei (2004) give a measure[4] of how closely linear movements in temperature affect gas demand. They deduce that there is a strong correlation between temperature and electricity/gas demand, which implies that either gas or electricity prices could be used in place of temperature contracts, as a partial hedge of a companys energy costs or profits. The link between weather and these other commodity spot prices is the main reason why weather derivatives were created to begin with. In Leggio and Lien (2002), the suitability of using weather derivatives to hedge gas bills is studied. Similarly, Pirrong and Jermakyan (2008) investigate the benefits of using weather derivatives to reduce the risk in trading electricity. Most authors, including, but not limited to Turvey (2005) and Platen and West (2004), follow the approach outlined in Cao and Wei (2000) who state that the market price of weather risk is negligible and hence the discount rate is the risk-free rate. This argument stems from the belief that weather is uncorrelated with most traditional investment assets. However, investors in the weather derivatives market are not

[3]When we refer to climate we are referring to the (occurred/expected) behaviour of the atmosphere over long time-periods. The behaviour of the atmosphere over short time horizons is referred to as the weather.

[4]They used the R^2 measure, which essentially describes how well an estimated model can predict futures outcomes. Cao and Wei (2004) find $R^2 = 0.9416$.

'representative' of the market, but face very specific risks that are induced by the weather. Thus it has been shown by Bellini (2005) that this assumption can lead to unsatisfactory prices. In the next section we assume that there exists a commodity, available for trading, that is sufficiently correlated with temperature so as to allow for the construction of at least partial hedging.

5.2 A new weather pricing PDE

As presented in §4.1 several models exist that attempt to describe the evolution of temperature. We adopt the model first purposed by Alaton et al. (2002), and confirm the choice of this model through empirical tests. To ensure an appropriate fit to UK historical data, we provide a new set of estimated parameters for the temperature model, but we shall defer explanations until §5.4.

To formulate the problem and create a weather derivatives valuation model, we first prescribe the state-space variables. The core variables are the daily temperature X, the degree-day index I, and time t. Let $V(X_t, I, t)$ be the value of a weather contingent claim written on these core variables. Additionally, we assume there to be a constant risk-free interest-rate r. Given that temperature is not traded we introduce a hedging instrument[5] H that is imperfectly correlated with temperature, and follows a GBM. This assumption of the correlated asset following a GBM is simple and is used so that the derivation is kept clear, but inclusion of say an OU process would result in the same procedure and a similar PDE. The equations that describe our problem are given by

$$\begin{aligned} \mathrm{d}H_t &= \mu_H H_t \mathrm{d}t + \sigma_H H_t \mathrm{d}Z_1, && (5.5)\\ \mathrm{d}X_t &= \mathrm{d}\theta(t) + \kappa\left[\theta(t) - X_t\right]\mathrm{d}t + \sigma_X(t)\mathrm{d}W_t, && (5.6)\\ \mathrm{d}I_t &= f(X_t, t)\mathrm{d}t, && (5.7)\\ \mathrm{d}M_t &= rM_t\mathrm{d}t, && (5.8) \end{aligned}$$

where u_H, σ_H are the respective drift and volatility of the correlated instrument H and are assumed constant. The temperature process in equation (5.6) drifts to the long-run seasonality mean $\theta(t)$ with mean-reversion speed κ. As explained

[5]This could take the form of a traded asset/commodity or liquid derivative such as a futures contract.

in §4.1.3, the forcing term $\mathrm{d}\theta(t)$ is included to ensure that the long-run average value of temperature tends to $\theta(t)$. The variability of the temperature is $\sigma_X(t)$ and is given as a piecewise constant function. In addition, $f(X_t, t)$ represents the drift of the underlying index, which for a HDD and CAT is given by

$$f(X_t, t) = (X_{ref} - X_t)^+ \tag{5.9}$$

and

$$f(X_t, t) = X_t. \tag{5.10}$$

respectively. As $\mathrm{d}H_t$ is correlated with $\mathrm{d}X_t$ we use Cholesky decomposition (Hull, 2006) to rewrite the Brownian increment $\mathrm{d}W_t$ as

$$\mathrm{d}W_t = \rho \mathrm{d}Z_1 + \sqrt{1-\rho^2}\mathrm{d}Z_2, \tag{5.11}$$

where where ρ is the correlation between $\mathrm{d}Z$ and $\mathrm{d}W_t$, Z_1 and Z_2 are two standard Brownian motions, and Z_1 is uncorrelated with Z_2,

$$\mathbb{E}(\mathrm{d}Z_1 \mathrm{d}Z_2) = 0. \tag{5.12}$$

Lastly we note the usual Wiener process properties of

$$\mathrm{d}W_t^2 = \mathrm{d}t, \tag{5.13}$$
$$\mathrm{d}Z_1^2 = \mathrm{d}t, \tag{5.14}$$
$$\mathrm{d}Z_2^2 = \mathrm{d}t, \tag{5.15}$$
$$\mathrm{d}Z_1 \mathrm{d}W_t = \rho \mathrm{d}t, . \tag{5.16}$$

5.2.1 The partial hedge

We follow a similar approach as laid out in Windcliff et al. (2007) by constructing a hedged portfolio, where a correlated asset is used as the hedging instrument rather than temperature. Consider a portfolio comprising of an option $V(X, I, t)$ less Δ contracts of the imperfectly correlated asset H_t. The portfolio is financed by selling a bond M_t. Hence

$$\Pi_t = V_t - \Delta H_t - M_t, \tag{5.17}$$

where it is assumed that

$$M_t = V_t - \Delta H_t \tag{5.18}$$

at time t, so that the self-financing property (3.7) holds. This means that no funds are either added or removed from the portfolio for the duration $0 < t < T$. The instantaneous variation of the portfolio is

$$\mathrm{d}\Pi_t = \mathrm{d}V_t - \Delta \mathrm{d}H_t - \mathrm{d}M_t. \tag{5.19}$$

Using Itô's Lemma we expand an increment of the option $\mathrm{d}V(X, I, t)$, so that

$$\begin{aligned} \mathrm{d}V_t &= \frac{\partial V}{\partial t}\mathrm{d}t + \frac{\partial V}{\partial X}\mathrm{d}X_t + \frac{1}{2}\frac{\partial^2 V}{\partial X^2}\mathrm{d}X_t^2 + \frac{\partial V}{\partial I}\mathrm{d}I \\ &= \left[\frac{\partial V}{\partial t} + \left(\kappa(\theta(t) - X_t) + \theta^{'}(t)\right)\frac{\partial V}{\partial X} + \frac{1}{2}\sigma_X^2(t)\frac{\partial^2 V}{\partial X^2} + f(X_t, t)\frac{\partial V}{\partial I}\right]\mathrm{d}t \\ &+ \sigma_X(t)\frac{\partial V}{\partial X}\mathrm{d}W_t. \end{aligned} \tag{5.20}$$

where $\theta^{'}(t)$ expresses the first derivative of θ with respect to time t. Substituting (5.11) into (5.20) leads to

$$\begin{aligned} \mathrm{d}V_t &= \left[\frac{\partial V}{\partial t} + \left(\kappa(\theta(t) - X_t) + \theta^{'}(t)\right)\frac{\partial V}{\partial X} + \frac{1}{2}\sigma_X^2(t)\frac{\partial^2 V}{\partial X^2} + f(X_t, t)\frac{\partial V}{\partial I}\right]\mathrm{d}t \\ &+ \sigma_X(t)\frac{\partial V}{\partial X}\left(\rho \mathrm{d}Z_1 + \sqrt{1-\rho^2}\mathrm{d}Z_2\right). \end{aligned} \tag{5.21}$$

We substitute (5.5), (5.6) and (5.21) into portfolio variation (5.19) to obtain

$$\begin{aligned} \mathrm{d}\Pi_t &= \left[\frac{\partial V}{\partial t} + \left(\kappa(\theta(t) - X_t) + \theta^{'}(t)\right)\frac{\partial V}{\partial X} + \frac{1}{2}\sigma_X^2(t)\frac{\partial^2 V}{\partial X^2} + f(X_t, t)\frac{\partial V}{\partial I}\right. \\ &- \left.\Delta\mu_H H_t - rM\right]\mathrm{d}t + \left(\sigma_X(t)\frac{\partial V}{\partial X}\rho - \Delta\sigma_H H_t\right)\mathrm{d}Z_1 \\ &+ \sigma_X(t)\frac{\partial V}{\partial X}\sqrt{1-\rho^2}\mathrm{d}Z_2. \end{aligned} \tag{5.22}$$

This portfolio is driven by two random sources of risk. Firstly, the risk from the temperature X_t, $\mathrm{d}Z_2$, and secondly, the risk from the imperfectly correlated asset $\mathrm{d}Z_1$. As shown by Black and Scholes (1973), a source of randomness can

be eliminated by solving for Δ such that coefficient of $\mathrm{d}Z_1$ is zero. This gives

$$\Delta = \rho \frac{\sigma_X(t)}{\sigma_H} \cdot \frac{\frac{\partial V}{\partial X}}{H_t}. \tag{5.23}$$

Substituting (5.18) and value for Δ into (5.22) gives

$$\begin{aligned} \mathrm{d}\Pi_t &= \left[\frac{\partial V}{\partial t} + \gamma(X_t,t)\frac{\partial V}{\partial X} + \frac{1}{2}\sigma_X^2(t)\frac{\partial^2 V}{\partial X^2} + f(X_t,t)\frac{\partial V}{\partial I} - rV\right]\mathrm{d}t \\ &+ \sigma_X(t)\frac{\partial V}{\partial X}\sqrt{1-\rho^2}\mathrm{d}Z_2, \end{aligned} \tag{5.24}$$

with

$$\gamma(X_t,t) = \kappa(\theta(t) - X_t) + \theta^{'}(t) - \frac{(\mu_H - r)}{\sigma_H}\rho\sigma_X(t). \tag{5.25}$$

Clearly this hedging strategy only partially hedges the derivative as the changes in the portfolio are still random. The portfolio becomes deterministic only if there exists a perfectly correlated instrument, i.e. when $|\rho| = 1$.

5.2.2 A special case

Lets consider a special case where the mean and standard deviation of temperature and the correlated asset are identical and are positively correlated. For example, this could be of two adjacent wind farms, where one is traded and the other is not, they have identical climates (since they have the same μ and σ) but non-identical weather (hence $\rho \neq 1$). We define the drift of temperature as μ_X, and apply this special case to (5.25) to obtain

$$\gamma(X,t) = \mu_X(1-\rho) + \rho r. \tag{5.26}$$

Choosing the drift in this way simplifies our problem and avoids the need to specify μ_H, which is difficult to estimate when $p \neq 1$ and is $\mu_H \neq \mu_X$. The removal of real-world drift is a significant step forward, as was the case in the derivation of the Black and Scholes (1973) PDE. When $\rho = 1$, a perfect hedge can be constructed. In this case, $\gamma(X,t) = r$, since the asset should grow at the risk-free rate. When the instrument is completely uncorrelated, i.e. $\rho = 0$, the hedge is completely ineffective and so the return is $\gamma(X,t) = \mu_X$. Also, for an imperfectly correlated instrument with $\rho = 0.5$, the hedged portfolio should

remove 50% of the the risk premium, and therefore $\gamma(X,t) = (\mu_X + r)/2$.

Consequently, for $|\rho| \neq 1$ the residual risk persists. We are unable to perfectly replicate the movements in the derivative's payoff and therefore can no longer rely on the straightforward Black and Scholes (1973) type analysis, and hence another approach is required to value the weather derivative within an incomplete markets setting. The following section outlines a possible approach.

5.2.3 Minimising risk in an incomplete market

As a starting point, we use the concept introduced by Föllmer and Sondermann (1985) of having a mean-self-financing portfolio, see §5.2.3. This property assumes that a portfolio Π_t has an expected value of zero. Considering a portfolio to be mean self-financing is an approach adopted by numerous academics to value various derivative contracts. Windcliff et al. (2007) adopt this method when pricing a segregated funds contract, and Ibáñez (2005) does the same in deriving a PDE for an option where short-selling of the underlying is restriction. The author is unaware of any work in the literature that has utilised this property ((5.27) below) in the context of pricing a weather derivatives contract. Given the portfolio defined in (5.17), we therefore assume that its variation has zero expectation:

$$\mathbb{E}[\mathrm{d}\Pi_t] = 0. \tag{5.27}$$

Under this assumption, we regard today's option value, $V(X_t, I, 0)$, as the *fair hedging price* (Schäl, 1994). Here it is assumed that the portfolio growth is expected to be zero (a local martingale) as opposed to taking the expected growth as equal to the risk-free rate, i.e. $\mathrm{d}\Pi_t = r\Pi_t \mathrm{d}t$. The reason for this is that by including the bond B in our portfolio we are already taking into account this growth and therefore do not need to incorporate it twice. Since the expectation of a Brownian motion is zero, the expectation of (5.24) is simply

$$\mathbb{E}\left[\mathrm{d}\Pi_t\right] = \left[\frac{\partial V}{\partial t} + \gamma(X_t,t)\frac{\partial V}{\partial X} + \frac{1}{2}\sigma_X^2(t)\frac{\partial^2 V}{\partial X^2} - rV + f(X_t,t)\frac{\partial V}{\partial I}\right]\mathrm{d}t, \tag{5.28}$$

It then follows from the mean-self financing property (5.27) that in expectation

$$\frac{\partial V}{\partial t} + \gamma(X_t,t)\frac{\partial V}{\partial X} + \frac{1}{2}\sigma_X^2(t)\frac{\partial^2 V}{\partial X^2} + f(X_t,t)\frac{\partial V}{\partial I} - rV = 0. \tag{5.29}$$

To give a PDE for a weather option, when the underlying is a HDD index we define

$$f(X_t, t) = (X_{ref} - X_t)^+. \tag{5.9}$$

From herein assume that $f(X_t, t)$ is given by (5.9), unless stated otherwise. PDE (5.29) is similar to convection-diffusion or advection PDEs that have been studied extensively in the applied mathematics literature. Morton and Kellogg (1996) provide a comprehensive and thorough examination of these types of problems and highlight the difficulties that arise in the numerical evaluation of such PDEs. Problems may arise if the PDE becomes convection-dominated in the X spatial dimension when the magnitude of the diffusion term with respect to X is smaller than its corresponding convection term, i.e.

$$\frac{1}{2}\sigma_X^2(t) < \gamma(X_t, t). \tag{5.30}$$

We demonstrate in chapter 6 the consequence of the above properties and show how the choice of which numerical scheme to apply is important, otherwise misleading results may be obtained. The solution to the above PDE will be used as a benchmark value, $V_{BE} = V(X, I, t = 0)$, throughout this thesis.

5.3 Boundary and final conditions

The valuation of a weather derivative requires the specification of boundary conditions to fully define the problem. A number of terminal conditions can be used, and depend on the type of contract to be valued. We present a few typical examples:

- A European call option:

$$V(X, I, T) = tick \cdot \max(I - K, 0). \tag{5.31}$$

- A European capped put option:

$$V(X, I, T) = \min(tick \cdot \max(K - I, 0), cap). \tag{5.32}$$

In the above payoffs, the form of I is dependent on the type of underlying index that is used. We outlined several possible forms in §2.2.1. Much of the computations performed in this thesis will be on European capped options because they are the mostly frequently traded type of derivative in the weather-risk market.

5.3.1 Truncation of computational domain

The value of an option that satisfies (5.29) is dependent on the value of the current temperature X_t. As we have a three-dimensional PDE, where we have first- and second-order derivatives in X, we are required to specify two boundary conditions. The domain for the PDE (5.29) is $X \times I \in [-a, \infty] \times [0, \infty]$, where a is the magnitude of absolute zero [6]. Motivated by numerical studies in chapter 6, we must first determine a finite domain in which we solve the PDE. Since the temperature is modeled as a mean-reverting process, its expectation and standard deviation are known. Therefore, the likely movement of the process in time can be specified, which then enables for truncation of the X domain. Given that the temperature process (4.4) at time $s < t$ admits the following strong solution:

$$X_t = [X_s - \theta(s)]e^{-\kappa(t-s)} + \theta(t) + \int_s^t e^{-\kappa(t-u)}\sigma_X(u)\mathrm{d}W_u. \tag{5.33}$$

It follows that the mean and variance are (Bellini, 2005)

$$\mathbb{E}\left[X(t)\right] = \theta(t) + (X_s - \theta(s))\, e^{-\kappa(t-s)}, \tag{5.34}$$

$$\mathrm{Var}\left[X(t)\right] = \int_s^t e^{-2\kappa(t-u)}\sigma_X^2(u)\mathrm{d}u. \tag{5.35}$$

To define the computational domain, the maximum standard deviation, denoted $\hat{\sigma}_X$, is chosen and substituted in place of $\sigma_X(t)$ in (5.35). This has the benefit of not needing to recompute new computational bounds at each time-step. Therefore, to value a contract within the specified domain at a given time t, say X_t, Andricopoulos, Widdicks, Duck, and Newton (2003) suggest setting the domain range to be at least 7.5 times standard deviation (i.e. set $D = 7.5$ in (5.36) below) either side of X_t. Andricopoulos et al. (2003) and Law (2009) considered this for ABM processes. Similar to Andricopoulos et al. (2003), the deviation from X_T

[6] This corresponds to 0 Kelvin or -273.15 °C

for an OU process is defined as

$$X_T^{\Delta} = D\frac{\hat{\sigma}_X}{\sqrt{2\kappa}}\left(1 - e^{-2\kappa T}\right)^{1/2}. \tag{5.36}$$

Consequently, the computational domain limits, X_T^{min} and X_T^{max}, may be given by

$$X_T^{min} = X_T - X_T^{\Delta}, \tag{5.37}$$

$$X_T^{max} = X_T + X_T^{\Delta}. \tag{5.38}$$

Equations (5.37) and (5.38) denote the minimum and maximum values that we allow temperature to reach within our computational domain. We perform numerical experiments to confirm that by truncating our domain the solution is not (significantly) affected. This is done by holding the grid spacing ΔX fixed, and then expanding the magnitudes of X^{min} and X^{max} to observe the effect this has on the solution. In the implementation, since ΔX is fixed, the number of grid points in X must be increased as the domain size is expanded. The diagrams in figure 5.1 illustrate how the solution changes as the truncated domain is varied. In figure 5.1(a) the value of the option is computed for four different domain sizes. The figure focuses on regions where distinct differences are observed. Comparing the red and green lines in the figure indicates that some information is lost when the domain size is as small as $X^{max} = 25$, and the difference between the solution when $X^{max} = 50$ and $X^{max} = 60$ is virtually zero (this is why the blue line is not easily visible in the diagram). Figure 5.1(b) shows the solution at $X = 17$ for different domain sizes. Again, small differences between the solutions when the domain limit is $X^{max} = 25$ and $X^{max} = 50$ are shown. The precise explanations of the method used to calculated the solutions in figure 5.1 are deferred until §6.2.3.

5.3.2 The value at extreme temperatures

By truncating the range in X, we next consider the behaviour of the system at the extremes X^{min} and X^{max} as defined in (5.37) and (5.38) respectively. In the context of weather derivatives the condition describes the behaviour of the option value when the temperature is either extremely warm or cold. Consider a capped

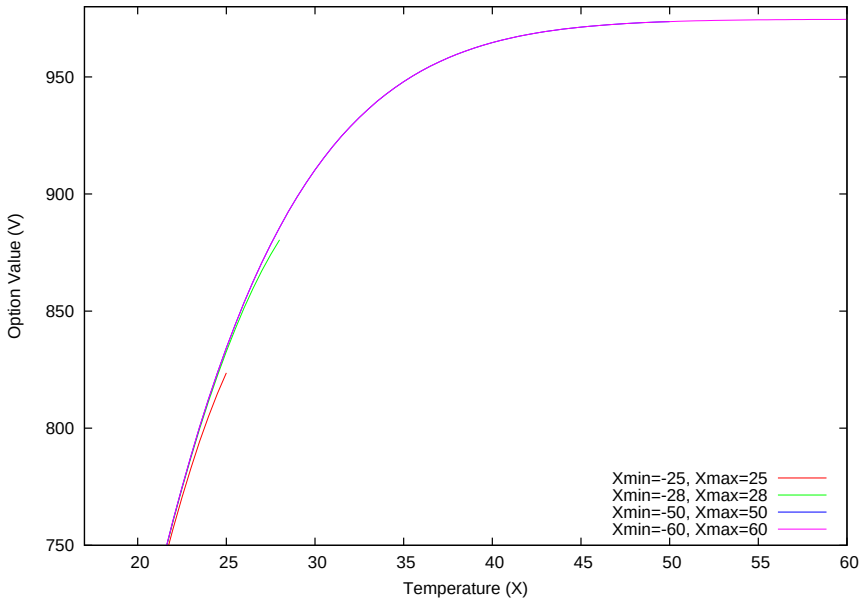

(a)

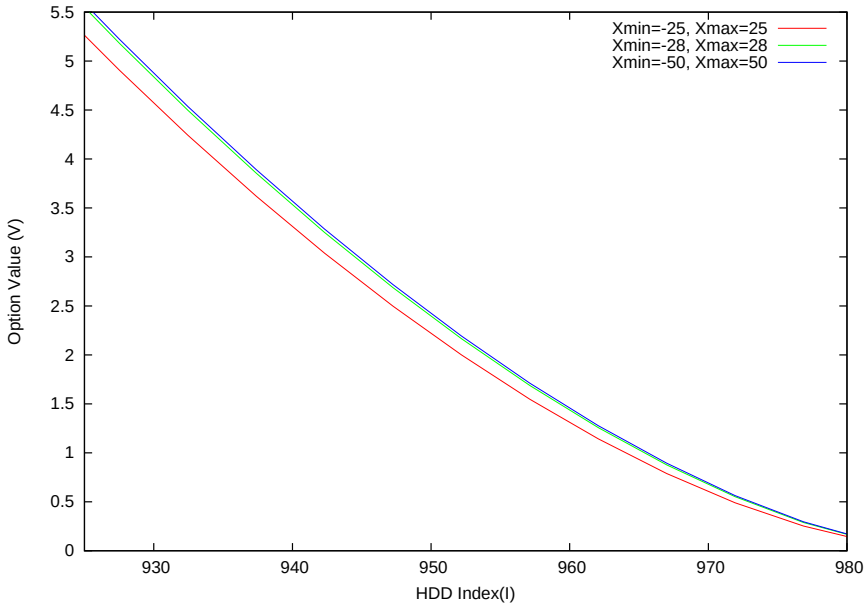

(b)

Figure 5.1: The figures plot the solution profiles of an uncapped HDD put option that are computed using differently sized computational domains. For each of the differently sized domains, ΔX is fixed. We use the Semi-Lagrangian method (which is explained in §6.2.3) to solve equation (5.29) with the following parameters: $K = 986.73, T = 90, r = 0.05/365, \rho = 0.9, \Delta I = 4.93365, \Delta\tau = 0.18$. Figure 5.1(a) plots the solutions as temperature changes, whereas in figure 5.1(b) we set $X = 17$ and plot the solution's (i.e. $V(17, 0, 0)$) behaviour for each domain size.

European HDD put option with payoff (5.32). As a reminder, the HDD weather index is given by

$$I_H(t) = \int_0^t (X_{ref} - X(s))^+ \mathrm{d}s, \tag{2.4}$$

where X_{ref} is the barrier temperature. In what follows, we suppress the use of subscript H in referring to the HDD index.

Condition as $X \to X^{min}$

If the temperature is very cold the HDD index becomes large, resulting in a put option being worthless. Therefore, a possible boundary condition is

$$V(X^{min}, I, t) = 0. \tag{5.39}$$

However this condition is too severe, and may unnaturally force the solution to reach zero within the computational domain. In order to avoid this we would have to set the range in X sufficiently large so that solutions in the regions of interest are not greatly effected. For computational convenience we impose the corresponding Robin boundary condition,

$$\begin{aligned} \frac{\partial V(X^{min}, I, t)}{\partial t} &+ \gamma(X^{min}, t)\frac{\partial V(X^{min}, I, t)}{\partial X} \\ &+ (X_{ref} - X^{min})^+ \frac{\partial V(X^{min}, I, t)}{\partial I} - rV = 0, \end{aligned} \tag{5.40}$$

as this enables a smaller domain truncation X^{min}, whilst giving a smoother solution profile. The specification of our boundary condition is an improvement on the simple Dirichlet condition of (5.39) that was used by Harris (2003) to value a similar weather PDE.

Condition as $X \to X^{max}$

Warm weather conditions result in a small accumulated HDD index, as no heating has been necessary. From observing the payoff condition (5.32), payoff is almost guaranteed (if the domain is large enough) since for warm conditions $I = 0$. This

suggests the Neumann boundary condition

$$\frac{\partial V}{\partial X}(X^{max}, I, t) = 0, \tag{5.41}$$

that implies that the option value is invariant at X^{max}.

Condition for the accumulating weather index along $I \to \infty$

Because we have an extra dimensional derivative appearing in the PDE (namely $\partial V/\partial I$) we are obliged to supply another boundary condition in this dimension. We can determine this by considering that $I \to \infty$ implies that $K - I < 0$. In other words the temperature must have been very cold to cause the accumulation index to reach such high levels, and thus the put option value is worthless. We obtain the Dirichlet boundary condition

$$\lim_{I \to \infty} V(X, I, t) = 0. \tag{5.42}$$

To ensure the problem remains well posed we only apply a condition at the maximum value of I, and then march backwards through decreasing I until reaching $I = 0$ (because the PDE is backwards parabolic in I).

Again, to numerically solve the PDE we need to determine where best to truncate our domain, so that I^{max} is finite. This will be the the largest value the weather index can reach on the grid. Since $X \in [X^{min}, X^{max}]$, we can make a suitable approximation by assuming that the maximum value I would reach if the temperature remained at X^{min} for the duration of the accumulation period, say T. This implies that

$$I^{max} = T * (X_{ref} + |X^{min}|). \tag{5.43}$$

This completes the specification of the boundary conditions for a capped put option that satisfies PDE (5.29) on a computational domain $X \times I \times t \in [X^{min}, X^{max}] \times [0, I^{max}] \times [0, T]$. Derivation of the boundary conditions for capped call options is similar and we define them at the relevant point in chapter 6.

5.4 Calculation of the temperature model parameters

To conclude this chapter we provide numerical estimates for the unknown parameters in the temperature SDE (5.6). The estimated parameter values are determined from using the data set *RTD* (see Appendix table B.2).

5.4.1 Estimating seasonal mean

Differing from Alaton et al. (2002), the method of non-linear least squares method (NLS) is used here to compute the parameters in seasonal mean (4.5). This involves searching for the parameter vector $\epsilon = (A, B, C, \phi)$ that solves

$$\min_{\epsilon} ||\mathbf{Y} - \mathbf{Z}||^2 \tag{5.44}$$

where $\mathbf{Y}$ is the vector with elements computed by (4.5) and $\mathbf{Z}$ is the real data vector. The statistical program R is used to perform the non-linear least squares fitting algorithm. The null hypothesis to be tested is that no one of the coefficients should appear in the model. The parameter estimates and their summary statistics are in table 5.1. For the A parameter, the t-statistic is large and its p-value is less than the computational precision level of $2\text{x}10^{-16}$, therefore assuming the absence of outliers, there is sufficient evidence to reject the null hypothesis that $A = 0$. The parameters C and ϕ are also significant. The t-statistic for B is not large enough to reject the null hypothesis. Therefore, B can safely be omitted from the model within the data range spanned by the sample. This leads to the following function for the seasonal mean temperature

$$\theta(t) = 11.56 + 2.87\text{x}10^{-6}t + 6.75\sin(\omega t - 1.90), \tag{5.45}$$

where t is measured in days and $\omega(= 2\pi/365)$ is the frequency. The constant -1.9 (measured in Radians) is a shift in the seasonal pattern, which when defined in units of t is approximately 110 days.

In order to validate the use of the developed model, a t-test is carried out. A two-tailed t-test is used to determine the likelihood that the proposed model

Parameter	Estimate	Std. Error	t-statistic	p-value (=Pr($>|t|$))
A	11.56	$7.735\text{x}10^{-02}$	149.41	$< 2\text{x}10^{-16}$ ***
B	$2.872\text{x}10^{-06}$	$2.393\text{x}10^{-05}$	0.12	0.904
C	6.749	$5.467\text{x}10^{-02}$	123.45	$< 2\text{x}10^{-16}$ ***
ϕ	-1.904	$8.107\text{x}10^{-03}$	-234.81	$< 2\text{x}10^{-16}$ ***

Table 5.1: The parameter values of the least-square model function (4.5). The standard error, t-statistic and its corresponding probability are shown for each parameter in columns three, four and five respectively. Where *** appears in the table it means that the significance level is approximately zero. 5599 observations were used. In the non-linear least square algorithm the parameters were initialise with the following values $A = 10$, $B = 0.002$, $C = 6$, $\phi = -1.90$

Parameter	Estimate	Standard Error
p-value	0.9860	N/A
t-statistic	0.01755	N/A
Mean of RTD	11.4755	$\pm$0.07459
Mean of proposed model	11.4772	$\pm$0.06382

Table 5.2: The table reports the $p - value$, the mean of RTD and mean of the proposed model (5.45). There are 11196 degrees of freedom. The significance level is at 5%.

(5.45) and RTD have the same mean (this is the null hypothesis). In this test, the significance level is set at 5%. It was confirmed from statistical analysis in table 5.2 indicates that there is not significant difference between the means RTD and the model (5.45). This is because the p-value(= 0.9860) is above the significance level. We also regress the proposed model (5.45) against the actual observed temperature at London Heathrow. Table 5.3 provides the statistics from the regression analysis and shows the similarity between the mean values of both the actual mean and approximated seasonal mean temperatures. Additionally, it highlights that almost 77% of temperature's behaviour can be explained by its seasonal mean.

The numerical results are consistent with our understanding of general weather conditions in the United Kingdom and the mean appears to visually match historical movements in figure 5.2. For example, the data shows that the difference between a typical winter day and a summer day is about 13°C, as the amplitude of the sine function is 6.75. We observe that the value of B is very small. This is to be expected since warming (or cooling) of the earth occurs over long time scales, and we have only taken the measurement over 15 years of historical data,

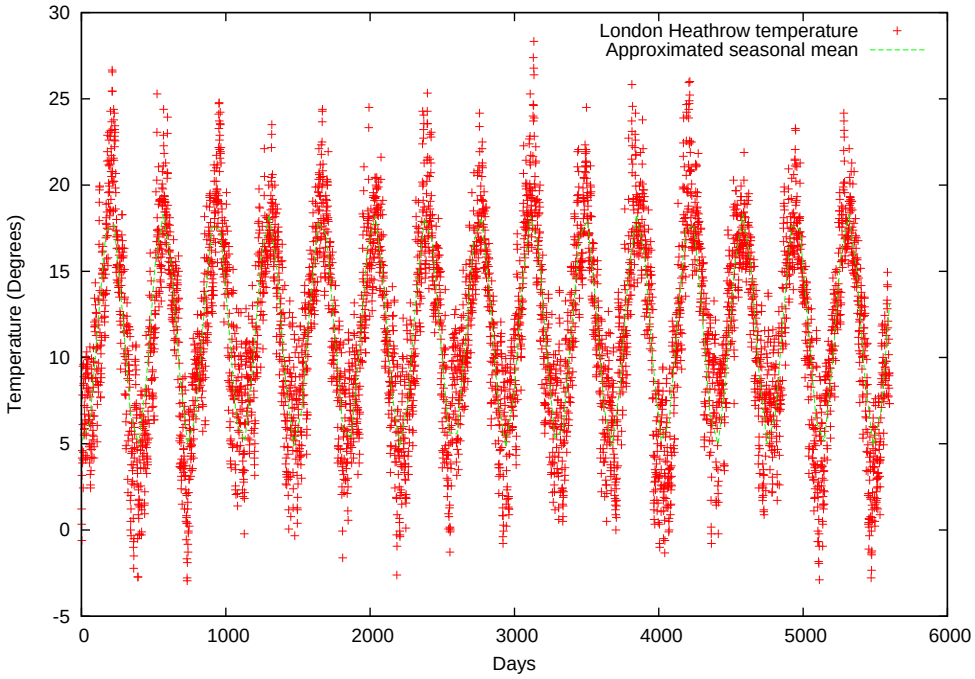

Figure 5.2: The figure plots the daily average temperature that is computed as the mean of the daily maximum and minimum values observed. The sample period extends from January 1st 1996 to May 12th 2010 with a total of 5599 observations. The green line displays the behaviour of the estimated seasonal mean.

from January 1st 1995 to May 12th 2010. Moreover, the rise in the temperature mean over the past 15 years is almost negligible at 0.0147°C.

5.4.2 Estimating $\sigma_X(t)$

Given that we are using a piecewise volatility function, the estimator is based on the quadratic variation (see Appendix A.1) of temperature $X(t)$:

$$\tilde{\sigma}_m^2 = \frac{1}{N_m} \sum_{j=0}^{N_m-1} (X(j+1) - X(j))^2, \tag{5.46}$$

where m is the specific month consisting of N_m days, with the observed temperatures during that month being denoted by $X(j)$ for $j = 1, \ldots, N_m$. This estimate is based on using one year of the *RTD* data set.

Differing from the study of Alaton et al. (2002), we do not simply take the estimate

Parameter	Value
Constant	0.0154
Beta	0.9985
R^2	0.7736
Mean of approximated seasonal mean temperature	11.4754
Mean of actual temperature	11.4772

Table 5.3: The statistics from the regression analysis.

Month	Estimation of $(\tilde{\sigma}_{avg})$	Estimation of $\tilde{\sigma}$
January	2.30974	2.51209
Febuary	2.09215	2.20502
March	1.88139	2.37840
April	1.83017	2.10051
May	1.83714	1.74256
June	1.75476	1.48755
July	1.62044	1.87269
August	1.54031	1.76075
September	1.64422	1.50615
October	1.94372	2.04457
November	2.32217	2.16213
December	2.48829	2.66395

Table 5.4: The calculated values for the two approximations for the function $\sigma_X(t)$ The first column calculations are based on formula (5.47) and the second column uses estimate (5.46) .

based on the most recent year's data, but make use of all the available data and average the respective volatility. It would be useful in future work to compare the two approaches on identical data sets. Then for each month we perform

$$(\tilde{\sigma}_{avg})_m^2 = \frac{\sum_{i=1}^{Y} \frac{1}{N_m} \sum_{j=0}^{N_m-1} (X^i(j+1) - X^i(j))^2}{Y} \tag{5.47}$$

where now, $X^i(j)$ is the observed temperature in year i on day j, again for $j = 1, \ldots, N_m$ and also $i = 1, \ldots, Y$, where Y represents the number of years used in the dataset. We present the results of both in table 5.4.

Parameter	Using $\tilde{\sigma}_m^2$	Using $(\tilde{\sigma_{avg}})_m^2$
$\hat{\kappa}$	0.2483	0.2546

Table 5.5: Estimated values of κ. We compute its value using the two different volatility estimates in equations (5.46) and (5.47).

5.4.3 Estimating κ

Next, to estimate the speed of mean reversion, the approach taken by Alaton et al. (2002), who use the martingale estimation functions method of Bibby and Sørensen (1995), is employed:

$$\hat{\kappa} = -\log\left(\frac{\sum_{i=1}^{n} G(t_{i-1})\left[X(t_i) - \theta(t_i)\right]}{\sum_{i=1}^{n} G(t_{i-1})\left[X(t_{i-1}) - \theta(t_{i-1})\right]}\right), \tag{5.48}$$

where

$$G(t_{i-1}) = \frac{X(t_{i-1}) - \theta(t_{i-1})}{\sigma^2(t_{i-1})}, \qquad i = 1, \ldots, n, \tag{5.49}$$

with $\theta(t)$ as defined in (4.4), and volatility values σ^2 as either (5.46) or (5.47). For ease of computation, the estimate of $\hat{\kappa}$ is computed by writing a C++ program. Table 5.5 shows the obtained estimated mean reversion parameter using the different estimates for volatility. A Welch two-sample t-test is performed to confirm the use of estimate $(\tilde{\sigma_{avg}})_m^2$ rather than $\tilde{\sigma}_m^2$. To do this, a 1000 possible temperature trajectories of (5.6) were obtained using the Monte-Carlo method and then averaged of these paths. The averaged trajectories are then used in the t-test to check the statistical likelihood that the mean is the same as the RTD. From the statistical analysis, it is confirmed that there is no significant difference between the mean of RTD and the mean temperature value produced when $\kappa = 0.2483$ because the $p - value(= 0.373)$ is above the significance level. A summary of the $p - value$ and the estimated means of the RTD data set and that of the model temperature values when $\kappa = 0.2483$ are presented in table 5.6. Therefore, it suggests that a suitable representation of the RTD is when the reversion rate is $\kappa = 0.2546$. For future work, it would useful to perform a statistical test to determine if the difference between the two levels of p are shown to be significant.

Statistic	Value
$p - value$	0.373
Mean of RTD	11.59
Mean of proposed model	11.49

Table 5.6: A summary of the results from the t-test used to compare the proposed model (5.6) ($\kappa = 0.2483$) with RTD. The table shows the $p - value$, which represents the probability that if the model is true, the difference between RTD and our model would be no larger than found here. Additionally we report the means of the proposed model and RTD. These values were computed using 5474 observations.

Empirical tests with real data

Given the derived estimates in §5.4.1 - §5.4.3, we can simulate possible trajectories and then make comparisons against the real temperature data. To do this, we use the Monte-Carlo method to simulate 1000 possible temperature trajectories, using the discrete version of the temperature process (5.6),

$$X_{t+1} = X_t + \theta^{'} \Delta t + \kappa \left[\theta(t) - X_t\right] \Delta t + \sigma_X(t) \sqrt{\Delta t} \phi, \tag{5.50}$$

and then take the average of these trajectories. Figure 5.3 shows a possible average temperature process compared with the RTD. To validate the use of this model, we perform a t-test, which measures the probability of the observed sample deviating from the null. Table 5.7 presents the summary of the statistical analysis. The $p - value$ obtained is larger than the critical value of 0.05 (95% confidence interval). This result indicates that there is not sufficient evidence to reject the hypothesis that the mean of the RTD and the mean of the developed model (5.6) are the same. The differences between the means of the two datasets are relatively small (see table 5.7). This finding suggest that the developed model is a valid representation for modelling the behaviour of temperature at London Heathrow. However, we do note that this model of weather does not allow for occasional very long, stably hot or cold spells to arise.

The choice of κ ensures that even if the weather today is wildly extreme, the temperature in the coming days will quickly return to a position about its seasonal mean. We illustrate such an example in figure 5.4(a) where we simulate a temperature path, but instead of setting the initial point at the seasonal mean

Statistic	Estimate	Standard Error
$p - value$	0.8335	N/A
Mean of RTD	11.59	± 0.0754
Mean of proposed model	11.61	± 0.0666
Std of RTD	5.567	± 0.0754
Std of proposed model	4.928	± 0.0666
Minimum value of RTD	-2.940	N/A
Minimum value of proposed model	-0.9895	N/A
Maximum value of RTD	28.33	N/A
Maximum value of proposed model	21.58	N/A

Table 5.7: A summary of the results from the t-test used to compare the proposed model (5.6) with RTD. The table shows the $p - value$, the mean of the proposed model and RTD, the standard deviation (denoted Std in the table) of both datasets. The standard error in these approximations is also shown. These values were computed using 5474 observations.

value on the day, we set the $X(0) = -50$. Figure 5.4(b) shows a possible simulated temperature path when $X(0) = 50$. In both instances it is apparent that after a few days the temperature has returned to more expected levels. More precisely, as $\kappa \approx 0.25$ it implies that there is about a 25% reduction per day in the difference between the current temperature and the seasonal mean. Thus it could take approximately 21 days for a temperature starting at $X = 50$ to reach the mean temperature of 5°C.

5.5 Summary

In this section a new model has been proposed that is based on the principles of mean-self financing and partial hedging. A PDE is consequently derived that values a weather-based contingent claim. The principle of mean-self financing implies that the expected change in the given portfolio is zero, which removes the remaining risk that existed due to the partial hedge. This is possible when the remaining weather risk can be diversified away, so as to leave a stable mean weather risk. The actual degree to which weather risk can be diversified is a key topic for future empirical research.

The mean-self financing assumption has been used in the literature and provides a suitable starting place from which to explore weather option pricing. The form

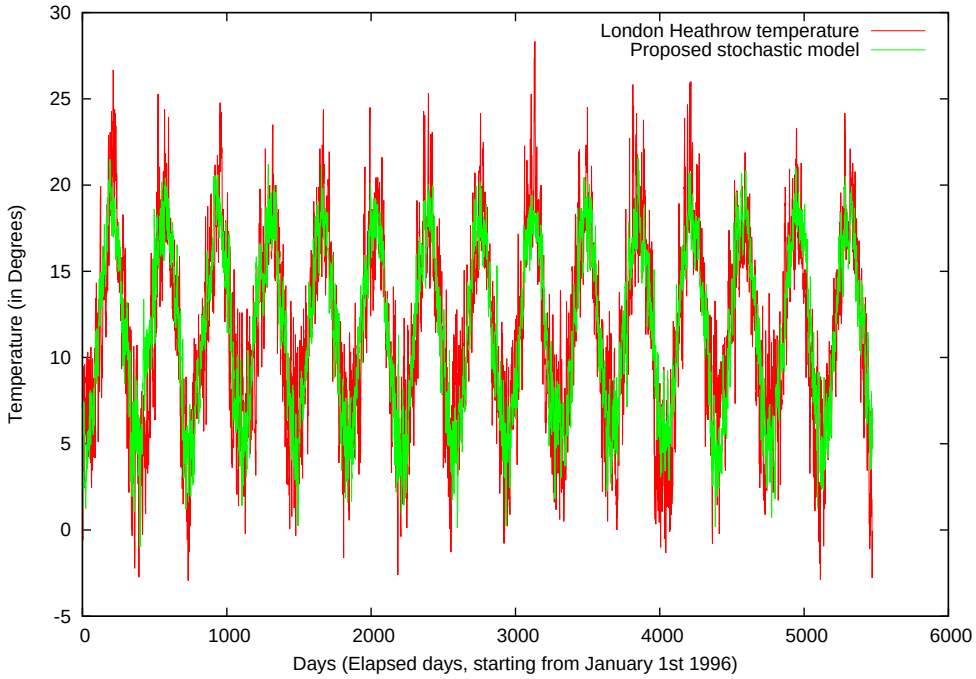

Figure 5.3: This figure plots the temperature data observed at London Heathrow from 1996 to 2010 and also the temperature values that are generated by the proposed stochastic process of temperature (4.4). The solid green line is computed by taking the average of several simulated paths of (4.4).

of our PDE is similar to that proposed Johnson (2007), with the exception that his derivation is for dividend paying asset with GBM. A similar PDE was also proposed by Windcliff et al. (2007), but we make use of a different underlying process (mean-reverting process). However, their model contains the real-world drift which is difficult to estimate. Avellaneda, Levy, and Paras (1995) suggest the use of worst case pricing when the real-world drift remains in the pricing equations, assuming that the parameter lies between known bounds. Our weather PDE model has the presence of the real-world drift (or more precisely the seasonal mean) but only for the temperature for which estimation of parameters is more robust than for those used to determine stock price drifts. Therefore, it is not a requirement in this case to rely on worst-case pricing. Furthermore, we demonstrated that in the special case where the drifts of X and H are identical the presence of the real-world percentage drift of the correlated instrument can be eliminated.

The model is an improvement on other weather pricing approaches for the following reasons:

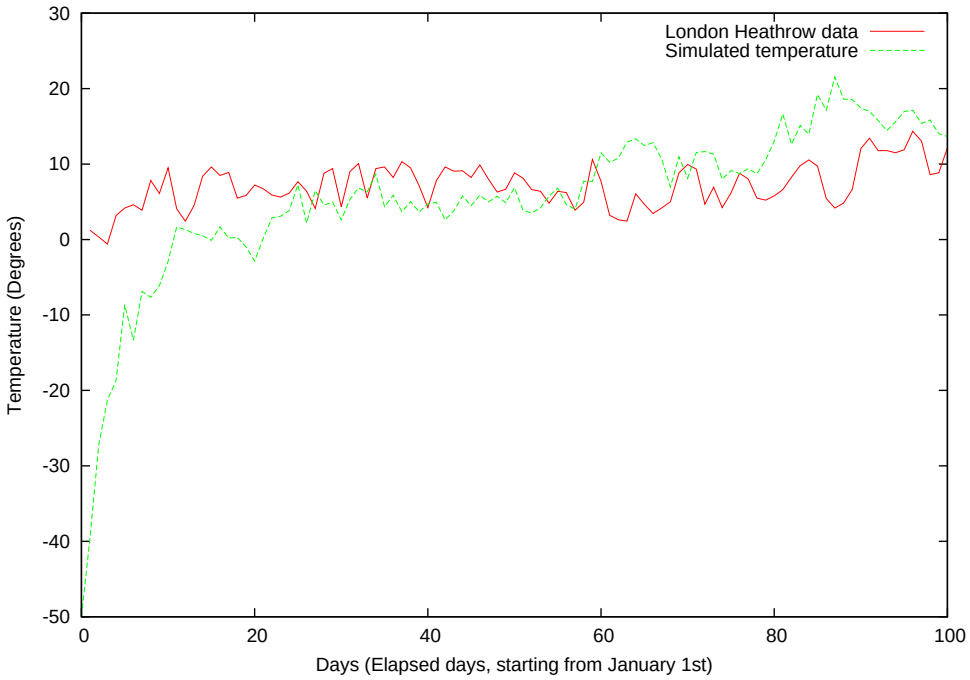

(a) $X = -50$

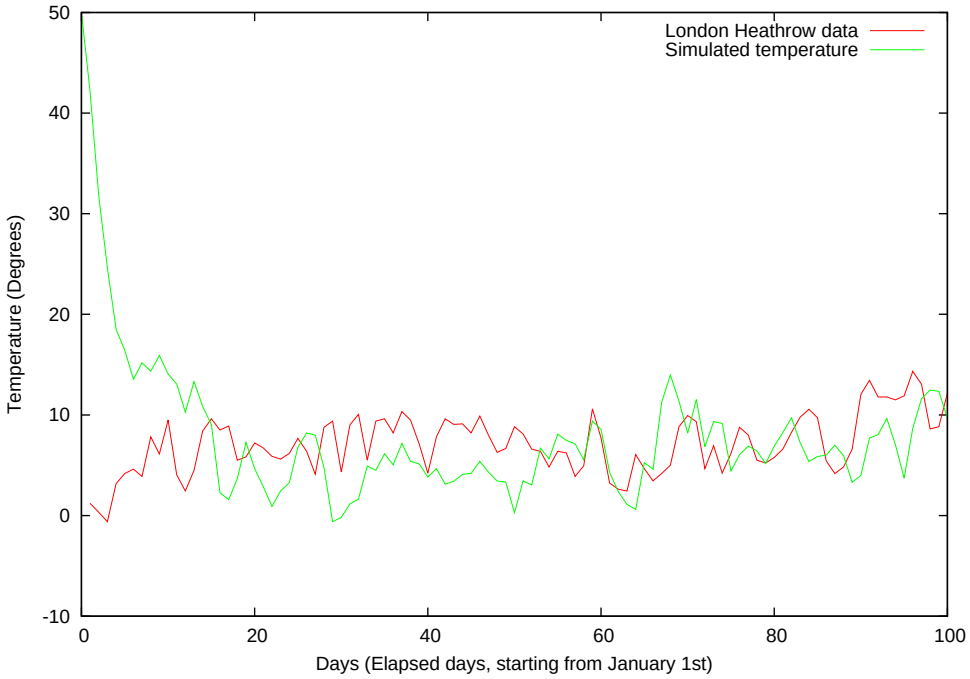

(b) $X = 50$

Figure 5.4: A simulated temperature path, generated using Monte Carlo method. This illustrates the speed at which the temperature process with revert back to its respective mean-level for that time of year given an extreme initial temperature.

- Using a PDE approach allows for the option value to be determined at any point in time, without re-computations.
- The model can be extended to include more complicated underlying processes, which perhaps more closely correlate with temperature throughout a particular time period.
- We can value weather options long before the start date of the averaging period. The value of the option in this instance will be similar to an Asian tail option, since in this case the averaging period does not start at the inception of the contract, but rather sometime after (Wilmott, 2000a). The start of the averaging window will now be expressed as t^* given that $t^* \in [0, T]$. We cite the work of Law (2009) as a guide on the computation of such an option.

The form of the derived PDE (5.29) makes it a challenging problem to solve, and we describe in the next chapter the issues that arise from the application of various numerical schemes. Since the PDE behaves like an advection PDE in certain regions, this requires the use of non-standard numerical techniques, which we demonstrate in detail in the next chapter.

Chapter 6

Numerical solutions of weather options

In this chapter, we consider the pricing of a weather derivative using our PDE from chapter 5, which we restate here

$$\frac{\partial V}{\partial t} + \frac{1}{2}\sigma_X^2 \frac{\partial^2 V}{\partial X^2} + \gamma(X_t, t)\frac{\partial V}{\partial X} + f(X_t, t)\frac{\partial V}{\partial I} - rV = 0, \tag{5.29}$$

where

$$\gamma(X, t) = \mu_X(1 - \rho) + \rho r, \tag{5.26}$$

and

$$\theta(t) = A + Bt + C\sin(\omega t + \phi). \tag{4.5}$$

Throughout this chapter, unless stated, we consider valuing HDD options such that

$$f(X_t, t) = (X_{ref} - X_t)^+. \tag{5.9}$$

The boundary conditions for pricing a European HDD capped put option (as explained in §5.3) are given as

$$\frac{\partial V(X, I, t)}{\partial t} + \gamma(X, t)\frac{\partial V(X, I, t)}{\partial X} + (X_{ref} - X)^+ \frac{\partial V(X, I, t)}{\partial I} - rV = 0, \quad \text{for} \quad X \to X^{min}, \tag{5.40}$$

$$\frac{\partial V}{\partial X}(X, I, t) = 0, \quad \text{for} \quad X \to X^{max}, \tag{5.41}$$

$$\lim_{I \to \infty} V(X, I, t) = 0, \quad \text{for} \quad I \to \infty, \tag{5.42}$$

with final condition

$$V(X, I, T) = \min(\max(K - I, 0) \cdot tick, cap). \tag{5.32}$$

This chapter is organised as follows. First, we explain the properties of the weather option PDE, and compare it with existing PDEs in the financial literature. Then, we provide descriptions of the numerical methods that may be used to appropriately determine the value of a weather derivative. When describing the numerical methods, we carefully examine their limitations when solving (5.29) and where possible highlight the necessary conditions under which these limitations are avoided or significantly reduced.

6.1 Similar PDEs

In pursuit of determining a suitable solution to the PDE (5.29), this section begins by comparing the PDE form to other similar models that have been presented. The fact that weather derivative contracts depend on an underlying that is an averaging of temperature suggests a strong link to Asian options. An Asian option has a payoff that depends on an average price or quantity of the underlying over a specified time horizon. The averaging may be discrete or continuous, and arithmetic or geometric. Taken from Law (2009), the continuous-time geometric and arithmetic averages of an asset S are given respectively by

$$\begin{aligned} I^G(t) &= \exp\left[\frac{1}{t}\int_0^t \ln(S(u))\mathrm{d}u\right], \\ I^A(t) &= \frac{1}{t}\int_0^t S(u)\mathrm{d}u. \end{aligned}$$

Explanations of either of the approaches can be found in Wilmott et al. (1995). Weather derivatives underlying index variables are typically of the arithmetic form and therefore we shall only consider them in this thesis. As we discussed in §2.2.2, discrete sampling of the average may be more realistic but here the main focus is on the continuous case for the reasons outlined in §2.2.1. It is helpful to view the pricing of a degree-day weather option as an arithmetic Asian option with no averaging being performed at maturity, and we observe that standard Asian

option pricing equations as found in Wilmott et al. (1995) and Zvan, Forsyth, and Vetzal (1996) bear a strong resemblance to PDE (5.29).

Ideally, the problem would be solved analytically, however, Wilmott et al. (1995) details that this is generally not possible. This happens if the payoff condition cannot be written in the form

$$S^{\eta}F(I/S,t), \tag{6.1}$$

for some constant η and function F. When this is possible, the dimensionality of problem can also be reduced through application of a similarity reduction. However, in the case of (5.29) this cannot be done because typical boundary conditions for weather options are not linearly homogeneous in X and I (see Wilmott et al., 1995, for an illustration of how to use a similarity reduction to simplify a PDE). Wilmott et al. (1995) states that to value arithmetic Asian options we must resort to numerical methods or approximations. Therefore, as the weather option is akin to valuing an arithmetic Asian option we too must utilise numerical approximations. Making this connection we are able to draw upon the vast array of numerical techniques presented for valuing Asian options. Kemna and Vorst (1990) prefer the simple implementation of Monte Carlo methods with a variance reduction. Adopting a PDE approach, Alziary, Décamps, and Koehl (1997) use an explicit finite-difference scheme to evaluate a European Asian option, though Zvan et al. (1996) show that standard finite-difference schemes (such as explicit schemes) are inaccurate and propose the use of a flux limiting technique to improve accuracy. Law (2009) utilises a hybrid finite-differencing scheme, which also uses the QUAD method as detailed in Andricopoulos et al. (2003), to value more complex Asian options. More details of the variety of available Asian options can be found in Wilmott (2000b) and we provide no further details on this topic.

Recall that by definition, a degree day is usually determined by examining the number of degrees above/below the barrier temperature that the temperature has reached over a given time period. The differences in degrees are then accumulated to form the index, which is subsequently used in the payoff function. Given the combination of the barrier component and the accumulation that occurs, it would be more appropriate to view a weather derivative contact as a ParAsian option (Xiao, 2007). This type of option monitors the cumulative time the underlying process has spent either above or below a specified barrier. Depending on the

accumulated quantity, the option may provide payoff (is activated) or not (is extinguished). If we consider the case of an 'up and in' ParAsian option, payoff will be made only if the underlying process has maintained a value greater than say B, for a given time length $\bar{t}$.

The idea of applying Asian options to pricing weather derivatives has been considered by Harris (2003) and Hamisultane (2008), who employ Asian options to capture the averaging feature of the weather index I. Here, the weather option is view as a ParAsian option since a weather derivative payoff typically contains an averaging and barrier feature. Sharp (2006) uses a ParAsian option to model mortgage valuation. To model bankruptcy, Johnson (2007) uses ParAsian options and consequently proposes a new option called the ParAsian Integral Time option. This option not only monitors the cumulative time spent above the barrier, but also the resulting area above/below the barrier. This area is defined by

$$I = \int_0^t \mathrm{d}I(t), \tag{6.2}$$

with

$$\mathrm{d}I = \begin{cases} 0 & \text{if } S(t) < B \\ \epsilon\,(S(t) - B)\,\mathrm{d}t & \text{if } S(t) \geq B \end{cases}, \tag{6.3}$$

where ϵ is a scaling parameter that is similar a *tick* multiplier. The resulting PDE in Johnson (2007) is of a similar form to our PDE (5.29) with the exception that his derivation is for dividend paying asset with GBM (3.4):

$$\frac{\partial V}{\partial t} + \frac{1}{2}\sigma^2 S^2 \frac{\partial^2 V}{\partial S^2} + (r-d)S\frac{\partial V}{\partial S} - rV = 0 \quad \text{if } S < B \quad , \tag{6.4}$$

$$\frac{\partial V}{\partial t} + \frac{1}{2}\sigma^2 S^2 \frac{\partial^2 V}{\partial S^2} + (r-d)S\frac{\partial V}{\partial S} + \epsilon\,(S-B)\,\frac{\partial V}{\partial I} - rV = 0. \quad \text{if } S \geq B \quad . \tag{6.5}$$

The introduction of the additional dimension I in (6.5) can lead to highly oscillatory solutions when using a standard Crank-Nicolson scheme (for more details of the Crank-Nicholson scheme refer to Smith, 1985). This happens as the scheme fails to deal with situations where the solution changes rapidly with respect to I. Johnson (2007) concludes that the use of a one-sided implicit scheme provides smoother solutions, though accuracy is lost without the use of excessively small grid spacing. Windcliff et al. (2007) use a fully implicit scheme and develop an algorithm to ensure that particular grid conditions are maintained by inserting a

finite number of nodes in an initial grid. In the following section the one-sided implicit scheme is outlined, and an improved numerical scheme is introduced in §6.2.

6.2 Numerical schemes for advection equations

Valuing a weather derivative based on numerically solving PDE (5.29) presents various challenges. As reported by Morton and Kellogg (1996), numerical evaluation of this type of PDE is difficult, and as mentioned above, the use of standard finite-difference schemes results in poor approximations due to the absence of a second-order derivative in I. By grouping particular terms in (5.29), the problem can be recast as an advection equation. To see this, we firstly make the usual transformation of $\tau = T - t$, with T being final time, and rewrite (5.29) to obtain

$$\frac{\partial V}{\partial \tau} - f(X,\tau)\frac{\partial V}{\partial I} = \frac{1}{2}\sigma_X^2 \frac{\partial^2 V}{\partial X^2} + \gamma(X,\tau)\frac{\partial V}{\partial X} - rV. \tag{6.6}$$

The left-hand side (LHS) is a classical example of an advection type equation and the RHS is a convection-diffusion equation. In this section we examine various schemes that may be used to obtain accurate solutions for advection PDEs. We introduce these methods in a simple context, to ensure clarity in the descriptions of the proposed numerical schemes.

Consider the one-dimensional linear advection equation

$$\frac{\partial U}{\partial \tau} + k\frac{\partial U}{\partial x} = 0, \tag{6.7}$$

with positive constant coefficient k. The first term on the LHS of the above equation is the local rate of change of U with respect to time and the second term is referred to as the advection term. This simple advection equation (6.7) has the well known general solution of

$$U(x,\tau) = U_0(x - k\tau), \tag{6.8}$$

which is obtained using the method of characteristics (Farlow, 1993). However, we consider evaluating this advection PDE numerically by discretising it on a uniform

two-dimensional mesh with spacing Δx and time step $\Delta\tau$ and then compare the numerical solution to the analytical one. The spatial nodes are denoted by i, and n denotes the time levels. Therefore the locations on our mesh are given by

$$x_i = x_0 + i\Delta x, \quad i = 0, 1, \ldots, i_{max} \quad , \tag{6.9}$$

$$\tau_n = \tau_0 + n\Delta\tau, \quad n = 0, 1, \ldots, n_{max} \quad . \tag{6.10}$$

As we are interested in solving the PDE for $U(x, \tau)$, we only consider the values of U at discrete points in the mesh, such that at node (i, n)

$$U(x, \tau) \to U(x_0 + i\Delta x, \tau_0 + n\Delta\tau) \equiv U_i^n \tag{6.11}$$

From this we have that a given numerical scheme is convergent if for successive grid refinements the numerical solution tends to the analytical one (or true solution), i.e.,

$$U_i^n \to U(x_i, \tau_n) \qquad \forall \quad i, n, \tag{6.12}$$

as $\Delta x \to 0$ and $\Delta\tau \to 0$. If this is not satisfied then we can conclude that the scheme is inappropriate for the problem.

There are several ways to discretise each of the differential terms in (6.7) and here we consider some typical examples, but for more details see Smith (1985).

6.2.1 Standard finite-difference schemes

Central differencing in space

Using a central difference scheme for the derivative with respect to x may result in spurious oscillations appearing the solution, as stated by Morton and Kellogg (1996) and further illustrated in Harris (2003). To see this oscillatory behaviour, write the difference equations as

$$\frac{\partial U(x, \tau)}{\partial x} = \frac{U_{i+1}^n - U_{i-1}^n}{2\Delta x} + O(\Delta x)^2, \tag{6.13}$$

$$\frac{\partial U(x, \tau + \Delta\tau)}{\partial \tau} = \frac{U_i^{n+1} - U_i^n}{\Delta\tau} + O(\Delta\tau). \tag{6.14}$$

The above discretisation is commonly referred to as a forward time and centred space scheme (FTCS). Equation (6.7) then becomes

$$\frac{U_i^{n+1} - U_i^n}{\Delta\tau} = -k\frac{U_{i+1}^n - U_{i-1}^n}{2\Delta x}, \tag{6.15}$$

where on rearrangement we obtain

$$U_i^{n+1} = U_i^n - \frac{k\Delta\tau}{2\Delta x}(U_{i+1}^n - U_{i-1}^n). \tag{6.16}$$

This scheme is said to be unstable and this can be confirmed using Von Neumann stability analysis. This consists of inserting a trial solution into the numerical scheme and determining if as time increases does the solution grow. To see this explicitly, consider the trial solution

$$U(x,\tau) = z(\tau)e^{ikx}, \tag{6.17}$$

however here we redefine i such that $i = \sqrt{-1}$. For the remainder of this subsection i denotes an imaginary number and we replace old subscripts i with m; thus, U_m^n denotes the solution at time-step n and grid point m. Using the discrete representations of the solution, substitute 6.17 into the equation of the scheme (6.16):

$$\begin{aligned} z_{n+1}e^{ik(m\Delta x)} &= z_n e^{ik(m\Delta x)} - \frac{k\Delta\tau}{2\Delta x}\left\{z_n e^{ik(m+1)\Delta x} - z_n e^{ik(m-1)\Delta x}\right\} \\ &= z_n e^{ik(m\Delta x)}\left\{1 - \frac{k\Delta\tau}{2\Delta x}[e^{ik\Delta x} - e^{-ik\Delta x}]\right\} \\ &= z_n e^{ik(m\Delta x)}\left\{1 - \frac{k\Delta\tau}{\Delta x}\cdot i\sin(k\Delta x)\right\}. \end{aligned} \tag{6.18}$$

The amplification factor is given by

$$|\zeta| = \sqrt{1 + \left(\frac{k\Delta\tau}{\Delta x}\right)^2 \sin^2(k\Delta x)}. \tag{6.19}$$

Clearly $|\zeta| \geq 1$ for all combination of grid sizes. Therefore it is not appropriate for solving (6.7) since the solution modulus $|U_m^n|$ grows exponentially.

Lax Method

To overcome the instability problems of the above scheme, it is possible to use the Lax method. We revert to using i subscript to denote a grid point location. The Lax method essentially replaces the value at U_i^n with its average. Therefore (6.16) becomes

$$U_i^{n+1} = \frac{1}{2}(U_{i+1}^n + U_{i-1}^n) - \frac{k\Delta\tau}{2\Delta x}(U_{i+1}^n - U_{i-1}^n). \tag{6.20}$$

If we consider the Taylor series expansions

$$\begin{aligned} U(x+\Delta x,\tau) &= U(x,\tau) + \Delta x\frac{\partial U}{\partial x} + \frac{\Delta x^2}{2}\frac{\partial^2 U}{\partial x^2} + \frac{\Delta x^2}{6}\frac{\partial^3 U}{\partial x^3} + \ldots, & (6.21)\\ U(x-\Delta x,\tau) &= U(x,\tau) - \Delta x\frac{\partial U}{\partial x} + \frac{\Delta x^2}{2}\frac{\partial^2 U}{\partial x^2} - \frac{\Delta x^2}{6}\frac{\partial^3 U}{\partial x^3} + \ldots, & (6.22) \end{aligned}$$

we find that

$$\begin{aligned} U(x+\Delta x,\tau) - U(x-\Delta x,\tau) &= 2\Delta x\frac{\partial U}{\partial x} - \frac{(\Delta x)^3}{3}\frac{\partial^2 U}{\partial x^2} + \ldots, & (6.23)\\ U(x+\Delta x,\tau) + U(x-\Delta x,\tau) &= 2U(x,\tau) + (\Delta x)^2\frac{\partial^2 U}{\partial x^2} + \ldots. & (6.24) \end{aligned}$$

Using the expressions of (6.23) and (6.24) and ignoring terms smaller than $(\Delta x)^2$, (6.20) can be expressed as

$$\frac{U(x,\tau+\Delta\tau) - U(x,\tau)}{\Delta\tau} = -k\frac{\partial U}{\partial x} + \frac{(\Delta x)^2}{2\Delta\tau}\frac{\partial^2 U}{\partial x^2}, \tag{6.25}$$

which is none other than

$$\frac{\partial U}{\partial \tau} = -k\frac{\partial U}{\partial x} + \frac{(\Delta x)^2}{2\Delta\tau}\frac{\partial^2 U}{\partial x^2}. \tag{6.26}$$

The presence of the second-derivative term clearly shows that artificial diffusion has been introduced into the equation. This is not necessarily undesirable, as diffusion smooths out the instabilities that previously existed. The scheme is stable if the time grid size is chosen to satisfy

$$\Delta\tau \leq \frac{\Delta x}{k}. \tag{6.27}$$

However, given that $\Delta\tau$ appears in the denominator of the coefficient of the diffusion term in (6.26), it implies that if $\Delta\tau \to 0$ faster than $(\Delta x)^2 \to 0$ then this coefficient will grow and result in the artificial diffusion dominating the solution.

One-sided differencing schemes

Wilmott (2000a) and Morton and Kellogg (1996) suggest that the differential operators of the spatial variable be approximated by a one-sided difference scheme. This scheme can be specified as either *downwind* or *upwind*, and the choice of scheme to use is dependent on the directional flow of information, denoted by k. In the mathematical finance literature, the terms upwind and downwind are sometimes referred to as upstream and downstream respectively. The terms ending with 'wind' refer to the flow of air, whereas those ending in 'stream' refer to the flow of fluid; in this thesis, we use the terms ending in 'wind'. Let us consider a given grid point i in our two-dimensional domain, at any given time the particle can only move in two directions: left or right. When $k \geq 0$, moving to the left side of the domain is referred to as the *upwind* side and the right side is known as the *downwind* side, The reverse is true when k is negative. Consequently, depending on the sign of k we are able to choose the appropriate one-sided discretisation scheme to solve the advection equation (6.7), which leads to the following (explicit) first-order approximations

$$\frac{U_i^{n+1} - U_i^n}{\Delta\tau} + k\frac{U_i^n - U_{i-1}^n}{\Delta x} = 0, \qquad \text{for } k \geq 0\ , \tag{6.28}$$

or

$$\frac{U_i^{n+1} - U_i^n}{\Delta\tau} + k\frac{U_{i+1}^n - U_i^n}{\Delta x} = 0, \qquad \text{for } k < 0\ . \tag{6.29}$$

A Taylor series analysis of the one-sided schemes above shows that these are first-order accurate in both space and time, i.e. $O(\Delta\tau)$ and $O(\Delta x)$. As with all explicit schemes, stability is only guaranteed when the Courant-Friedrichs-Lewy condition (CFL) is satisfied (see Courant, Friedrichs, and Lewy, 1928), namely

$$\left| k\frac{\Delta\tau}{\Delta x} \right| \leq D. \tag{6.30}$$

where the constant D depends on the equation being solved, and the number $C = k \cdot \Delta\tau/\Delta x$ is called the Courant number. The inequality (6.30) imposes

restrictions on the time-step spacing $\Delta\tau$. In other words, the discrete step forward in τ must be smaller than the time taken for the particle to travel to the an adjacent grid point.

Using an implicit version of the one-sided difference scheme removes the CFL restriction and ensures stability. This is at the expense of introducing artificial diffusion in regions with large gradients. We see this by performing the same analysis as used to derive (6.26) to determine that using this scheme the PDE has errors that equal the RHS of the following equation

$$\frac{\partial U}{\partial \tau} + \frac{\partial U}{\partial x} = -\frac{\Delta\tau}{6}\frac{\partial U}{\partial \tau} + \frac{\Delta x}{2}\frac{\partial^2 U}{\partial x^2}. \tag{6.31}$$

Using an example we illustrate this introduction of artificial diffusion. Consider an implicit finite-difference scheme, with $k = 1$ and initial condition

$$U(x,0) = \begin{cases} 0 & x < 0 \\ 1 & x \geq 0 \end{cases}. \tag{6.32}$$

Using different grid sizes for ΔX and Δt the solution is computed and then compared with the analytic solution ($U(x-\tau)$), see figure 6.1. to make visual comparisons between the different solutions. In regions where the first-order derivative in x is not defined, i.e. near $x \approx 0$, this initially causes the second-order derivative to be unbounded and large, meaning that the diffusive term will dominate. This can be observed in figure 6.1 where the solution appears excessively smoothed in the region $x = 1$, which is the location where there is a discontinuity in the first derivative at $t = 1$. The analytical solution shows that from definition of the PDE (6.7) the initial condition profile must be preserved throughout time. The figure highlights that by significantly reducing the grid size in x, the diffusion can be suppressed.

To reduce the diffusive nature of an *upwind* scheme it may be appropriate to use higher-order versions of the scheme. We state the formulas for just the upwind schemes as the downwind schemes are symmetrical. In the case of a *upwind* scheme, equation (6.28) can be represented by the following second-order scheme only in x,

$$\frac{U_i^{n+1} - U_i^n}{\Delta\tau} - k\frac{3U_i^n - 4U_{i-1}^n + U_{i-2}^n}{2\Delta x} = 0 \tag{6.33}$$

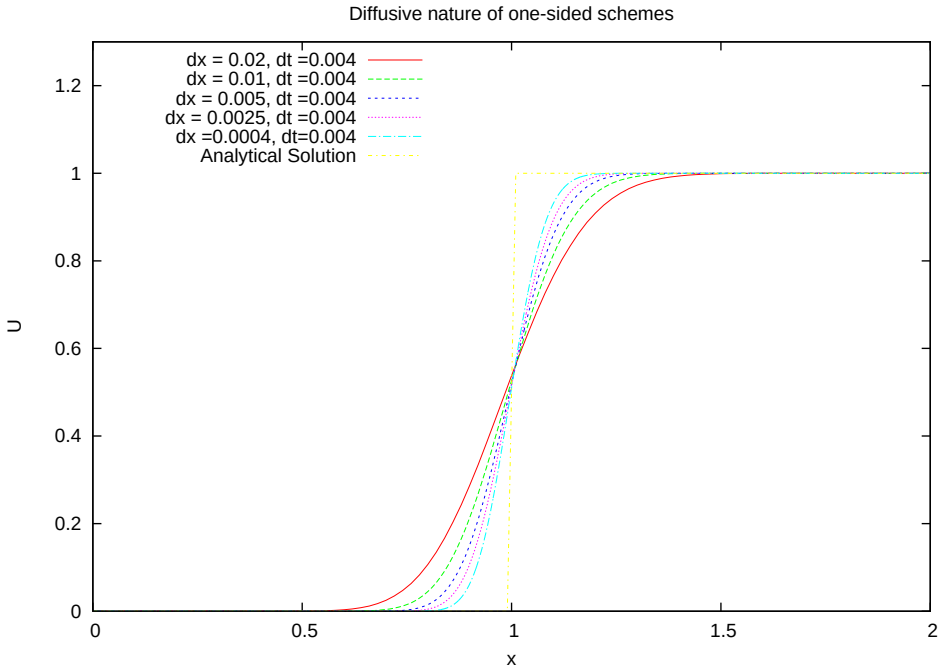

Figure 6.1: Diffusion that persists in a one-sided finite difference scheme. Here $c = 1$. The analytical solution shown in the figure is $U(x - \tau)$

and the third-order scheme is

$$\frac{U_i^{n+1} - U_i^n}{\Delta\tau} - k\frac{2U_{i+1}^n + 3U_i^n - 6U_{i-1}^n + U_{i-2}^n}{6\Delta x} = 0. \tag{6.34}$$

6.2.2 The Lagrangian derivative

Rather than using traditional Eulerian-based methods, such as the methods discussed in the previous section, we now consider using Lagrangian-based schemes. A Lagrangian description of a system is often used in fluid dynamics, and is a way of observing the properties of a fluid while travelling along an individual fluid parcel[1] as it moves in space and time (Batchelor, 2000). This differs from an Eulerian description, whereby fluid properties would be measured from a fixed location in space. For example, suppose we have two researchers Dan and Tom, who wish to measure the temperature change over time in a river. Tom records the temperature changes at uniform time intervals by attaching a thermometer

[1]A fluid parcel is simply a small collection of very small fluid particles moving in a fluid flow Batchelor (2000)

to a rock that lies on the river bed. This is an example of measuring a property of the fluid from a fixed location as the fluid flows by, and is referred to as the Eulerian description. On the other hand, Dan attaches a thermometer to a free floating buoy, and records the temperature of the river as the buoy (and hence thermometer) moves along with the flow of the river. So rather than having a fixed co-ordinate system, we have a moving co-ordinate system that is known as the Lagrangian description of a fluid (Batchelor, 2000). Furthermore, this gives rise to the term the *Lagrangian derivative*, which is a derivative taken with respect to a moving co-ordinate system.

Next we derive the Lagrangian derivative, using the above temperature example. Let $U(x,\tau)$ denote temperature of the fluid in one-dimension, with τ being time. Suppose that the fluid parcel moves with velocity $g(x,\tau)$. By using a Lagrangian description of the system, our location x is no longer fixed as time passes, but instead moves along with the fluid with velocity $g(x,\tau)$. This gives rise to the following definition for the Lagrangian derivative

$$\frac{DU}{D\tau} = \lim_{\Delta\tau\to 0} \frac{U(x+f\Delta\tau, \tau+\Delta\tau) - U(x,\tau)}{\Delta\tau}. \tag{6.35}$$

Using the Taylor series expansion of the term at time $\tau+\Delta\tau$, and assuming that $\Delta\tau$ is small enough such that the quadratic and higher order terms are negligible, gives,

$$U(x+f\Delta\tau, \tau+\Delta\tau) = U(x,\tau) + \Delta\tau\frac{\partial U}{\partial\tau} + f\Delta\tau\frac{\partial U}{\partial x}. \tag{6.36}$$

Taking this series and substituting into (6.35), we obtain after simplifications

$$\frac{DU}{D\tau} = \frac{\partial U}{\partial\tau} + \frac{\mathrm{d}x}{\mathrm{d}\tau}\frac{\partial U}{\partial x}, \tag{6.37}$$

and use the fact that the velocity f is equivalent to $\frac{\mathrm{d}x}{\mathrm{d}\tau}$. The Lagrangian derivative operator can be given as

$$\frac{D}{D\tau} \equiv \frac{\partial}{\partial\tau} + \frac{\mathrm{d}x}{\mathrm{d}\tau}\frac{\partial}{\partial x} \tag{6.38}$$

or as is typically seen in fluids textbooks (such as Batchelor, 2000), in multiple dimensions

$$\frac{D}{D\tau} \equiv \frac{\partial}{\partial\tau} + \mathbf{k}\cdot\nabla \tag{6.39}$$

where $\mathbf{k}$ is the velocity field and $\nabla \equiv (\frac{\partial}{\partial x}, \frac{\partial}{\partial y}, \frac{\partial}{\partial z})$ is the rate of change in U in three

spatial variables x, y and z. The ordinary differential equation (ODE) (6.37) tells us that the total rate of change of temperature as the fluid parcel travels with velocity f is equal to the sum of the local rate of change and convective rate of change of U. Here it is appropriate to use $\frac{D}{D\tau}$ rather than $\frac{\mathrm{d}}{\mathrm{d}\tau}$ to distinguish from the ordinary understanding in mathematics for the derivative of a function of one variable.

If we consider our original example (6.7), the Lagrangian derivative is given by

$$\frac{DU}{Dt} = \frac{\partial U}{\partial t} + \frac{\mathrm{d}x}{\mathrm{d}t}\frac{\partial U}{\partial x} \tag{6.40}$$

along the trajectory

$$\frac{\mathrm{d}x}{\mathrm{d}t} = k. \tag{6.41}$$

This reduces equation (6.7) to the ODE

$$\frac{DU}{Dt} = 0. \tag{6.42}$$

A physical interpretation of this ODE could be that the quantity U is conserved under transport along a fluid path (or characteristic).

6.2.3 Semi-Lagrangian Scheme

Semi-Lagrangian schemes (hereafter SLS) were first introduced by Douglas Jr and Russell (1982) for numerical atmospheric and weather predictions, which is fitting, as we shall employ this technique in the case of weather derivatives. This scheme has attracted considerable interest since its introduction, and Randall (2009) suggests that this interest is because SLS provide the same level of accuracy for larger time steps than those used in Eulerian-based schemes, and more easily maintains properties such as monotonicity. Although SLS have several advantages over other finite-difference schemes, there are a few inherent issues:

1. severe truncation errors may cause misleading results;
2. the integration of Lagrangian trajectories and interpolations of the particles may increase computational time.

The reasons for using SLS is to attempt to exploit the benefits of having a fixed computational grid, as found in Eulerian-based schemes but with the enhanced stability of Lagrangian methods, implying that computational times can be reduced, as the time-step $\Delta\tau$ can be larger than those required in Eulerian-based schemes; in others words the CFL condition need not be met. As the name implies, the SLS is a hybrid of the Eulerian and Lagrangian methods. As mentioned in §6.2.2, in an Eulerian scheme an observer stays at a fixed location and watches the world evolve around him, whereas in a Lagrangian scheme the observer watches the world evolve as he moves along a fluid path. A SLS allows the observer to travel along a fluid path whilst ensuring that at the end of each time-step the arrival location is exactly at a computation grid point.

The application of SLS within finance is very limited. The popularity of this method remains with the fluid dynamics community. In the mathematical finance literature, we start with the work of Parrott and Clarke (1998) who use the SLS to value an American-Asian option and demonstrate that it accurately integrates the convection terms appearing in their Asian option PDE. They also introduce a parallelised version of the SLS to enable the valuation of American-Asian options with stochastic volatility. For valuation of a weather derivative where, differing from our work in chapter 5, the underlying is the actual weather index, Harris (2003) illustrates that due to the convection-dominance of her derived PDE, application of SLS eliminates spurious oscillating solutions. We give special credit to Forsyth, who has provided a extensive collection of papers on the use of SLS and their applications in a variety of settings. The following are works which have involved Forsyth and made use of SLS: d'Halluin, Forsyth, and Labahn (2006) demonstrate the scheme's ability to enable the pricing of Asian options with jumps, and also those that follow Levy processes in Wang, Wan, and Forsyth (2007); the solution of an optimal gas storage problem is in Chen and Forsyth (2007); and in Forsyth, Kennedy, Tse, and Windcliff (2009) the scheme is used to decouple the linear and nonlinear components of the PDE used in determining the optimal liquidation strategy in the presence of price impact. In addition to Forsyth, we note that recently the method has been applied by Evatt et al. (2010a) and Evatt et al. (2010b) to the valuing of a mine, under price, interest and convenience yield uncertainties.

The next three sections provide a review of the application of SLS by applying the method to a simple problem to demonstrate its effectiveness, and illustrate the numerical errors that are associated with using the scheme. In section §6.3 our weather PDE (5.29) is then solved using SLS.

Application of the SLS

Consider a 1D advection equation similar to that of (6.7), but now with a variable coefficient of advection $g(x, \tau)$ such that,

$$\frac{\partial U}{\partial \tau} - g(x, \tau)\frac{\partial U}{\partial x} = 0. \tag{6.43}$$

where $x_{min} \leq x \leq x_{max}$. The initial condition here is given when $t = 0$, which occurs when $\tau = T$ (by definition that $\tau = T - t$); therefore,

$$U(x, 0) = g(x, T), \tag{6.44}$$

and the we impose the Dirichlet boundary condition,

$$U(x_{min}, \tau) = 0. \tag{6.45}$$

Using the Lagrangian derivative operator (6.38), the PDE (6.43) reduces to the ODE

$$\frac{DU}{D\tau} = 0 \tag{6.46}$$

along the trajectory

$$\frac{\mathrm{d}x}{\mathrm{d}\tau} = -g(x, \tau). \tag{6.47}$$

The essence of the SLS is to approximately integrate the PDE (6.43) along the trajectory given by (6.47) (Randall, 2009). To integrate along this trajectory, the point where a given parcel originated is calculated at every time step. We refer to the point of origination as the *departure point* and its current position as the *arrival point*. The departure point is calculated by solving

$$\frac{\mathrm{d}x}{\mathrm{d}\tau} = -g(x, \tau) \tag{6.48}$$

backwards from $\tau = \tau_{n+1}$ to $\tau = \tau_n$. The reason for doing this is that we are interested in finding out the position at the previous step but using the characteristic line at (x_a^{n+1}, τ_{n+1}). Using Euler's discretisation the above equation becomes

$$\frac{x_a^{n+1} - \tilde{x}_d^n}{\Delta\tau} = -g(x_a^{n+1}, \tau_{n+1}), \tag{6.49}$$

where x_a^{n+1} and $\tilde{x}_d^n$ denotes the arrival and departure points at the respective time-levels $n+1$ and n. As we are using an Euler scheme to solve (6.48), we have introduced $\tilde{x}_d^n$ to denote the approximate value of the actual departure point x_d^n. Therefore the Euler approximated departure point $\tilde{x}_d^n$ at time τ_n is simply calculated from

$$\tilde{x}_d^n = x_a^{n+1} + g(x_a^{n+1}, \tau_{n+1})\Delta\tau. \tag{6.50}$$

Applying the SLS with implicit time-stepping, we write (6.46) as the discrete equation

$$\frac{U_a^{n+1} - U_d^n}{\Delta\tau} = 0. \tag{6.51}$$

The schematic view of the SLS is illustrated in Figure 6.2. The solid curve, AC, in figure 6.2 shows the exact path that a particle would have to take in order to arrive at $x_a^{\tau^{n+1}}$ at time τ^{n+1}, with its current velocity specified by $g(x, \tau^{n+1})$. The dashed-line $A'C$ is the path from C to the Euler-approximated departure point $\tilde{x}$. Note that the location of the departure point will not necessarily lie on a grid point in the $x \times t$ plane, and so the precise location of $\tilde{x}_d^n$ will generally not coincide with the Eulerian grid points. Hence, we must utilise an interpolation scheme to estimate the dependent variable U_d^n at grid points surrounding $\tilde{x}_d^n$.

Interpolation

Suppose that a particle resides at $x = x_a^{n+1}$ and has a departure point at time step $\tau = \tau_n$ given by

$$\tilde{x}_d^n = x_a^{n+1} + g(x_a^{n+1}, \tau_{n+1})\Delta\tau. \tag{6.52}$$

Furthermore, suppose, for simplicity, that the mesh is spatially uniform, that $g(x, \tau) > 0$, and that the departure point lies between two consecutive grid points

$$x_a < \tilde{x}_d^n < x_{a+1}. \tag{6.53}$$

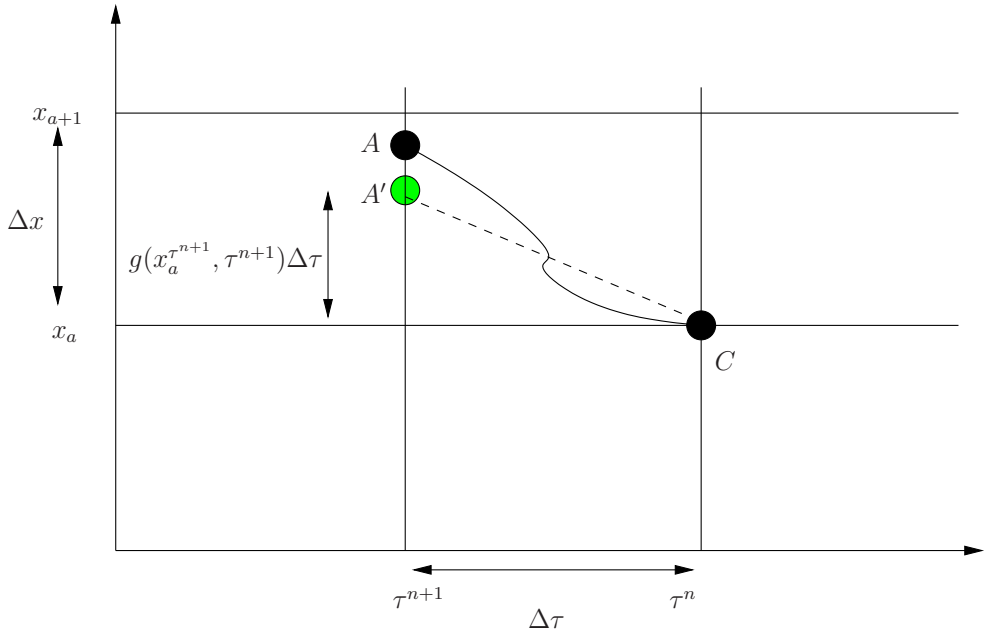

Figure 6.2: Schematic view for two-time-level advection. The vertical axis is the displacement and the horizontal axis denotes time τ. Actual (solid curve) and approximated (dashed-line) trajectories that arrive at mesh point $x_a^{\tau^{n+1}}$. Here $g(x_a^{\tau^{n+1}}, \tau^{n+1})\Delta\tau$ is the displacement of the particle during the time-interval $\Delta\tau$

Using linear interpolation we can determine an estimate of U at $\tilde{x}_d^n$, denoted by $\tilde{U}_d^n$, as

$$\tilde{U}_d^n = U_a^n + \Big[\frac{\tilde{x}_d^n - x_a}{\Delta x}\Big](U_{a+1}^n - U_a^n). \tag{6.54}$$

Substituting (6.52) into the above equation

$$\tilde{U}_d^n = U_a^n + \Big[\frac{x_a^{n+1} + g(x_a^{n+1}, \tau_{n+1}) - x_a}{\Delta x}\Big](U_{a+1}^n - U_a^n) \tag{6.55}$$

and then simplifying terms, yields

$$\tilde{U}_d^n = (1-\alpha)U_a^n + \alpha U_{a+1}^n, \tag{6.56}$$

where

$$\alpha = \frac{g(x_d^{n+1}, \tau_{n+1})\Delta\tau}{\Delta x}. \tag{6.57}$$

By initially assuming that the departure point is located between two consecutive points x_a and x_{a+1}, this results in the following condition

$$0 < \alpha < 1, \tag{6.58}$$

because from (6.53)

$$\begin{aligned} x_a < \tilde{x}_d^n < x_{a+1}, \\ 0 < g(x_d^{n+1}, \tau^{n+1})\Delta\tau < \Delta x, \\ 0 < \alpha < 1. \end{aligned}$$

The inequality (6.53) is the same stability condition for upwind schemes (see §6.2).

A strong assumption is made here: the speed of advection (denoted by $g(x, \tau)$) is sufficiently slow such that during any given time-step, $\tilde{x}_d^n$ will be between consecutive grid points. It is possible for this not to be the case, and so the scheme may appear as illustrated in figure 6.3, where $\tilde{x}_d^n$ is no longer between the blue dots at x_a and x_{a+1}. This schematic view occurs when the particle displacement is large, which implies that either the particle is moving rapidly (i.e., $g(x, \tau)$ is large) and/or the time step size $\Delta\tau$ is large. In other words if

$$g(x, \tau)\Delta\tau > \Delta x, \tag{6.59}$$

then the departure point location will no longer satisfy (6.53) and $\alpha > 1$. Here, the CFL condition would be violated and therefore the use of an explicit scheme would result in unstable solutions being obtained. To include the case where condition (6.59) is met, we specify the more general inequality,

$$x_{a+b} < \tilde{x}_d^n < x_{a+1+b}, \tag{6.60}$$

where $b \geq 0$. The value of b is dependent on the values of $g(x, \tau)$, Δx and $\Delta\tau$, and is given by

$$b = \Big\lfloor \frac{g(x, \tau)\Delta\tau}{\Delta x} \Big\rfloor, \tag{6.61}$$

where $\lfloor z \rfloor$ evaluates the largest integer not greater than z, and is referred to as

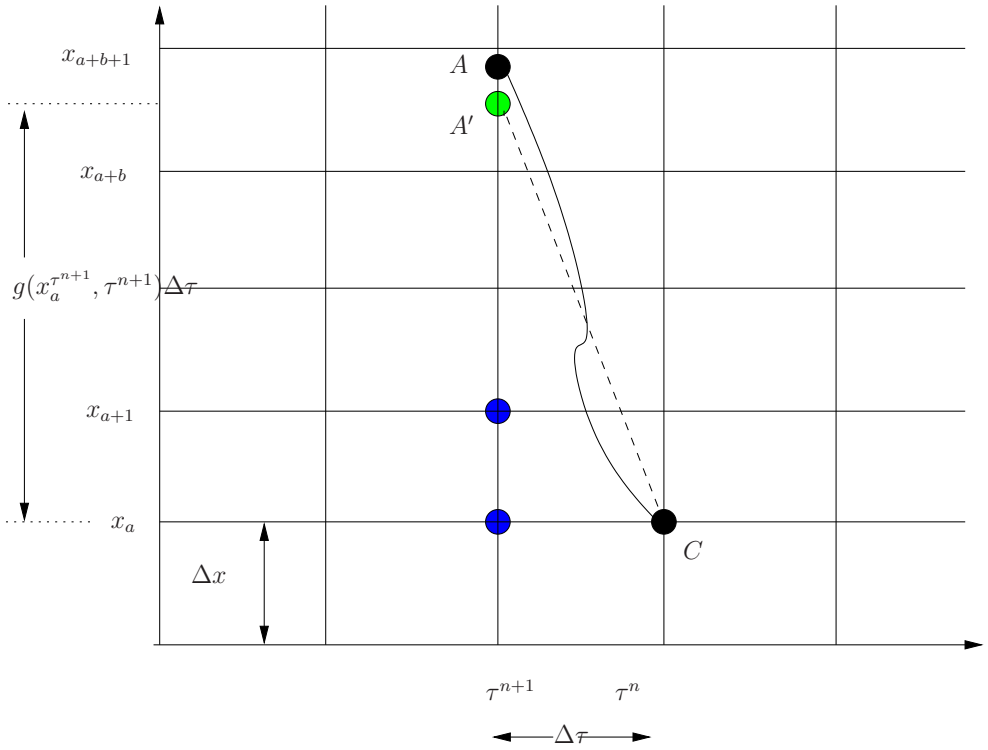

Figure 6.3: A view of a fast moving particle over the domain. Actual (solid curve) and approximated (dashed-line) trajectories that arrive at mesh point x_a at τ^{n+1}. Here $g(x_a^{\tau^{n+1}}, \tau^{n+1})\Delta\tau$ is approximated backward displacement of the particle during the time period $\Delta\tau$.

the *floor* of a real number z. Furthermore, the CFL number is now

$$C = \frac{g(x_a^{n+1}, \tau_{n+1})\Delta\tau}{\Delta x} - b. \tag{6.62}$$

Again, by using linear interpolation, we obtain

$$\begin{aligned}
\tilde{U}_d^n &= U_{a+b}^n + \left[\frac{\tilde{x}_d^n - x_{a+b}}{\Delta x}\right]\Big(U_{a+b+1}^n - U_{a+b}^n\Big), \\
&= U_{a+b}^n + \left[\frac{x_a^{n+1} + g(x_a^{n+1}, \tau_{n+1}) - x_a - b\Delta x}{\Delta x}\right]\Big(U_{a+b+1}^n - U_{a+b}^n\Big), \\
&= \Big(1 + b - \frac{g(x_a^{n+1}, \tau_{n+1})\Delta\tau}{\Delta x}\Big)U_{a+b}^n + \Big(\frac{g(x_a^{n+1}, \tau_{n+1})\Delta\tau}{\Delta x} - b\Big)U_{a+b+1}^n,
\end{aligned}$$

then by simplifying and letting

$$\hat{\alpha} = \alpha - b \tag{6.63}$$

this gives

$$\tilde{U}_d^n = (1 - \hat{\alpha})U_{a+b}^n + \hat{\alpha}U_{a+b+1}^n. \tag{6.64}$$

This is a more general formula to use, and will ensure that we are approximating the solution at the correct departure point. Again, from (6.60) it is clear that

$$0 < \hat{\alpha} \leq 1. \tag{6.65}$$

When $b = 0$, it implies that no steps have been skipped in the x space, and we return to the original case with $\hat{\alpha} = \alpha$.

Errors in Semi-Lagrangian scheme

As the solution of U_d^n typically involves interpolation, it is important to understand the errors this introduces. First, from equation (6.64) the Taylor expansion of $U(x_i + \Delta x, \tau)$ (expanding about x_i) is given as

$$U(x_i + \Delta x, \tau) = U(x_i, \tau) + \Delta x \frac{\partial U}{\partial x}(x_i, \tau) + \frac{1}{2}(\Delta x)^2 \frac{\partial^2 U}{\partial x^2}(x_i, \tau) + O(\Delta x)^3 \tag{6.66}$$

Rearranging this equation provides the Taylor series approximation for the first derivative in x:

$$\frac{\partial U}{\partial x}(x_i, \tau) = \frac{U(x_i + \Delta x, \tau) - U(x_i, \tau)}{\Delta x} - \frac{1}{2}\Delta x \frac{\partial^2 U}{\partial x^2}(x_i, \tau) + O(\Delta x)^3. \tag{6.67}$$

Next, write the departure point as $\tilde{x}_d^n = x + \alpha \Delta x$ because

$$\alpha \Delta x = g(x_i, \tau^{n+1})\Delta \tau,$$

and then obtain the Taylor expansion at $x + \alpha\Delta x$:

$$U(x_i + \alpha\Delta x, \tau) = U(x_i, \tau) + \alpha\Delta x \frac{\partial U}{\partial x}(x_i, \tau) + \frac{1}{2}\alpha^2\Delta x^2 \frac{\partial^2 U}{\partial x^2}(x_i, \tau) + O(\Delta x)^3. \tag{6.68}$$

Replacing the first derivative term in (6.68) with the derivative expression in (6.67) yields

$$\begin{aligned} U(x_i + \alpha\Delta x, \tau) &= U(x_i, \tau) + \alpha\Delta x \left(\frac{U(x_i + \Delta x, \tau) - U(x_i, \tau)}{\Delta x} - \frac{1}{2}\Delta x \frac{\partial^2 U}{\partial x^2}(x_i, \tau) \right) \\ &+ \frac{1}{2}\alpha^2\Delta x^2 \frac{\partial^2 U}{\partial x^2}(x_i, \tau) + O(\Delta x)^3. \end{aligned}$$

which simplifies to give

$$\begin{aligned} U(x_i + \alpha\Delta x, \tau) &= U(x_i, \tau) + \alpha\big(U(x_i + \Delta x, \tau) - U(x_i, \tau)\big) \\ &+ \frac{1}{2}\alpha(\alpha - 1)\Delta x^2 \frac{\partial^2 U}{\partial x^2}(x_i, \tau) + O(\Delta x)^3. \end{aligned} \tag{6.69}$$

This is the expansion of the solution at $\tilde{x}_d^n$ and indicates the associated errors that results when using linear interpolation. It is clear from the presence of the diffusion term in (6.69) that artificial smoothing may occur, which leads to inaccurate results. As expected, when $\alpha = 0$ no interpolation is required since it implies that the particle is exactly at x_i. Similarly when $\alpha = 1$, it is at x_{i+1}. Also we note that the maximum source of diffusion comes is introduced when the interpolation is taken half-way between two consecutive grid points, i.e. when $\alpha = 1/2$. In this case it implies that

$$\max_{0 \le \alpha \le 1} \alpha(\alpha - 1) = \frac{1}{4}. \tag{6.70}$$

Using the above equation, we can determine the error bounds of our approximated solution under linear interpolation. Simply rearrange the expansion of $U(x_i + \alpha\Delta x, t)$, and ignore terms smaller than $O(\Delta x)^2$, to obtain

$$U(x_i + \alpha\Delta, \tau) - \Big\{ U(x_i, \tau) + \alpha\big(U(x_i + \Delta x, \tau) - U(x_i, \tau)\big) \Big\} = \frac{\Delta x^2}{2}\alpha(\alpha - 1)\frac{\partial^2 U}{\partial x^2}(x_i, \tau). \tag{6.71}$$

If we express error of the approximation as

$$R = U(x_i + \alpha\Delta x, \tau) - \tilde{U}(x_i + \alpha\Delta x, \tau), \tag{6.72}$$

where U is the exact value and $\tilde{U}$ is the linear interpolated value from (6.69), then using (6.70) we see that this error is bounded by

$$|R| \leq \max_{0\leq\alpha\leq 1} \frac{1}{8}\Delta x^2 \left| \frac{\partial^2 U}{\partial x^2}(x_i, \tau) \right|. \tag{6.73}$$

This inequality states that the approximation between two points on a given function increases with the second derivative of the function that is approximated (assuming U has a continuous second derivative). The above derivation, and the fact that we have shown that it is consistent with the standard error bound for linearly interpolated functions, see Press et al. (2002), is a contribution of our work. Deriving the accuracy of the solution using higher-order interpolation schemes can be performed in the same manner.

Therefore, using an SLS with the linear interpolated approximation $\tilde{U}^n_{i^*}$, the PDE (6.7) expressed in discrete form is

$$\frac{1}{\Delta\tau}\left[U^{n+1}_i - U^n_{i^*} - \alpha\big(U^n_{i^*+1} - U^n_{i^*}\big)\right] = \frac{\Delta x^2}{2\Delta\tau}\alpha(\alpha-1)\frac{\partial^2 U^n_{i^*}}{\partial x^2} - \frac{\Delta\tau}{2}\frac{\partial^2 U^n_i}{\partial\tau^2}, \tag{6.74}$$

where we intentionally differentiate between i and i^*, to stress that depending on the grid sizes in the spatial or time dimensions or the speed of the information flow (denoted by $g(x,\tau)$), the location where the interpolation is performed may not be near i, or near the ath point as shown in figure 6.3. Thus, we find that the error associated with SLS for our PDE is given by

$$O\left(\frac{(\Delta x)^2}{\Delta\tau}, \Delta\tau\right), \tag{6.75}$$

and is also found to be identical to the error of the Lax method (see (6.26)). However, the SLS is superior as in the special cases we noted above (i.e. $\alpha = \{0, 1\}$), there is no longer spurious smoothing in the x dimension. Furthermore the magnitude of the first error term found in (6.74) is consistently smaller than the diffusive error term in (6.26).

What is surprising here, is that we typically find (in standard difference schemes)

Figure 6.4: Solution of the PDE (6.43) as a function of x, at $\tau = 1$, using different discretisations (as stated in table 6.1). Here $g(x,\tau) = 1$, the computational domains are given as $x_{min} = -20$ and $x_{max} = 20$, and the Dirichlet boundary condition is $U(x_{min},\tau) = 0$. The analytical solution is $U = U(x-1)$.

that making refinements in τ, and keeping Δx fixed, usually offers convergence (see Smith, 1985). However, for an SLS this will lead to misleading results due to the excessive smoothing . Additionally, these errors are exaggerated in regions where the solution rapidly changes since the second-order derivative in x becomes large and unbounded. To make appropriate use of SLS, we suggest that $\Delta x \to 0$ faster than $\Delta\tau \to 0$, $\Delta x \neq \sqrt{g(x,\tau)\Delta\tau}$, and by choosing $\Delta x = g(x,\tau)\Delta\tau$. Following this, results in the useful removal of numerical diffusion that is inherent in the SLS scheme.

To conclude this review and analysis of the SLS, numerical examples are provided and compared with the analytical solution of (6.7). Equation (6.43) is solved using the previously stated initial condition,

$$U(x,0) = \begin{cases} 0 & x < 0 \\ 1 & x \geq 0 \end{cases}, \tag{6.32}$$

and compared with the solutions obtained when using different discretisations (as outlined in table 6.1). In figure 6.4, these solutions are presented and confirm that when $\hat{\alpha} = 1$ the result is very accurate (see the solid dashed blue line in the figure). The red line in the figure shows the artificial smoothing as the ratio between Δx and $\Delta\tau$ results in α becoming less than unity. Table 6.2 also shows that the artificial diffusion is not explicitly caused when the speed of the particle is fast, and so bypassing the two nearest grid points (see figure 6.3), but occurs as the value of $\hat{\alpha}$ varies between fractional values. In order to visualise the numerical diffusion occurring we take two representative points in x space, at $x = g(x,\tau)\tau - \Delta x$ and $x = g(x,\tau)\tau + \Delta x$ and then plot out their respective solutions (see figure 6.5). These points are chosen as they are either side of a discontinuity in the solution. The solution has significant errors when $\hat{\alpha} = 0.5$ and decreases either side of this value. The bottom graph in figure 6.5 shows how the value of $\hat{\alpha}$ changes as the speed of advection $f(x,\tau)$ is varied, while keeping the values of Δx and $\Delta\tau$ fixed. This indicates that if the speed of advection varies, then careful selection of grid sizes is required in order to suppress artificial

diffusion. Note that the results in table 6.2 were obtained using large grid-spacing, yet achieve the exact result when $\hat{\alpha} = 0$ and $\hat{\alpha} = 1$.

Case	$\#x$	$\#\tau$	Δx	$\Delta\tau$	$\hat{\alpha}$	$\frac{\hat{\alpha}}{2}(1-\hat{\alpha})$	Numerical Diffusion
1	4000	100	0.01	0.01	1	0	No
2	4000	200	0.01	0.005	0.5	0.125	Yes
3	4000	67	0.01	0.0149	0.4925	0.1249	Yes

Table 6.1: The specification of the grid sizes and resulting values of α that are used to solve PDE (6.43). Here $x_{min} = -20$ and $x_{max} = 20$. The speed of advection is a constant $g(x, \tau) = 1$.

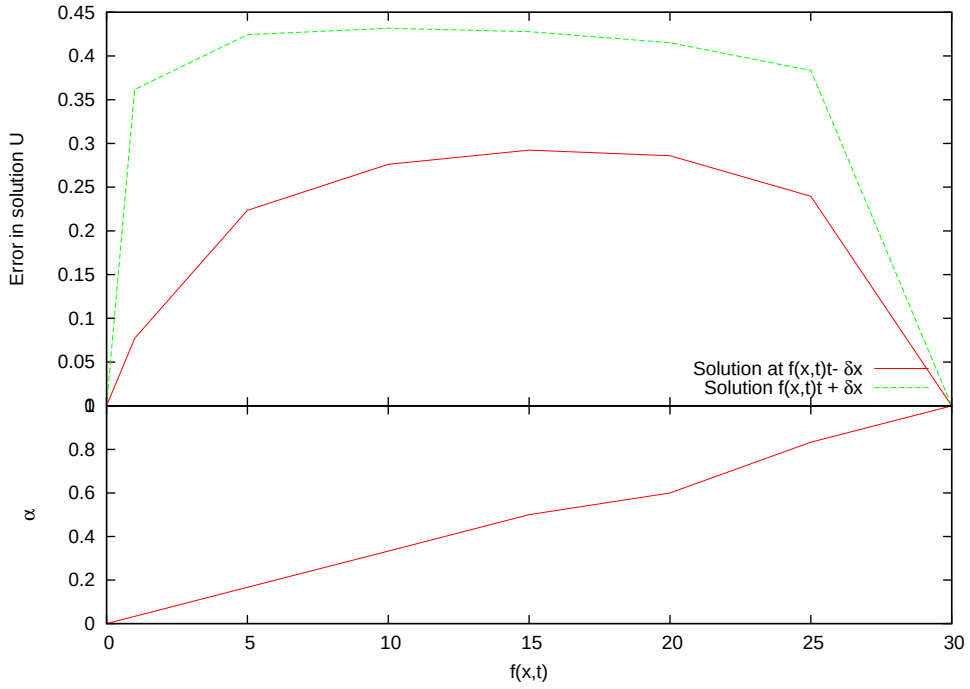

Figure 6.5: Top half of figure indicates how the error in the numerical solution of PDE (6.43) at the points $x = f(x, \tau)\tau - \Delta x$ and $x = f(x, \tau)\tau + \Delta x$ vary as a function of the speed of advection $f(x, \tau)$. The values of x are shown in table 6.2, and the resulting values of $\hat{\alpha}$ are then plotted on the bottom section of the figure.

6.3 Discretising the weather PDE

Having surveyed the numerous numerical schemes that may be used to discretise a PDE of the form (6.7), this section considers the application of the SLS for the

case	$g(x,\tau)$	$\hat{\alpha}$	$g(x,\tau)\Delta\tau - \Delta x$	$g(x,\tau)\Delta\tau + \Delta x$
1	0	0	0	1
2	1	0.0333	0.361662	0.92286
3	5	0.1666	0.424434	0.776537
4	10	0.333	0.431744	0.723864
5	15	0.5	0.427768	0.707668
6	20	0.6	0.41524	0.713984
7	25	0.8333	0.383553	0.76038
8	30	1	0	1

Table 6.2: Test cases to show the presence of numerical diffusion as the speed of advection varies. Here, we fixed the grid sizes at $\Delta x = 1$ and $\Delta\tau = 0.0\dot{3}$. The solution of (6.7) is computed for the locations either side of the location where the solution rapidly changes.

reasons outlined previously. Starting from the PDE for a HDD option,

$$\frac{\partial V}{\partial \tau} - (X_{ref} - X)^+ \frac{\partial V}{\partial I} = \frac{1}{2}\sigma_X^2 \frac{\partial^2 V}{\partial X^2} + \gamma(X,\tau)\frac{\partial V}{\partial X} - rV, \tag{6.6}$$

let $\mathcal{L}$ be the differential operator represented by

$$\mathcal{L}\{V\} \equiv \frac{1}{2}\sigma_X^2 \frac{\partial^2 V}{\partial X^2} + \gamma(X,t)\frac{\partial V}{\partial X} - rV, \tag{6.76}$$

such that (6.6) can be rewritten as

$$\frac{\partial V}{\partial \tau} - (X_{ref} - X)^+ \frac{\partial V}{\partial I} = \mathcal{L}\{V\}. \tag{6.77}$$

The Lagrangian derivative along a trajectory $I(X,\tau)$, through the domain $I \times \tau$ (hence X is fixed), is

$$\frac{DV}{D\tau} = \frac{\partial V}{\partial \tau} + \frac{\mathrm{d}I}{\mathrm{d}\tau}\frac{\partial V}{\partial I}. \tag{6.78}$$

Equating (6.78) with the LHS of (6.77) yields

$$\frac{DV}{D\tau} = \mathcal{L}\{V\} \tag{6.79}$$

along the trajectory

$$\frac{\mathrm{d}I}{\mathrm{d}\tau} = -(X_{ref} - X)^+. \tag{6.80}$$

Let $V(X_i, I_j, \tau_n) = V_{i,j}^n$ denote the approximated value of the option at node X_i,

Parameter	Value
X_{min}	-50
X_{max}	50
X_{ref}	18
I_{min}	0
I_{max}	$T \cdot (X_{ref} + \lvert X_{min} \rvert)$

Table 6.3: The computational domain values used to compute the solution of PDE (5.29). The value of I_{max} varies depending on the length of the contract period T.

weather index value I_j, and discrete time τ_n. For simplicity we discretise the system with an equally-spaced grid in all directions, such that

$$\begin{aligned} X_i &= X_{min} + i\Delta X, \qquad i = 0, \cdots, A \quad , \\ I_j &= I_{min} + j\Delta I, \qquad j = 0, \cdots, J \quad , \\ \tau^n &= \tau_N - n\Delta\tau \qquad n = 0, \cdots, N \quad , \end{aligned} \tag{6.81}$$

where A, J and N are the maximum number of points in each dimension respectively. We have used the unusual notation of A because the natural use of I would cause confusion with the weather index value I_j. If we are valuing a weather contract at initiation then the value of the index will be zero, since there has been no HDD values recorded; therefore take $I_{min} = 0$. Also, the values of X_{min}, and the maximum values of X_i, I_j are as given in table 6.3.

Construction of a semi-Lagrangian scheme is performed by assuming that the solution is known at $\tau = \tau^n$. Discretising (6.79) along the trajectory, using a fully implicit scheme for both time and spatial dimensions, yields

$$\frac{V_{i,j}^{n+1} - V_{i,d}^{n}}{\Delta\tau} = (\mathcal{L}\{V\})_{i,j}^{n+1}, \tag{6.82}$$

where $V_{i,d}^n = V(X_i, I_d, \tau^n)$ is the value of the option price at the departure point. To determine the location of the departure point, (6.80) must be solved. Staniforth and Côté (1991) stated that usually the trajectory must be estimated numerically, using, perhaps an iterative based root finder. However, since the value of X along the trajectory is fixed, the LHS of (6.80) is a constant function and so its solution can be determined exactly. Therefore, integrating

$$\frac{\mathrm{d}I}{\mathrm{d}\tau} = -(X_{ref} - X)^+. \tag{6.83}$$

from $\tau = \tau^{n+1}$ to $\tau = \tau^n$, yields

$$I_d^n = I_a^{n+1} + (X_{ref} - X)^+ \Delta\tau, \tag{6.84}$$

where I_d^n is the departure point and I_a^{n+1} is the arrival point. With knowledge of the location of I_d, $V_{i,d}^n$ can be determined by interpolation:

$$V_{i,d}^n = (1 - \hat{\alpha}) V_{i,a+b}^n + \hat{\alpha} V_{i,a+b+1}^n \tag{6.85}$$

where $\hat{\alpha}$ redefined here as

$$\hat{\alpha} = \frac{(X_{ref} - X)^+ \Delta\tau}{\Delta I} - \left\lfloor \frac{(X_{ref} - X)^+ \Delta\tau}{\Delta I} \right\rfloor. \tag{6.86}$$

Using standard finite-difference techniques, the RHS of (6.82) becomes

$$(\mathcal{L}\{V\})_{i,j}^{n+1} = \frac{1}{2}\sigma_H^2 \left(\frac{V_{i+1,j}^{n+1} - 2V_{i,j}^{n+1} + V_{i-1,j}^{n+1}}{(\Delta X)^2} \right) + \gamma(X_i, \tau^{n+1}) \left(\frac{V_{i+1,j}^{n+1} - V_{i-1,j}^{n+1}}{2\Delta X} \right) - r V_{i,j}^{n+1}. \tag{6.87}$$

Combining (6.82) and (6.87) the following implementation is obtained

$$V_{i,d}^n = a_i V_{i-1,j}^{n+1} + b_i V_{i,j}^{n+1} + c_i V_{i+1,j}^{n+1}, \tag{6.88}$$

with

$$a_i = \frac{\Delta\tau}{2(\Delta X)^2} \left(\Delta X \gamma(X_i, \tau^{n+1}) - \sigma_X^2 \right) \tag{6.89}$$

$$b_i = 1 + \frac{\sigma_H^2 \Delta\tau}{(\Delta X)^2} + r\Delta\tau \tag{6.90}$$

$$c_i = -\frac{\Delta\tau}{2(\Delta X)^2} \left(\Delta X \gamma(X_i, \tau^{n+1}) + \sigma_X^2 \right) \tag{6.91}$$

$$d_i = V_{i,d}^n. \tag{6.92}$$

This can be represented this in matrix form as

$$\mathbf{A}\mathrm{V}^{n+1} = \mathbf{D}^n, \tag{6.93}$$

where $\mathbf{A}$ is the matrix of coefficients

$$\begin{pmatrix} b_0 & c_0 & 0 & 0 & . & . & . & . & 0 \\ a_1 & b_1 & c_1 & 0 & . & . & . & . & . \\ 0 & a_2 & b_2 & c_2 & . & . & . & . & . \\ . & . & . & . & . & . & . & . & . \\ . & . & . & 0 & a_i & b_i & c_i & 0 & . \\ . & . & . & . & . & . & . & . & . \\ 0 & . & . & . & . & . & 0 & a_{imax} & b_{imax} \end{pmatrix}, \tag{6.94}$$

and $\mathbf{D}^n$ is the solution at each point i:

$$\begin{pmatrix} d^n_{0,j} \\ d^n_{01,j} \\ . \\ . \\ . \\ d^n_{imax-1,j} \\ d^n_{imax,j} \end{pmatrix}. \tag{6.95}$$

Equation (6.93) is then solved using an LU solver. Due to the time-dependence of the mean-reverting drift parameter the LU matrices must be calculated at each time-step. Using an SLS with linear interpolation the global truncation error is given by

$$O\left((\Delta X)^2, \frac{(\Delta I)^2}{\Delta \tau}, \Delta \tau\right), \tag{6.96}$$

implying that there is second-order convergence X due to the central differencing used; first-order convergence in τ and the errors in the I dimension are exclusively from the errors of interpolation, of size $\frac{(\Delta I)^2}{\Delta \tau}$.

6.4 Analysis of numerical schemes on option prices

As discussed earlier in §6.2.3, the SLS can lead to inaccurate solutions as numerical diffusion may be introduced. In this section, the SLS is applied to value a weather derivative contract and the peculiarities of the scheme are investigated.

Additionally, further illustrations are provided that compare SLS against other numerical techniques based on standard finite-difference schemes from §6.2.1.

Consider the weather PDE for a HDD option

$$\frac{\partial V}{\partial \tau} - (X_{ref} - X)^{+}\frac{\partial V}{\partial I} = \frac{1}{2}\sigma_X^2(\tau)\frac{\partial^2 V}{\partial X^2} + \gamma(X,\tau)\frac{\partial V}{\partial X} - rV, \tag{6.6}$$

with the same boundary conditions as stated in equation (5.39), (5.41) and (5.42), and initial condition for an uncapped option,

$$V(X, I_H, T) = \max(K - I_H, 0). \tag{6.97}$$

PDE (6.6) has wave-like behaviour (in the I dimension) in the region where $X < X_{ref}$. It is in this region where the use of SLS may result in artificial smoothing appearing in the solution space, since $\hat{\alpha}$ will often remain fractional, implying that a form of interpolation is required. We investigate, via numerical experiments, if SLS is appropriate for solving (6.6). To uncover the numerical diffusion it is helpful to begin the analysis by considering the trivial case of when $\sigma_X(\tau) = 0$ and also $\gamma(X,\tau) = 0$, which has the effect of restricting the directional influences to just the I dimension. In this case (6.6) reduces to

$$\frac{\partial V}{\partial \tau} - (X_{ref} - X)^{+}\frac{\partial V}{\partial I} = -rV. \tag{6.77}$$

This equation has a known analytical solution of

$$V(X, I, \tau) = e^{-r\tau}\max(K - I - (X_{ref} - X)^{+}\tau, 0), \tag{6.98}$$

which can then be used to compare the accuracy of the numerical solution obtained using SLS. We use a sample set of parameters that we shall refer to as *EBM-01* (we adopt this naming convention to illustrate that these parameters are chosen by the author purely for experimental purposes, where details of the parameters are provided in table 6.4). Equation (6.6) is solved at $\tau = T$ (i.e. $t = 0$) where $I = 0$. The computed errors are shown in figure 6.6 for the solution at $X = 11$, through to $X = 16$. We chose to focus on this region as in this neighbourhood lies another discontinuity in $\frac{\partial V}{\partial X}$, which differs from the other, and more typical, discontinuity found at the reference level X_{ref}. This additional

discontinuity is denoted X_{dis} and is defined such that (at $I = 0$)

$$X_{dis} = \left(X_{ref} - \frac{K}{\tau} \right). \tag{6.99}$$

This discontinuity exists only when $X < X_{ref}$, otherwise, from (6.6) and (6.98), the solution is simply $V = e^{-r\tau}K$ that has no sharp changes. The five panels in figure 6.6 show the variations in the error of the solution for different values of X, as ΔI and Δt are varied. Given the parameter set *EBM-01*, we find that $X_{dis} = (18 - 80/20) = 14$, which explains why in figure 6.6(d) large errors are found in the solution, and also the numerical scheme shows the largest errors around this region as depicted by figure 6.6(c) and 6.6(e). The oscillations in figure 6.6(d) represent the non-linearity errors in the scheme because as we make refinements in ΔI, the resulting grid points may not coincide with the location where there is a discontinuity Johnson (2007) therefore recommends selecting the sizes and the origins of ΔI and $\Delta\tau$ such that the discontinuity lies exactly at a grid point. For an analysis of the impact of non-linearity errors found in finite-difference schemes (and other lattice-based schemes) refer to chapter 8. Now, in the region where this discontinuity lies the second derivative is large and unbounded, therefore if the ratio $(\Delta I)^2/\Delta\tau$ is not sufficiently small, then the artificial diffusion will grow. This explains why in figures 6.6(c) and 6.6(e) there is an increase in the errors of the solution in the region where $\Delta\tau$ is sufficiently smaller than ΔI (this occurs in the top right-hand corner of both images) because this makes $(\Delta I)^2/\Delta\tau$ large. Alternatively, when ΔI is much smaller than $\Delta\tau$, its evident from figure 6.7 that numerical diffusion diminishes as the errors are virtually zero.

The convergence results obtained from refining the mesh spacing and time-step size are shown in table 6.5, where we have used both linear and quadratic interpolation in the SLS scheme. The sizes of domain spacings $\Delta\tau$ and ΔI are successively halved whilst we hold $\Delta X(= 1)$ constant. The ratio is computed

$$ratio = \frac{V_{z+1} - V_z}{V_{z+2} - V_{z+1}}, \tag{6.100}$$

where V_z, V_{z+1} and V_{z+2} are the option values at successive grid levels. To compute the value V_{z+1} we use twice as many nodes in the τ and I dimensions as we did to compute V_z. Similarly, V_{z+2} is calculated using four times as many nodes

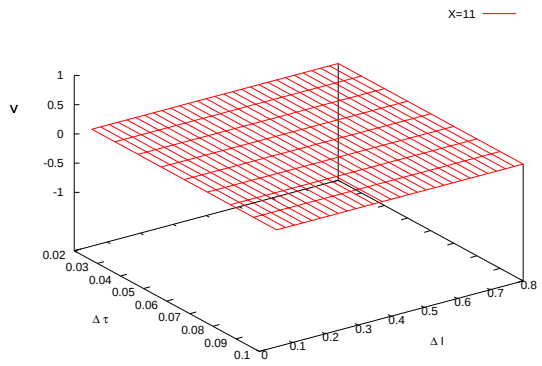

(a) X=11

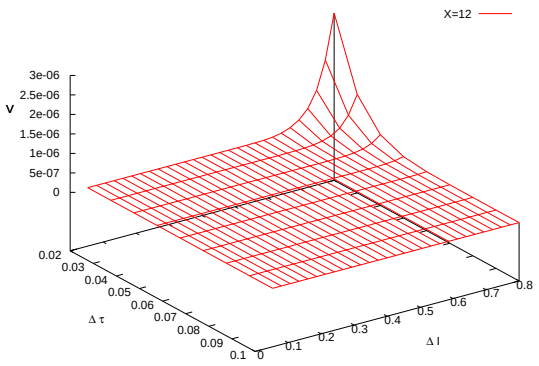

(b) X=12

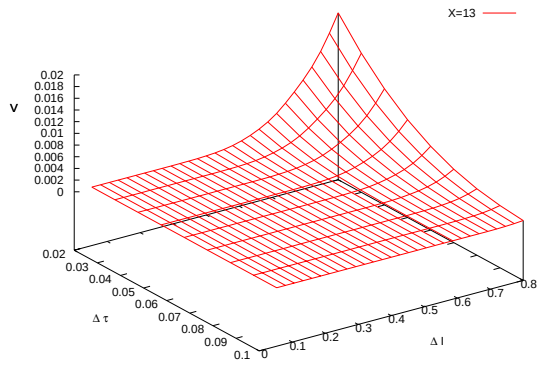

(c) X=13

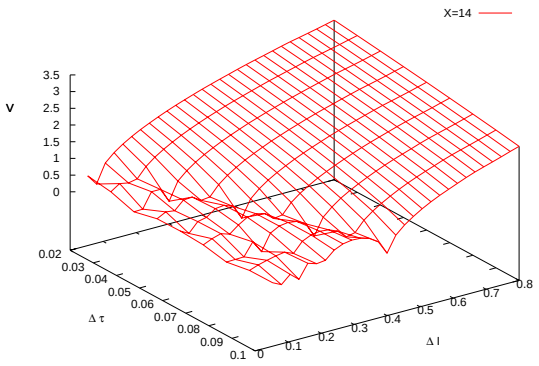

(d) X=14

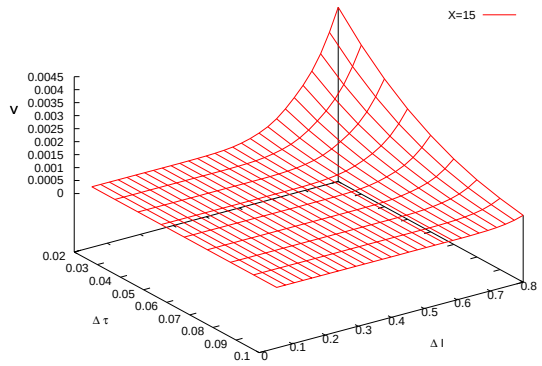

(e) X=15

Figure 6.6: Error of the numerical solution (obtained using SLS) when compared to the analytical solution for different values of X. The solution is evaluated at $t = 0, I = 0$, using parameters *EBM-01*

Data set	**EBM-01**	**EBM-02**	**EBM-03**
Parameter			
r	0.05/365	0.05/365	0.05/365
K	80	80	986.73
T	20 days	31 days	90 days
$\rho^{0.5}$	0	0	0.9
κ	0.254577	0.254577	0.254577
σ_X	0	{ 2.51209, 2.20502, 2.37840, 2.10051, 1.74256, 1.48755, 1.87269, 1.76075, 1.50615, 2.04457, 2.16213, 2.66395 }	same as for EBM-02
X_{min}	-50	-50	-50
X_{max}	50	50	50
I_{min}	0	0	0
I_{max}	160	160	1980
X_{ref}	18	18	18
$\Delta\tau$	$0.1\dot{3}$	$0.10\dot{3}$	0.1
ΔX	1	1	1
ΔI	0.8	0.8	0.8
$\theta(t)$	$11.56 + 2.87\text{x}10^{-6}t + 6.75\sin(\omega t - 1.90)$		

Table 6.4: This parameter set is used to demonstrate the effectiveness of the derived weather model (5.29) for pricing a collection of European weather options using SLS. The value of r is scaled so that it is represented in days. The expression of $\theta(t)$ is used for all parameter sets.

as used to compute V_z. So, $V_z = V(\Delta\tau, \Delta I), V_{z+1} = V(\Delta\tau/2, \Delta I/2), V_{z+2} = V(\Delta\tau/4, \Delta I/4)$. First-order convergence is achieved, since the ratio is very close to 2 when using both forms of interpolation. Notable, in the table, it was ensured that $\Delta I < \Delta\tau$ so that numerical diffusion is minimised. The precise removal of artificial diffusion is difficult because $\hat{\alpha}$ is not constant but varies as $(X_{ref} - X)$ changes (see table 6.2). Therefore, the computational grid sizes at each X value would need to be adjusted. This approach is not performed, but instead we utilise the weak condition that

$$\Delta I < \Delta\tau. \tag{6.101}$$

Additionally, we choose to employ quadratic interpolation to compute an approximation for U_d^n, since figure 6.8 shows that quadratic interpolation reduces the error by 50%, even at locations where the solution changes rapidly (Staniforth and Côté, 1991, also recommend the use of quadratic interpolation).

Next we consider the behaviour of the solution as $\Delta X \to 0$. We fix the size of

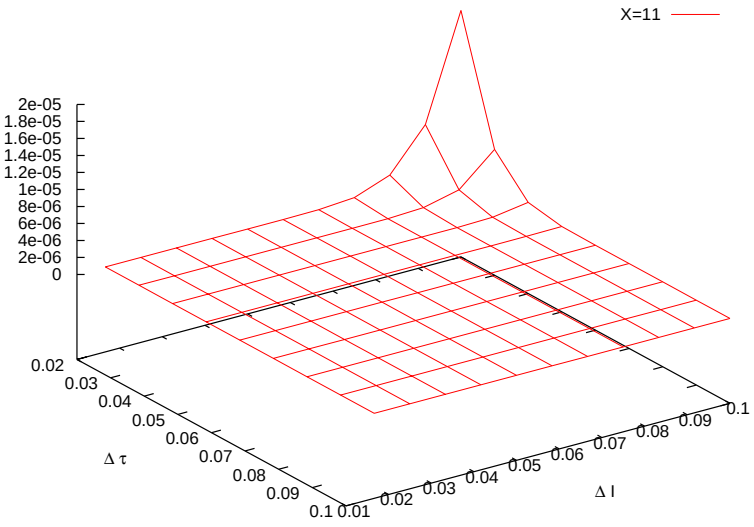

Figure 6.7: An illustration of how the artificial diffusion for small values of ΔI and $\Delta\tau$ causes errors in the solution of a HDD put option (obtained using SLS). The option is computed at $X = 11$, $t = 0, I = 0$, using parameters $K = 25, r = 0.05, T = 25, \rho = 0, \sigma_X = 0.2285, \mu_X = 0, \Delta X = 1$

.

ΔI and $\Delta\tau$ and plot in figure 6.9 the various solution profiles for different sizes of ΔX. The change in the solution can be relatively significant. We show this by observing the different option values that are obtained when $X = 0$. If we compare the solutions for when $\Delta X = 1$ and $\Delta X = 0.0625$ we see that there is almost a 6% difference in value. As expected, when the value of ΔX gets small, say $\Delta X = 0.015625$, the difference between the solution here and when $\Delta X = 0.0625$ is less than 0.2%.

Case where $X \geq X_{ref}$

Again consider PDE (6.6), where $\sigma_X(X)$ and $\gamma(X, \tau)$ are functions and not zero for all values of X and τ. When solving the PDE in the region where $X \geq X_{ref}$, we are able to use standard-finite difference techniques because the advection disappears as $(X_{ref} - X)^+ = 0$ (and therefore $\hat{\alpha} = 0$ from (6.86) on page 151). This means that in this region we solve the reduced PDE (5.29):

$$\frac{\partial V}{\partial \tau} = \frac{1}{2}\sigma_X^2 \frac{\partial^2 V}{\partial X^2} + \gamma(X, \tau)\frac{\partial V}{\partial X} - rV. \tag{6.102}$$

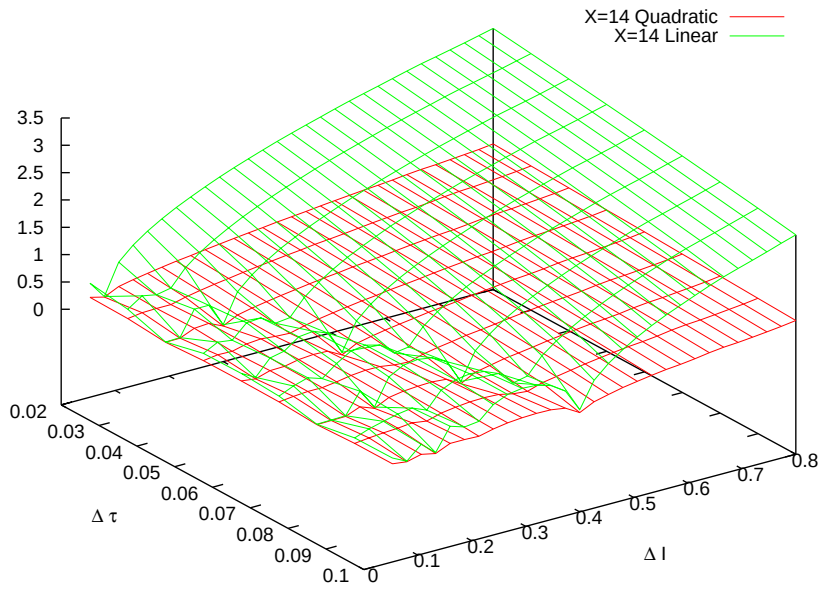

Figure 6.8: Illustration of the errors of the solution obtained when using either a linear or quadratic interpolate in the SLS. To compute the errors we compare our solution against the analytical solution $V(X = 14, 0, 0)$ using parameters *EBM-01*.

n	I grid nodes	$\Delta\tau$	ΔI	$V(X,0,0)$	ratio
Semi-Lagrangian with linear interpolation					
21	201	1.0	0.8	39.8905684288	N/A
41	401	0.5	0.4	39.8905646865	N/A
81	801	0.25	0.2	39.8905628152	1.9998631590
161	1601	0.125	0.1	39.8905618796	1.9999301732
321	3201	0.0625	0.05	39.8905614117	1.9999672400
641	6401	0.03125	0.025	39.8905611778	1.9999831114
Semi-Lagrangian with quadratic interpolation					
21	201	1.0	0.8	39.8905684288	N/A
41	401	0.5	0.4	39.8905646865	N/A
81	801	0.25	0.2	39.8905628152	1.9998631514
161	1601	0.125	0.1	39.8905618796	1.9999302567
321	3201	0.0625	0.05	39.8905614117	1.9999668907
641	6401	0.03125	0.025	39.8905611778	1.9999837493

Table 6.5: The exact value of the option at $X = 16$. The exact value is given by the analytic formula (6.98) as 39.8905609439 (to 10 d.p). The option is a put option with parameters *EBM-01*. We use n nodes in τ. Here the value of $\Delta X = 1$.

Note that there is no boundary condition required at $X = X_{ref}$, since in the implementation we are using the values computed at the previous time-step as the initial conditions for this reduced PDE in this region. In figure 6.10 when the values of $\Delta I \to 0$ and $\Delta\tau \to 0$, the solution begins to approach a stable value as no numerical diffusion is present.

6.5 Results - Weather options

In this section we value a series of European HDD weather put options using the SLS scheme for the LHS and an implicit scheme for the RHS of PDE (5.27). First, we take a preliminary look at solution profiles using a simple data set *EBM-02* to get an impression of the behaviour of the prices with respect to the state variables I and X. Then we highlight the key subtleties of the numerical implementation and also provide the real-world interpretations of the results, followed by a more robust example similar to a real weather option contract. In the valuation of the following contracts we keep maturity dates short, as in practice the contract maturities are usual only weeks, months or a season. In general we value capped

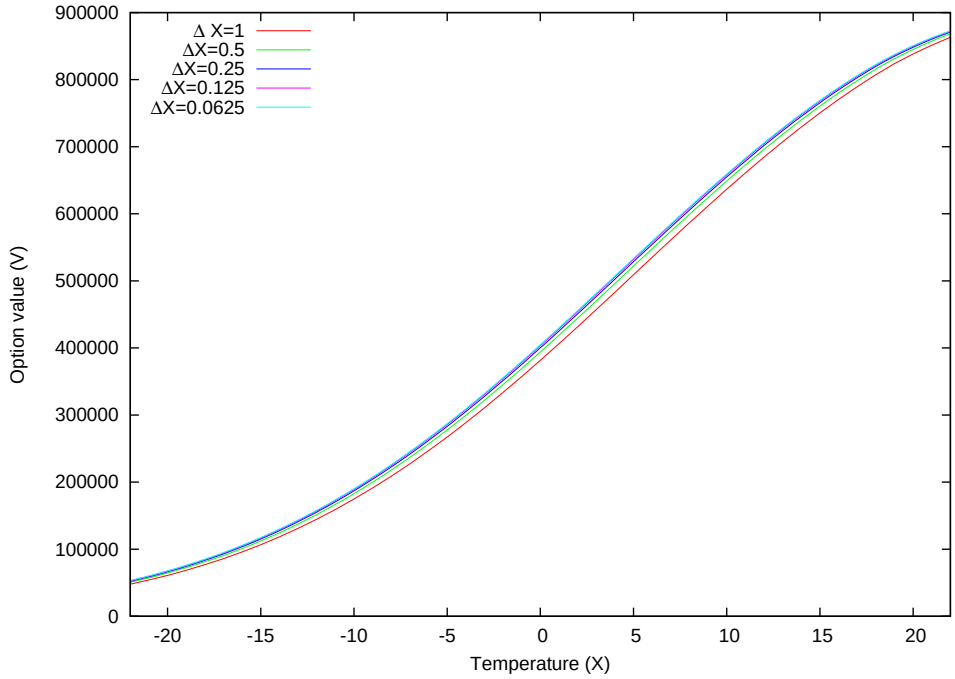

Figure 6.9: The variation in the solution of a European put option as ΔX is refined. The parameters used are $K = 1750$, $T = 151$ days, $\rho = 0.9$, $r = 0.0001$. Here $\Delta t = 0.94375$ and $\Delta I = 70$.

options but to aid understanding we begin with a simple uncapped put option.

Preliminary results

Consider a European HDD put option with payoff

$$V(X, I, T) = (K - I)^+ \tag{6.103}$$

and parameter set *EBM-02*. Specifying $\rho = 0$ implies that they there is no correlated instrument available, thus the drift term in the PDE is completely driven by the mean-reverting drift. The contract length is specified at 31 days, starting on January 1st (which corresponds to $t = 0$) until January 31st ($t = 31$). As we are valuing a put option we set the truncation I_{max} equal to twice the strike value, so that unnecessary computations are avoided.

For our PDE model, the presence of the term $(X_{ref} - X^+)$ implies that movement in the option V through I is linked not just to time, but also to its position in X space. When X becomes negative and large, $(X_{ref} - X)^+$ becomes large which

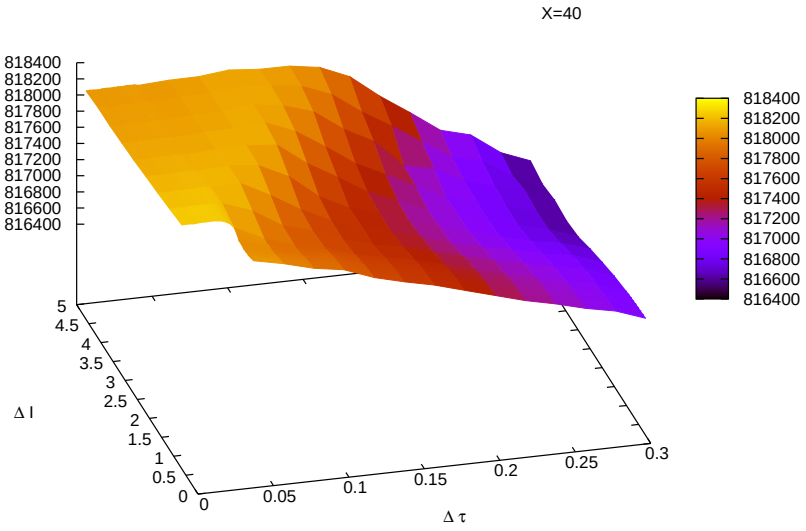

(a) $X = 40$

Figure 6.10: Variation of the solution for options with starting temperature $X > X_{ref}$ as the computational grid sizes are refined. The solutions, are obtained by solving (6.102) at time $t = 0$ (i.e. finding $V(X, 0, 0)$), with parameters *EBM-01*, with $\Delta X = 1$.

n	I grid nodes	$\Delta\tau$	ΔI	$V(X,0,0)$	ratio
Semi-Lagrangian with quadratic interpolation					
11	201	2.0	0.4	13.2069618186	N/A
21	401	1.0	0.2	13.0246779117	N/A
41	801	0.5	0.1	12.9409856629	2.1780261566
81	1601	0.25	0.05	12.9010440680	2.0953657204
161	3201	0.125	0.025	12.8815549012	2.0494254721
321	6401	0.0625	0.0125	12.8719314306	2.0251703042
641	12800	0.03125	0.0062504883	12.8671497060	2.0125522223
1281	25600	0.015625	0.0031251221	12.8647668931	2.0067562770

Table 6.6: Value of a HDD put option at $X = 16$ and $I = 0$, with parameter set *EBM-02*. We use n nodes in τ and 100 grid points is used in the X dimension. The payoff is given in (6.103). $\Delta X = 1$, since the number of nodes in the X is $A = 100$.

results in V rapidly moving through I space. In this region an implicit central-difference scheme (see 6.2.1) produces highly oscillatory solutions, see 6.11(a). This is resolved by employing a one-sided difference scheme, which is shown in figure 6.11(b), although this reduces the accuracy of the scheme since the order of errors are large in a one-sided difference scheme. We confirm that the use of SLS is appropriate in solving PDE (5.29) as from table 6.6 we see second order convergence, with desired ratio of 2. The final computation in the table was derived using over 3 billion nodes in the computational domain.

We present four plots in figure 6.12 that show how weather option prices with different expiry date behave through X and I. From these diagrams we can see that as the length of the contract increases the option value decays, since there is increased probability of I having value and hence of the payoff being small. Since the strike level is relatively low the option has little value (see figure 6.12(d)). Today's option price is given at $\tau = T$, with $I = 0$ as at the start of the contract the HDD index is zero. An illustration of the solution profiles as X varies is provided in figure 6.13 and confirms that if the starting temperature is very hot, the option price still has little value, since as the option evolves through time the underlying variable X will revert back to its seasonal mean $\theta(\tau)$ that results in I increasing in value (since temperatures in January are usually below 18°C). Consequently this reduces the option's payoff and therefore its value today. The reason why the option price is not exactly zero, is because it can take a few days before the model adjusts the temperature back to normal levels and therefore in

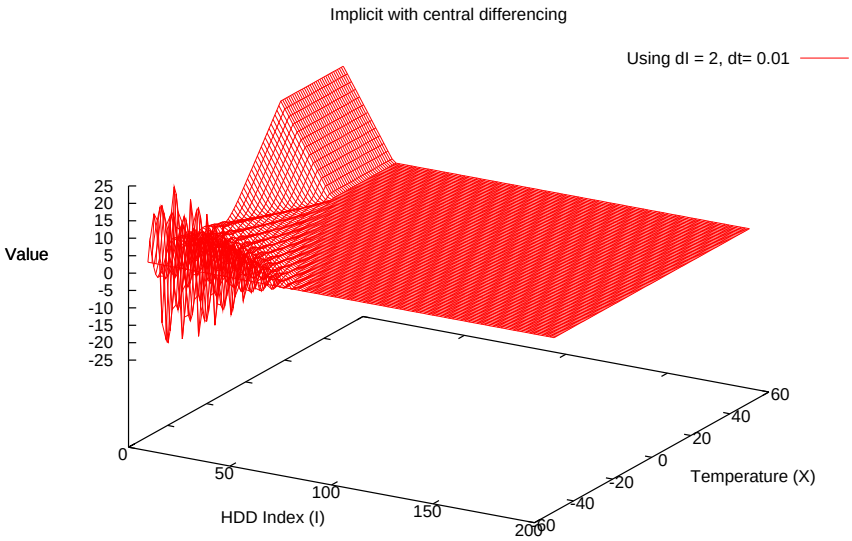

(a)

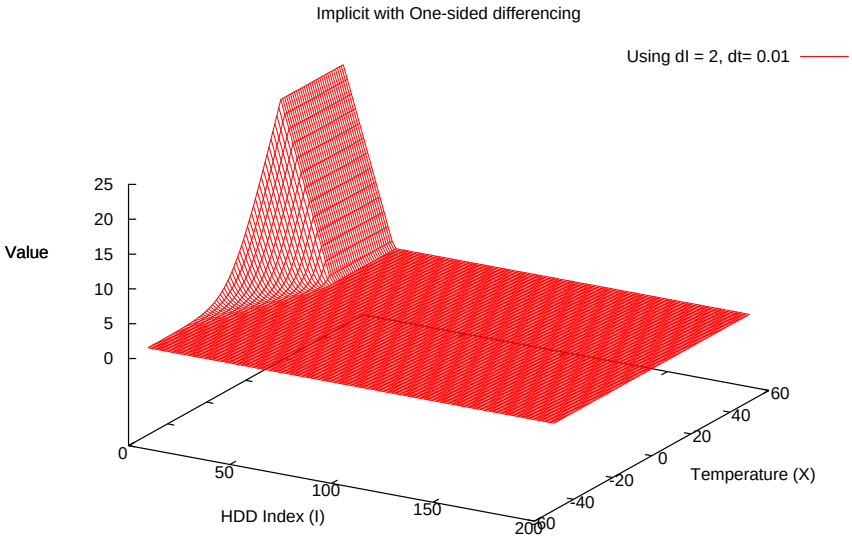

(b)

Figure 6.11: Oscillatory behaviour that occurs in regions where the solution of PDE (5.29) changes rapidly. Here the values of the grid are fixed with $\Delta\tau = 0.01$, $\Delta I = 2$ and $\Delta X = 1$. The solution profiles in both figures is for when $t = 0$ and uses parameters *EBM-02*.

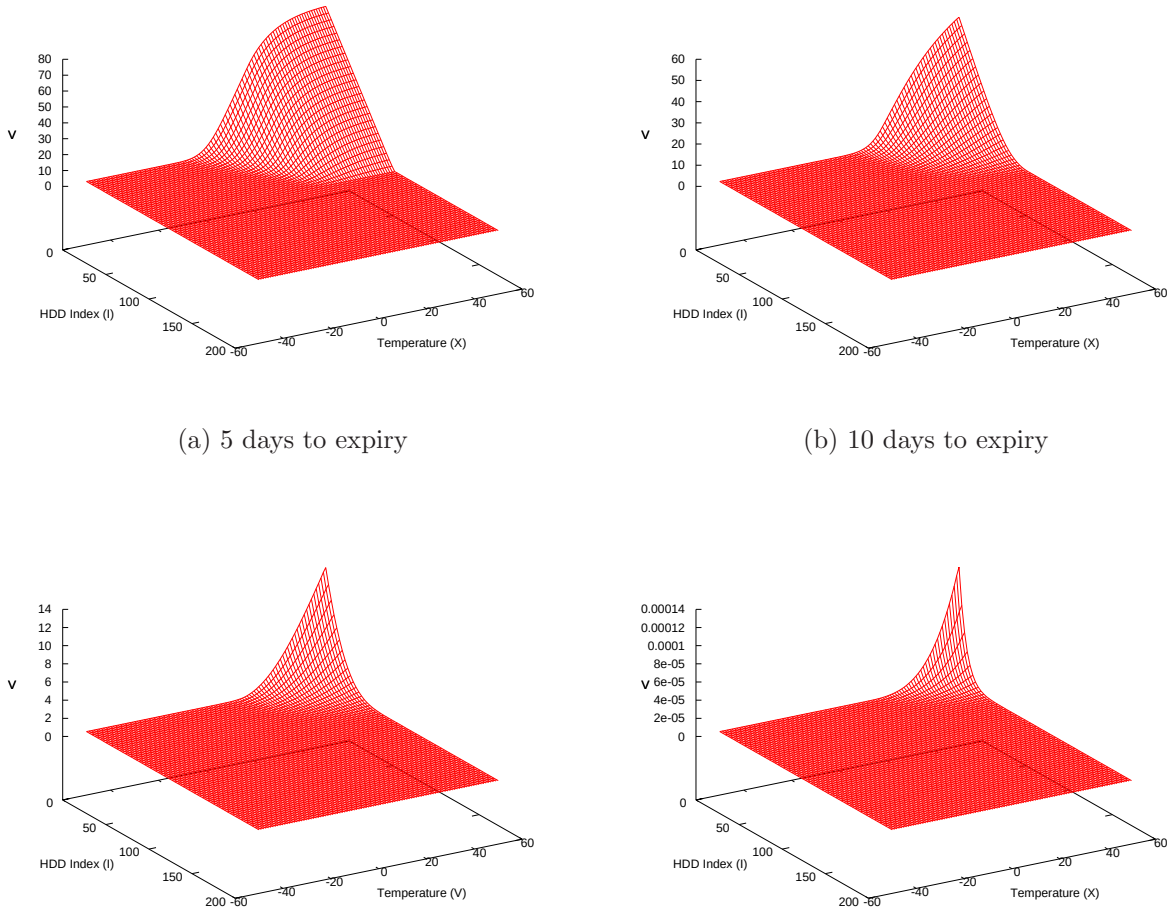

(a) 5 days to expiry

(b) 10 days to expiry

(c) 15 days to expiry

(d) 31 days to expiry

Figure 6.12: The variation in the solution profiles in time for a put option with parameters *EBM-02*.

that elapsed time I has little or no value. At extreme negative values, say at $X = -50$, by the time the temperature has returned to usual levels the value of the HDD index is large, and will generally continue to grow throughout the typically cold month of January. This is intuitive, as the temperature today should not greatly affect a weather derivatives value, unless the contract period is unusually short. Such an example is shown in figure 6.12(a) where the contract length is just 5 days. If the strike level is large enough such that I is unlikely to surpass it then the price would behave as shown in figure 6.14, but notice that even in regions with extremely warm weather the option prices is significantly

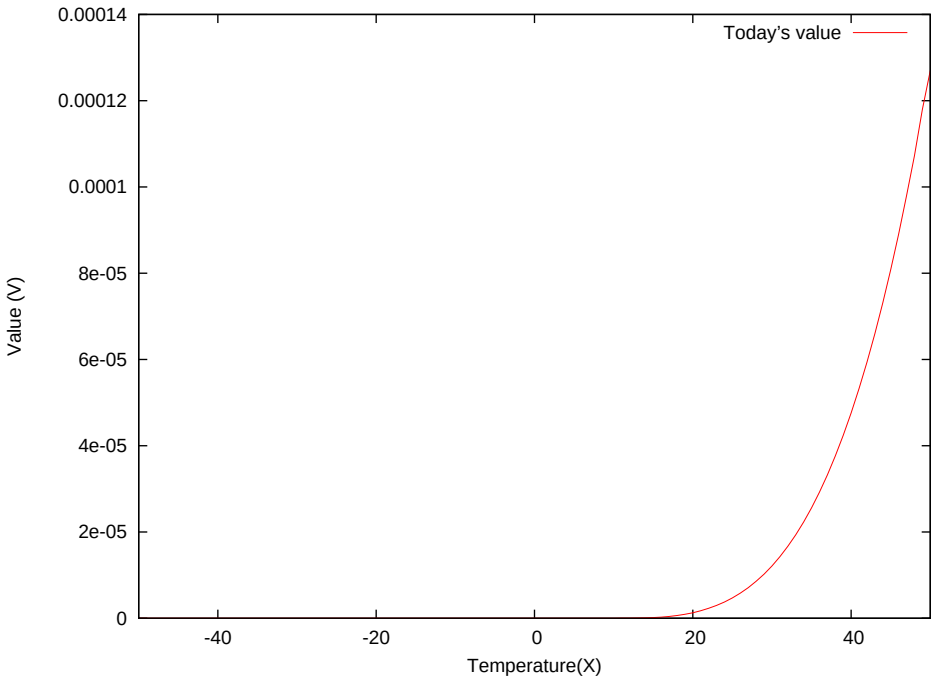

Figure 6.13: European HDD put option price at time $t = 0$, for a range of different initial temperatures. At time $t = 0$, $I = 0$ since no averaging has been performed. Based on the *EBM-01* parameter set.

below K since over the contract period the index will still accumulated value.

We compare the solutions from (5.29) to those of Harris (2003) where the valuation of a HDD put weather option was obtained, assuming that the underlying temperature followed a ABM process with yearly averaged constant volatility and drift. Our empirical results in §5.4 show this assumption is incorrect. We illustrate in figure 6.15 our derived solutions for a put option using three different values for the correlation $\rho^{0.5}$, and compare these with the solution obtained using Harris (2003) model. The values obtained differ significantly, since Harris (2003) assumes that temperature follows an ABM process, which would suggest that if the temperature was to have begun at an extreme value then it is likely to remain near this starting point for all time. Our model is more consistent with real-world dynamics of temperature. Furthermore the model produces option prices that are not largely dependent on temperature today but more on its general behaviour during the contract period, since abnormal temperatures soon revert back to normal levels. Harris's model completely neglects this, which results in her model being extremely sensitive to the changes in initial temperature. As the hedging

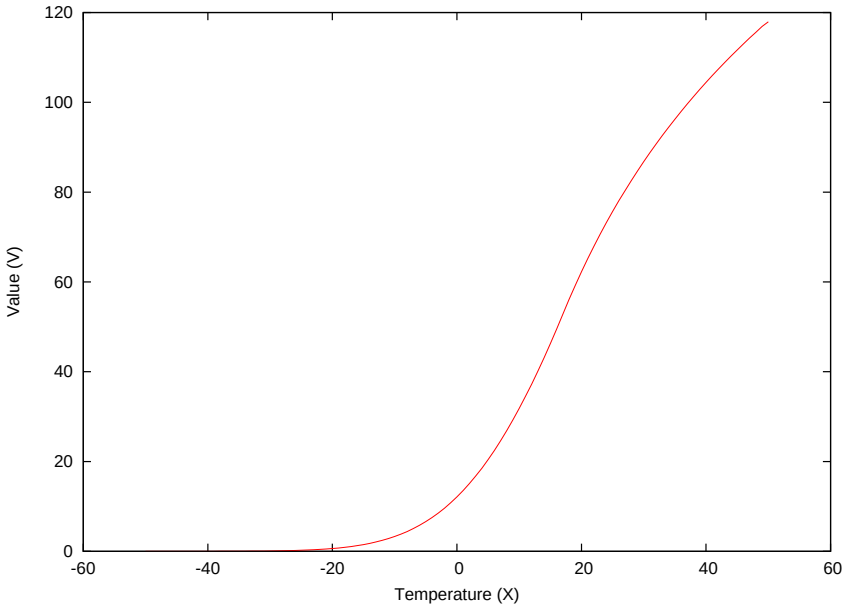

(a)

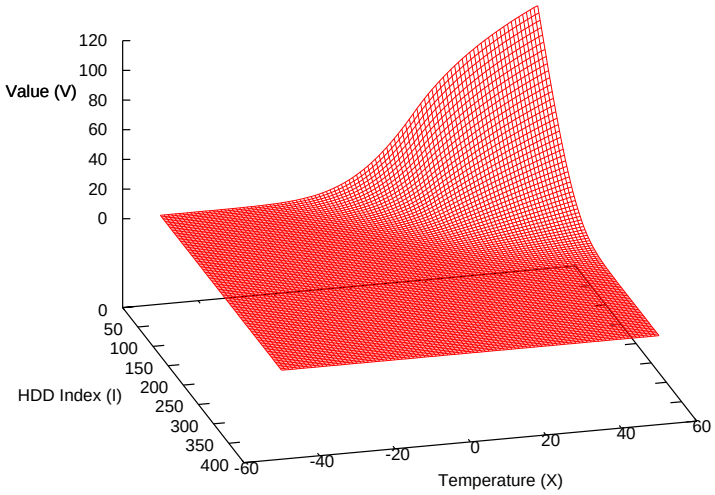

(b)

Figure 6.14: European put option price, with parameter set *EBM-01* but with $K = 400$. In figure 6.14(a) , $I = 0$ since at the start of the contract the index has no value. We show the solution profile in X and I dimensions in figure 6.14(b).

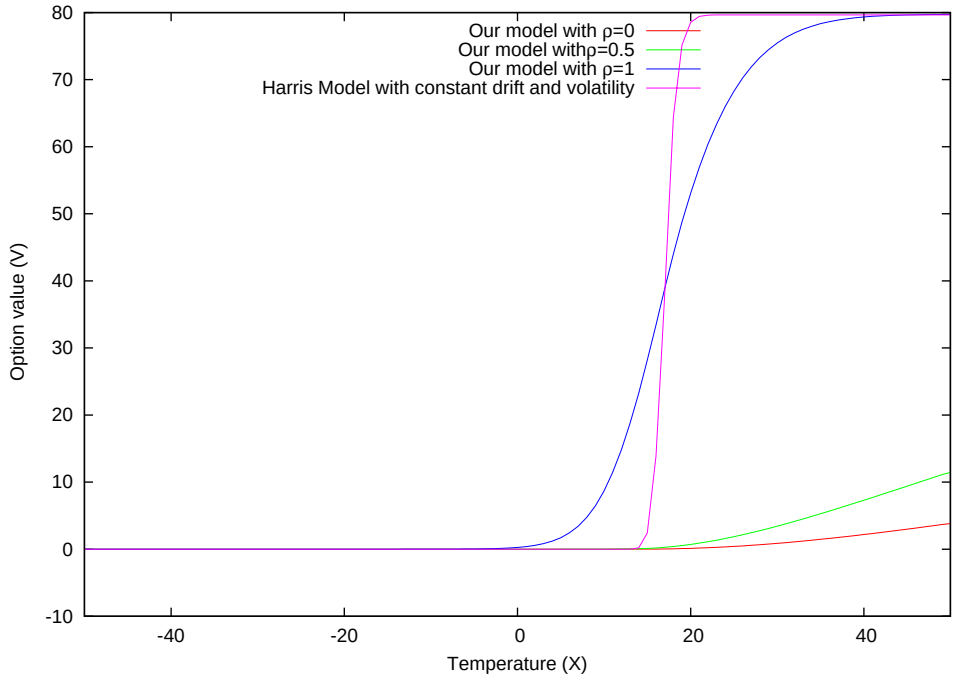

Figure 6.15: A comparison of the option values derived using the proposed model of (5.29) and that of Harris (2003). The parameters are given by *EBM-01*. For constant volatility and drift the values are $\sigma_X = 0.2285$ and $\mu_X = -0.0252$.

instruments correlation increases the dominance of the mean-reverting drift is lessen and when $|\rho| = 1$ the solution profile appears similar to that of Harris. However, our solution has a smoother profile since the specified volatilities are different.

A concrete example

Consider a capped European put option with parameter set *EBM-03*, payoff

$$V(X, I_H, T) = \min(\max(K - I_H, 0) \cdot tick, cap). \tag{6.104}$$

and additionally parameters $tick = £5,000$ and $cap = £1,000,000$. Notable from the parameter set, we have assumed there exists a suitable correlated instrument, with $\rho = 0.9$ such that a partial hedge is effective. The contract starts from January 1st to March 31st. We begin by illustrating in table 6.6 that the SLS provides convergence.

The general shape of the capped European put option price in figure 6.16 is very

similar to the one shown in figure 6.14(b). However, the observed temperature today now greatly impacts the option price. As an example, consider the option prices

$$V(X = 3, 0, 0) = 229,996,$$
$$V(X = 4, 0, 0) = 248,129,$$
$$V(X = 5, 0, 0) = 266,948,$$

we can then compute the delta of the option to be, $\frac{\partial V}{\partial X}(X_0, 0) = 18,476$. This is significant because using our model, incorrect observations of today's temperature can lead to large mis-pricing depending on the structure of the payoff. The reasons for this increased sensitivity stems from the inclusion of the *tick* multiplier in the payoff condition (6.104). Consequently, at expiry for every unit that I decreases leads to an increase of $5,000$ in the final payoff. As expected, the sensitive is reduced as the we move towards the limits X_{min} and X_{max}. Increasing the speed of mean-reversion κ reduces the option's sensitivity to initial temperature, the reverse is true when $\kappa \to 0$. We present this result in figure 6.17. However, this parameter should be measured according to historical weather data or accurate forecasts, to ensure that the underlying temperature dynamics behave realistically.

6.5.1 Effects of ρ on the weather option price

A particular point of interest, and one which is crucial in the specification of our new weather option PDE, is the relationship between option prices and the observed correlation between temperature and the traded asset. Moreover, from the arbitrage arguments which led to the definition of $\gamma(X, \tau)$, ρ is a free parameter which can be independently changed. The temperature drift and volatility structures could be altered as weather changes, but this is usually fixed and based on estimates from historical weather data. According to (5.29), increasing $|\rho|$ implies that a more suitable hedge is available, hence the risk for the issuer of the contract decreases, as shown by Windcliff et al. (2007). However, in the case of a mean-reverting process the situation is quite subtle. If $\rho = 0$, then the drift

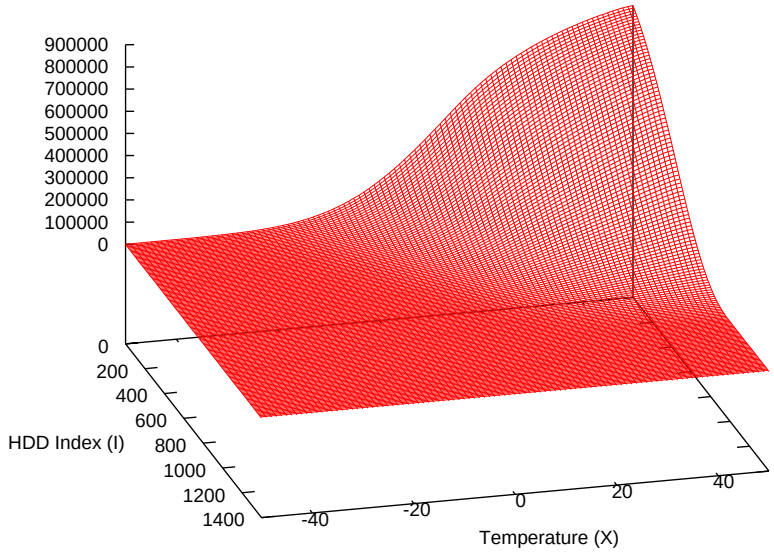

Figure 6.16: A 3D illustration of the option price's behaviour at $t = 0$, using parameters *EBM-03*.

term is purely driven by the mean-reverting temperature drift, i.e.

$$\gamma(X, \tau) = \mathrm{d}\theta(t) + \kappa\left[\theta(t) - X\right]\mathrm{d}t.$$

As we illustrated previously, the put option price increases through the X domain, starting from negative then through to positive values. Figure 6.18 shows how the solution of a capped European HDD put option, using parameter set *EBM-03* and payoff (6.104), behaves as $\rho^{0.5}$ varies. For $\rho^{0.5} \neq 0$ the sign of γ changes depending on the position of V in X space. In the region where $X \approx -50$, the movement in the X domain is dominated by a positive temperature drift such that we have $\gamma \approx \mathrm{d}\theta(t) + \kappa\left[\theta(t) - X\right]\mathrm{d}t > 0$. A positive drift term has the effect of making the option price more expensive, which explains the behaviour of the solution depicted in figure 6.18(b). When $X \approx 50$, the mean-reverting drift becomes large and negative and subsequently this depresses the option price. This is not unusual because the market price is not equivalent to the hedging price, and therefore being able to hedge will not translate necessarily into the option value being reduced.

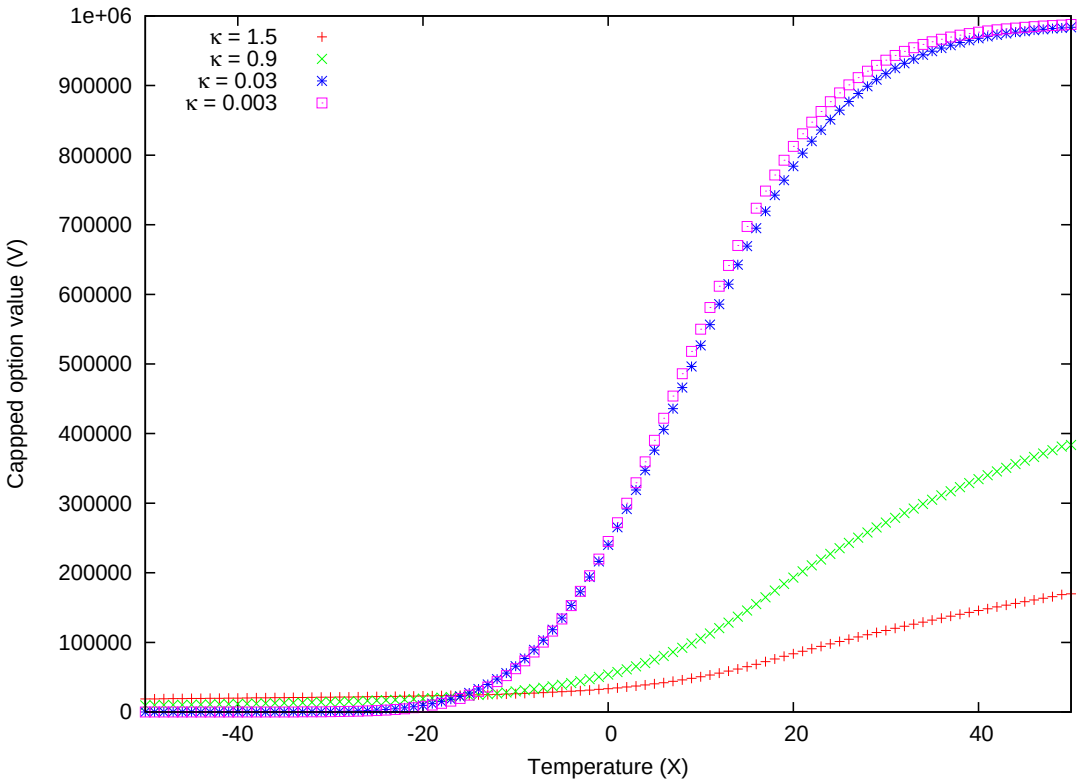

Figure 6.17: The behaviour of the option price as the specification of mean-reversion changes. The parameters used here are given by *EBM-03*, for a capped European HDD put option with payoff (6.104).

6.5.2 Further numerical enhancements

To improve the accuracy of the scheme further, Richardson extrapolation could be used (but this was not used in our implementation). First suggested by Geske and Johnson (1984), it forms an integral part of the methods for Andricopoulos et al. (2003) and Widdicks, Andricopoulos, Newton, and Duck (2002). The idea is as follows: Let V_E be the exact price of the option, and take V_n as the value given by the numerical method with n steps. If the rate of convergence, as $n \to \infty$, is known to be $1/(n)^c$, where c is the order of convergence, then V_n is assumed to have form:

$$V_n = V_E + \frac{h_1}{n^c} + \text{smaller terms}, \tag{6.105}$$

where h_1 is unknown but stays constants for different n. Take approximations V_{n_1} and V_{n_2} which used n_1 and n_2 steps respectively, and equate equations in

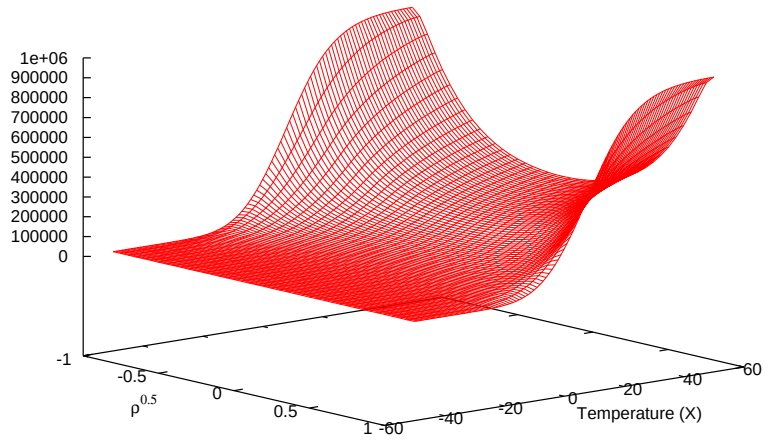

(a)

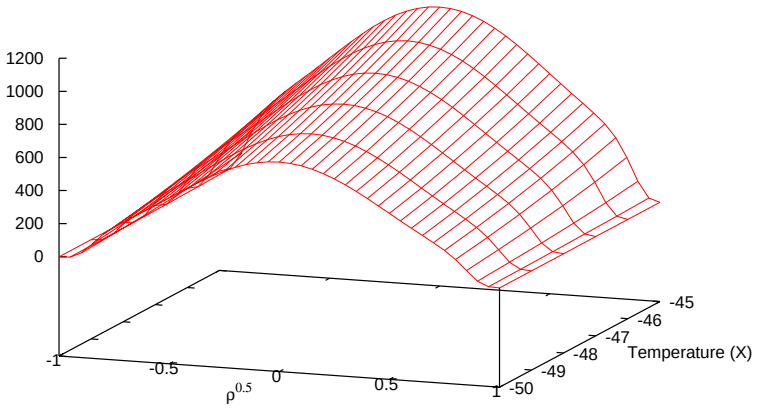

(b) Solution in a subsection of the X domain

Figure 6.18: The behaviour of the option price caused by varying the correlation between temperature and the hedging asset H. $\rho^{0.5}$ is observed at intervals of size 0.05. The bottom graph highlights the hidden curvature that exists in the region where X is large and negative.

terms of h_1

$$h_1 = (n_1)^c V_{n_1} - (n_1)^c V_E = (n_2)^c V_{n_2} - (n_2)^c V_E. \tag{6.106}$$

This is simple rearranged to give

$$V_E = \frac{(n_1)^c V_{n_1} - (n_2)^c V_{n_2}}{(n_1)^c - (n_2)^c}. \tag{6.107}$$

Alternatively, the use of more densely spaced grid points in the region where the solution changes rapidly might offer improvement, but at a considerable increase in computational effort. Another possibility for investigating the very slight central bulge in (b) of 6.18 would be to test alternative forms of boundary condition, such as a Robin condition in the direction of $\rho^{0.5} = 1, -1$ along the X boundaries at $\rho^{0.5} = 1, -1$.

6.6 Summary

This chapter has discussed a variety of numerical schemes and examined some of the difficulties of using an implicit central-difference scheme. These drawbacks can be overcome by using an SLS, and by imposing the weak condition of (6.101) to suppress errors introduced from interpolation.

We observed an objectively small but qualitatively interesting result when $\rho \neq 0$ and X is very small. In practical terms we would anticipate that if $\rho = 0$, hedging is no longer possible and therefore a put issuer's selling price will increase, relative to the case when $|\rho| = 1$. The price that the issuer is charging is best referred to as the market price, since this is what participants are prepared to pay. In this chapter we are computing the fair hedging price, but by assuming the hedge portfolio to provide mean zero returns, we have neglected the additional random risk. Relaxing this assumption of having a mean self-financing portfolio greatly affects the prices of weather derivatives, and we consider this impact in the next chapter.

Chapter 7

Weather Options with an added risk-premium

> *If we drop the assumption that markets are always correct and that financial modelling is at best an approximate science, then there is no such thing as risk-free hedging .... [An] alternative approach assumes uncertain volatility: if volatility is so difficult to measure, why not accept this situation and instead work on volatility ranges? A consequence is that there is no such thing as a single fair value for an option, all prices within a given range are possible.*
>
> ***Paul Wilmott***

This chapter develops the weather option valuation model proposed in chapter 5, where we now relax the assumption that in expectation the change in the portfolio is mean self-financing, i.e. $\mathbb{E}[\mathrm{d}\Pi_t] = 0$. Recall from chapter 5 that the portfolio is random since the process of delta-hedging does not eliminate all sources of risk. This issue of random payoffs which are not hedgeable appears in the insurance pricing literature. For example, Moller (1998) approaches the valuation of a unit-linked life insurance contract from this perspective, and Windcliff et al. (2007) price a segregated funds contract that provides guarantees on mutual funds held in pension plan investment accounts. The resulting pricing equations of these papers differ greatly, with the former using principles of self-financing strategies and martingale theory, whereas a PDE approach is used in the latter paper. We adopt a similar approach to that outlined in Windcliff et al. (2007),

to derive a new weather option PDE which is non-linear in the instances where the payoff structure is more complicated than simple put and call options. Using the extended model produces option prices that have been priced relative to the magnitude of risk that remains after the partial hedge. To our knowledge use of these principles for the valuation of weather derivatives has not been covered in the literature previously.

7.1 Extension to the weather option PDE

Considering a portfolio to be mean self-financing is perhaps an over-simplification used in the derivation of the weather derivative pricing equation (5.29). As discussed by Windcliff et al. (2007), insolvency problems can arise for an investor (or insurer) who charges a price based on equation (5.29). Jewson et al. (2005) provide an illustration of this point by performing trading simulations, where the option is repeatedly issued at the fair price, for independent realisations of the weather index. Their results show that issuing a weather option at its fair price will lead to an expected loss in the trade, unless trading continues for almost 100 hundred years into the future. Over this time horizon, the mean profit reaches zero. Therefore, trading at the fair price can result in insolvency problems (Windcliff et al., 2007). Since weather derivatives typically have short maturities, investors are thus concerned about managing their short-term risks and will therefore charge more than the derived fair price. This difference between the fair option price and the price charged by the issuer is captured by the market price of risk (3.13). Møller (2001) indicates that if residual risk is not diversifiable, then the option writer should be compensated for bearing this extra risk. In this incomplete market situation, there are various approaches that can be used to value the contract. We have already discussed in chapters 3, 4 and 5 the works of several authors who value derivatives in an incomplete market. We therefore do not repeat this literature review in this chapter, but instead present our extension to the previously derived weather pricing model. Such weather option prices incorporate an extra premium that is awarded for bearing unhedgable risk.

We begin by reconsidering the variation in the portfolio (5.24)

$$\begin{aligned} \mathrm{d}\Pi_t &= \left[\frac{\partial V}{\partial t} + \gamma(X,t)\frac{\partial V}{\partial X} + \frac{1}{2}\sigma_X^2(t)\frac{\partial^2 V}{\partial X^2} + f(X,t)\frac{\partial V}{\partial I} - rV\right]\mathrm{d}t \\ &+ \sigma_X \frac{\partial V}{\partial X}\sqrt{1-\rho^2}\mathrm{d}Z_2, \end{aligned}$$

which was obtained by using the hedging strategy of

$$\Delta = \rho\frac{\sigma_X}{\sigma_H}\cdot\frac{\frac{\partial V}{\partial X}}{H}. \tag{5.23}$$

In order to continue, we briefly review principles of actuarial premium calculations. From Møller (2001), the two most widely used calculation principles are referred to as the *variance principle*

$$V_{var} = \mathbb{E}[V] + \lambda \mathrm{Var}[V]. \tag{7.1}$$

and the *standard deviation principle*

$$V_{sd} = \mathbb{E}[V] + \lambda\sqrt{\mathrm{Var}[V]}. \tag{7.2}$$

We use principle (7.2) in §4.3.2, to appropriately adjust the fair price obtained from burn analysis for both a swap and option contract. The second term in equation (7.1) and (7.2) should be regarded as the level of reserve the issuer must have (or obtain from the buyer of the contract) so that any payouts can be honoured. These terms are frequently referred to as *safety loadings* in the context of insurance pricing. These principles suggest that the option value can be determined as its expected value plus some compensation. As pointed out by Ibáñez (2005) and Windcliff et al. (2007), it is not unreasonable for an investor to expect to earn a premium at a rate that is proportional to his risk. More precisely, during a time-interval Δt the portfolio's value should appreciate in accordance to the size of the risk, so that by using the standard deviation principle (7.2) we obtain

$$\mathbb{E}[\mathrm{d}\Pi_t] = \lambda\sqrt{\frac{\mathrm{Var}[\mathrm{d}\Pi_t]}{\mathrm{d}t}}\mathrm{d}t. \tag{7.3}$$

This is equivalent to defining a market price of risk associated with the residual risk $\mathrm{d}Z_2$, and has been used by Ibáñez (2005) and Cochrane and Saa-Requejo

(2000) to value real options. Therefore, LHS of (7.3) becomes

$$\begin{aligned} \text{LHS} &= \lambda\sqrt{\frac{\text{Var}[\text{d}\Pi_t]}{\text{d}t}} \\ &= \lambda\sigma_X\left|\frac{\partial V}{\partial X}\right|\sqrt{1-\rho^2} \\ &= \text{sgn}\left(\frac{\partial V}{\partial X}\right)\lambda\sigma_X\frac{\partial V}{\partial X}\sqrt{1-\rho^2}, \end{aligned} \tag{7.4}$$

and $\text{sgn}(z)$ denotes the sign of z. Taking the expectation of (5.24) and combining the result with (7.4) produces the following PDE

$$\frac{\partial V}{\partial t}+\left(\gamma(X,t)-\text{sgn}\left(\frac{\partial V}{\partial X}\right)\lambda\sigma_X\sqrt{1-\rho^2}\right)\frac{\partial V}{\partial X}+\frac{1}{2}\sigma_X^2(t)\frac{\partial^2 V}{\partial X^2}+f(X,t)\frac{\partial V}{\partial I}-rV=0. \tag{7.5}$$

The solution to this PDE is a weather option price that incorporates a risk premium to compensate for the fact that temperature cannot be traded and no perfect hedge is available. This is analogous to the case of paying dividends to investor for holding a risky financial stock. Of particular interest here is that this PDE is valid only for a long position in V. Notice that in the definition of our portfolio, we have assumed we are long the option, which implies that since prefect replication is not possible, the risk the investor is exposed to is mainly upside-risk (with the downside being the option's premium), whereas for the option writer there is a possibility of making a large payout. Therefore we would expect these prices to now be different as the risks involved are no longer symmetrical. A similar PDE for the short position can be easily derived by first considering the portfolio

$$(\Pi_t)_s = -V_t + \Delta H_t + M_t, \tag{7.6}$$

where we have used the subscript s to distinguish this from our original portfolio (5.17). Then by choosing Δ as defined in (5.23), the change in the portfolio (7.6) is

$$\begin{aligned} (\text{d}\Pi_t)_s &= -\left[\frac{\partial V}{\partial t}+\gamma(X,t)\frac{\partial V}{\partial X}+\frac{1}{2}\sigma_X^2(t)\frac{\partial^2 V}{\partial X^2}+f(X,t)\frac{\partial V}{\partial I}-rV\right]\text{d}t \\ &+ \sigma_X\frac{\partial V}{\partial X}\sqrt{1-\rho^2}\text{d}Z_2. \end{aligned}$$

Since the change in the portfolio is not deterministic, the holder would expect to be compensated. Therefore, we make use of principle (7.3) and then find that the PDE for the weather option's short position is given by

$$\frac{\partial V}{\partial t}+\left(\gamma(X,t)+\operatorname{sgn}\left(\frac{\partial V}{\partial X}\right)\lambda\sigma_X\sqrt{1-\rho^2}\right)\frac{\partial V}{\partial X}+\frac{1}{2}\sigma_X^2(t)\frac{\partial^2 V}{\partial X^2}+f(X,t)\frac{\partial V}{\partial I}-rV=0. \tag{7.7}$$

We can express PDEs (7.5) and (7.7) succinctly as

$$\frac{\partial V}{\partial t}+\left(\gamma(X,t)+q\lambda\sigma_X\sqrt{1-\rho^2}\right)\frac{\partial V}{\partial X}+\frac{1}{2}\sigma_X^2(t)\frac{\partial^2 V}{\partial X^2}+f(X,t)\frac{\partial V}{\partial I}-rV=0, \tag{7.8}$$

where q is

$$q=\begin{cases}-\operatorname{sgn}\left(\frac{\partial V}{\partial X}\right) & \text{if long,}\\ \operatorname{sgn}\left(\frac{\partial V}{\partial X}\right) & \text{if short.}\end{cases} \tag{7.9}$$

Depending on the payoff structure, $\partial V/\partial X$ is not single-signed. A straddle would be a good example of this since the combination of both a call and put implies that its delta will change signs in certain regions. We value straddles in §7.2. In this case we cannot drop the modulus sign in (7.8), therefore the equation is non-linear and must be solved numerically. Hoggard, Whalley, and Wilmott (1994) introduced one of the first non-linear PDEs in their model for options with transaction costs. More recently, Glover (2008) derives a non-linear PDE to price an illiquid option with a price impact factor feeding back into the governing asset price process. Non-linear PDEs can result in non-unique prices being obtained (Glover, Duck, and Newton, 2010, provides insights and cautionary notes). Consequently, we no longer obtain single prices for the option, but rather determine pricing bands that indicate the cheapest and most expensive price to be paid for the derivative. This is typical of an incomplete market problem. So rather than naïvely following the existing literature on weather derivatives, we assume that $\lambda \neq 0$. This approach is very much in line with the quote from Willmott at the start of this chapter; that financial modelling is an approximate science and thus a band of prices exists.

If we denote the value of the short position as V^s and long position V^l then in order for a weather market to exist the condition $V^s \geq V^l$ must be satisfied, otherwise no one would ever write an option. Both V^s and V^l are positive. We can confirm that our PDE model (7.8) satisfies this condition by considering the valuation of a simple call option. For this option $\partial V/\partial X \geq 0$ which implies $q > 0$

for the short position which has the effect of increasing the value of the option, whereas in the long position $q < 0$ which reduces the price. Therefore $V^s \geq V^l$. Similarly for a put option $q < 0$ in the short position, and from figure 7.1 this will translate the payoff condition to the right, thus increasing the value of the option. In the long position this option's value is decreased because when $q > 0$ the payoff condition is translated to the left.

7.2 Valuation

Following the detailed analysis in chapter 6, we make use of the SLS to discretise and then solve the non-linear PDE (7.8). As the discretisation of the PDE is almost identical to (6.88), we omit reproducing the derivation and state that the only differences is that $\gamma(X, \tau_{n+1})$ in equations (6.89) and (6.90) is replaced by the new drift term

$$\gamma(X, \tau_{n+1}) + q\lambda\sigma_X(\tau_{n+1})\sqrt{1-\rho^2}.$$

We demonstrate that in this incomplete market setting, there exist large spreads between the bid (long) and ask (short) prices of weather options. The non-linear component of the (7.8) is then considered, as we price a straddle option.

Parameter choices

In our numerical examples, the results obtained are not directly comparable to the weather derivative market because the choices of parameters are not derived from market data. Until the UK weather derivatives markets' liquidity increases, robust estimates of model parameters through methods of calibration are not available. The level of compensation an investor demands for risk is difficult to set accurately. Turvey (2005) considers $\lambda = 0$, however Bellini (2005) demonstrates empirically that the value of λ is very different from zero and that it is time-dependent. Alaton et al. (2002) attempt to determine the value of λ by calibrating their model prices with two quoted OTC weather derivative prices, though this is too limited a data set to be confident of the market's value for λ. Instead, we use the numerical values for λ presented in Møller (2001), since this provides a selection of possible option prices for investors with different risk appetites

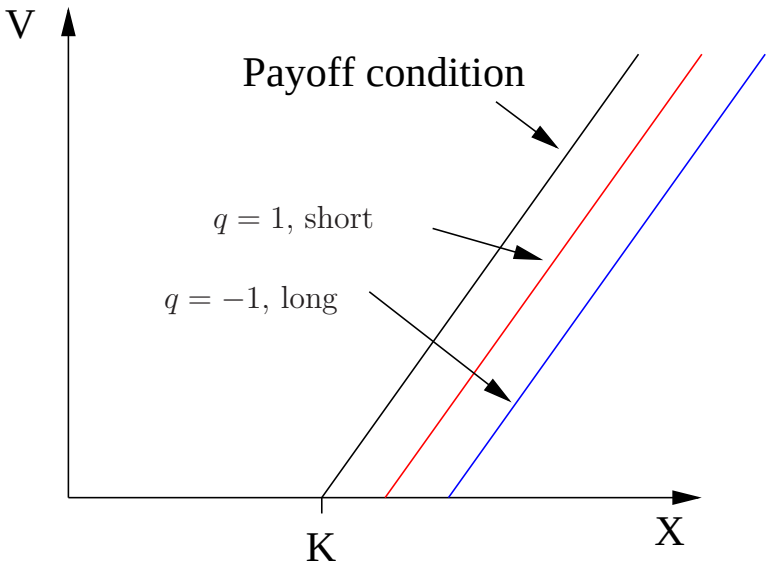

(a) Call option payoff

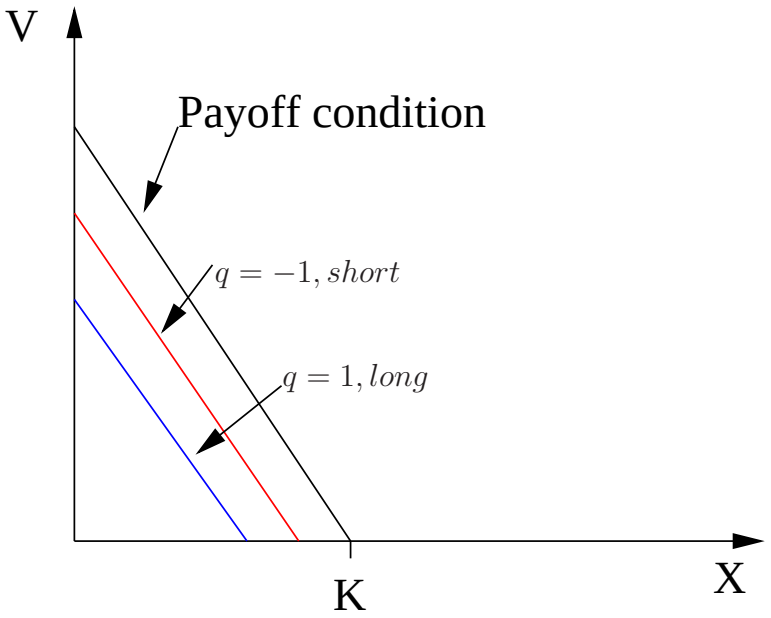

(b) Put option payoff

Figure 7.1: The movement of a call and put option as the magnitude of the $\partial V/\partial X$ coefficient increases/decreases.

λ	0.01	0.1	0.25	0.5	1	2

Table 7.1: Numerical choices for the market price of risk, λ. Source: Møller (2001). The larger the value of λ the greater the level of compensation awarded.

(these values are listed in table 7.1). The volatility of temperature is given by the averaged monthly volatility estimate (5.47), where the numerical values of each month are presented in the second column of table 5.4. The mean reversion and seasonal mean are as specified in parameter set *EBM-03*. In all the examples we take $tick = £5,000$ and $cap = £1,000,000$, unless specified otherwise.

Results

In figure 7.2(a) we show the numerical solution of a capped European HDD put option, where virtually no additional compensation is awarded for the residual risk. In this case we have taken $\lambda = 0.01$. Also in this example, we have assumed a sufficiently accurate partial hedge as $\rho = 0.9$; the results are intuitive. Because the portfolio only earns a small premium for carrying additional risk, the short and long position option values V^s and V^l in the figure are very close. In particular, the spread between the short and long position prices decreases as the temperature becomes extremely cold (i.e. where $X \to -50$). This is because when the initial temperature is very cold the probability that it will rise above 18°C is small, which implies that the HDD index will be large. Thus the probability for which the option will expire with a positive payoff is very low. A HDD weather contract that has an initial temperature below the barrier X_{ref} can be regarded as being out of the money (OTM). For contracts that begin far OTM the values of V^s and V^l tend to the value of the fair premium. The difference between the prices changes significantly as we increase the market price of risk, λ. In figure 7.3 the option has been valued using a variety of values for λ, such that for increasing values of λ the difference in the short and long position put prices grows. However, there is a bound to the level of increases since the option's value has an upper bound. This point is illustrated clearly in figure 7.3(d). Taking $\lambda = 1$, and pricing an uncapped put option we can see from figure 7.4 that prices far exceed those found in 7.3(d) and only begin to approach the maximum value of $e^{-rT}K \cdot tick$ for $X > 10$, as opposed to reaching its maximum value from $X = -10$ onwards. To understand the significance of our findings, we examine

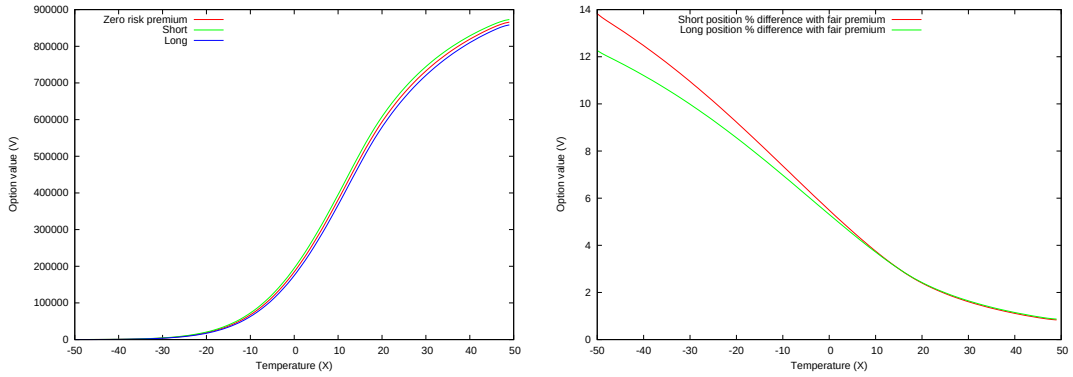

Figure 7.2: The figure on the left gives the value of a put in the long and short positions. Also included is the value of the fair premium that is computed using PDE (5.29). Here the partial hedge is effective, $\rho = 0.9$. $\lambda = 0.01$, with other parameters from *EBM-03*. The right-hand figure shows the percentage differences of these option prices against the fair premium for a put option.

the percentage difference of the short position and long position prices above and below the fair premium, respectively. For $X = 4$, and $\lambda = 0.01$ (implying that the investor should earn a premium that is a 1/10 of the standard deviation of the residual risk), the short position price is 4.58% more expensive that the fair premium and the long position price 4.68% cheaper. We illustrate the percentage difference of the short and long prices relative to the fair price in figure 7.2(b).

The solution of a call option is similar and is presented in figure 7.5. However, we use a different boundary condition along I_{max} since in this region a call option will likely have value. We specify the following Dirichlet boundary condition

$$V(X, I_{max}, t) = e^{-r\tau}K. \tag{7.10}$$

We purposely defined the boundary conditions at X_{min} and X_{max} in a general manner so that they could be applied to value a variety of options with different payoff structures, such as straddles.

As (7.8) becomes non-linear when an option's delta is not singled-signed, we consider the valuation of a portfolio of options. Specifically we value a straddle, with payoff

$$V(T) = \max(I - K, 0) + \max(K - I, 0). \tag{7.11}$$

In figure 7.6, we show solution of an option with payoff (7.11) at different times

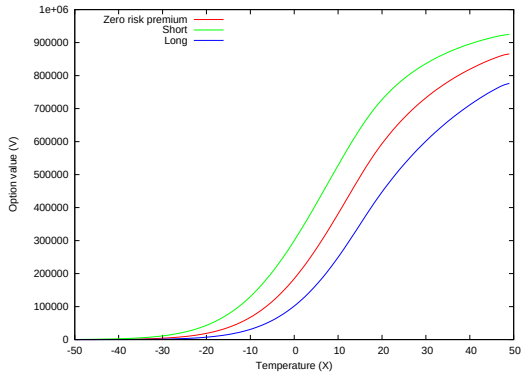

(a) $\lambda = 0.1$

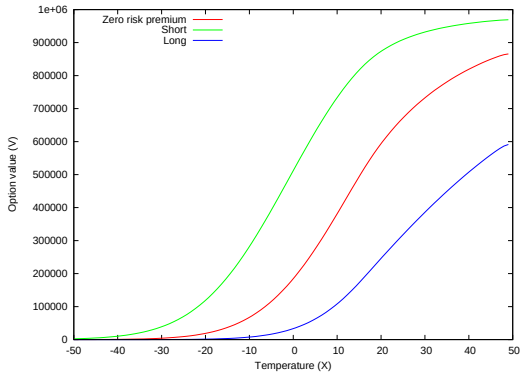

(b) $\lambda = 0.25$

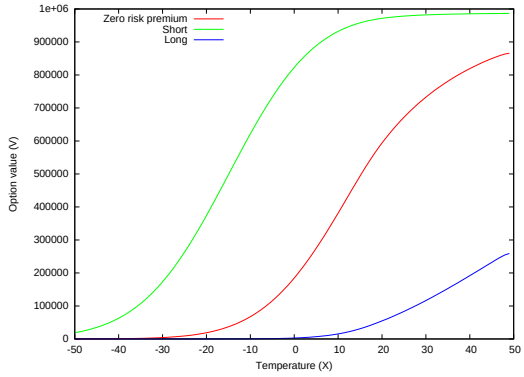

(c) $\lambda = 0.5$

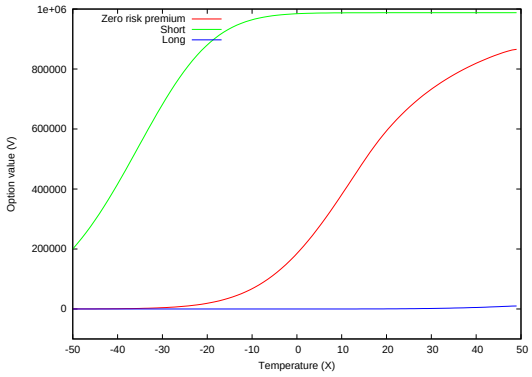

(d) $\lambda = 1$

Figure 7.3: Option prices for the long and short positions for different values of λ. The fair premium price is included. $\rho = 0.9$, with other parameters as given by *EBM-03*. We adjust the range of the last diagram so that the last line can be seen clearly.

t. Interestingly, the capped straddle option prices in figure 7.6(d) exhibit much smoother (and flatter) solution profiles through X than an uncapped straddle, shown in figure 7.6(b). This confirms that constructing weather options as a capped straddle can reduce an investor's risk as payoff is likely in these instances.

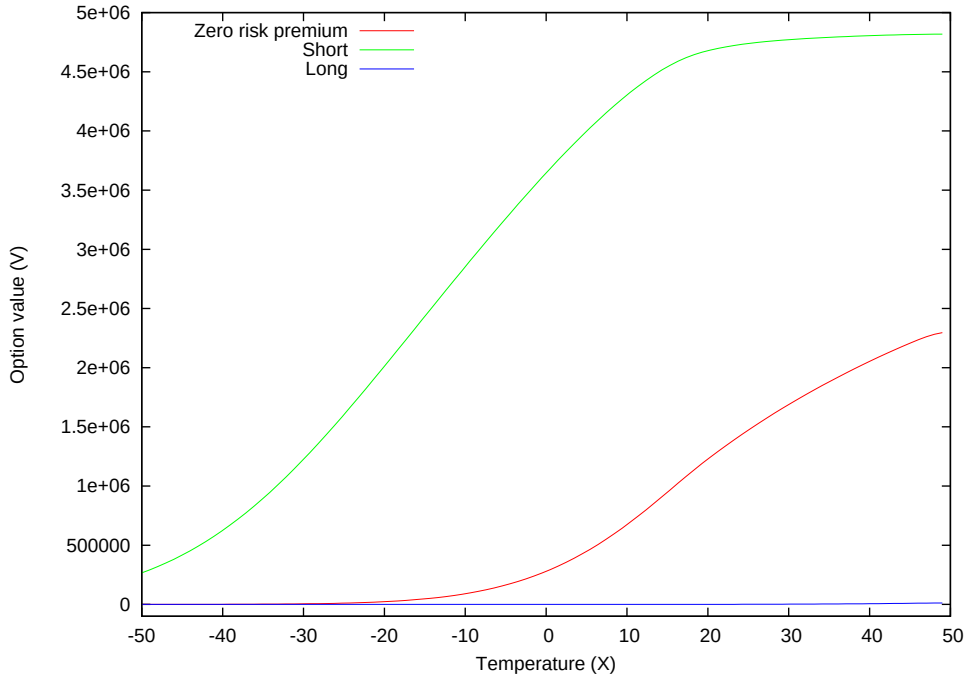

Figure 7.4: Put option price for an uncapped put. Parameter set *EBM-03*, $\lambda = 1$, $\rho = 0.9$. We adjust the range of the last diagram so that the last line can be seen clearly.

7.3 Summary

In this chapter we extend the previous model from chapter 5, to obtain a PDE that produces prices for weather options that include an added risk-premium, which is relative to the magnitude of risk that the investor is exposed to, due to not being able to trade the underlying quantity to create full hedge. Using our model, the option values for a counterparty holding the long or short position are no longer equal, unless the correlated asset being used in the hedging of the contract is perfectly correctly with temperature (i.e. $|\rho| = 1$) or ($\lambda = 0$). We demonstrate the non-linear nature of the PDE, in the case of valuing a straddle weather option.

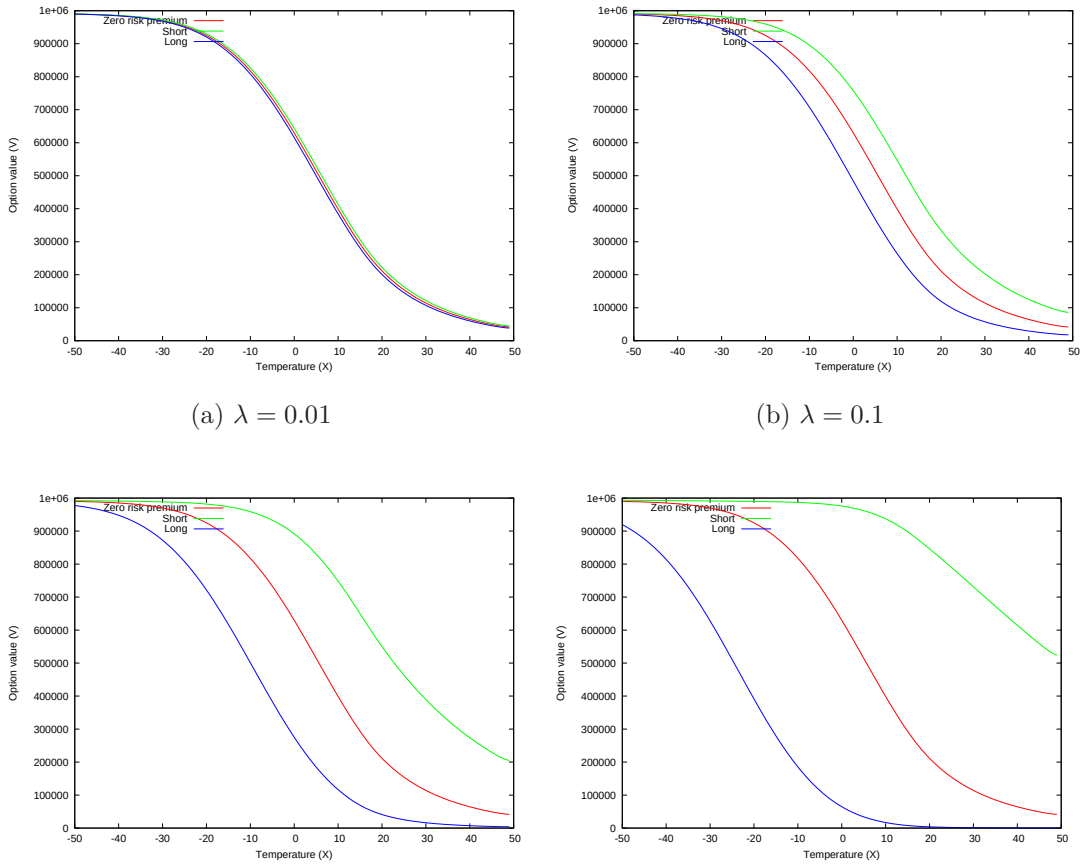

(a) $\lambda = 0.01$ (b) $\lambda = 0.1$

(c) $\lambda = 0.25$ (d) $\lambda = 0.5$

Figure 7.5: Call option prices for the long and short positions for different values of λ. The fair premium price is included. $\rho = 0.9$, with other parameters as given by *EBM-03*.

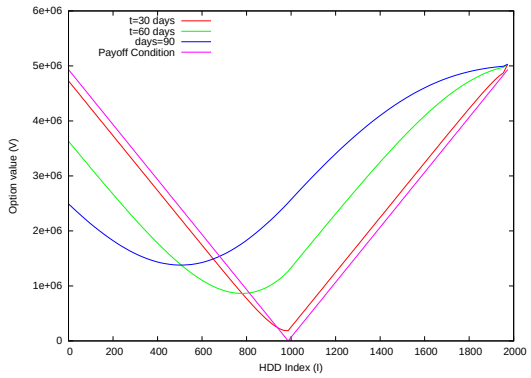

(a) Uncapped straddle time evolution

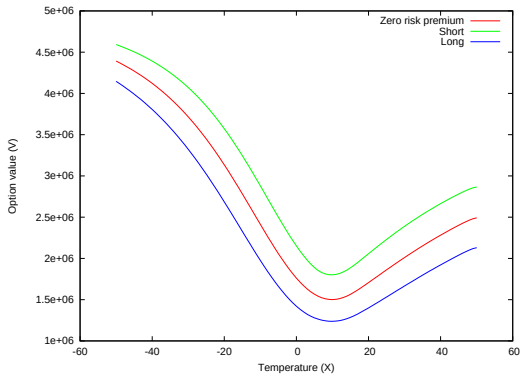

(b) Uncapped straddle prices

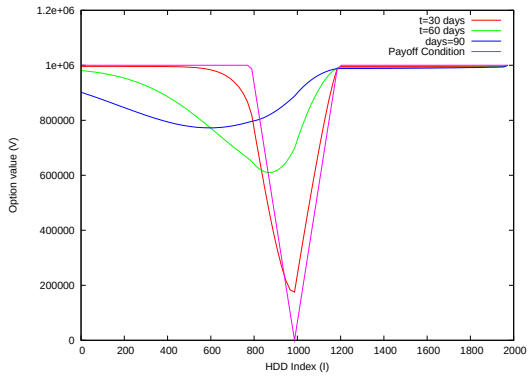

(c) Capped straddle time evolution

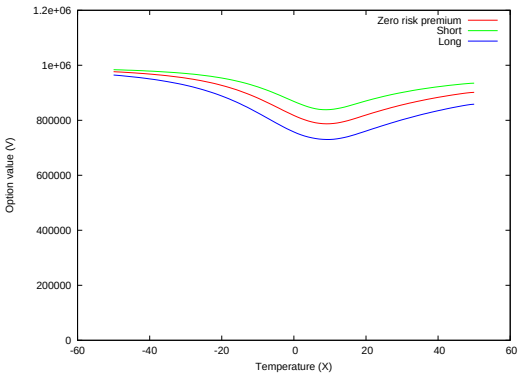

(d) Capped straddle prices

Figure 7.6: The evolution of a capped and uncapped straddle option price through time and I space. Here $\lambda = 0.1$, $\rho = 0.9$, and parameter set *EBM-03*.

Chapter 8

Improved numerical techniques for alleviating non-linearity errors

Parts of this chapter were presented at the 6th World Congress of the Bachelier Finance Society, June 22nd-26th 2010, Toronto, Canada

> *Change is the law of life. And those who look only to the past or present are certain to miss the future.*
>
> **John Fitzgerald Kennedy**

In the previous chapter we introduced the valuation of derivatives involving more complex payoff structures. These types of weather derivative contracts are becoming increasingly traded as industry participants attempt to mitigate their weather risks. Jewson et al. (2005) note that a company's weather-related financial returns may not be derived from the weather conditions at one specific location, but rather across multiple locations. Therefore, the purchase of a weather basket option would be more attractive than needing to individually manage separate contracts, one for each location. The pricing of a basket option using finite-difference or other lattice-based schemes, such as a binomial tree, can be problematic since it is difficult in multiple dimensions to ensure that computational grid points will lie on discontinuities. When grid points are not correctly

aligned oscillatory solutions can be introduced, as we saw in figure 6.6(d). The problem of locating these discontinuities becomes more complex as the number of underlying weather indices increases.

The aims of this chapter are twofold. Firstly, to introduce a quadrature scheme that can be used to value weather derivatives and other financial derivatives with precision. Secondly, we propose and develop a generic methodology for overcoming this non-linearity error that is typically found in lattice-based option pricing, such as binomial trees or finite-difference (Widdicks et al., 2002). The proposed methodology's effectiveness is demonstrated by pricing options on multiple underlyings.

8.1 The QUAD method

The use of numerical quadrature to price options was introduced by Andricopoulos et al. (2003) and then later extended to the case where the option has multiple underlying in Andricopoulos, Widdicks, Newton, and Duck (2007). In both papers, the authors employ simple numerical integration techniques, namely the trapezium and Simpson's rule to solve the resulting integral (8.3) (which is presented the following section). We modify their work, and suggest the use of the tanh-sinh scheme (explained in §8.1.3), which consequently increases the numerical accuracy of option prices and reduces computational times. In this section we begin by describing briefly the key aspects of the QUAD method.

8.1.1 Building blocks of QUAD

In our description of the method, we assume the same Black & Scholes framework as proposed in Andricopoulos et al. (2003) and so begin with PDE

$$\frac{\partial V}{\partial t} + \frac{1}{2}\sigma^2 S^2 \frac{\partial^2 V}{\partial S^2} + rS\frac{\partial V}{\partial S} - rV = 0. \tag{8.1}$$

where σ is the volatility, r is the risk-free rate and S is the underlying. QUAD exploits the fact that this PDE can be represented as an integral equation which consists of the payoff function and the Green's function representation of (3.10).

By considering K to be the strike value, and then performing the change of variable

$$x = \ln\left(\frac{S_t}{K}\right), \quad y = \ln\left(\frac{S_{t+\Delta t}}{K}\right) \tag{8.2}$$

with Δt being the time interval between two time observations, the value of the option $V(S_t, t)$ can be expressed as

$$V(x,t) = A(x)\int_{-\infty}^{\infty} B(x,y)V(y,t+\Delta t)\mathrm{d}y \tag{8.3}$$

where

$$A(x) = \frac{1}{\sqrt{2\sigma^2\pi\Delta t}}\exp\left(-\frac{kx}{2} - \frac{\sigma^2k^2\Delta t}{8} - r\Delta t\right), \tag{8.4}$$

$$B(x,y) = \exp\left(\frac{ky}{2} - \frac{(x-y)^2}{2\sigma^2\Delta t}\right) \tag{8.5}$$

and

$$k = \frac{2r}{\sigma^2} - 1. \tag{8.6}$$

Theoretically, we are required to evaluate the integral over a doubly-infinite range in order to solve the problem correctly. Expression (8.5) reveals that our interval of integration need not necessarily be large, to accurately evaluate our option. This is evident because our value for x is fixed over the integration and remains modestly small due to its log-normal nature. However, as $|y| \to \infty$, the exponential term in $B(x,y)$ behaves as e^{-y^2}, which rapidly approaches zero and consequently results in an insignificant contribution to the overall integral. This then permits the truncation of the range of integration in order to practically solve (8.3) (Andricopoulos et al., 2003). In accordance with (8.2) define

$$x_0 = \ln(S_0/K), \tag{8.7}$$

where S_0 is the value of the asset and x_0 is our log-transformed variable, both at $t = t_0$. The truncated range of integration shall be referred to as $[y_{min}, y_{max}]$ and take the value

$$y_{max} = x_0 + x_\Delta \tag{8.8}$$

$$y_{min} = x_0 - x_\Delta \tag{8.9}$$

where

$$x_{\Delta} = D\sigma\sqrt{T}. \tag{8.10}$$

In (8.10) D denotes the number of standard deviations we anticipate x to move within the next time-step. We mentioned this parameter earlier in chapter 6 but omitted much of the detail so as to not disturb the flow of the text; here we expand slightly. The value of D is important and should not be set too small or large. Choosing a small value for D results in significant contributions being neglected, since the range of integration is too small which consequently impacts the quality of the final solution. Conversely, if chosen too large, then either the computational time is dramatically extended as more points are evaluated or the size of Δy needs to be increased; ultimately affecting the accuracy of the result. Practically, the size of D is chosen to lie between 7 and 20, and Andricopoulos et al. (2003), and Law (2009) indicate that a suitable choice is for $D = 7.5$.

As with all quadrature schemes, it is necessary to determine the number of knot-points we wish to use in order to approximate the given integral. Let us define

$$N_{above} = \text{NEINT}\left(\frac{y_{max} - b}{\Delta y}\right) \tag{8.11}$$

$$N_{below} = \text{NEINT}\left(\frac{b - y_{min}}{\Delta y}\right) \tag{8.12}$$

to be the number of knot-points above and below the discontinuity point, b, respectively. The function NEINT(.), in both expressions (8.11) and (8.12), returns the nearest positive even number. This differs from the implementation given by Andricopoulos et al. (2003, 2007) but it then allows for the easy substitution of other numerical quadrature schemes which require a even number of grid points, such as Simpson's rule.

A subtle point here is that taking points above/below the strike value guarantees that a node will lie at b. In this instance monotonic and smooth convergence is permitted; in §8.5 we consider the effect of not having a grid point on the discontinuity.

Imposing equations (8.8) and (8.9) in equation (8.3), we obtain

$$V(x_0,t) \approx A(x) \int_{y_{min}}^{y_{max}} B(x_0,y)V(y,t+\Delta t)\mathrm{d}y, \tag{8.13}$$

where $V(y,t+\Delta t)$ is the option payoff. Depending on the nature of the option to be evaluated, integral (8.13) in general cannot be expressed analytically, unless we are concerned with evaluating simple European options. An important consideration when selecting a numerical scheme is the relative trade-off between numerical accuracy and computational efficiency. Usually the more complicated the scheme, the longer it takes to evaluate an integral, although it may offer fast convergence rates. The trapezoidal scheme is of $O(\Delta x^2)$, whereas the Simpson's is $O(\Delta x^4)$ accurate. The latter scheme is preferred as even though it is more computationally expensive this is not significant enough to prevent a higher-order approximation.

Other types of schemes are available such as Gaussian quadrature or Clenshaw-Curtis quadrature, where the main differences between these two and the Newton-Côtes schemes are that which allow for the flexible placement of evaluation grid points within the domain. Comparison of the tanh-sinh (see §8.1.3 below) against further quadrature schemes would be an interesting area of study to consider in the future.

We summarise the QUAD algorithm below

1. Set the number of knot-points, n, to obtain the required accuracy.
2. Define $x_0 = \ln(S_0/K)$ and set D such that $7 \leq D \leq 20$.
3. Calculate the value of y_{min}, y_{max}, and Δy.
4. Determine N_{below} and N_{above}.
5. Apply the final conditions:

   for $i = 0$ to N_{above} **do**
   Set $y_i = b + i\Delta y$
   Set the value of payoff $V(y_i, T)$
   end for
   for $i = N_{below}$ to 1 **do**

Set $y_i = b - i\Delta y$
Set the value of payoff $V(y_i, T)$
end for

6. Use the chosen quadrature scheme to integrate (8.13), and then multiply by $A(x)$ to obtain the value of the option.

8.1.2 Extension of QUAD to price discretely monitored options

QUAD can be extended to value options that have early exercise features, such as Bermudan and American options. Here we briefly show how this can be achieved for a Bermudan option, and refer the reader to Andricopoulos et al. (2007) for further details and examples.

In pricing a Bermudan put option with strike value K and maturity T, we define V_m to be the value of the option at time t_m where $m = 1, 2, 3 \ldots, M$ denotes the distinct exercise times. The option value at expiry, V_M, is

$$V_M(x, t_M) = \max(K - Ke^y, 0). \tag{8.14}$$

At each time where the holder can exercise the option we must determine whether the option is worth holding onto or not. This is determined via the early exercise condition

$$V_m(x, t_m) = \max(V_{m+1}(y, t_m), K - Ke^x). \tag{8.15}$$

Given that the pricing process begins from the final condition, i.e. going backward in time, the notation V_{m+1} is used to distinguish the option value at the previous time step from the currently evaluated option value V_m. It is evident that there is a discontinuity, b_m, at the point where $V_m = K - Ke^x$ at each time-step t_m. Therefore we split the range of integration in order to eliminate non-linearity error. To determine the value of b_m, we apply Newton-Raphson iteration to find an approximation to the zeros of some real-valued function, here defined as

$$p(z) = (K - Ke^z) - V_m(z, t_m). \tag{8.16}$$

As this is an iterative solver, estimates for the initial of z and Δz must be set,

which then allows for new values of z to be obtained by

$$z^* = z + \Delta z. \tag{8.17}$$

The values of $p(z)$ and $p(z^*)$ are calculated by integrating (8.3) using a chosen quadrature scheme. We then apply the Newton-Raphson method (Press et al., 2002) to obtain a new value of Δz^*,

$$\Delta z^* = \frac{-\Delta z p(z^*)}{p(z^*) - p(z)}. \tag{8.18}$$

This iterative process is continued until we obtain an acceptably accurate [1] approximation to the zero of (8.16), and then take $b_m = z$. This process of determining the location of discontinuity is performed at each time-step.

Equipped with a method to determine the locations of the free boundary, b_m, the range of integration can be 'centred' about it: removing non-linearity error. The evaluation process for pricing a Bermudan option is equivalent to calculating a European option over numerous consecutive observation times. Therefore, rather than repeat the algorithm (presented at the end of §8.1.1) we will outline the extension made to the European pricing algorithm:

1. We generate a set of values for y_{max_m} and y_{min_m} at each time-step t_m, such that

$$y_{max_m} = x_0 + (x_\Delta)_m \tag{8.19}$$
$$y_{min_m} = x_0 - (x_\Delta)_m \tag{8.20}$$

   where

$$(x_\Delta)_m = D\sigma\sqrt{T - m\Delta t}. \tag{8.21}$$

   Defining $(x_\Delta)_m$ in this manner provides an estimate of the maximum movement of the underlying asset, from x_0 during a small time Δt.

2. Starting at maturity, we compute the free boundary b_M, and then generate the set of points

$$y_i = b_M + i\Delta y, \tag{8.22}$$

[1] Iterations ceased once the value of $p(z)$ reached below 10^{-11} .

and store the option value at each point using condition (8.15).

3. Move to the next time-step and determine b_m using the Newton-Raphson method.

4. Using a chosen quadrature scheme, evaluate the option at each x_i using

$$\begin{aligned} V(x_i, t_m) &= A(x_i)\Bigg[\int_{b_{m+1}}^{y_{max_{m+1}}} B(x_i, y)V(y, t+\Delta t)\mathrm{d}y \\ &+ \int_{y_{min_{m+1}}}^{b_{m+1}} B(x_i, y)V(y, t+\Delta t)\mathrm{d}y\Bigg]. \end{aligned} \tag{8.23}$$

5. Repeat the previous two steps until the option price for the underlying asset with value x_0 is determined.

8.1.3 The tanh-sinh scheme

Having outlined the details of QUAD, we next introduce a high-precision quadrature scheme that can be used in conjunction with QUAD. Tanh-sinh quadrature is a sophisticated numerical integration technique that is well suited for deriving vastly accurate numerical solutions of integrals. Takahashi and Mori (1974) first introduced tanh-sinh quadrature as a means of achieving accuracy of hundreds or even thousands of digits. Convergence of the scheme is exponential for well-behaved integrands. Bailey and Borwein (2006) have shown the method to be superior to Gaussian quadrature and error function quadrature. For clear descriptions of Gaussian and error function quadrature see Press et al. (2002).

The tanh-sinh scheme is based on the Euler-Maclaurin summation formula[2] (Bailey and Borwein, 2006), which implies that for certain **bell-shaped** integrands, approximating the integral by a simple step-function is remarkably accurate. The idea of the scheme is as follows: transform the integral on the interval $[-1, 1]$ to an integral on $(-\infty, \infty)$ by using the change of variable

$$x = g(t) \qquad \text{where} \qquad g(t) = \tanh(\frac{\pi}{2}\sinh(t)). \tag{8.24}$$

Then using the knowledge that, firstly, $g(x)$ is some monotonic function with the

[2]This is used to approximate integrals by using finite sums

property that $g(x) \to 1$ as $x \to \infty$ and $g(x) \to -1$ as $x \to -\infty$ and, secondly, that all derivatives of $g(x)$ rapidly approach zero for large positive and negative values of x, we can evaluate our integral using the equation below:

$$\int_{-1}^{1} f(x)dx = \int_{-\infty}^{\infty} f(g(t))g'(t)dt \approx \Delta x \sum_{j=-N}^{N} w_j f(x_j) \tag{8.25}$$

where

$$x_j = g(j\Delta x) = \tanh(\frac{\pi}{2}\sinh(\Delta x j)), \tag{8.26}$$

$$w_j = g'(j\Delta x) = \frac{\frac{\pi}{2}\cosh(\Delta x j)}{\cosh^2(\frac{\pi}{2}\sinh(\Delta x j))}, \tag{8.27}$$

Δx is the interval of integration, and N is chosen such that the contributions of the terms greater than N are smaller than some required arithmetic precision measure ϵ. Typically, the measure is set at $\epsilon = 10^{-p}$, where p is the level of precision in digits.

The tanh-sinh scheme requires that the interval of integration, prior to the change of variable, is $[-1, 1]$. In scenarios where this interval is $[c, d]$ where $|c| \neq |d|$, one must apply some affine transformation to map the interval to $(-1, 1)$. This transformation is given by

$$\frac{(d-c)}{2}\int_{-1}^{1} f\left(\frac{(d-c)y + (d+c)}{2}\right)\mathrm{d}y. \tag{8.28}$$

Implementation detail

From the above definition of our approximated integral (8.25), it is evident that

$$x_{-j} = -x_j \tag{8.29}$$

$$w_{-j} = w_j \tag{8.30}$$

This is extremely useful as it means that we do not need to calculate the weight and knot-points for $j < 0$: saving considerable computational time. The knot-point x_j and weight w_j can be computed once for some given h. Now suppose we have evaluated equation (8.25) and the value produced is above our error threshold, we can decrease our interval of integration Δx to improve the accuracy.

Typically we refine Δx through the expression $\Delta x = 2^{-k}$, for some level k; each successive refinement is termed a 'level'. This expression for Δx is chosen because of the exponential convergence of the scheme, where the number of correct digits is doubled when Δx is halved. For a more detailed examination of the scheme's convergence see Borwein and Ye (2007). The number, say n, of knot-points and weights required at level k depends on the precision the user needs: the implementation here uses $n = 3.3\text{x}2^k$.

Accuracy and Computational Time

In this results section, all computations were obtained using an AMD Athlon XP 2600+ 2.09 GHz with only 256MB of RAM computer, and the executables were created using the Microsoft Visual Studio .Net Version 7 under optimized Release mode.

To show the improved accuracy obtained by changing the underlying quadrature scheme, we consider the pricing of a European put option, which has strike K and matures at time T with payoff

$$V(S,T) = \max(K - S, 0). \tag{8.31}$$

The values of K, T, and the other parameters of the contract are given by *EBM-04* in table 8.1. Applying the final-time condition, our integrand in (8.3) is

$$B(x,y)\max(K - Ke^y). \tag{8.32}$$

Clearly the first derivative, $\frac{\partial V}{\partial S}$, is discontinuous at the strike level (i.e. when $y = 0$). Therefore, to eliminate non-linearity error we split the interval of integration into two components based on the location of the strike price. Hence, the two intervals of integration are $[-\infty, 0]$ and $[0, \infty]$. We can then evaluate each integral using the tanh-sinh method as described before to obtain the option's value. Since there is an analytical solution for a simple European put option (via the Black and Scholes (1973) formula), we use it in order to compute errors. Table 8.2 presents the error of QUAD when using different numbers of segments. Using just 56 segments we can clearly see that the QUAD tanh-sinh implementation is 5.53 x 10^{12} times more accurate than the Simpson's Rule implementation

Parameter	*EBM-04*
S_0	100
X	95
σ	0.2
r	0.1
T	1.0
D	10
y_{min}	-1.97
y_{max}	2.022

Table 8.1: Values for an European put option parameters

	Trapezium QUAD	**Simspons QUAD**	**tanh-sinh QUAD**
Segments	Error	Error	Error
4	2.40	2.39	1.20
14	$9.69\text{x}10^{-1}$	$5.21\text{x}10^{-1}$	$2.57\text{x}10^{-3}$
26	$2.76\text{x}10^{-1}$	$4.95\text{x}10^{-3}$	$5.27565\text{x}10^{-8}$
54	$6.34\text{x}10^{-2}$	$7.23\text{x}10^{-4}$	$3.9968\text{x}10^{-15}$
106	$1.64\text{x}10^{-2}$	$4.94\text{x}10^{-5}$	$5.32907\text{x}10^{-15}$
212	$4.10\text{x}10^{-3}$	$3.09\text{x}10^{-6}$	$5.77315\text{x}10^{-15}$
422	$1.03\text{x}10^{-3}$	$1.97\text{x}10^{-7}$	$5.32907\text{x}10^{-15}$
846	$2.58\text{x}10^{-4}$	$1.22\text{x}10^{-8}$	$4.44089\text{x}10^{-15}$
1690	$6.45\text{x}10^{-5}$	$7.67\text{x}10^{-10}$	$1.77635\text{x}10^{-15}$

Table 8.2: Comparison of option values using different underlying quadrature schemes for a European put option using parameters *EBM-04* as shown in table 8.1. The errors are determined by comparing the solutions obtained using the QUAD method with the analytical solution, which is 2.39820 (to 5 d.p).

and 6.30 x 10^{14} times more accurate than the trapezium implementation. Notice that after 106 segments the error in the tanh-sinh implementation begins to oscillate; this is due to round-off error that occurs in memory during the calculation process. This demonstrates that the tanh-sinh scheme, using the QUAD method implementation, produces far superior accuracy and astonishingly fast convergence compared to Simpson's rule (see figure 8.1).

Table 8.3 shows the comparison of error and computational time of the tanh-sinh QUAD and Crank-Nicolson method with respect to the exact solution for a European put option. Unlike the QUAD method which requires only one time step in its calculation, the Crank-Nicolson method here uses 60 time steps. This larger number of time steps means that obtaining high accuracy with the Crank-Nicolson method incurs a time penalty. This results in the tanh-sinh QUAD

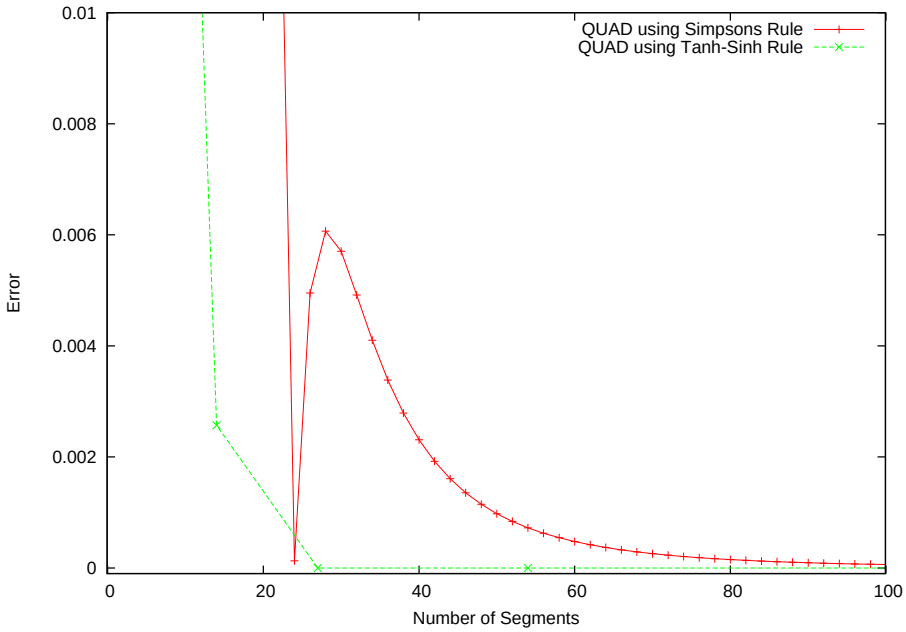

Figure 8.1: Comparison of different underlying quadratures schemes.

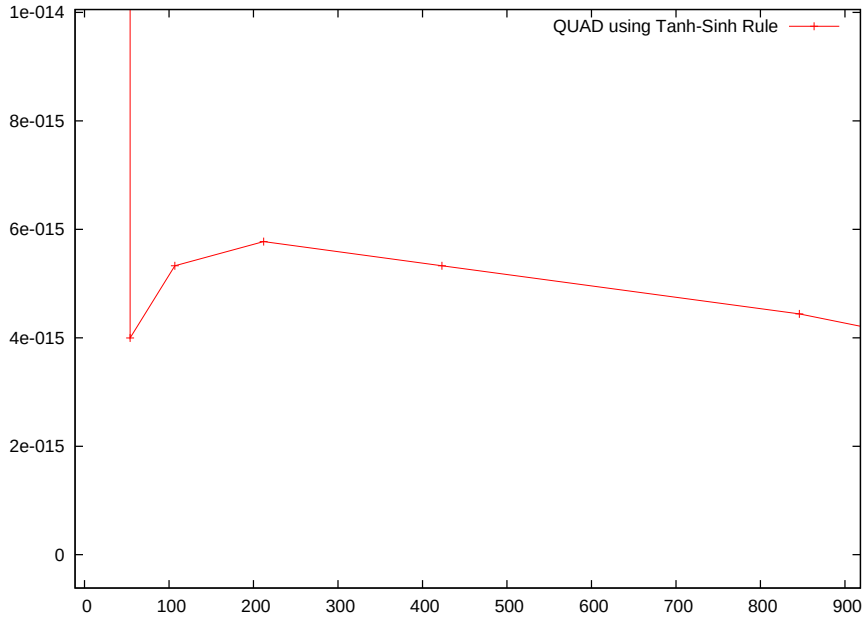

Figure 8.2: A closer look at the high accuracy achieved by using the tanh-sinh scheme.

tanh-sinh QUAD		**Crank-Nicolson**	
Segments	Error (*time(s)*)	Nodes	Error(*time(s)*)
106	$5.33\text{x}10^{-15}(0.00045)$	106	$2.18\text{x}10^{-3}(0.49906)$
422	$5.33\text{x}10^{-15}(0.00129)$	422	$4.97\text{x}10^{-5}(0.54856)$
1690	$1.78\text{x}10^{-15}(0.00449)$	1690	$4.55\text{x}10^{-5}(1.12510)$

Table 8.3: Comparing tanh-sinh QUAD with other numerical methods for a European put option

method being 250 times faster than Crank-Nicolson method, taking only 0.00449 seconds.

8.2 Appraisal of tanh-sinh method

The computational time is significantly shorter than for a finite-difference approximation. In the instance of pricing one-dimensional options even with early-exercise features, we therefore recommend the application of the tanh-sinh quadrature. The tanh-sinh scheme described previously can be extended to two or more dimensions (see Appendix §A.6 for the formulation in two dimensions). In two dimensions the method's computational effort greatly increases since the number of function evaluations in a 2-D system is vastly greater than for the 1-D case. Bailey and Borwein (2005) state that for each increase in the level k (i.e. doubling the knot-points), the computational cost is quadrupled instead of doubled, since there are four times as many function evaluations required. For well-behaved integrands accuracy to over 100-digit can be achieved within a few minutes using only a single CPU processor (see table 3 in Bailey and Borwein, 2005). However, when the number of dimensions of a problem is larger than 5 this tradeoff between accuracy and efficiency takes over, and we must consider other techniques.

In multiple dimensions QUAD still fails to provide the flexibility required to price options with dimensions higher than 5. Additionally, as the dimensions of the option increase, determining the exact topology of the free boundaries proves extremely difficult and significantly increases computational time. This is the main reason why Monte Carlo simulation is still the preferred method for valuing derivatives in high dimensions. To make QUAD a viable numerical technique of practical use in high dimensions issues with locating free boundaries and increases

in computational time must be addressed and possible solutions obtained. This is the focus of the next section.

8.3 An enhanced methodology to suppress non-linearity errors

The valuation of financial derivatives may be computed via the application of lattice-based methods, such as binomial trees (Cox et al., 1979), finite-difference schemes (see §6.2.1 for example), and quadrature methods. However, issues of stability often occur for even the simplest option payoffs, for example a European put option V with standard payoff

$$\max(K - S, 0),$$

where K is the strike price and S the underlying asset. A discontinuity exists in the delta of the option at the strike value. If the nodes in a lattice-based scheme are misaligned in regions where the delta is discontinuous, then convergence is frequently non-monotonic. This phenomenon is typically known as 'non-linearity' error, and has been observed by Figlewski and Gao (1999), Widdicks et al. (2002), amongst others. A similar observation was found in our numerical solution of a weather option in figure 6.6(d). To achieve acceptable accuracy, vast amounts of calculations are required because of the non-monotonic convergence, which makes the use of Richardson extrapolation inappropriate.

Use of higher-order lattice-based schemes, such as the QUAD method as described previously in §8.1, will exaggerate the magnitude of errors in the option price, since higher-order schemes have error terms involving higher order derivatives. In the region near the strike value these will be large and unbounded.

Techniques have been presented to reduce the 'non-linearity' error. Figlewski and Gao (1999) present their Adaptive Mesh Model as a method to reduce the non-linearity error in binomial trees by refining the lattice around the exercise region, since this is where the most significant solution variation occurs. Widdicks et al. (2002) seek to improve the accuracy of binomial trees by defining a parameter which measures the distance between the strike price and the nearest node,

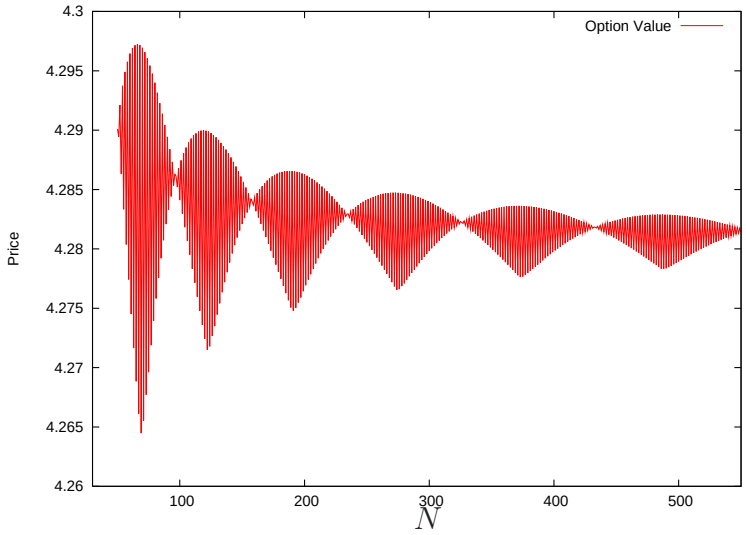

Figure 8.3: A graph of the price against number of node points N for a American call, using binomial model (Cox et al., 1979).

normalised with respect to the lattice size. They show that if this parameter is held constant, then it is possible to produce smooth monotonic convergence, and Richardson extrapolation can then be used to obtain accurate values; see Chapter 6.6 for a brief description of Richardson extrapolation.

Though the Widdicks et al. (2002) method is applicable to binomial, trinomial and finite-difference schemes, it has less application when pricing American-style options, since at each time step the location of all the nodes is important, due to the presence of the free boundary, which intersects through the mesh in a manner unknown a priori.

As much of the errors stem from not successfully tracking the locations of discontinuities, Johnson (2007) uses a transformation to explicitly solve the location of the moving free boundary at each time-step (present when pricing American style options), and subsequently aligning the grid with this location; this effectively removes the non-linearity error. As per Widdicks et al. (2002), Johnson (2007) improves the boundary-fitted coordinate (BFC) method's efficiency by applying Richardson extrapolation. From this, Johnson (2007) then compares and further develops an Enhanced boundary-fitted coordinate method. He shows that the method's calculation of the free-boundary location is superior to that of the Project Successive Over Relaxation (PSOR) method [3]. However, as stated

[3]The PSOR method is simply an extension to the Successive Over Relaxation (SOR) method

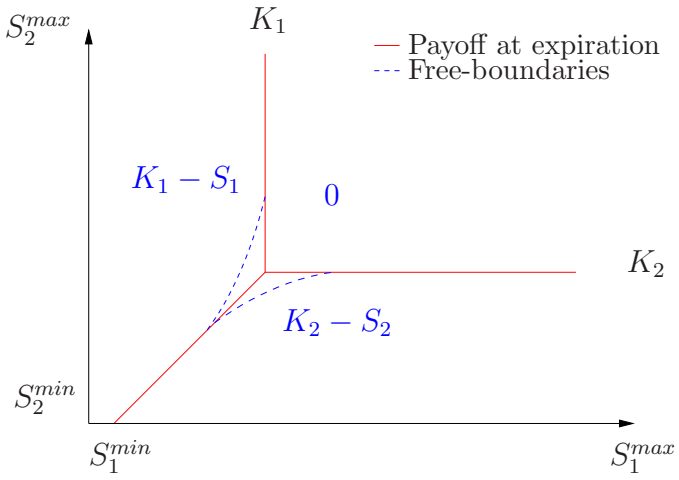

Figure 8.4: Topology of free-boundary surface of a 2D basket American put option. Solid line is the payoff at expiration, $\max(K_1 - S_1, K_2 - S_2, 0)$; dashed line represents the free-boundaries at a subsequent time-step.

by Johnson, Sharp, Duck, and Newton (2007), it is impractical to use the BFC method to price an option on multiple assets, as formulation of the topology of the free boundary is extremely complex. More recently, Lord, Fang, Bervoets, and Oosterlee (2007) proposed an alternative to locating the discontinuity. They use simple linear (or cubic) interpolation to determine an approximate location of the free boundary, which by-passes the need for a Newton-Raphson iteration and in so doing reduces the computational effort somewhat. Once obtained, the grid is then shifted so that the discontinuity lies on the grid, although this can lead to some inaccuracies, since interpolating across the free boundary introduces errors due to the underlying data being non-differentiable, because of the discontinuity in the delta.

However, the effectiveness of the methods described above is limited once the number of state variables (i.e. dimensions) increases or when pricing more exotic options, as the topology of the domain hyper-surfaces becomes extremely complicated, thus locating precise node locations becomes problematic. Figure 8.4 depicts the two-dimensional topology for a basket option with two underlyings. Consequently, the highly rigorous task of determining the exact topology may be a disincentive to practitioners without a strong theoretical background. Our aim is to provide a simple methodology to solve complex options using existing lattice-based methods, which is applicable in multi-dimensions.

and the reader is directed to Smith (1985) for specifics on the method.

The remainder of this chapter proceeds as follows: in §8.4 we propose a generic methodology for the pricing of simple vanilla options and also multi-dimensional options, which is based on a least-squares approach (see Press et al., 2002, for an in depth view of the algorithm). In addition we outline how the method can be incorporated within an existing option pricing framework, based on virtually any lattice method. Then in §8.5 we demonstrate the method's effectiveness through numerical experiments.

8.4 Methodology

The main focus will be on how to effectively minimise the non-linearity error to obtain an accurate representation of the true option value. Unlike previous literature, this approach performs post-processing on the computed results. In particular, it permits the use of extrapolation techniques by analysing data that is non-monotonic (but convergent). A least-squares approach is used in order to determine the curve of 'best' fit. In statistics, it is typical to apply some regression analysis on (scattered) data sets to identify a trend. Once determined, it can enable the prediction of subsequent data, which has not yet been obtained (or calculated). Observing the graph in figure 8.3 it is clear that the data-set converges (even though non-monotonically) and so we wish to determine the 'curve of best-fit', using the method of least squares (Dahlquist and Björck, 2003).

For clarity, we outline the basic concept of the least-squares method in this context.

8.4.1 Representation of a model function

The least-squares method requires the specification of a model function $V(N, \beta)$, from which it estimates the parameter(s) β that best fit the computed data, and where N is the number of grid (data) points[4]. This is similar to techniques of regression analysis that we show earlier in §4.3.1, when fitting a linear trend to historical weather data. The least squares method attempts to determine the 'best' curve which fits through observed data points, whilst minimising the

[4]When using binomial trees, we are concern in the number of time-steps

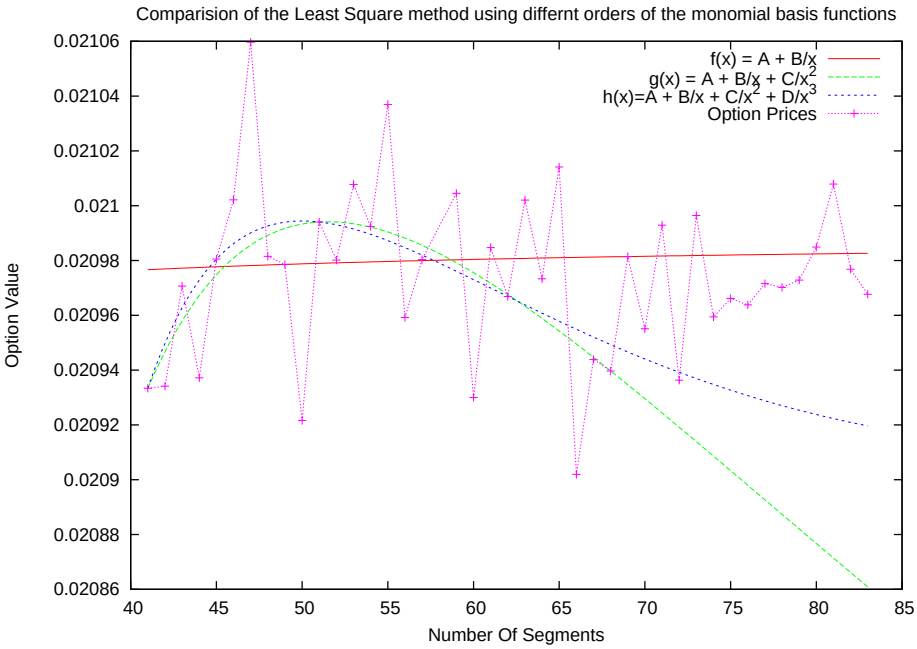

Figure 8.5: Fitting with higher order polynomial results in the function trying to replicate the data set.

residual (for details on different approaches on how residuals are minimise, see Appendix A.7); however, in this context, we do not require this. Since in the presence of non-linearity error the observed values oscillate, meaning that a function which faithfully replicates this behaviour cannot be used for extrapolation (see figure 8.5). In the numerical experiments, the form of the model function was consider as

$$V(N,\beta) = V_{\epsilon}(N) + \sum_{i=1}^{M} \frac{\beta_i}{N^i}. \tag{8.33}$$

where M represents the number of basis functions $\{1/N, 1/N^2, 1/N^3, \ldots, 1/N^M\}$, and β_i is the estimated error for the basis function. Using the trapezium rule, several option values were computed using a different number of grid points and then attempted to apply the our methodology. Figure 8.6 illustrates the results, and confirms that introducing extra terms actually reduces the accuracy of the methodology. Rather, we require the asymptotic value of the option prices in the limit of infinitesimal lattice spacing.

α	1	2	4
	binomial tree 1st order finite-difference	2nd order finite-difference Point successive over relaxation trapezium rule	Simpson's rule

Table 8.4: The appropriate value for α in equation (8.34), when a given numerical scheme has been used to derive the option price data.

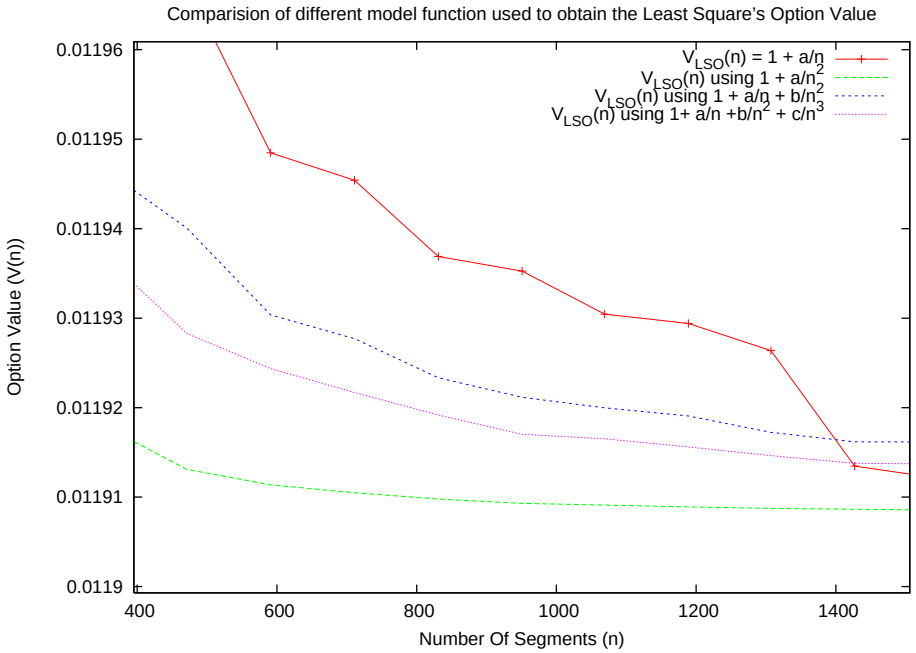

Figure 8.6: Showing how varying alpha and the form of the model function does not improve accuracy. And in fact the best model function chosen is the one which best follows the trapezium rule's rate of convergence.

The method

Rather than minimising the residuals, we require that as $N \to \infty$, $V(N, \beta)$ gives the precise value of the option price. Numerical experiments suggest a model function of the form

$$V(N, \beta) = V_\epsilon(N) + \frac{\beta_0}{N^\alpha}, \tag{8.34}$$

where V_ϵ is the precise value of the option, β_0 is the coefficient of the leading-order error term and α represents the rate of convergence of the chosen numerical technique (e.g. $\alpha = 2$ for the trapezium rule, see table 8.4 for an outline of the various selections for α).

To determine β_0 and V_ϵ, we construct a lattice containing N grid points, and then

apply a chosen numerical scheme (e.g finite-difference, QUAD, binomial tree) to obtain a value for the option, say V_1. We then repeat the previous process with a refined lattice using $N_{i+1} = N_i + 1$ grid points, where i denotes the ith choice of grid size, which will generate a set of computed option values $V = \{V_1, V_2, \ldots, V_i\}$. The small increment in grid points ensures that we observe the points which are near the location of discontinuity in the delta.

Naturally, we ask: how many choices of N do we use before applying the least-squares method? Firstly, the least squares algorithm can only be applied once the number of computed option values exceeds the number of basis functions appearing in (8.34), and so $i > 2$. Secondly, it is *optimal*[5] to perform the method once the following conditions are satisfied:

$$V(N_{i-4}) > V(N_{i-2}) \quad \text{and} \quad V(N_{i-2}) < V(N_i), \tag{8.35}$$

This is equivalent to saying, compare the two previous option values, which were computed using node points N_{i-4} and N_{i-2} respectively, with the current option value obtained using N_i node points. When this condition is satisfied we may refer to option value at N_{i-2} as a *sweet spot*, due to the fortuitous alignment of the node points in regions of rapidly-varying solutions, and refer to it as V_*^1. Once the two conditions are satisfied, we perform the method of least-squares to find the curve of 'best' fit across the computed values $\{V_1, \ldots, V_{i-2}\}$ (i.e. only use points up to the *sweet spot*), to obtain values for β_1 and $V_{\epsilon,1}$, which are the initial estimates of β and V_ϵ respectively. We show the locations of the *sweet spots* in figure 8.7, and these are the points where the methodology is applied.

As we increase the number of node points (and evaluate the value of the option), we check to see if (8.35) is satisfied, and if so, we record this value as the next *sweet spot* V_*^2. Now, we perform the least squares method again, but this time fitting the curve over the dataset $\{V_*^1, \ldots, V_*^2\}$, in other words, discard all information before V_*^1 and only use the data between the two successive *sweet spots*. We can summarise this by stating that the least-squares method is performed over dataset $\{V_*^{w-1}, \ldots, V_*^w\}$, where w refers to the number of *sweet spots* that have been encountered so far. Continuing this process, produces a set of approximate values, $V_\epsilon = \{V_{\epsilon,1} \ldots V_{\epsilon,w}\}$. Note that the errors of the approximations for V_ϵ

[5] In the sense that the obtained Least-Square option prices generated using our methodology converge monotonically and hence extrapolation techniques can be applied.

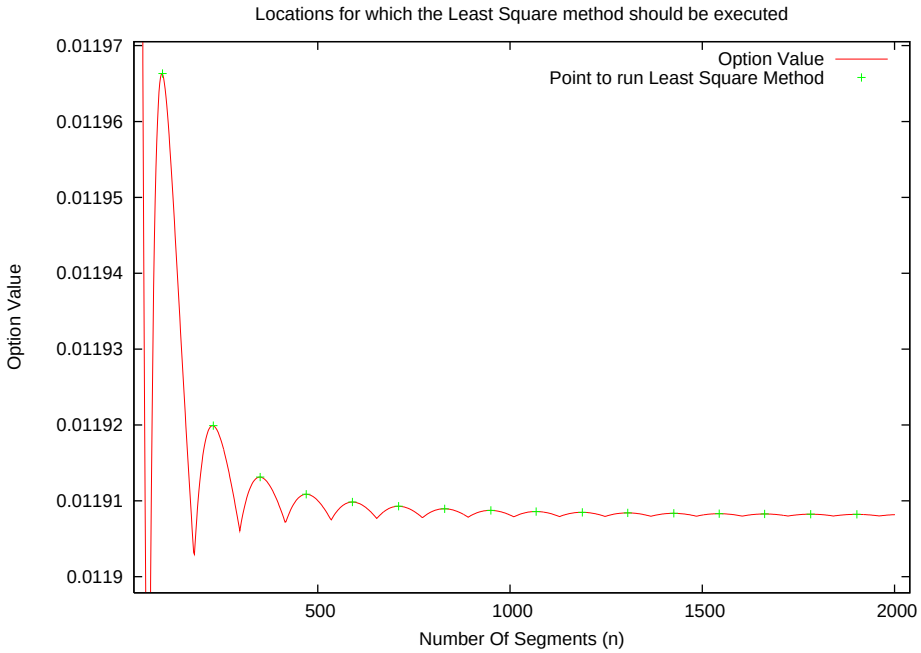

Figure 8.7: The *sweet spot* locations at which the methodology is applied.

monotonically decrease, for payoff functions that do not have numerous discontinuities, and so $V_{\epsilon,w}$ is the best approximation for the option price. Therefore, the application of our methodology permits the use of extrapolation to further enhance accuracy (here we employ Richardson extrapolation), because of the monotonic convergent property.

8.5 Numerical results of the proposed methodology

Through various numerical experiments we illustrate the application and effectiveness of the methodology, valuing both European and Bermudan options (both on multiple underlyings). Section 8.5.3 further demonstrates the significance of our methodology as it is not possible (with the current technologies) to solve numerically a highly dimensional problem using a high number of knot points. In this section we outline the pricing of options where the underlying stock process follows the usual, GBM (3.4), though as our methodology is generic it may be applied irrespective of the underlying price process.

European	$\sigma_1 = 0.1$	$\sigma_2 = 0.1$	$r = 0.1$	$T = 1.0$	$\rho = 0.4$
	$S_1 = 1.0$	$K_1 = 1.0$	$S_2 = 0.49$	K_2 =0.5	
Bermudan	$\sigma_{1,2} = 0.2$	$\sigma_2 = 0.2$	$r = 0.1$	$T = 1.0$	$\rho = 0.4$
	$S_1 = 1.0$	$K_1 = 1.0$	$S_2 = 0.49$	K_2 =0.5	$M = 6$

Table 8.5: Values for a European put option parameters. The asset values are given by S_1 and S_2, with volatilities σ_1 and σ_2. The option strike values are given by K_1 and K_2. The number of exercise opportunities is given by M

To obtain an accurate option price, denoted as V_{ref}, the QUAD method (Andricopoulos et al., 2003) is employed with a sufficiently small Δy ($\approx 2.4\text{x}10^{-4}$). This amounts to integrating over a coarse grid of around 100 million knot points for an European put option on two underlying assets. This value is extremely accurate and will be used as a benchmark in our error analysis.

8.5.1 Multi-dimensional European option

We begin by considering a European put option which has two underlying assets with values, S_1 and S_2 respectively, and matures at time T with constant interest rate r. The volatilities of the two assets are given by σ_1 and σ_2 respectively, and ρ denotes the correlation between the assets. The payoff is defined as

$$V(S_1, S_2, T) = \max(K_1 - S_1, K_2 - S_2, 0), \tag{8.36}$$

where K_1 and K_2 are the strike values. The values of the parameters used to value the European put option are shown in the top of table 8.5. Figure 8.4 is an illustration of the locations of discontinuities for an option on two underlyings.

We compute the value of the option using the methodology proposed in §8.4.1 and also the value obtained when using the original QUAD method, and then determine the associated errors by comparing the two values with V_{ref}. Table 8.6 presents the percentage error found when using our methodology (which we refer to as LSO-QUAD, to indicate that we are using our methodology on numerical results produced by the QUAD scheme) and original QUAD method. In both cases the trapezoidal integration method is used to compute the integral (8.13). In table 8.6, when $N = 97$, one "sweet-spot" has been reached and therefore the least-square algorithm is performed. Each entry in the table denotes another

"sweet-spot" being reached. The location of these points is shown by the green plus signs in figure 8.8. At these locations we perform our methodology and obtain a series of computed option prices (that are shown by blue crosses in figure 8.8). After only one "sweet-spot" has been reached we achieve accuracy that is within 0.48% of the *true* option price.

We make a comparison between our proposed methodology and the original QUAD method in order to demonstrate that little improvement is gained by determining the location of the discontinuity and positioning the grid accordingly. Our proposed methodology rapidly suppresses the 'non-linearity' error using a limited number of knot-points for the QUAD-based implementation. The blue crosses in figure 8.8 show that the option values obtained using our methodology are monotonically decreasing, and therefore, enables the use of extrapolation to further improved estimates. Additionally, computational time is significantly reduced, and enables previously infeasible problems to be approached. An important observation is that using a sizable truncated range of integration will speed up convergence and improve accuracy (see Andricopoulos et al., 2003).

LSO-QUAD		**QUAD**	
N	Error	N	Error
97	0.48 %	97	0.25 %
229	0.19 %	229	0.047 %
351	0.08 %	361	0.019 %
471	0.04 %	493	0.010 %
591	0.03 %	625	0.006 %
711	0.02 %	757	0.004 %
831	0.015 %	889	0.003 %
951	0.01 %	1021	0.002%
1069	0.009 %	1153	0.0019%
1189	0.007 %	1285	0.0015%
European option, payoff $= \max(K_1 - S_1, K_2 - S_2, 0)$			
$V_{ref} = 0.011908043$			

Table 8.6: Comparison of the percentage error found when applying methodology and the original error. Note that titles with the prefix 'LSO' indicates the application of the Least Square Optimisation Methodology. Both implementations use the trapezoidal integration method.

In the implementation of the methodology, we used the the trapezoidal and Simpson's rule numerical integration techniques. It is striking that typically the Simpson's rule has superior accuracy over the trapezoidal method, with an error of

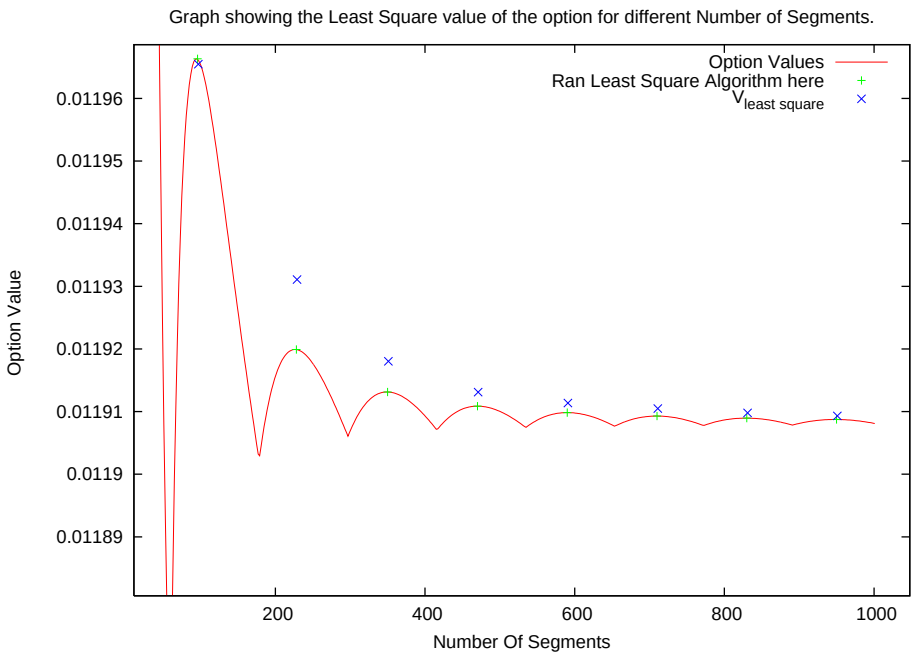

Figure 8.8: An illustration of the locations of the "sweet-spots" and also the option values that are computed using our methodology. The solid red line, is the raw underlying option prices computed using the QUAD method without discontinuities being alignment with the grid points.

$O(\Delta y^4)$ where Δy represents the width between two knot points. However, the introduction of non-linearity error reverses this, as at the location of discontinuity the approximations of the higher order derivative terms are more inaccurate (indeed, unbounded) terms, and because the trapezoidal method only approximates up to the second derivative (unlike the Simpson's rule, which involves the fourth derivative) it is less effected by the error. We may observe in table 8.7 that there are greater differences in the errors found between QUAD and our methodology when the integral is computed using Simpson's rule as opposed to the trapezium method. When using the trapezium method, the error with our methodology is at most twice as large, whereas when using the Simpson's rule this difference can be 5-6 times the size of the error when using original QUAD. Additionally, setting α to the rate of the convergence of the quadrature scheme employed (in the case of the Simpson's rule, $\alpha = 4$) produces smaller errors. We show this result in figure 8.9, where the red and green lines represents the percentage errors obtain using our methodology for when $\alpha = 4$ and $\alpha = 2$ respectively.

We next apply the methodology to the Cox et al. (1979) binomial tree (hereafter

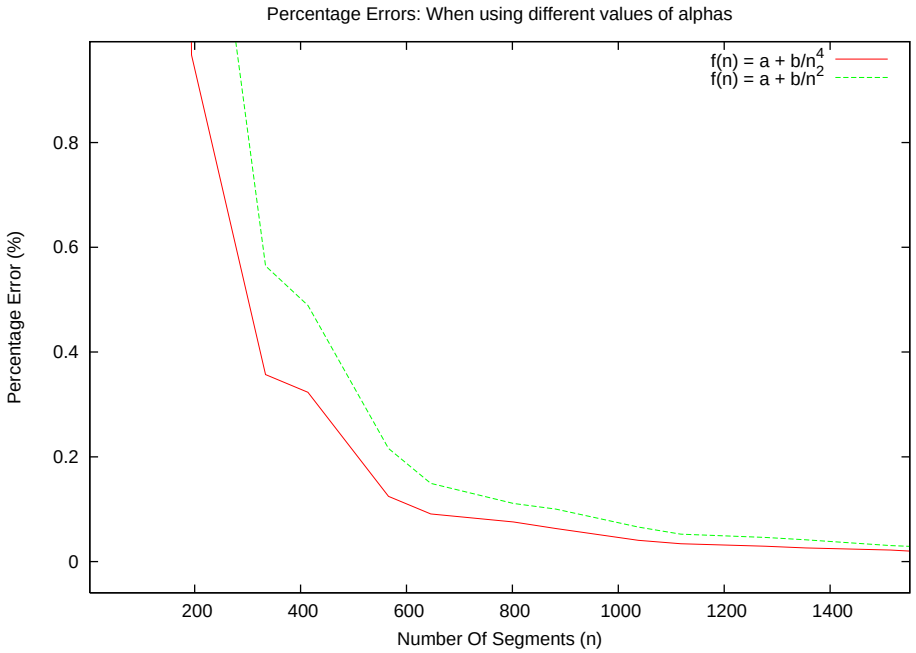

Figure 8.9: Illustrates the percentage error of our proposed methodology, with different values for α in model function (8.34), where Simpson's rule has been used to compute integral (8.13). This is for valuing a European put option with parameters as given in table 8.5 and payoff (8.36).

denoted as CRR) and show that the non-linearity error is suppressed, and it produces surprisingly accurate results. It should be noted that in the binomial tree method the rate of convergence is typically of $O(1/N)$, and so when applying the proposed methodology we set $\alpha = 1$ in equation (8.34), and we then proceed as outlined in the proposed methodology algorithm. In figure 8.10 we present the obtained option values using our methodology, using three different specifications for the model function (8.34). The figure illustrates that using $\alpha = 1$ provides more accurate results, since the solution profile is closer to the value of V_{ref}.

8.5.2 Multi-dimensional Bermudan option

We now present the results for a six-times exercisable Bermudan put option on two underlying assets, S_1 and S_2 respectively, with payoff

$$V(S_1, S_2, T) = \max(K_1 - S_1, K_2 - S_2, 0), \tag{8.37}$$

QUAD: Trapezium		**LSO-QUAD: Trapezium**	**QUAD: Simpson's**		**LSO-QUAD: Simpson's**
N	%Error	% Error	N	% Error	% Error
15	26.3422	14.2835	18	32.7180	33.1754
97	0.4800	0.4852	194	0.3143	0.9671
229	0.1931	0.0994	334	0.0859	0.3569
351	0.0838	0.0427	414	0.0569	0.3232
471	0.0425	0.0237	566	0.0292	0.1246
591	0.0279	0.0151	646	0.0225	0.0909
711	0.0206	0.0104	802	0.0145	0.0758
951	0.0106	0.0058	1038	0.0086	0.0407
1069	0.0090	0.0046	1118	0.0074	0.0341
1189	0.0073	0.0037	1278	0.0057	0.0292
European option, payoff $= \max(K_1 - S_1, K_2 - S_2, 0)$					
$V_{ref} = 0.011908043$					

Table 8.7: Table comparing percentage errors for when the QUAD method has been implemented to not align the lattice about the discontinuity found at the expiry and then the improvement with utilising the LSO methodology.

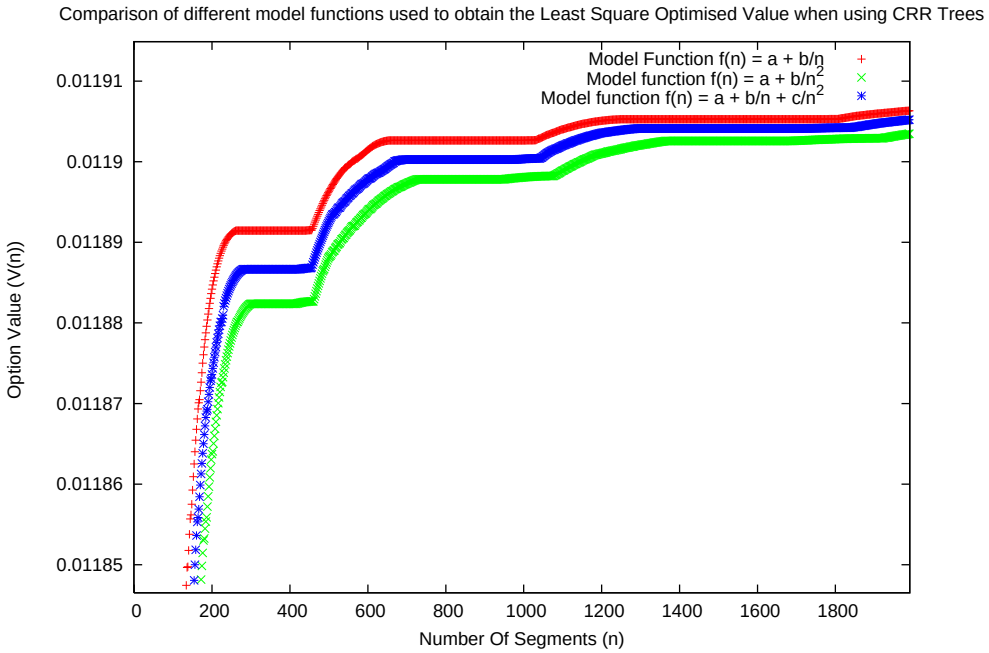

Figure 8.10: The option values obtained using our methodology with the CRR binomial tree method. The *true* value is given as $V_{ref} = 0.011908043$. The three lines in the figure are for different types of model functions.

where K_1 and K_2 are the strike values. The parameter values are specified in bottom of table 8.5. Since no analytical solution is available for early-exercise style options, we obtain the value for V_{ref} by employing the QUAD method with 2^{16} knot points used in the computation.

Table 8.8 reports the absolute error found when using our proposed method with QUAD. Notice that the experiments were completed using fewer segments than when computing the European option, because of the extended computational time required to price multiple observed options. At each exercise opportunity, at say τ, we need to value the option at a series of asset prices x_i (in all dimensions), and continue this process moving backward in time. Applying LSO-QUAD achieves excellent accuracy with an error as small as approximately 10^{-7}.

In our results we ensured that in implementing the PSOR method that the strike price was not aligned with the grid in an attempt to produce the non-monotonic behaviour observed in other lattice methods. We slightly perturbed the option data from table 8.5 and from oscillations that are visible in red line in figure 8.11 it is evident that without careful nodal placement the non-linearity error persists.

LSO-QUAD	
N	Error
50	0.000032561
75	0.000007415
100	0.000002622
125	0.000000799
150	0.000000137
Bermudan option, payoff $= \max(K_1 - S_1, K_2 - S_2, 0)$	
$V_{ref} = 0.0201941230315239$	

Table 8.8: The absolute errors of the proposed method for different grid segments N. The parameter values used to compute these values are specified in bottom half of table 8.5

Table 8.9 also highlights the importance of choosing the appropriate model function as by using $f(x) = \alpha_1 + \alpha_2/x^2$ the accuracy is significantly improved by 99%. Note that in figure 8.11, the blue line is not a least square fit of the solid red line (which is the raw data) but rather is a fit of the option prices at the most recent "sweet-spots". So by examining the true convergence of the chosen scheme and then setting the model function to reflect this, will typically lead to reduction in the magnitude of errors.

8.5.3 Ten-Dimensional European Basket Option

To fully appreciate our methodology's applicability, we use the method to value a European put option on 10 underlyings. The valuation of an option on multiple-assets may be obtain through solving the Black-Scholes partial differential equation (Andricopoulos et al., 2007):

$$\frac{\partial V}{\partial t} + \frac{1}{2}\sum_{i=1}^{N}\sum_{j=1}^{N}\sigma_i\sigma_j\rho_{ij}S_iS_j\frac{\partial^2 V}{\partial S_i \partial S_j} + \sum_{i=1}^{N}(r-d_i)S_i\frac{\partial V}{\partial S_i} - rV = 0 \qquad (8.38)$$

where S_i are the underlying assets, σ_i and d_i represent the corresponding volatilities and continuous dividend yield respectively and ρ_{ij} the correlation coefficient between underlying assets S_i and S_j. The risk-free rate is denoted as r, t is time, and $V(S_1, \ldots, S_{10}, t)$ is the price of the derivative. Here $i = 1, 2, \ldots, 10$. Note that $|\rho_{ij}| < 1$, $\rho_{ii} = 1$ and $\rho_{ij} = \rho_{ji}$.

Following the same procedure as performed in §8.1.1 to solve (3.10), let K_i be

LS-PSOR($f(x) = \beta_0 + \beta_1/x$)		**LS-PSOR**($f(x) = \beta_0 + \beta_1/(x^2)$)
K	Error	Error
20	0.000809034	0.000391210
30	0.000662721	0.000085861
40	0.000433197	0.000008267
50	0.000404582	0.000018631
60	0.000314935	0.000015135
70	0.000252584	0.000006045
80	0.000212729	0.000003192
90	0.000187271	0.000004083
100	0.000176882	0.000001429
110	0.000160062	0.000000949
Bermudan option, payoff $= \max(E_1 - S_1, E_2 - S_2, 0)$ $V_{ref} = 0.00259345594581309$		

Table 8.9: Error of the proposed method when applied to explicit finite difference method (using PSOR) to value a Bermudan option with parameters as stated in table 8.5. The model function is defined as $f(x) = \beta_0 + \beta_1/x$.

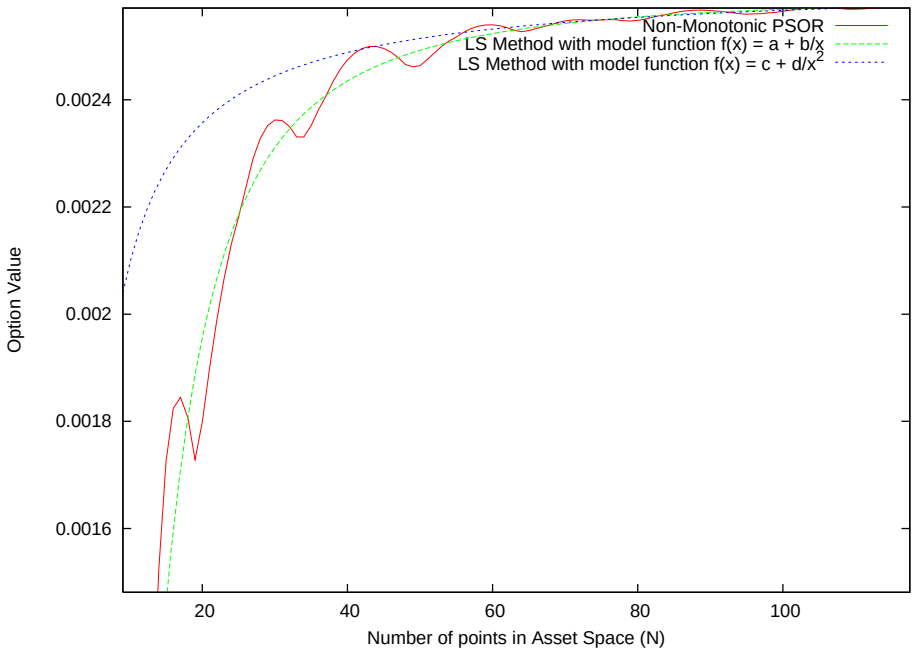

Figure 8.11: Results observed when pricing an American two-dimensional basket option, using the PSOR method to obtain the underlying non-monodic data. The two curves show the approximation of the proposed method when using different basis functions for Least Square model function.

the exercise prices, and then make the suitable logarithmic transformations

$$x_i = \ln((S_i)_t/K_i) \quad \text{and} \quad y_i = \ln((S_i)_{t+\Delta t}/K_i). \tag{8.39}$$

Here x_i and y_i are chosen nodes at t and $t+\Delta t$ respectively. Now let $\mathbf{R}$ represent the correlation matrix such that the elements $R(i,j) = \rho_{ij}$. The solution is then given by (Wilmott, 2000a)

$$V(x_1, \ldots, x_{10}, t) = \tag{8.40}$$
$$C \int_{-\infty}^{\infty} \ldots \int_{-\infty}^{\infty} V(y_1, \ldots, y_{10}, t+\Delta t) B(x_1, \ldots, x_{10}, y_1, \ldots, y_{10}) \mathrm{d}y_1 \ldots \mathrm{d}y_n,$$

where

$$C = e^{-r\Delta t}(2\pi\Delta t)^{-10/2}(|\mathbf{R}|)^{-1/2}(\sigma_1, \ldots, \sigma_{10})^{-1}, \tag{8.41}$$

the Green's function

$$B(x_1, \ldots, x_{10}, y_1, \ldots, y_{10}) = \exp(-\frac{1}{2}\alpha_i^T \mathbf{R}^{-1} \alpha_i), \tag{8.42}$$

and column vector

$$\alpha_i = \frac{1}{\sigma_i(\Delta t)^{-1/2}}\Big(x_i - y_i + \big(r - D_i - \frac{\sigma_i^2}{2}\big)\Delta t\Big). \tag{8.43}$$

The range of integration in equation (8.40) can be truncated, provided that the contributions of the integrals outside this range are insignificant (Andricopoulos et al., 2003). This simple amounts to having a set of values for y_{min} and y_{max} for each ith underlying.

For this basket put option we define the payoff as

$$V(S_1, S_2, \ldots, S_{10}, T) = \max(K_1 - S_1, \ldots, K_{10} - S_{10}, 0). \tag{8.44}$$

where the values of S_i, K_i and the other contract parameters are given in table 8.10. Trying to determine the topology of the free-boundaries in this case is difficult, and therefore we ignore them and instead make use of our methodology to determine the option's value. As the tensor-product grid is large, we choose to use few knot points (at most 12), so that CPU times are minimal. The results of these are shown graphically in figure 8.12, where the option prices are computed

Parameter	Value
r	0.1
σ	0.1
S_1	1.0
S_2, S_5, S_8	0.49
S_3, S_6, S_9	0.49
S_4, S_7, S_{10}	0.8
K_1	1.0
K_2, K_5, K_8	0.5
K_3, K_6, K_9	0.5
K_4, K_7, K_{10}	0.8
T	1
D	7

Table 8.10: The parameter values for pricing a European basket put option on 10 underlyings.

for grids with different number of segments and results in the values oscillate violently due to the misalignment with discontinuities (see the solid red line in figure 8.12). The green line in the figure is our approximate option values using our proposed methodology. We see that even with this many dimensions we can still observe the suppression of the non-linearity error by utilising our methodology. In future work, we intend to use parallel computing to further reduce computational times and to allow for the pricing of more complex derivatives, in higher dimensions, i.e. American style basket options.

8.6 Conclusion

In this chapter we have presented a canonical least-squares based methodology for suppressing the non-linearity errors present when pricing options. Our method is flexible with respect to the type of option to be priced and the underlying method used to compute that option, which is demonstrated in the numerical experiments for European, Bermudan, and up to 10 dimension European basket option. Numerous types of contracts can be accurately valued given an appropriate numerical scheme exists to obtain a set of (non-monotonic) prices. The generic nature of the scheme implies that it would be useful for solving an array of different financial instruments. An example would be in the solving of weather basket options.

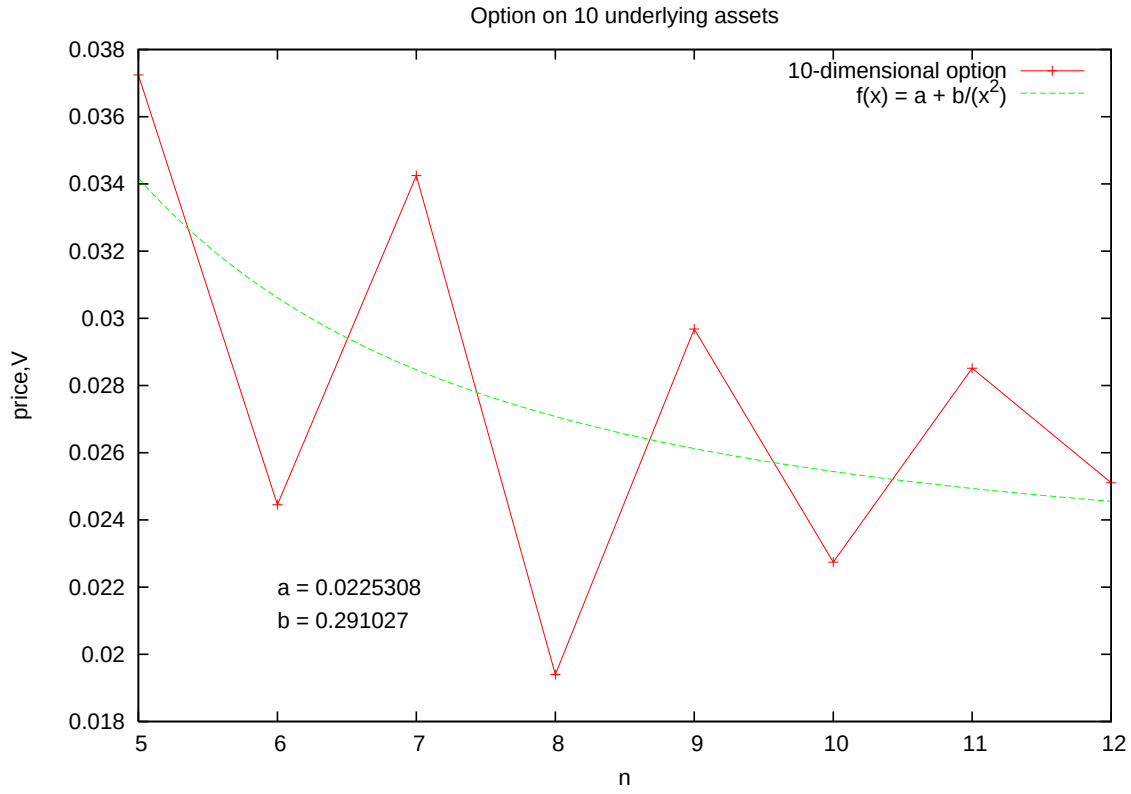

Figure 8.12: Using a limited number of points, we can see the non-monotonic option prices obtained through QUAD (using the trapezium rule) oscillates violently. Application of the methodology highlights that a smooth price profile can be obtained in order to get an approximated price.

Chapter 9

Conclusions

Under the assumptions of *mean self-financing* portfolios and *the standard deviation principle*, weather derivatives pricing is investigated. Using an imperfectly correlated asset, a suitable partial hedge is constructed and is shown to remove a source of randomness observed in the portfolio. The approach of using correlated asset as substitutes for the purpose of hedging has been considered in the literature (as discussed in chapter 5). We assume initially that the expected value of the portfolio is zero, which consequently eliminates the second residual risk. This then allows the derivation of a new two-dimensional backward parabolic PDE which includes the weather index I. Calculation of temperature model parameters are estimated, so that we can adequately model the behaviour of temperature. Modifications as to how these parameters are calculated are given and justified.

In chapter 6, an investigation of finite-difference for solving advection or convection-dominated PDEs ruled out application of several standard schemes. Noting the difficulties in numerically solving these PDEs, we subsequently introduced SLS and showed it to be the best suited for a PDE of the form (5.29). We specified weak conditions under which accurate solution can be obtained when using SLS. We provided a specification of the boundary conditions, and allowed for the truncation of the computational domain which led to a reduction in unnecessary computations. Results indicated that for standard put and call options the starting temperature only slightly alters the option's price, because equation (5.29) has a mean-reverting drift process.

An extension to the work in chapter 5 is developed in chapter 7, where the valuation of a weather derivative is viewed from an incomplete markets perspective. This results in a non-linear two-dimensional PDE which gives rise to option prices of different values depending on if the option is long or short. This is practically important, as in the weather derivatives markets there is often a sizeable spread between the bid and ask prices. The approach is similar to those considered in actuarial science where a risk premium is added to compensate the investor for holding undiversifiable risk.

We introduce into this literature the tanh-sinh quadrature scheme in chapter 8, and demonstrate its superior accuracy when compared to other lattice methods, such as QUAD using either a Simpson's or trapezium, or a Crank-Nicolson finite-difference scheme. The scheme was incorporated into the QUAD method, and through numerical experiments was shown to exhibit exponential convergence, and be 250 times faster than Crank-Nicolson method. The second contribution of this chapter is in the development of a generic methodology which suppresses the non-linearities that are often found in lattice-based schemes. It was shown that our approach is easily extended into multiple dimensions and applicable to various lattice schemes, such as QUAD, finite-difference schemes, and binomial trees.

9.1 Future work

Several interesting avenues of future research can be extended from this thesis.

An important development would to model more precisely the correlation between temperature and various commodity contracts. This could be extended to model the known lag between movements in load versus movements in prices.

The weather option model developed here could be extended to include more complex dynamic models of the behaviour of temperature. We neglected this since the estimated temperature model appeared to approximate the temperature patterns (at London Heathrow).

With regards to the numerical techniques presented in this thesis, a comparison of the tanh-sinh scheme versus other non-Newton-Côtes quadrature schemes would

be an interesting area to consider in the future. The Least Square Optimisation methodology developed in chapter 8 may have applications for valuing previously intractable basket options, not only in weather derivatives but in other fields.

References

P. Alaton, B. Djehiche, and D. Stillberger. On modelling and pricing weather derivatives. *Applied Mathematical Finance*, 9(1):1–20, 2002.

B. Alziary, J.P. Décamps, and P.F. Koehl. A PDE approach to Asian options: analytical and numerical evidence* 1. *Journal of Banking & Finance*, 21(5): 613–640, 1997. ISSN 0378-4266.

A.D. Andricopoulos, M. Widdicks, P.W. Duck, and D.P. Newton. Universal option valuation using quadrature methods. *Journal of Financial Economics*, 67(3):447–471, 2003.

A.D. Andricopoulos, M. Widdicks, D.P. Newton, and P.W. Duck. Extending quadrature methods to value multi-asset and complex path dependent options. *Journal Of Financial Economics*, 83(2):471–499, 2007.

M. Avellaneda, A. Levy, and A. Paras. Pricing and hedging derivative securities in markets with uncertain volatilities. *Applied Mathematical Finance*, 2(2): 73–88, 1995. ISSN 1350-486X.

D.H. Bailey and J.M. Borwein. Highly Parallel, High-Precision Numerical Integration. 2005.

D.H. Bailey and J.M. Borwein. Effective Bounds in Euler-Maclaurin-Based Quadrature (Summary for HPCS06). *Proceedings of the 20th International Symposium on High-Performance Computing in an Advanced Collaborative Environment*, 2006.

G.K. Batchelor. *An introduction to fluid dynamics*. Cambridge Univ Pr, 2000.

F. Bellini. *The Weather Derivative Market: Modelling and Pricing Temperature*. PhD thesis, Institute for Economic Research, University of Lugano, Switzerland, 2005.

F.E. Benth and J. Benth. The volatility of temperature and pricing of weather derivatives. *Quantitative Finance*, 7(5):553, 2007.

F.E. Benth and J. Šaltytė-Benth. Stochastic modelling of temperature variations with a view towards weather derivatives. *Applied Mathematical Finance*, 12 (1):53–85, 2005.

B.M. Bibby and M. Sørensen. Martingale estimation functions for discretely observed diffusion processes. *Bernoulli*, pages 17–39, 1995.

T. Björk. *Arbitrage theory in continuous time*. Oxford Univ Pr, 2009. ISBN 019957474X.

F. Black and M. Scholes. The Pricing of Options and Corporate Liabilities. *The Journal of Political Economy*, 81(3):637–654, 1973.

J.M. Borwein and L. Ye. Quadratic Convergence of the Tanh-Sinh Quadrature Rule. 2007. "`http://www.cs.dal.ca/jborwein/tanhsinh.pdf, 2006`".

A. Brix, S. Jewson, and C. Ziehmann. Weather derivative modelling and valuation: a statistical perspective. *Climate Risk and the Weather Market*, pages 127–150, 2002.

P.L. Brockett, M. Wang, and C.C. Yang. Weather derivatives and weather risk management. *Risk Management & Insurance Review*, 8(1):127–140, 2005.

D. Brody, J. Syroka, and M. Zervos. Dynamical pricing of weather derivatives. *Quantitative Finance*, 2(3):189–198, 2002.

M. Cao and J. Wei. Equilibrium valuation of weather derivatives. *Preprint, Queens University, Kingston, Ontario*, 2000.

M. Cao and J. Wei. Weather derivatives valuation and market price of weather risk. *Journal of Futures Markets*, 24(11):1065–1089, 2004.

M. Cao, A. Li, and J. Wei. Weather Derivatives: A New Class of Financial Instruments. 2003. "Available at SSRN: `http://ssrn.com/abstract=1016123`".

S. Chantarat, C.G. Turvey, A.G. Mude, and C.B. Barrett. Improving humanitarian response to slow-onset disasters using famine-indexed weather derivatives. *Agricultural Finance Review*, 68(1):169–195, 2008.

Z. Chen and P.A. Forsyth. A semi-Lagrangian approach for natural gas storage valuation and optimal operation. *SIAM Journal on Scientific Computing*, 30 (1):339–368, 2007.

Group CME. Weather Products. 2011. "Avaiable at: `http://www.cmegroup.com/trading/weather/weather-products-brochure.html`".

J.H. Cochrane and J. Saa-Requejo. Beyond arbitrage: Good-deal asset price bounds in incomplete markets. *Journal of Political Economy*, 108(1):79–119, 2000.

R. Courant, K. Friedrichs, and H. Lewy. Über die partiellen Differenzengleichungen der mathematischen Physik. *Mathematische Annalen*, 100(1):32–74, 1928.

J.C. Cox, S.A. Ross, and M. Rubinstein. Option Pricing: A Simplified Approach. *Journal of Financial Economics*, 7(3):229–263, 1979.

G. Dahlquist and Å. Björck. *Numerical Methods*. Courier Dover Publications, 2003.

M. Davis. Pricing weather derivatives by marginal value. *Quantitative Finance*, 1(3):305–308, 2001. ISSN 1469-7688.

Y. d'Halluin, PA Forsyth, and G. Labahn. A Semi-Lagrangian approach for American asian options under jump diffusion. *SIAM Journal on Scientific Computing*, 27(1):315–345, 2006.

B. Dischel. "Black-Scholes won't do". *Risk*, 10:8–9, 1998a.

B. Dischel. At last: A model for weather risk. *Energy & Power Risk Management*, 11(3):20–21, 1998b.

B. Dischel and W.M. Observer. Dry market in need of liquidity. *Risk Magazine: Risk Management for Investor, September*, pages 20–22, 2002.

F. Dornier and M. Queruel. Weather Derivatives Pricing-Caution to the Wind. *Energy and Power Risk Management*, pages 30–32, 2000.

J. Douglas Jr and T.F. Russell. Numerical methods for convection-dominated diffusion problems based on combining the method of characteristics with finite element or finite difference procedures. *SIAM Journal on Numerical Analysis*, pages 871–885, 1982.

T.E. Duncan, Y.Z. Hu, and B. Pasik-Duncan. Stochastic calculus for fractional brownian motion. i. theory. *Decision and Control, 2000. Proceedings of the 39th IEEE Conference on*, 1:212–216 vol.1, 2000.

C.L. Dunis and V. Karalis. Weather derivatives pricing and filling analysis for missing temperature data. *Derivatives Use, Trading & Regulation*, 9:61–83, 2003.

D. Durand. Growth stocks and the Petersburg paradox. *Journal of Finance*, 12 (3):348–363, 1957. ISSN 0022-1082.

J.A. Dutton. Opportunities and priorities in a new era for weather and climate services. *Bulletin of the American Meteorological Society*, 83(9):1303–1311, 2002.

GW Evatt, PV Johnson, PW Duck, and SD Howell. Finite resource valuations: Insights into optimal extraction rate regimes. *Under Review*, 2010a.

GW Evatt, PV Johnson, PW Duck, SD Howell, and J. Moriarty. The expected lifetime of an extraction project. *Proceedings of the Royal Society A: Mathematical, Physical and Engineering Science*, 2010b. ISSN 1364-5021.

S.J. Farlow. *Partial differential equations for scientists and engineers*. Dover Pubns, 1993. ISBN 048667620X.

S. Figlewski and B. Gao. The adaptive mesh model: a new approach to efficient option pricing. *Journal of Financial Economics*, 53(3):313–351, 1999.

H. Föllmer and D. Sondermann. Hedging of non-redundant contingent claims. *Contributions to Mathematical Economics. In Honor of Gerard Debreu*, 1985.

PA Forsyth, JS Kennedy, ST Tse, and H. Windcliff. Optimal trade execution: a mean quadratic variation approach. *Submitted to Quantitative Finance*, 2009.

FSA. Fsa confirms extension of short selling disclosure regime, January 2009. `http://www.fsa.gov.uk/pages/Library/Communication/PR/2009/009.shtml`.

M. Garman, C. Blanco, and R. Erickson. Weather Derivatives: Instruments and Pricing Issues. *Environmental Finance*, 2000.

N. Gatzert, H. Schmeiser, and D. Toplek. An analysis of pricing and basis risk for industry loss warranties. *Zeitschrift für die gesamte Versicherungswissenschaft*, pages 1–21, 2007.

H. Geman. *Commodities and commodity derivatives: modelling and pricing for agriculturals, metals and energy*. John Wiley & Sons, 2005.

R. Geske and H.E. Johnson. The american put option valued analytically. *Journal of Finance*, pages 1511–1524, 1984.

P. Glasserman. *Monte Carlo methods in financial engineering*. Springer Verlag, 2004. ISBN 0387004513.

K.J. Glover. *The Analysis of PDEs Arising in Nonlinear and Non-Standard Option Pricing*. PhD thesis, Department of Mathematics, University of Manchester, 2008.

Kristoffer J. Glover, Peter W. Duck, and David P. Newton. On nonlinear models of markets with finite liquidity: some cautionary notes. *SIAM Journal on Applied Mathematics*, 70(8):3252–3271, 2010. ISSN 0036-1399.

H. Hamisultane. Extracting information from the market to price the weather derivatives. *ICFAI Journal of Derivatives Markets*, Vol. 4:17–46, 2006.

H. Hamisultane. Which Method for Pricing Weather Derivatives? 2008. "`http://helene-hamisultane.voila.net/`".

W.K. Härdle and B. López Cabrera. Implied market price of weather risk. *SFB 649 Discussion Papers*, 2009.

C. Harris. *The Valuation of Weather Derivatives using Partial Differential Equations*. PhD thesis, Department of Mathematics, University of Reading, 2003.

V. Henderson. Valuation of claims on nontraded assets using utility maximization. *Mathematical Finance*, 12(4):351–373, 2002. ISSN 1467-9965.

V. Henderson. The impact of the market portfolio on the valuation, incentives and optimality of executive stock options. *Quantitative Finance*, 5(1):35–47, 2005.

S.L. Heston. A closed-form solution for options with stochastic volatility with applications to bond and currency options. *Review of financial studies*, 6(2): 327–343, 1993.

T. Hoggard, AE Whalley, and P. Wilmott. Hedging option portfolios in the presence of transaction costs. *Advances in Futures and Options Research*, 7(1): 21–35, 1994.

J. Hull and A. White. The pricing of options on assets with stochastic volatilities. *The Journal of Finance*, 42(2):281–300, 1987.

J.C. Hull. *Options, Futures and Other Derivatives. Ed.* Prentice Hall (6th ed.), New Jersey, 2006.

H.E. Hurst. {Long-term storage capacity of reservoirs}. *Trans. Amer. Soc. Civil Eng.*, 116:770–808, 1951.

A. Ibáñez. Option-Pricing in Incomplete Markets: The Hedging Portfolio plus a Risk Premium-Based Recursive Approach. *Nº.: UC3M Working Papers. Bussiness Economics 2005-21*, 2005.

S. Jewson and A. Brix. Weather derivative pricing and the year ahead forecasting of temperature part 1: empirical results. 2004. "Available at SSRN: `http://ssrn.com/abstract=535142`".

S. Jewson, A. Brix, and C. Ziehmann. *Weather derivative valuation: the meteorological, statistical, financial and mathematical foundations*. Cambridge Univ Pr, 2005.

P. Johnson. *Improved Numerical Techniques For Occupation-Time Derivatives And Other Complex Financial Instruments*. PhD thesis, Department of Mathematics, University of Manchester, 2007.

P.V. Johnson, N.J. Sharp, P. Duck, and D.P. Newton. Enhanced Finite-Difference Techniques for Early-Exercise Options on Single and Multiple Underlyings. 2007.

M.S. Joshi. *The concepts and practice of mathematical finance*. Cambridge Univ Pr, 2003.

E. Kalnay. *Atmospheric modeling, data assimilation, and predictability*. Cambridge Univ Pr, 2003. ISBN 0521796296.

A.G.Z. Kemna and ACF Vorst. A pricing method for options based on average asset values. *Journal of Banking & Finance*, 14(1):113–129, 1990. ISSN 0378-4266.

S.H Law. *On The Modelling, Design, and Valuation of Commodity Derivatives*. PhD thesis, Department of Mathematics, University of Manchester, 2009.

K.B. Leggio and D. Lien. Hedging gas bills with weather derivatives. *Journal of Economics and Finance*, 26(1):88–100, 2002. ISSN 1055-0925.

H.E. Leland. Option pricing and replication with transactions costs. *The journal of finance*, 40(5):1283–1301, 1985.

R. Lord, F. Fang, F. Bervoets, and K. Oosterlee. A Fast and Accurate FFT-Based Method for Pricing Early-Exercise Options Under Lévy Processes. *Center for Mathematics and Computer Science (CWI)*, 2007.

P. Lynch. The origins of computer weather prediction and climate modeling. *Journal of Computational Physics*, 227(7):3431–3444, 2008. ISSN 0021-9991.

B.B. Mandelbrot and J.W. Van Ness. Fractional Brownian motions, fractional noises and applications. *SIAM review*, 10(4):422–437, 1968. ISSN 0036-1445.

J.S Matthews. Dog Days and Degree Days. January 2009. "Available at: `http://www.cmegroup.com/trading/weather/files/weather-white-paper.pdf`".

R. McIntyre and S. Doherty. An Example from the UK. *Energy and Power Risk Management*, 1999.

N Mehta. On-line fx trading for pros, February 2000.

R.C. Merton. Theory of Rational Option Pricing. *The Bell Journal of Economics and Management Science*, 4(1):141–183, 1973.

Met-Office. Companies not forecasting the hidden cost of weather. 2001. "Available at: `www.met-office.gov.uk/corporate/pressoffice/pr20011126.html.` ".

T. Moller. Risk-minimizing hedging strategies for unit-linked life insurance contracts. *Astin Bulletin*, 28(1):17–48, 1998.

T. Møller. On transformations of actuarial valuation principles. *Insurance: Mathematics and Economics*, 28(3):281–303, 2001.

M. Moreno. Riding the temp. *Weather Derivatives, FOW Special Supplement*, 2000.

J. Morrison. Managing Weather Risk: Will Derviatives Use Rise? *Futures Industry*, 2009.

K.W. Morton and R.B. Kellogg. *Numerical solution of convection-diffusion problems*. Springer, 1996.

M. Mraoua. Temperature stochastic modeling and weather derivatives pricing: empirical study with Moroccan data. *Afrika Statistika*, 2(1), 2009.

R. Myers. What Every CFO Needs To Know Now About Weather Risk Management. 2009. "Available at: `http://www.cmegroup.com/trading/weather/files/WeatherRisk_CEO.pdf`".

S.N. Neftci. *An introduction to the mathematics of financial derivatives*. Academic Pr, 2000. ISBN 0125153929.

M. Nicholls. Confounding the forecasts. *Environmental Finance*, 10:5–7, 2004.

M. Odening, O. Musshoff, and W. Xu. Analysis of rainfall derivatives using daily precipitation models: opportunities and pitfalls. *Agricultural Finance Review*, 67(1):135–156, 2007. ISSN 0002-1466.

M. Otaka and Y. Kawaguchi. Hedging and pricing of real estate securities under market incompleteness. In *Quantitative Methods in Finance Conference, Cairns, Australia*, 2002.

K. Parrott and N. Clarke. A parallel solution of early exercise Asian options with stochastic volatility. In *Proceedings of the 11th Domain Decomposition Conference, Greenwich*. Citeseer, 1998.

H. Pham, T. Rheinländer, and M. Schweizer. Mean-variance hedging for continuous processes: new proofs and examples. *Finance and Stochastics*, 2(2): 173–198, 1998.

C. Pirrong and M. Jermakyan. The price of power: The valuation of power and weather derivatives. *Journal of Banking & Finance*, 32(12):2520–2529, 2008.

E. Platen and J. West. A fair pricing approach to weather derivatives. *Asia-Pacific Financial Markets*, 11(1):23–53, 2004. ISSN 1387-2834.

P. Poncet and V.E. Vaugirard. The valuation of nature-linked bonds with exchange rate risk. *Journal of Economics and Finance*, 25(3):293–307, 2001.

W.H. Press, S.A. Teukolsky, and W.T. Vetterling. *Numerical recipes in C++: the art of scientific computing*. Cambridge University Press, 2002.

D Randall. *An Introduction to Atmospheric Modeling*. 2009. "Available at: `http://www.4shared.com/document/nTNX3TZC/An_Introduction_to_Atmospheric.html`".

L.F. Richardson. *Weather prediction by numerical process*. Cambridge Univ Pr, 2007.

D. Ruppert. *Statistics and Data Analysis for Financial Engineering*. Springer Verlag, 2010.

P.A. Samuelson. St. Petersburg paradoxes: Defanged, dissected, and historically described. *Journal of Economic Literature*, 15(1):24–55, 1977. ISSN 0022-0515.

M. Schäl. On quadratic cost criteria for option hedging. *Mathematics of Operations Research*, 19(1):121–131, 1994.

F. Schiller, G. Seidler, and M. Wimmer. Temperature Models for Pricing Weather Derivatives. 2008. "Quantitative Finance, Forthcoming. Available at SSRN: `http://ssrn.com/abstract=1280826`".

M. Schweizer. Approximation pricing and the variance-optimal martingale measure. *The Annals of Probability*, 24(1):206–236, 1996.

N. J. Sharp. *Advances in Mortgage Valuation: An Option-Theorectic Approach*. PhD thesis, Department of Mathematics, University of Manchester, 2006.

K.R. Sircar and G.C. Papanicolaou. Stochastic volatility, smile & asymptotics. *Applied Mathematical Finance*, 6(2):107–145, 1999.

G.D. Smith. *Numerical Solution of Partial Differential Equations: Finite Difference Methods*. Oxford University Press, 1985.

A. Staniforth and J. Côté. Semi-lagrangian integration schemes for atmospheric models: A review. *Monthly Weather Review*, 119(9):2206–2223, 1991.

STORM. Weather derivatives volume plummets. *STORM*, 2009.

H. Takahashi and M. Mori. Double exponential formulas for numerical integration. *Publ. RIMS, Kyoto Univ*, 9:721–741, 1974.

J. Tigler and T. Butte. Weather derivatives: A quantitative analysis. *Research Thesis, Institute of Finance and Banking, Department of Business Administration, Economics and Law, Darmstadt University of Technology*, 2001.

C.G. Turvey. Weather derivatives for specific event risks in agriculture. *Review of Agricultural Economics*, 23(2):333, 2001. ISSN 1058-7195.

C.G. Turvey. The pricing of degree-day weather options. *Agricultural Finance Review*, 65(1):59, 2005.

C.G. Turvey. The Pricing, Structure and Function of Weather-Linked Bonds, Mortgages and Operating Credit. *Agricultural Finance Review*, 68(1):135–150, 2008.

O. Vasicek. An equilibrium characterization of the term structure. *Journal of financial economics*, 5(2):177–188, 1977.

G Village. Credit crunch dampens weather market in 2008, July 2008. http://ilaw.prod.informaprofessional.com/ilaw/doc/view.htm?id=225921.

I.R. Wang, J.W.L. Wan, and P.A. Forsyth. Robust numerical valuation of European and American options under the CGMY process. *Journal of Computational Finance*, 10(4):31, 2007. ISSN 1460-1559.

P. Wessa. Free statistics software, office for research and development and education, 2010. "`http://www.wessa.net/`".

M. Widdicks, A.D. Andricopoulos, D.P. Newton, and P.W. Duck. On the enhanced convergence of standard lattice methods for option pricing. *Journal of Futures Markets*, 22(4):315–338, 2002.

P. Wilmott. *Paul Wilmott on Quantitative Finance*. London; New York: Springer, 2002., 2000a.

P. Wilmott. Quantative Finance, volume 2, 2000b.

P. Wilmott, S. Howison, and J. Dewynne. *The Mathematics of Financial Derivatives: A Student Introduction*. Cambridge University Press, 1995.

P. Wilmott, J. Dewynne, and S. Howison. *Option pricing: mathematical models and computation*. Oxford financial press Oxford, 2000.

H. Windcliff, J. Wang, PA Forsyth, and KR Vetzal. Hedging with a correlated asset: Solution of a nonlinear pricing PDE. *Journal of Computational and Applied Mathematics*, 200(1):86–115, 2007.

X Xiao. *Advanced Monte Carlo Techniques: An Approach for foreign exchange derivative pricing*. PhD thesis, Department of Mathematics, University of Manchester, 2007.

G. Zanotti, G. Gabbi, and Laboratore. Climate Variables and Weather Derivatives: Gas Demand, Temperature and Seasonality Effects in the Italian Case. 2003. "Available at SSRN: `http://ssrn.com/abstract=488745d`".

R. Zvan, P.A. Forsyth, and K.R. Vetzal. *Robust numerical methods for PDE models of Asian options*. University of Waterloo, Faculty of Mathematics, 1996.

Appendix A

Additional mathematical details

A.1 Quadratic Variation

The quadratic variation of a process is an extension of the notion of the total variation of a function, but rather than summing the absolute values of changes of a function sampled at a sequence of times, the squares are summed. Suppose X_t is a stochastic process, with $t = 0, 1, 2, \ldots$ then the quadratic variation is the processes

$$[X]_t = \sum_{s=1}^{t} (X_s - X_{s-1})^2 \tag{A.1}$$

A.2 Proof for including seasonal variation term

Take

$$\mathrm{d}X_t = \mathrm{d}\theta(t) + \kappa(t)\left[\theta(t) - X_t\right]\mathrm{d}t + \sigma(t)\mathrm{d}W_t. \tag{A.2}$$

we wish to prove that the expectation of the process is $\theta(t)$. First we introduce a variable

$$Z_t = e^{\int_0^t \kappa(s)\mathrm{d}s}\left[\theta(t) - X_t\right], \tag{A.3}$$

where we define $Z_0 = 0$. Using Itô's lemma, we find that

$$\begin{aligned} \mathrm{d}Z_t &= \frac{\partial Z}{\partial t}\mathrm{d}t + \frac{\partial Z}{\partial X}\mathrm{d}X_t \\ &= e^{\int_0^t \kappa(s)\mathrm{d}s}\frac{\mathrm{d}\theta}{\mathrm{d}t} + \kappa(t)e^{\int_0^t \kappa(s)\mathrm{d}s}\left[\theta(t) - X_t\right]\mathrm{d}t - e^{\int_0^t \kappa(s)\mathrm{d}s}X_t\mathrm{d}X_t \\ &= e^{\int_0^t \kappa(s)\mathrm{d}s}\frac{\mathrm{d}\theta}{\mathrm{d}t} + \kappa(t)e^{\int_0^t \kappa(s)\mathrm{d}s}\left[\theta(t) - X_t\right]\mathrm{d}t \\ &- e^{\int_0^t \kappa(s)\mathrm{d}s}\left[\mathrm{d}\theta(t) + \kappa(t)\left[\theta(t) - X_t\right]\mathrm{d}t\right] + e^{\int_0^t \kappa(s)\mathrm{d}s}\sigma(t)\mathrm{d}W_t \\ &= -e^{\int_0^t \kappa(s)\mathrm{d}s}\sigma(t)\mathrm{d}W_t. \end{aligned} \tag{A.4}$$

Integrating both sides yields,

$$Z_t = Z_0 - \int_0^t e^{\int_0^t \kappa(s)\mathrm{d}s}\sigma(t)\mathrm{d}W_t. \tag{A.5}$$

From the definition of the variable Z_t in equation (A.3), we obtain

$$X_t = \theta(t) + e^{-\int_0^t \kappa(s)\mathrm{d}s}\int_0^t e^{\int_0^t \kappa(s)\mathrm{d}s}\sigma(t)\mathrm{d}W_t \tag{A.6}$$

Taking expectations of the previous equation produces

$$\mathbb{E}[X_t] = \theta(t) \tag{A.7}$$

as required (since $\mathbb{E}[\mathrm{d}W] = 0$).

A.3 The strong solution to Dornier/Alaton's model

With initial condition T_0, using the method of variation of parameters and Itô's formula, we can derive the solution to (4.4). Let

$$f(\hat{T}_t, t) = \hat{T}_t e^{\alpha t} \tag{A.8}$$

and then differentiate to give,

$$\frac{\partial f}{\partial t} = \hat{T}_t \alpha e^{\alpha t}, \quad \frac{\partial f}{\partial \hat{T}_t} = e^{\alpha t}, \quad \frac{\partial^2 f}{\partial \hat{T}_t^{\,2}} = 0$$

. Using Itô's Lemma to express df we obtain:

$$\begin{aligned} \mathrm{d}f &= \hat{T}_t \alpha e^{\alpha t}\mathrm{d}t + e^{\alpha t}\mathrm{d}\hat{T}_t \\ \mathrm{d}f &= e^{\alpha t}\mathrm{d}S + \alpha e^{\alpha t}S(t)\mathrm{d}t + e^{\alpha t}\sigma_t \mathrm{d}W_t \end{aligned} \tag{A.9}$$

Integrating we obtain,

$$\int_0^t \mathrm{d}f = \int_0^t e^{\alpha\tau}\mathrm{d}S(\tau) + \int_0^t \alpha e^{\alpha\tau}S(\tau)\mathrm{d}\tau + \int_0^t e^{\alpha\tau}\sigma_\tau \mathrm{d}W_\tau, \tag{A.10}$$

where through evaluation we see reduces to

$$\hat{T}_t e^{\alpha t} - \hat{T}_0 = e^{\alpha t}\Big(S(t) - S(s)\Big) + S(t)\Big(e^{\alpha t} - 1\Big) + \int_0^t e^{\alpha\tau}\sigma_\tau \mathrm{d}W_\tau, \tag{A.11}$$

which then yields the strong solution to the SDE (4.4)

$$\hat{T}_t = \Big(\hat{T}_0 - S(t)\Big)e^{-\alpha t)} + \Big(S(t) - S(0)\Big) + S(t) + \int_0^t e^{\alpha(\tau - t)}\sigma_\tau \mathrm{d}W_\tau. \tag{A.12}$$

A.4 Fractional Brownian motion

An associated fBm W^H is a Gaussian stochastic process that must satisfy the following properties:

1. the process W^H has continuous sample paths with $W_0^H = 0$,
2. W_t^H is a zero-mean Gaussian random variable for $t \geq 0$ (i.e. $\mathbb{E}[W_t^H] = 0$),
3. The covariance relation between to stationary increments of the process W^H is defined as:

$$\mathbb{E}[W_t^H W_s^H] = \frac{1}{2}(t^{2H} + s^{2H} - |t-s|^{2H}), \qquad \text{for all } t, s \geq 0, \tag{A.13}$$

   where here $\mathbb{E}$ denotes the expectation with respect to probability measure $\mathbb{P}$.

From observation, when $H = 1/2$ the FBM reduces to a standard Brownian motion; if $H > 1/2$ the Gaussian process models long-range dependence. It ss

important to note that when $H \neq 1/2$ the standard methods of stochastic calculus are not readily applicable, as by definition the process W^H is no longer a semi-martingale or Markov process. Intuitively this can be understood as implying that the process now depends on more information in the past than just the present value, which violates the definition of a Markov process. Brody et al. (2002) use the results from Duncan et al. (2000) to derive the model of temperature dynamics using FBM, and similar to Alaton et al. (2002), employ an Ornstein-Uhlenbeck process to model the evolution of daily temperature, giving

$$\mathrm{d}\hat{T}_t = \alpha(\theta(t) - \hat{T}_t)dt + \sigma_t dW_t^H. \tag{A.14}$$

Here, the parameters $\alpha, \theta(t), \sigma_t$ are defined as in equation (4.4), with W_t^H being a FBM.

Using the methods developed in Duncan et al. (2000), the strong solution of (4.14) yields

$$X = \hat{T}_0 K_t + K_t \int_0^t \alpha S(\tau) K_\tau^{-1} \mathrm{d}\tau + K_t \int_0^t \sigma_\tau K_\tau^{-1} dW_\tau^H, \tag{A.15}$$

with

$$K_t = exp\bigg(- \int_0^t \alpha \mathrm{d}\tau \bigg). \tag{A.16}$$

A.5 Linear regression formulas

For a linear regression model, the least square estimates are given by the simple formulae

$$\hat{\alpha} = \frac{S_{xx}S_y - S_x S_{xy}}{NS_{xx} - S_x^2}, \tag{A.17}$$

$$\hat{\beta} = \frac{NS_{xy} - S_x S_y}{NS_{xx} - S_x^2}, \tag{A.18}$$

where (Press et al., 2002; Jewson et al., 2005)

$$S_y = \sum_{i=1}^{N} y_i \quad , \quad S_x = \sum_{i=1}^{N} x_i \quad , \tag{A.19}$$

$$S_{xx} = \sum_{i=1}^{N} x_i^2 \quad , \quad S_{xy} = \sum_{i=1}^{N} x_i y_i \quad , \tag{A.20}$$

$$\bar{y} = \frac{1}{N} S_y \quad , \quad \bar{x} = \frac{1}{N} S_x \quad . \tag{A.21}$$

A.6 Tanh-Sinh in two dimensions

Below shows the formulation of the tanh-sinh quadrature scheme, for an integral

$$\int_{-1}^{1} \int_{-1}^{1} f(x, y) \mathrm{d}x \mathrm{d}y. \tag{A.22}$$

Make the change of variable

$$x = g(t) \qquad \text{where} \qquad g(t) = \tanh(\frac{\pi}{2} \sinh(t)), \tag{A.23}$$

$$y = g(u) \qquad \text{where} \qquad g(u) = \tanh(\frac{\pi}{2} \sinh(u)). \tag{A.24}$$

It then follows that we can evaluate the integral using the following equation

$$\int_{-1}^{1} \int_{-1}^{1} f(x, y) \mathrm{d}x \mathrm{d}y = \int_{-\infty}^{\infty} \int_{-\infty}^{\infty} f(g(t), g(u)) g^{'}(t) g^{'}(u) \mathrm{d}t \mathrm{d}u \tag{A.25}$$

$$\approx \Delta x \Delta y \sum_{k=-\infty}^{\infty} \sum_{j=-\infty}^{\infty} w_j w_k f(x_j, x_k), \tag{A.26}$$

where x_j and w_j are the 1-D abscissas and weights defined by equations (8.26) and (8.27) respectively. The other set of absicissas and weights are given by

$$x_k = g(j\Delta y) = \tanh(\frac{\pi}{2} \sinh(\Delta x k)), \tag{A.27}$$

$$w_k = g'(j\Delta y) = \frac{\frac{\pi}{2} \cosh(\Delta x k)}{\cosh^2(\frac{\pi}{2} \sinh(\Delta x j))}. \tag{A.28}$$

Δx and Δy are the intervals of integration in x and y.

A.7 L-p Norms

Two approaches commonly used to minimise the residuals are the l_1 or l_∞ approximations. We provide a very brief description of both. Given the set of residuals

$$\mathbf{r} = \begin{pmatrix} r_1 \\ r_2 \\ \vdots \\ r_n \end{pmatrix} \tag{A.29}$$

we may calculate an l_1 solution, which minimises the l_1 norm of the residuals

$$|\mathbf{r}|_1 = \sum_{i=1}^{N} |r_i|. \tag{A.30}$$

Alternatively an l_∞ solution is obtained through minimising the absolutely largest residual

$$|\mathbf{r}|_\infty = \max_{x \in [a,b]} |r_i|. \tag{A.31}$$

For small values of N the error in the value produced by the numerical technique will be large; therefore, computation of an l_1 solution is necessary. This will be more crucial when applying the methodology in multiple dimensions where, due to the curse of dimensionality, few node points can be used. The reader is referred to Dahlquist and Björck (2003) for more formal specifics and details with regard to the various norms.

Appendix B

Table data

B.1 Statistics

Bins	Midpoint	Abs. Frequency	Rel. Frequency	Cumul. Rel. Freq.	Density
-9,-8	-8.5	3	0.000536	0.000536	0.000536
-8,-7	-7.5	2	0.000357	0.000893	0.000357
-7,-6	-6.5	9	0.001607	0.0025	0.001607
-6,-5	-5.5	40	0.007144	0.009645	0.007144
-5,-4	-4.5	90	0.016074	0.025719	0.016074
-4,-3	-3.5	202	0.036078	0.061797	0.036078
-3,-2	-2.5	406	0.072513	0.13431	0.072513
-2,-1	-1.5	794	0.141811	0.276121	0.141811
-1,0	-0.5	1181	0.210931	0.487051	0.210931
0,1	0.5	1212	0.216467	0.703518	0.216467
1,2	1.5	871	0.155563	0.859082	0.155563
2,3	2.5	446	0.079657	0.938739	0.079657
3,4	3.5	217	0.038757	0.977496	0.038757
4,5	4.5	78	0.013931	0.991427	0.013931
5,6	5.5	37	0.006608	0.998035	0.006608
6,7	6.5	8	0.001429	0.999464	0.001429
7,8	7.5	3	0.000536	1	0.000536

Table B.1: A frequency table of the statistics absolute frequency, relative frequency, cumulative relative frequency, midpoints, and density of the temperature data observed at London Heathrow from January 1st 1995 to May 30th 2010.

B.2 Temperature Data

Date	Temperature	Date	Temperature	Date	Temperature
01/01/1995	1.22	02/01/1995	0.33	03/01/1995	-0.61
04/01/1995	3.17	05/01/1995	4.17	06/01/1995	4.61
07/01/1995	3.89	08/01/1995	7.83	09/01/1995	6.11
10/01/1995	9.5	11/01/1995	4.06	12/01/1995	2.44
13/01/1995	4.5	14/01/1995	8.39	15/01/1995	9.61
16/01/1995	8.5	17/01/1995	8.89	18/01/1995	5.5
19/01/1995	5.83	20/01/1995	7.22	21/01/1995	6.72
22/01/1995	5.89	23/01/1995	5.61	24/01/1995	6.17
25/01/1995	7.67	26/01/1995	6.39	27/01/1995	4.11
28/01/1995	8.78	29/01/1995	9.39	30/01/1995	4.33
31/01/1995	9	01/02/1995	10.06	02/02/1995	5.5
03/02/1995	9.39	04/02/1995	9.61	05/02/1995	8.22
06/02/1995	10.33	07/02/1995	9.5	08/02/1995	7.11
09/02/1995	4.22	10/02/1995	7.83	11/02/1995	9.61
12/02/1995	9.06	13/02/1995	9.11	14/02/1995	8.22
15/02/1995	9.89	16/02/1995	8	17/02/1995	6.28
18/02/1995	6.67	19/02/1995	8.83	20/02/1995	8.11
21/02/1995	6.61	22/02/1995	6.39	23/02/1995	4.83
24/02/1995	6.39	25/02/1995	6.22	26/02/1995	3.89
27/02/1995	4.94	28/02/1995	10.61	01/03/1995	7.72
02/03/1995	3.22	03/03/1995	2.61	04/03/1995	2.44
05/03/1995	6.06	06/03/1995	4.67	07/03/1995	3.44
08/03/1995	4.17	09/03/1995	5	10/03/1995	8.83
11/03/1995	9.94	12/03/1995	9.33	13/03/1995	4.67
14/03/1995	6.94	15/03/1995	4.22	16/03/1995	6.17
17/03/1995	8.78	18/03/1995	8	19/03/1995	5.5
20/03/1995	5.22	21/03/1995	5.78	22/03/1995	6.61
23/03/1995	8.28	24/03/1995	9.78	25/03/1995	10.56
26/03/1995	9.72	27/03/1995	5.44	28/03/1995	4.17
29/03/1995	4.83	30/03/1995	6.61	31/03/1995	12.06
01/04/1995	13.44	02/04/1995	11.78	03/04/1995	11.78
04/04/1995	11.5	05/04/1995	11.89	06/04/1995	14.33
07/04/1995	13.06	08/04/1995	8.61	09/04/1995	8.83
10/04/1995	12.17	11/04/1995	12.61	12/04/1995	11.28
13/04/1995	10.5	14/04/1995	12.56	15/04/1995	10.56
16/04/1995	9.33	17/04/1995	10.61	18/04/1995	8.61
19/04/1995	5.11	20/04/1995	6.06	21/04/1995	7.28
22/04/1995	8.61	23/04/1995	10.61	24/04/1995	9.22
25/04/1995	13.39	26/04/1995	8.44	27/04/1995	8
28/04/1995	8.39	29/04/1995	9.67	30/04/1995	11.89
01/05/1995	13.33	02/05/1995	16.56	03/05/1995	17.94
04/05/1995	19	05/05/1995	19.72	06/05/1995	19.89
07/05/1995	19.94	08/05/1995	13.89	09/05/1995	11.44
10/05/1995	10.67	11/05/1995	8.56	12/05/1995	7.67
13/05/1995	7.72	14/05/1995	9.06	15/05/1995	10.22
16/05/1995	10.72	17/05/1995	8.83	18/05/1995	9.39
19/05/1995	11	20/05/1995	11.17	21/05/1995	12.28
22/05/1995	13.78	23/05/1995	16.11	24/05/1995	14.83
25/05/1995	14.89	26/05/1995	15.17	27/05/1995	16.17
28/05/1995	16.44	29/05/1995	14.61	30/05/1995	13.33

Date	Temperature	Date	Temperature	Date	Temperature
31/05/1995	15.06	01/06/1995	13.72	02/06/1995	15.06
03/06/1995	13.61	04/06/1995	13.67	05/06/1995	14.61
06/06/1995	15.11	07/06/1995	15.44	08/06/1995	12.39
09/06/1995	12.33	10/06/1995	12.06	11/06/1995	12.67
12/06/1995	11.28	13/06/1995	11.17	14/06/1995	13
15/06/1995	13.67	16/06/1995	14.83	17/06/1995	13.72
18/06/1995	16.94	19/06/1995	17.78	20/06/1995	18.89
21/06/1995	18.11	22/06/1995	17.72	23/06/1995	15.72
24/06/1995	13.89	25/06/1995	17.06	26/06/1995	17.5
27/06/1995	18.44	28/06/1995	21.39	29/06/1995	21.94
30/06/1995	22.89	01/07/1995	17.06	02/07/1995	15.33
03/07/1995	15.78	04/07/1995	17.44	05/07/1995	19.56
06/07/1995	18.94	07/07/1995	20.11	08/07/1995	21.17
09/07/1995	21.44	10/07/1995	22.61	11/07/1995	23.06
12/07/1995	21.11	13/07/1995	19.94	14/07/1995	19.61
15/07/1995	18.22	16/07/1995	18.56	17/07/1995	18.56
18/07/1995	21.22	19/07/1995	22.83	20/07/1995	24.28
21/07/1995	23.17	22/07/1995	18.5	23/07/1995	19.17
24/07/1995	20.78	25/07/1995	22.11	26/07/1995	21.72
27/07/1995	20.5	28/07/1995	21.44	29/07/1995	23.67
30/07/1995	23.17	31/07/1995	25.44	01/08/1995	26.67
02/08/1995	26.56	03/08/1995	25.44	04/08/1995	20.78
05/08/1995	20.17	06/08/1995	20.22	07/08/1995	18.5
08/08/1995	17.61	09/08/1995	18.5	10/08/1995	21.56
11/08/1995	24.39	12/08/1995	23.78	13/08/1995	21.44
14/08/1995	20.22	15/08/1995	22.61	16/08/1995	24.17
17/08/1995	22.22	18/08/1995	22.83	19/08/1995	23.22
20/08/1995	23.44	21/08/1995	23.06	22/08/1995	22.56
23/08/1995	19.83	24/08/1995	18.61	25/08/1995	20.67
26/08/1995	19.56	27/08/1995	17.39	28/08/1995	15.22
29/08/1995	14.94	30/08/1995	17	31/08/1995	18
01/09/1995	17.33	02/09/1995	16.33	03/09/1995	14.5
04/09/1995	15.39	05/09/1995	14.33	06/09/1995	15.33
07/09/1995	17.11	08/09/1995	17	09/09/1995	16.83
10/09/1995	15.22	11/09/1995	16.33	12/09/1995	14.44
13/09/1995	13.78	14/09/1995	14.06	15/09/1995	14.06
16/09/1995	14.17	17/09/1995	15.28	18/09/1995	15.94
19/09/1995	16.28	20/09/1995	13.78	21/09/1995	13.5
22/09/1995	15.39	23/09/1995	14.94	24/09/1995	12.67
25/09/1995	12.11	26/09/1995	15.33	27/09/1995	12.5
28/09/1995	9.33	29/09/1995	10.83	30/09/1995	11.89
01/10/1995	15.83	02/10/1995	14.17	03/10/1995	14.94
04/10/1995	15.78	05/10/1995	13.72	06/10/1995	14.61
07/10/1995	17.11	08/10/1995	18.28	09/10/1995	18.28
10/10/1995	16.33	11/10/1995	16.33	12/10/1995	16.78
13/10/1995	16.33	14/10/1995	16.11	15/10/1995	15.78
16/10/1995	15	17/10/1995	15.89	18/10/1995	12.44
19/10/1995	12.28	20/10/1995	11.89	21/10/1995	10.22
22/10/1995	11.5	23/10/1995	11.44	24/10/1995	16.33
25/10/1995	13.39	26/10/1995	15.11	27/10/1995	13.5
28/10/1995	7.89	29/10/1995	10.06	30/10/1995	10.5
31/10/1995	9.67	01/11/1995	9.17	02/11/1995	7.83

Date	Temperature	Date	Temperature	Date"	Temperature
03/11/1995	7.83	04/11/1995	6.28	05/11/1995	4.72
06/11/1995	4.89	07/11/1995	6.72	08/11/1995	11.56
09/11/1995	11.83	10/11/1995	9.89	11/11/1995	12.39
12/11/1995	13.17	13/11/1995	11.94	14/11/1995	10.39
15/11/1995	11.39	16/11/1995	8.78	17/11/1995	2.94
18/11/1995	2.17	19/11/1995	5.17	20/11/1995	5.5
21/11/1995	9.56	22/11/1995	10.17	23/11/1995	9.22
24/11/1995	11.78	25/11/1995	11.78	26/11/1995	9.56
27/11/1995	9.22	28/11/1995	8.67	29/11/1995	9
30/11/1995	5.72	01/12/1995	8.28	02/12/1995	11.61
03/12/1995	11.22	04/12/1995	6.89	05/12/1995	1.72
06/12/1995	0	07/12/1995	0.5	08/12/1995	2
09/12/1995	1.22	10/12/1995	-0.33	11/12/1995	3.78
12/12/1995	5.72	13/12/1995	6.22	14/12/1995	4.44
15/12/1995	2.67	16/12/1995	4.44	17/12/1995	4.72
18/12/1995	4.56	19/12/1995	5.28	20/12/1995	3.44
21/12/1995	2.83	22/12/1995	10.67	23/12/1995	6.17
24/12/1995	3.78	25/12/1995	0.67	26/12/1995	-1
27/12/1995	-0.67	28/12/1995	-2.22	29/12/1995	-1.5
30/12/1995	-0.5	31/12/1995	2.61	01/01/1996	4.17
02/01/1996	5.94	03/01/1996	4.78	04/01/1996	5.56
05/01/1996	7.22	06/01/1996	7.11	07/01/1996	9.56
08/01/1996	9.89	09/01/1996	9.78	10/01/1996	9
11/01/1996	8.44	12/01/1996	10.61	13/01/1996	10.72
14/01/1996	9.28	15/01/1996	7.33	16/01/1996	6.5
17/01/1996	7	18/01/1996	5.06	19/01/1996	6.67
20/01/1996	3.94	21/01/1996	2.67	22/01/1996	4.67
23/01/1996	3.61	24/01/1996	3.28	25/01/1996	-0.5
26/01/1996	-2.72	27/01/1996	-2.72	28/01/1996	1.5
29/01/1996	0.89	30/01/1996	2.33	31/01/1996	2.5
01/02/1996	0.67	02/02/1996	1.44	03/02/1996	1.78
04/02/1996	1.72	05/02/1996	-0.28	06/02/1996	-0.28
07/02/1996	-0.22	08/02/1996	1.33	09/02/1996	4.06
10/02/1996	6.67	11/02/1996	7.06	12/02/1996	5.11
13/02/1996	4.61	14/02/1996	3.56	15/02/1996	2.56
16/02/1996	7.83	17/02/1996	8.06	18/02/1996	6.67
19/02/1996	1.39	20/02/1996	-0.28	21/02/1996	-0.11
22/02/1996	1.17	23/02/1996	5.17	24/02/1996	7.83
25/02/1996	6.22	26/02/1996	4.83	27/02/1996	4.89
28/02/1996	4.28	29/02/1996	5.22	01/03/1996	5.89
02/03/1996	6	03/03/1996	6.56	04/03/1996	6.28
05/03/1996	6.22	06/03/1996	6.11	07/03/1996	3.61
08/03/1996	4.44	09/03/1996	3.89	10/03/1996	5.5
11/03/1996	1.44	12/03/1996	1.56	13/03/1996	0.94
14/03/1996	2.22	15/03/1996	5.5	16/03/1996	5.61
17/03/1996	5.78	18/03/1996	6.33	19/03/1996	4.94
20/03/1996	3.56	21/03/1996	7.33	22/03/1996	8.06
23/03/1996	11.28	24/03/1996	8.17	25/03/1996	7.78
26/03/1996	4.78	27/03/1996	3.28	28/03/1996	4.17
29/03/1996	5.56	30/03/1996	4.28	31/03/1996	5.06

Date	Temperature	Date	Temperature	Date"	Temperature
01/04/1996	3.94	02/04/1996	4.11	03/04/1996	3.78
04/04/1996	5.22	05/04/1996	6.89	06/04/1996	6.39
07/04/1996	8.17	08/04/1996	10.06	09/04/1996	11.5
10/04/1996	9.72	11/04/1996	10.72	12/04/1996	5.33
13/04/1996	6.17	14/04/1996	7.78	15/04/1996	11.78
16/04/1996	13.61	17/04/1996	12.17	18/04/1996	10.78
19/04/1996	11.67	20/04/1996	15	21/04/1996	16.06
22/04/1996	10.28	23/04/1996	10.39	24/04/1996	10.83
25/04/1996	11.33	26/04/1996	13.5	27/04/1996	14.44
28/04/1996	11.72	29/04/1996	8.67	30/04/1996	8.78
01/05/1996	10.56	02/05/1996	8.72	03/05/1996	7.78
04/05/1996	7.11	05/05/1996	7.83	06/05/1996	9.17
07/05/1996	9.28	08/05/1996	7.94	09/05/1996	7.61
10/05/1996	7.17	11/05/1996	7.72	12/05/1996	10.78
13/05/1996	11.61	14/05/1996	11.11	15/05/1996	10.33
16/05/1996	6.39	17/05/1996	6.61	18/05/1996	6.39
19/05/1996	8.83	20/05/1996	10.5	21/05/1996	11.67
22/05/1996	11.17	23/05/1996	13.33	24/05/1996	12.56
25/05/1996	12.72	26/05/1996	11.44	27/05/1996	12.5
28/05/1996	11.72	29/05/1996	16.11	30/05/1996	19.61
31/05/1996	15.78	01/06/1996	13.83	02/06/1996	13.5
03/06/1996	13.61	04/06/1996	16.72	05/06/1996	20.28
06/06/1996	23.06	07/06/1996	25.28	08/06/1996	18.11
09/06/1996	17.39	10/06/1996	17.39	11/06/1996	17.11
12/06/1996	17	13/06/1996	16.22	14/06/1996	15.78
15/06/1996	16.72	16/06/1996	18.89	17/06/1996	21.06
18/06/1996	17.44	19/06/1996	17.28	20/06/1996	12.94
21/06/1996	13.72	22/06/1996	13.83	23/06/1996	15.39
24/06/1996	16.33	25/06/1996	19.06	26/06/1996	19.11
27/06/1996	19.17	28/06/1996	16.56	29/06/1996	14.5
30/06/1996	16.56	01/07/1996	14.39	02/07/1996	15.28
03/07/1996	15.17	04/07/1996	15.83	05/07/1996	14.06
06/07/1996	13.28	07/07/1996	14.94	08/07/1996	15.33
09/07/1996	16.28	10/07/1996	19.22	11/07/1996	19.83
12/07/1996	18.83	13/07/1996	20.06	14/07/1996	20.78
15/07/1996	18.78	16/07/1996	16	17/07/1996	17.17
18/07/1996	19.78	19/07/1996	19.17	20/07/1996	21.11
21/07/1996	22.89	22/07/1996	24.39	23/07/1996	22.28
24/07/1996	17.17	25/07/1996	19	26/07/1996	21.83
27/07/1996	19.39	28/07/1996	19.17	29/07/1996	19.33
30/07/1996	18.44	31/07/1996	19.06	01/08/1996	17.61
02/08/1996	16.67	03/08/1996	18.11	04/08/1996	19
05/08/1996	21.28	06/08/1996	18.44	07/08/1996	17.5
08/08/1996	17.56	09/08/1996	17.78	10/08/1996	18.61
11/08/1996	16.56	12/08/1996	17.11	13/08/1996	18.28
14/08/1996	18.22	15/08/1996	17.33	16/08/1996	20.39
17/08/1996	20.72	18/08/1996	23	19/08/1996	23.94
20/08/1996	20.67	21/08/1996	18.83	22/08/1996	17.72
23/08/1996	17.06	24/08/1996	16.17	25/08/1996	16.22
26/08/1996	15.56	27/08/1996	15.06	28/08/1996	15.11
29/08/1996	15.11	30/08/1996	14.89	31/08/1996	14.06

Date	Temperature	Date	Temperature	Date"	Temperature
01/09/1996	16.11	02/09/1996	18.11	03/09/1996	17.67
04/09/1996	16.22	05/09/1996	17.28	06/09/1996	15.78
07/09/1996	15.78	08/09/1996	15.5	09/09/1996	14.83
10/09/1996	14.28	11/09/1996	14.17	12/09/1996	14.83
13/09/1996	12.83	14/09/1996	13	15/09/1996	15.06
16/09/1996	15.5	17/09/1996	14.56	18/09/1996	13.06
19/09/1996	12.22	20/09/1996	13.33	21/09/1996	13.61
22/09/1996	12.5	23/09/1996	12.33	24/09/1996	12.11
25/09/1996	15.33	26/09/1996	14.17	27/09/1996	15.06
28/09/1996	14.94	29/09/1996	16.83	30/09/1996	13.28
01/10/1996	12.06	02/10/1996	11.56	03/10/1996	13.22
04/10/1996	11	05/10/1996	10.44	06/10/1996	10.44
07/10/1996	13.78	08/10/1996	14.78	09/10/1996	12.72
10/10/1996	12.33	11/10/1996	11.11	12/10/1996	12.89
13/10/1996	15.33	14/10/1996	15.56	15/10/1996	12.61
16/10/1996	11	17/10/1996	10.11	18/10/1996	11.78
19/10/1996	12.78	20/10/1996	15.17	21/10/1996	14
22/10/1996	13.28	23/10/1996	13.89	24/10/1996	14.33
25/10/1996	14.5	26/10/1996	11.61	27/10/1996	14.72
28/10/1996	14.22	29/10/1996	10.89	30/10/1996	8.72
31/10/1996	12.28	01/11/1996	13.39	02/11/1996	15.89
03/11/1996	15	04/11/1996	13.44	05/11/1996	10.89
06/11/1996	12.83	07/11/1996	9.67	08/11/1996	6.61
09/11/1996	8.28	10/11/1996	5.17	11/11/1996	3.67
12/11/1996	7.33	13/11/1996	5.33	14/11/1996	3.83
15/11/1996	5.5	16/11/1996	3.67	17/11/1996	6.56
18/11/1996	3.61	19/11/1996	3.89	20/11/1996	5.06
21/11/1996	2.39	22/11/1996	3.11	23/11/1996	2.89
24/11/1996	4.11	25/11/1996	8.33	26/11/1996	5.44
27/11/1996	3.56	28/11/1996	1.5	29/11/1996	8.28
30/11/1996	7.39	01/12/1996	7.89	02/12/1996	6.72
03/12/1996	8.78	04/12/1996	5.94	05/12/1996	3.72
06/12/1996	3.33	07/12/1996	4.67	08/12/1996	4.72
09/12/1996	3.89	10/12/1996	4	11/12/1996	4.28
12/12/1996	3.11	13/12/1996	3.56	14/12/1996	1.22
15/12/1996	7.17	16/12/1996	6.72	17/12/1996	6.33
18/12/1996	8.89	19/12/1996	8.11	20/12/1996	6.11
21/12/1996	3.17	22/12/1996	3.72	23/12/1996	2.33
24/12/1996	0.5	25/12/1996	2.11	26/12/1996	-0.56
27/12/1996	0.83	28/12/1996	0.72	29/12/1996	0.39
30/12/1996	2	31/12/1996	-1.67	01/01/1997	-2.78
02/01/1997	-2.94	03/01/1997	-1.89	04/01/1997	0.39
05/01/1997	1.22	06/01/1997	1.61	07/01/1997	-0.83
08/01/1997	-1.28	09/01/1997	-0.17	10/01/1997	-0.06
11/01/1997	2.17	12/01/1997	6.89	13/01/1997	6.83
14/01/1997	2.94	15/01/1997	0.22	16/01/1997	2.94
17/01/1997	5.89	18/01/1997	6.39	19/01/1997	4.83
20/01/1997	5.28	21/01/1997	3.56	22/01/1997	5.78
23/01/1997	7	24/01/1997	5.78	25/01/1997	5
26/01/1997	3.11	27/01/1997	4.11	28/01/1997	4.83
29/01/1997	5.17	30/01/1997	4.28	31/01/1997	4.44

Date	Temperature	Date	Temperature	Date"	Temperature
01/02/1997	4.89	02/02/1997	4.94	03/02/1997	3.44
04/02/1997	8.56	05/02/1997	6.67	06/02/1997	8.39
07/02/1997	9.06	08/02/1997	3.56	09/02/1997	8.89
10/02/1997	8.44	11/02/1997	7.5	12/02/1997	11.11
13/02/1997	6.56	14/02/1997	4.17	15/02/1997	5.28
16/02/1997	5.83	17/02/1997	8.83	18/02/1997	7.22
19/02/1997	6.89	20/02/1997	9	21/02/1997	10.72
22/02/1997	9.89	23/02/1997	10.78	24/02/1997	8.78
25/02/1997	10.33	26/02/1997	8.17	27/02/1997	7.5
28/02/1997	9.61	01/03/1997	8.89	02/03/1997	10.44
03/03/1997	6.44	04/03/1997	8.17	05/03/1997	9.33
06/03/1997	8.11	07/03/1997	9.67	08/03/1997	9.83
09/03/1997	9.11	10/03/1997	8.94	11/03/1997	9.39
12/03/1997	9.11	13/03/1997	10.06	14/03/1997	11.39
15/03/1997	12.5	16/03/1997	11.5	17/03/1997	10.56
18/03/1997	9.94	19/03/1997	9.72	20/03/1997	8.72
21/03/1997	8.61	22/03/1997	7.11	23/03/1997	9.83
24/03/1997	8.22	25/03/1997	9.56	26/03/1997	11.22
27/03/1997	11.33	28/03/1997	8.78	29/03/1997	8.28
30/03/1997	9	31/03/1997	10	01/04/1997	10.56
02/04/1997	10.83	03/04/1997	10.17	04/04/1997	8.67
05/04/1997	12.5	06/04/1997	10.28	07/04/1997	8.39
08/04/1997	9.94	09/04/1997	12.44	10/04/1997	13.44
11/04/1997	9.61	12/04/1997	7.67	13/04/1997	11.39
14/04/1997	10.83	15/04/1997	9.39	16/04/1997	9
17/04/1997	9.83	18/04/1997	8.06	19/04/1997	7.28
20/04/1997	5.72	21/04/1997	7.17	22/04/1997	8.72
23/04/1997	10.33	24/04/1997	11	25/04/1997	9.22
26/04/1997	10.5	27/04/1997	13.28	28/04/1997	14.39
29/04/1997	13.83	30/04/1997	13.83	01/05/1997	15.78
02/05/1997	18.17	03/05/1997	17.17	04/05/1997	14.89
05/05/1997	13.5	06/05/1997	6.11	07/05/1997	6.33
08/05/1997	8.83	09/05/1997	9.5	10/05/1997	11.17
11/05/1997	11.89	12/05/1997	11	13/05/1997	12.56
14/05/1997	13.39	15/05/1997	12.89	16/05/1997	15.78
17/05/1997	18.78	18/05/1997	16.83	19/05/1997	14.83
20/05/1997	12.89	21/05/1997	12	22/05/1997	11.44
23/05/1997	11.33	24/05/1997	10.89	25/05/1997	12.61
26/05/1997	15.72	27/05/1997	15	28/05/1997	11.78
29/05/1997	15.61	30/05/1997	17.56	31/05/1997	17.17
01/06/1997	15.56	02/06/1997	17.06	03/06/1997	16.39
04/06/1997	15.56	05/06/1997	18.72	06/06/1997	19.39
07/06/1997	19.28	08/06/1997	17.33	09/06/1997	16.56
10/06/1997	19.5	11/06/1997	19.11	12/06/1997	16.78
13/06/1997	17.83	14/06/1997	14.78	15/06/1997	14.94
16/06/1997	15.44	17/06/1997	15.67	18/06/1997	16.22
19/06/1997	13.17	20/06/1997	12.67	21/06/1997	13.89
22/06/1997	13.61	23/06/1997	15.56	24/06/1997	14.56
25/06/1997	13.61	26/06/1997	14.11	27/06/1997	12.56
28/06/1997	13	29/06/1997	15.28	30/06/1997	13.61

Date	Temperature	Date	Temperature	Date"	Temperature
01/07/1997	14.33	02/07/1997	13.89	03/07/1997	13.61
04/07/1997	14.83	05/07/1997	16.89	06/07/1997	19
07/07/1997	21.17	08/07/1997	20.22	09/07/1997	20.83
10/07/1997	17.61	11/07/1997	18.06	12/07/1997	18.5
13/07/1997	19.22	14/07/1997	18.39	15/07/1997	19.39
16/07/1997	18.39	17/07/1997	16.67	18/07/1997	16.11
19/07/1997	19.06	20/07/1997	19.61	21/07/1997	20.22
22/07/1997	21	23/07/1997	21.72	24/07/1997	19.5
25/07/1997	18.89	26/07/1997	17.56	27/07/1997	19.78
28/07/1997	19.72	29/07/1997	21.17	30/07/1997	19.17
31/07/1997	15.5	01/08/1997	19	02/08/1997	19.11
03/08/1997	17.78	04/08/1997	18.44	05/08/1997	19.06
06/08/1997	19.39	07/08/1997	22.17	08/08/1997	24.11
09/08/1997	23.28	10/08/1997	24.72	11/08/1997	24.78
12/08/1997	23.72	13/08/1997	22.61	14/08/1997	20.78
15/08/1997	22.06	16/08/1997	22.89	17/08/1997	21.56
18/08/1997	23.56	19/08/1997	24.22	20/08/1997	23.5
21/08/1997	21.94	22/08/1997	21.83	23/08/1997	22.17
24/08/1997	21.28	25/08/1997	18.94	26/08/1997	17.33
27/08/1997	16.72	28/08/1997	15.5	29/08/1997	16.83
30/08/1997	17.11	31/08/1997	18.61	01/09/1997	18.11
02/09/1997	16.61	03/09/1997	17.17	04/09/1997	17.78
05/09/1997	15.11	06/09/1997	15.17	07/09/1997	17.33
08/09/1997	16.44	09/09/1997	16.83	10/09/1997	15.72
11/09/1997	16.44	12/09/1997	14.67	13/09/1997	12.06
14/09/1997	13	15/09/1997	14.83	16/09/1997	16.56
17/09/1997	16.17	18/09/1997	17.94	19/09/1997	16.56
20/09/1997	15.56	21/09/1997	13.67	22/09/1997	14.39
23/09/1997	14.83	24/09/1997	15.5	25/09/1997	16.67
26/09/1997	16.61	27/09/1997	15.78	28/09/1997	14.72
29/09/1997	17.61	30/09/1997	18.89	01/10/1997	19.56
02/10/1997	15.89	03/10/1997	15	04/10/1997	15.06
05/10/1997	14	06/10/1997	15.22	07/10/1997	13.72
08/10/1997	15.39	09/10/1997	17.33	10/10/1997	14.33
11/10/1997	10.56	12/10/1997	10.11	13/10/1997	8.67
14/10/1997	6.94	15/10/1997	11.94	16/10/1997	13.67
17/10/1997	16.44	18/10/1997	16	19/10/1997	15.22
20/10/1997	12.56	21/10/1997	10	22/10/1997	8.56
23/10/1997	9.11	24/10/1997	8.33	25/10/1997	5.94
26/10/1997	6.28	27/10/1997	8.17	28/10/1997	5.17
29/10/1997	4	30/10/1997	3.83	31/10/1997	5.28
01/11/1997	5	02/11/1997	3.61	03/11/1997	8.06
04/11/1997	8.94	05/11/1997	13.78	06/11/1997	11.89
07/11/1997	10.28	08/11/1997	11.06	09/11/1997	8.33
10/11/1997	8.28	11/11/1997	7.78	12/11/1997	4.78
13/11/1997	4.94	14/11/1997	6.78	15/11/1997	13.72
16/11/1997	15.11	17/11/1997	13.89	18/11/1997	11.83
19/11/1997	11.78	20/11/1997	10.5	21/11/1997	7.61
22/11/1997	7.56	23/11/1997	7.83	24/11/1997	7.72
25/11/1997	7.61	26/11/1997	10.11	27/11/1997	10.06
28/11/1997	11.39	29/11/1997	9.61	30/11/1997	8.06

Date	Temperature	Date	Temperature	Date"	Temperature
01/12/1997	3.78	02/12/1997	2.33	03/12/1997	2.56
04/12/1997	3.5	05/12/1997	2.06	06/12/1997	8.11
07/12/1997	8.67	08/12/1997	10.94	09/12/1997	10.61
10/12/1997	12.83	11/12/1997	11.72	12/12/1997	6.72
13/12/1997	4.83	14/12/1997	6.56	15/12/1997	4.89
16/12/1997	2.11	17/12/1997	1.39	18/12/1997	8.11
19/12/1997	8	20/12/1997	8.83	21/12/1997	5.78
22/12/1997	6.5	23/12/1997	9.5	24/12/1997	12.61
25/12/1997	10.06	26/12/1997	7.78	27/12/1997	5.67
28/12/1997	4.56	29/12/1997	6.22	30/12/1997	9.33
31/12/1997	8	01/01/1998	6.22	02/01/1998	8.28
03/01/1998	8.17	04/01/1998	7	05/01/1998	4.89
06/01/1998	6.17	07/01/1998	8.33	08/01/1998	10.11
09/01/1998	12.61	10/01/1998	9.61	11/01/1998	8.33
12/01/1998	10.78	13/01/1998	9.89	14/01/1998	7.83
15/01/1998	8.89	16/01/1998	7.39	17/01/1998	6.89
18/01/1998	7.5	19/01/1998	5.33	20/01/1998	2.33
21/01/1998	3.33	22/01/1998	4	23/01/1998	1.94
24/01/1998	4.39	25/01/1998	3.5	26/01/1998	3.44
27/01/1998	2.94	28/01/1998	2.78	29/01/1998	4.44
30/01/1998	4.56	31/01/1998	4.39	01/02/1998	-0.22
02/02/1998	1.83	03/02/1998	2.17	04/02/1998	3.44
05/02/1998	6.17	06/02/1998	7.94	07/02/1998	6.11
08/02/1998	6.22	09/02/1998	8.17	10/02/1998	9.56
11/02/1998	10.56	12/02/1998	10.83	13/02/1998	12.83
14/02/1998	10.22	15/02/1998	9.78	16/02/1998	10.89
17/02/1998	9	18/02/1998	6.89	19/02/1998	10.06
20/02/1998	10.94	21/02/1998	10.28	22/02/1998	6.61
23/02/1998	7.06	24/02/1998	8.83	25/02/1998	8.39
26/02/1998	7.83	27/02/1998	8.89	28/02/1998	5.33
01/03/1998	6.28	02/03/1998	8.78	03/03/1998	12.39
04/03/1998	9.94	05/03/1998	7.44	06/03/1998	10.39
07/03/1998	10.78	08/03/1998	7.56	09/03/1998	4.44
10/03/1998	4.94	11/03/1998	7.5	12/03/1998	5.22
13/03/1998	8.78	14/03/1998	7.44	15/03/1998	9.72
16/03/1998	9.44	17/03/1998	10.28	18/03/1998	10.44
19/03/1998	8.44	20/03/1998	8.72	21/03/1998	9.44
22/03/1998	8.67	23/03/1998	6.67	24/03/1998	5.78
25/03/1998	6.83	26/03/1998	10.33	27/03/1998	12.22
28/03/1998	12	29/03/1998	14.17	30/03/1998	13
31/03/1998	10	01/04/1998	10	02/04/1998	10.94
03/04/1998	10.89	04/04/1998	10.89	05/04/1998	10.06
06/04/1998	9.89	07/04/1998	9	08/04/1998	8.06
09/04/1998	7.67	10/04/1998	5.61	11/04/1998	5.89
12/04/1998	4.17	13/04/1998	3.78	14/04/1998	4.56
15/04/1998	3.17	16/04/1998	5	17/04/1998	6.33
18/04/1998	6.17	19/04/1998	8.78	20/04/1998	10.06
21/04/1998	10.11	22/04/1998	15.33	23/04/1998	11.78
24/04/1998	11.83	25/04/1998	11.72	26/04/1998	10.33
27/04/1998	9.11	28/04/1998	9.44	29/04/1998	11.61
30/04/1998	10.56	01/05/1998	8.89	02/05/1998	10.78

Date	Temperature	Date	Temperature	Date"	Temperature
03/05/1998	9.11	04/05/1998	10	05/05/1998	11.28
06/05/1998	13.22	07/05/1998	13.17	08/05/1998	16
09/05/1998	17.78	10/05/1998	16.94	11/05/1998	15.56
12/05/1998	15.33	13/05/1998	17.89	14/05/1998	19.78
15/05/1998	18.72	16/05/1998	17.22	17/05/1998	15.89
18/05/1998	16.11	19/05/1998	17.39	20/05/1998	18.67
21/05/1998	15.56	22/05/1998	13.22	23/05/1998	13.78
24/05/1998	14.44	25/05/1998	14.44	26/05/1998	12.44
27/05/1998	9.44	28/05/1998	12.67	29/05/1998	14.78
30/05/1998	16.11	31/05/1998	15.5	01/06/1998	15.28
02/06/1998	15.5	03/06/1998	14.89	04/06/1998	13.22
05/06/1998	14.28	06/06/1998	17.61	07/06/1998	15.56
08/06/1998	14.39	09/06/1998	16.61	10/06/1998	13.72
11/06/1998	10.5	12/06/1998	12.17	13/06/1998	12.5
14/06/1998	14.11	15/06/1998	13.72	16/06/1998	14.83
17/06/1998	13.78	18/06/1998	15.56	19/06/1998	19.39
20/06/1998	22.11	21/06/1998	20.5	22/06/1998	16.44
23/06/1998	16.44	24/06/1998	18.22	25/06/1998	15.61
26/06/1998	14.67	27/06/1998	15.17	28/06/1998	16.22
29/06/1998	14.89	30/06/1998	16.22	01/07/1998	16.17
02/07/1998	14.06	03/07/1998	15	04/07/1998	15.78
05/07/1998	18.11	06/07/1998	16.83	07/07/1998	16.17
08/07/1998	15.78	09/07/1998	18.11	10/07/1998	17.83
11/07/1998	15.89	12/07/1998	17.22	13/07/1998	15.39
14/07/1998	15.39	15/07/1998	16	16/07/1998	17.06
17/07/1998	16.94	18/07/1998	16.61	19/07/1998	18
20/07/1998	20	21/07/1998	17.83	22/07/1998	17.39
23/07/1998	18.11	24/07/1998	17.06	25/07/1998	17.56
26/07/1998	16.61	27/07/1998	17.11	28/07/1998	17.06
29/07/1998	17.39	30/07/1998	16.72	31/07/1998	17.06
01/08/1998	15.89	02/08/1998	16.17	03/08/1998	15.72
04/08/1998	18.56	05/08/1998	19.39	06/08/1998	19
07/08/1998	20.22	08/08/1998	22.17	09/08/1998	20.44
10/08/1998	22.94	11/08/1998	23.5	12/08/1998	18.94
13/08/1998	16.89	14/08/1998	19.89	15/08/1998	18.61
16/08/1998	20.61	17/08/1998	19.17	18/08/1998	18.44
19/08/1998	18.11	20/08/1998	17.22	21/08/1998	18.78
22/08/1998	16	23/08/1998	14.61	24/08/1998	15.28
25/08/1998	15.89	26/08/1998	15.56	27/08/1998	14.67
28/08/1998	14.44	29/08/1998	16.39	30/08/1998	17.39
31/08/1998	16.83	01/09/1998	20	02/09/1998	18.17
03/09/1998	17.72	04/09/1998	16.28	05/09/1998	16.78
06/09/1998	17	07/09/1998	18.89	08/09/1998	18.33
09/09/1998	18.39	10/09/1998	16.44	11/09/1998	14
12/09/1998	10.22	13/09/1998	11.22	14/09/1998	12.89
15/09/1998	13.72	16/09/1998	13.56	17/09/1998	14.06
18/09/1998	16.83	19/09/1998	18.61	20/09/1998	16.56
21/09/1998	17.28	22/09/1998	15.78	23/09/1998	16.06
24/09/1998	16.83	25/09/1998	17.56	26/09/1998	17.28
27/09/1998	15.83	28/09/1998	16.17	29/09/1998	14.89
30/09/1998	15.39	01/10/1998	14.5	02/10/1998	11.67

Date	Temperature	Date	Temperature	Date"	Temperature
03/10/1998	9	04/10/1998	10.06	05/10/1998	9.89
06/10/1998	10.89	07/10/1998	11.22	08/10/1998	10.89
09/10/1998	11.89	10/10/1998	12.5	11/10/1998	13.11
12/10/1998	12.11	13/10/1998	13.44	14/10/1998	15.56
15/10/1998	11.33	16/10/1998	12.56	17/10/1998	11.89
18/10/1998	7.44	19/10/1998	7.94	20/10/1998	9.78
21/10/1998	15.61	22/10/1998	16.56	23/10/1998	15.22
24/10/1998	10.78	25/10/1998	10.44	26/10/1998	8.33
27/10/1998	13.94	28/10/1998	12.61	29/10/1998	9.33
30/10/1998	8.61	31/10/1998	8.28	01/11/1998	7.22
02/11/1998	7.94	03/11/1998	7.83	04/11/1998	4.83
05/11/1998	6.72	06/11/1998	9.22	07/11/1998	9.78
08/11/1998	12.28	09/11/1998	14.17	10/11/1998	9.5
11/11/1998	6.33	12/11/1998	8.67	13/11/1998	7.44
14/11/1998	6.33	15/11/1998	5.94	16/11/1998	3.83
17/11/1998	2.67	18/11/1998	4.17	19/11/1998	5.33
20/11/1998	3.39	21/11/1998	3.22	22/11/1998	2.61
23/11/1998	3.06	24/11/1998	6.33	25/11/1998	5.83
26/11/1998	6.67	27/11/1998	7.89	28/11/1998	9.33
29/11/1998	4.78	30/11/1998	4.83	01/12/1998	4.39
02/12/1998	3.33	03/12/1998	2	04/12/1998	2.94
05/12/1998	1.17	06/12/1998	0.06	07/12/1998	3.11
08/12/1998	8.22	09/12/1998	10	10/12/1998	9.11
11/12/1998	7.72	12/12/1998	12.61	13/12/1998	9.83
14/12/1998	13.28	15/12/1998	11.89	16/12/1998	8.39
17/12/1998	8.06	18/12/1998	9.06	19/12/1998	5.89
20/12/1998	3.06	21/12/1998	0.78	22/12/1998	5.5
23/12/1998	7.83	24/12/1998	8.89	25/12/1998	8.61
26/12/1998	6.5	27/12/1998	5.78	28/12/1998	8.89
29/12/1998	7.56	30/12/1998	7.06	31/12/1998	11.78
01/01/1999	12.33	02/01/1999	12	03/01/1999	6.33
04/01/1999	4.61	05/01/1999	3.33	06/01/1999	1.28
07/01/1999	2.39	08/01/1999	5.22	09/01/1999	6.5
10/01/1999	9.44	11/01/1999	7.89	12/01/1999	5.67
13/01/1999	7.11	14/01/1999	11.33	15/01/1999	11.06
16/01/1999	5.5	17/01/1999	-0.33	18/01/1999	5.44
19/01/1999	8.28	20/01/1999	10.28	21/01/1999	6.06
22/01/1999	5.72	23/01/1999	8.89	24/01/1999	5.17
25/01/1999	4.11	26/01/1999	4.61	27/01/1999	7.61
28/01/1999	7.5	29/01/1999	7.61	30/01/1999	10.61
31/01/1999	8.06	01/02/1999	7.28	02/02/1999	3.17
03/02/1999	1.28	04/02/1999	0.39	05/02/1999	1.17
06/02/1999	1.89	07/02/1999	4.56	08/02/1999	3.83
09/02/1999	2.67	10/02/1999	5.94	11/02/1999	7
12/02/1999	6.67	13/02/1999	10	14/02/1999	11
15/02/1999	7.56	16/02/1999	8	17/02/1999	4.94
18/02/1999	4.56	19/02/1999	4.22	20/02/1999	4.72
21/02/1999	8.89	22/02/1999	8.11	23/02/1999	8.17
24/02/1999	11.83	25/02/1999	11.78	26/02/1999	8.17
27/02/1999	5.72	28/02/1999	4.28	01/03/1999	3.78

Date	Temperature	Date	Temperature	Date	Temperature
02/03/1999	4.33	03/03/1999	5.67	04/03/1999	5.5
05/03/1999	3	06/03/1999	4.89	07/03/1999	10.28
08/03/1999	10.67	09/03/1999	8.39	10/03/1999	9
11/03/1999	9.72	12/03/1999	12.83	13/03/1999	9.67
14/03/1999	7.78	15/03/1999	7.39	16/03/1999	8.5
17/03/1999	7.83	18/03/1999	11.11	19/03/1999	9.78
20/03/1999	9.28	21/03/1999	7.28	22/03/1999	7.83
23/03/1999	9	24/03/1999	11.61	25/03/1999	11.33
26/03/1999	13.78	27/03/1999	14.17	28/03/1999	12.78
29/03/1999	10.39	30/03/1999	12.89	31/03/1999	13.17
01/04/1999	12.83	02/04/1999	10.17	03/04/1999	11.44
04/04/1999	12.44	05/04/1999	10.78	06/04/1999	9.22
07/04/1999	9.39	08/04/1999	6.44	09/04/1999	4.39
10/04/1999	5.5	11/04/1999	5.83	12/04/1999	6.83
13/04/1999	6.67	14/04/1999	6.67	15/04/1999	9.33
16/04/1999	11.44	17/04/1999	10.78	18/04/1999	10.06
19/04/1999	11.72	20/04/1999	11.22	21/04/1999	13.06
22/04/1999	13.78	23/04/1999	12.78	24/04/1999	11.56
25/04/1999	13.06	26/04/1999	14.5	27/04/1999	14.72
28/04/1999	15.22	29/04/1999	13.72	30/04/1999	12.78
01/05/1999	13.67	02/05/1999	12.94	03/05/1999	12.83
04/05/1999	16.22	05/05/1999	14.83	06/05/1999	14.56
07/05/1999	13.5	08/05/1999	12.78	09/05/1999	13.56
10/05/1999	12	11/05/1999	11.78	12/05/1999	11.67
13/05/1999	12.56	14/05/1999	15.72	15/05/1999	16
16/05/1999	14.83	17/05/1999	12.89	18/05/1999	14.83
19/05/1999	14.78	20/05/1999	13.56	21/05/1999	15.28
22/05/1999	19.06	23/05/1999	17.61	24/05/1999	18.39
25/05/1999	13.11	26/05/1999	13.28	27/05/1999	16.72
28/05/1999	15.67	29/05/1999	14.39	30/05/1999	13.94
31/05/1999	11.94	01/06/1999	13.33	02/06/1999	12.72
03/06/1999	12.5	04/06/1999	13.56	05/06/1999	13.83
06/06/1999	14.39	07/06/1999	13.67	08/06/1999	15.44
09/06/1999	17.56	10/06/1999	18.94	11/06/1999	19.89
12/06/1999	17.28	13/06/1999	17.5	14/06/1999	16.78
15/06/1999	16.17	16/06/1999	13.28	17/06/1999	13.89
18/06/1999	16.94	19/06/1999	17.61	20/06/1999	16.89
21/06/1999	18.78	22/06/1999	16.11	23/06/1999	14.39
24/06/1999	15.78	25/06/1999	16.11	26/06/1999	17
27/06/1999	19.89	28/06/1999	19.61	29/06/1999	17.83
30/06/1999	18.5	01/07/1999	19.56	02/07/1999	20.33
03/07/1999	22.11	04/07/1999	20.72	05/07/1999	20
06/07/1999	20.61	07/07/1999	19.39	08/07/1999	18.56
09/07/1999	16	10/07/1999	16.33	11/07/1999	17.56
12/07/1999	20.33	13/07/1999	21.17	14/07/1999	20.44
15/07/1999	19.33	16/07/1999	16.83	17/07/1999	14.67
18/07/1999	18.06	19/07/1999	22.33	20/07/1999	21.78
21/07/1999	17.61	22/07/1999	17	23/07/1999	18.94
24/07/1999	19.89	25/07/1999	22.5	26/07/1999	23.67
27/07/1999	24.28	28/07/1999	24.39	29/07/1999	20.06
30/07/1999	20.83	31/07/1999	20.5	01/08/1999	21.22

Date	Temperature	Date	Temperature	Date	Temperature
02/08/1999	19	03/08/1999	18.06	04/08/1999	17.94
05/08/1999	15.56	06/08/1999	16.11	07/08/1999	17.17
08/08/1999	17.78	09/08/1999	17.22	10/08/1999	15.89
11/08/1999	13.61	12/08/1999	13.83	13/08/1999	14.89
14/08/1999	15.83	15/08/1999	15.28	16/08/1999	14.61
17/08/1999	14.67	18/08/1999	16.89	19/08/1999	16.39
20/08/1999	19.39	21/08/1999	19.17	22/08/1999	17.44
23/08/1999	18.5	24/08/1999	18.72	25/08/1999	18.33
26/08/1999	18.22	27/08/1999	19.11	28/08/1999	20.33
29/08/1999	20.22	30/08/1999	20	31/08/1999	20
01/09/1999	20.17	02/09/1999	18.78	03/09/1999	18
04/09/1999	17.28	05/09/1999	18.11	06/09/1999	21.94
07/09/1999	17.89	08/09/1999	14.5	09/09/1999	13
10/09/1999	12.83	11/09/1999	14.67	12/09/1999	14.89
13/09/1999	15.39	14/09/1999	16.44	15/09/1999	15.33
16/09/1999	15.83	17/09/1999	16.44	18/09/1999	16.67
19/09/1999	16.72	20/09/1999	15.94	21/09/1999	14.33
22/09/1999	15.17	23/09/1999	14.83	24/09/1999	15.72
25/09/1999	14.61	26/09/1999	14.22	27/09/1999	12.61
28/09/1999	10.61	29/09/1999	9.67	30/09/1999	8.61
01/10/1999	8.78	02/10/1999	10.94	03/10/1999	14.44
04/10/1999	15.5	05/10/1999	16.11	06/10/1999	12.67
07/10/1999	9.83	08/10/1999	10.28	09/10/1999	10.56
10/10/1999	12.78	11/10/1999	11.67	12/10/1999	10.67
13/10/1999	9.89	14/10/1999	9.61	15/10/1999	8.89
16/10/1999	10.11	17/10/1999	13.33	18/10/1999	12.67
19/10/1999	11.67	20/10/1999	11.72	21/10/1999	11.11
22/10/1999	10.89	23/10/1999	12.61	24/10/1999	10.72
25/10/1999	14.17	26/10/1999	13	27/10/1999	14.17
28/10/1999	10.56	29/10/1999	10.61	30/10/1999	10.94
31/10/1999	10.5	01/11/1999	8.61	02/11/1999	8

Date	Temperature	Date	Temperature	Date	Temperature
03/11/1999	10.78	04/11/1999	10.44	05/11/1999	9.39
06/11/1999	8.83	07/11/1999	8.11	08/11/1999	8.39
09/11/1999	9.22	10/11/1999	7.5	11/11/1999	5.94
12/11/1999	3.89	13/11/1999	4.17	14/11/1999	4.83
15/11/1999	4.89	16/11/1999	4.72	17/11/1999	5.28
18/11/1999	7.67	19/11/1999	11.61	20/11/1999	12.11
21/11/1999	10.72	22/11/1999	8.72	23/11/1999	11.83
24/11/1999	8.89	25/11/1999	7.17	26/11/1999	10.56
27/11/1999	7.5	28/11/1999	9.06	29/11/1999	4.67
30/11/1999	4	01/12/1999	10.89	02/12/1999	8.94
03/12/1999	8.17	04/12/1999	7.17	05/12/1999	5.94
06/12/1999	10.28	07/12/1999	7.39	08/12/1999	4.17
09/12/1999	2.06	10/12/1999	2.5	11/12/1999	3.83
12/12/1999	8.33	13/12/1999	3.44	14/12/1999	-0.06
15/12/1999	-1.61	16/12/1999	3.67	17/12/1999	8.11
18/12/1999	8.11	19/12/1999	10.78	20/12/1999	5.83
21/12/1999	5.39	22/12/1999	3.22	23/12/1999	2.94
24/12/1999	2.17	25/12/1999	4.11	26/12/1999	5.89
27/12/1999	7.94	28/12/1999	8.5	29/12/1999	9.17
30/12/1999	5.72	31/12/1999	6.5	01/01/2000	8.83
02/01/2000	7.89	03/01/2000	7.28	04/01/2000	2.89
05/01/2000	2.89	06/01/2000	8.11	07/01/2000	7.28
08/01/2000	3.89	09/01/2000	3.56	10/01/2000	4.72
11/01/2000	3.89	12/01/2000	4.56	13/01/2000	5.44
14/01/2000	5.78	15/01/2000	2.11	16/01/2000	5.44
17/01/2000	5	18/01/2000	3.94	19/01/2000	3
20/01/2000	1.11	21/01/2000	2.5	22/01/2000	0.56
23/01/2000	5	24/01/2000	11	25/01/2000	11.44
26/01/2000	11.06	27/01/2000	9.67	28/01/2000	8.17
29/01/2000	6.33	30/01/2000	9.28	31/01/2000	8.78
01/02/2000	10.33	02/02/2000	7.72	03/02/2000	9.28
04/02/2000	7.33	05/02/2000	6.94	06/02/2000	5.28
07/02/2000	7.33	08/02/2000	6.94	09/02/2000	4.89
10/02/2000	6.5	11/02/2000	4.44	12/02/2000	5.33
13/02/2000	8.72	14/02/2000	6.44	15/02/2000	3.89
16/02/2000	6.11	17/02/2000	4.78	18/02/2000	9.5
19/02/2000	9.67	20/02/2000	5.83	21/02/2000	6
22/02/2000	10.56	23/02/2000	7.94	24/02/2000	7.78
25/02/2000	5.67	26/02/2000	6.89	27/02/2000	8.44
28/02/2000	4.17	29/02/2000	5.11	01/03/2000	8.72
02/03/2000	11.39	03/03/2000	12.5	04/03/2000	13.17
05/03/2000	11.28	06/03/2000	10.33	07/03/2000	8.78
08/03/2000	10.17	09/03/2000	9.94	10/03/2000	7.78
11/03/2000	8.94	12/03/2000	9.56	13/03/2000	8.5
14/03/2000	7.22	15/03/2000	7.56	16/03/2000	8.28
17/03/2000	9.17	18/03/2000	10.72	19/03/2000	10.39
20/03/2000	7.44	21/03/2000	6.28	22/03/2000	6.17
23/03/2000	5.56	24/03/2000	5.67	25/03/2000	6.44
26/03/2000	6.94	27/03/2000	7	28/03/2000	10.17
29/03/2000	7.11	30/03/2000	3.22	31/03/2000	5.67

Date	Temperature	Date	Temperature	Date	Temperature
01/04/2000	5.83	02/04/2000	8.17	03/04/2000	9.78
04/04/2000	9.89	05/04/2000	7.83	06/04/2000	5.33
07/04/2000	3.89	08/04/2000	5.56	09/04/2000	6.72
10/04/2000	4.39	11/04/2000	6.83	12/04/2000	8.33
13/04/2000	9.39	14/04/2000	11.17	15/04/2000	12.33
16/04/2000	11.89	17/04/2000	11.44	18/04/2000	9.83
19/04/2000	10.44	20/04/2000	12.06	21/04/2000	11.5
22/04/2000	11.67	23/04/2000	11.72	24/04/2000	13.61
25/04/2000	11.83	26/04/2000	12.06	27/04/2000	10.94
28/04/2000	9.72	29/04/2000	9.78	30/04/2000	13
01/05/2000	16.33	02/05/2000	18.33	03/05/2000	14.56
04/05/2000	17.11	05/05/2000	14.94	06/05/2000	13.39
07/05/2000	14.39	08/05/2000	18.17	09/05/2000	19.67
10/05/2000	21.06	11/05/2000	17.56	12/05/2000	12.44
13/05/2000	11.11	14/05/2000	11.44	15/05/2000	11.17
16/05/2000	11.72	17/05/2000	13.78	18/05/2000	12.78
19/05/2000	12.17	20/05/2000	12.39	21/05/2000	11.11
22/05/2000	10.28	23/05/2000	10.28	24/05/2000	11.89
25/05/2000	12.22	26/05/2000	13.22	27/05/2000	14.17
28/05/2000	15.44	29/05/2000	17.33	30/05/2000	15.44
31/05/2000	13.61	01/06/2000	14.06	02/06/2000	14.78
03/06/2000	17.78	04/06/2000	16.22	05/06/2000	14.33
06/06/2000	15.28	07/06/2000	18.5	08/06/2000	18.06
09/06/2000	17.94	10/06/2000	17.56	11/06/2000	18.17
12/06/2000	20.33	13/06/2000	23.33	14/06/2000	24.5
15/06/2000	18.17	16/06/2000	16.83	17/06/2000	15.39
18/06/2000	15.17	19/06/2000	12.39	20/06/2000	14.44
21/06/2000	15.72	22/06/2000	17.06	23/06/2000	16.72
24/06/2000	16.89	25/06/2000	16.06	26/06/2000	17.11
27/06/2000	17.5	28/06/2000	18.61	29/06/2000	16.28
30/06/2000	15.17	01/07/2000	17.22	02/07/2000	15.33
03/07/2000	14.56	04/07/2000	15.5	05/07/2000	13.28
06/07/2000	12.72	07/07/2000	13.72	08/07/2000	16.17
09/07/2000	14.06	10/07/2000	14.11	11/07/2000	13.94
12/07/2000	16.61	13/07/2000	18.11	14/07/2000	19.28
15/07/2000	19.56	16/07/2000	19.39	17/07/2000	16.67
18/07/2000	15.78	19/07/2000	14.5	20/07/2000	15.83
21/07/2000	18.22	22/07/2000	19.11	23/07/2000	17.44
24/07/2000	18.44	25/07/2000	19.28	26/07/2000	20.44
27/07/2000	19.22	28/07/2000	17.28	29/07/2000	16.28
30/07/2000	17.72	31/07/2000	18.39	01/08/2000	20.39
02/08/2000	20	03/08/2000	19.33	04/08/2000	18.56
05/08/2000	19.89	06/08/2000	19.78	07/08/2000	20.44
08/08/2000	18.83	09/08/2000	19.78	10/08/2000	18.67
11/08/2000	18.67	12/08/2000	17.22	13/08/2000	16.78
14/08/2000	18.28	15/08/2000	17.44	16/08/2000	16
17/08/2000	16.89	18/08/2000	18.22	19/08/2000	19.89
20/08/2000	20.17	21/08/2000	18.72	22/08/2000	16.39
23/08/2000	15.78	24/08/2000	16.22	25/08/2000	16.83
26/08/2000	16.17	27/08/2000	14.94	28/08/2000	15.39
29/08/2000	14	30/08/2000	13.89	31/08/2000	15.5

Date	Temperature	Date	Temperature	Date	Temperature
01/09/2000	16.44	02/09/2000	15.22	03/09/2000	18.28
04/09/2000	18.56	05/09/2000	20.33	06/09/2000	21.61
07/09/2000	18.89	08/09/2000	17.11	09/09/2000	17
10/09/2000	16.22	11/09/2000	15.39	12/09/2000	15.56
13/09/2000	14.44	14/09/2000	13.61	15/09/2000	13.5
16/09/2000	13.61	17/09/2000	18.28	18/09/2000	19.11
19/09/2000	14.89	20/09/2000	13.61	21/09/2000	17.11
22/09/2000	14.72	23/09/2000	14.94	24/09/2000	15.33
25/09/2000	14.61	26/09/2000	13	27/09/2000	12.33
28/09/2000	13.67	29/09/2000	13.83	30/09/2000	11.67
01/10/2000	10.44	02/10/2000	10.94	03/10/2000	12.44
04/10/2000	9.5	05/10/2000	9.39	06/10/2000	9.78
07/10/2000	10.94	08/10/2000	11	09/10/2000	11.44
10/10/2000	12.22	11/10/2000	11.5	12/10/2000	10.33
13/10/2000	13.83	14/10/2000	11.17	15/10/2000	11
16/10/2000	10.78	17/10/2000	11.33	18/10/2000	13.17
19/10/2000	11.56	20/10/2000	12.89	21/10/2000	10.28
22/10/2000	13	23/10/2000	13.11	24/10/2000	10.5
25/10/2000	10.67	26/10/2000	10.11	27/10/2000	9.11
28/10/2000	7.94	29/10/2000	7.61	30/10/2000	6.72
31/10/2000	7.39	01/11/2000	9.22	02/11/2000	8.61
03/11/2000	7.83	04/11/2000	7.83	05/11/2000	7.67
06/11/2000	10.94	07/11/2000	8.56	08/11/2000	5.94
09/11/2000	4.44	10/11/2000	3.33	11/11/2000	8
12/11/2000	4.89	13/11/2000	8.33	14/11/2000	8.33
15/11/2000	4.83	16/11/2000	6.06	17/11/2000	8.89
18/11/2000	6.94	19/11/2000	6.5	20/11/2000	10.06
21/11/2000	8.39	22/11/2000	8.61	23/11/2000	14.11
24/11/2000	12.39	25/11/2000	9.83	26/11/2000	11.83
27/11/2000	10.28	28/11/2000	8.11	29/11/2000	11.56
30/11/2000	12.44	01/12/2000	11.56	02/12/2000	9.83
03/12/2000	10.67	04/12/2000	9.44	05/12/2000	10.5
06/12/2000	13.22	07/12/2000	13.33	08/12/2000	10.22
09/12/2000	6.33	10/12/2000	4.33	11/12/2000	2.44
12/12/2000	3.94	13/12/2000	6.39	14/12/2000	8.5
15/12/2000	8.89	16/12/2000	6.28	17/12/2000	4.83
18/12/2000	4.72	19/12/2000	5.67	20/12/2000	3.94
21/12/2000	1.89	22/12/2000	1.83	23/12/2000	-0.28
24/12/2000	-2.61	25/12/2000	-0.94	26/12/2000	0.89
27/12/2000	9.5	28/12/2000	9.61	29/12/2000	6.89
30/12/2000	8.94	31/12/2000	7	01/01/2001	5.72
02/01/2001	4.61	03/01/2001	4.56	04/01/2001	3.22
05/01/2001	5.17	06/01/2001	4.67	07/01/2001	5.61
08/01/2001	4.28	09/01/2001	4.17	10/01/2001	2.5
11/01/2001	0.67	12/01/2001	0.44	13/01/2001	-0.06
14/01/2001	-0.28	15/01/2001	-0.39	16/01/2001	2
17/01/2001	6.61	18/01/2001	8.89	19/01/2001	8.61
20/01/2001	6	21/01/2001	5.22	22/01/2001	3.78
23/01/2001	2.33	24/01/2001	2.17	25/01/2001	3.67
26/01/2001	4.5	27/01/2001	1.5	28/01/2001	5.89
29/01/2001	7.44	30/01/2001	7.89	31/01/2001	9.17

Date	Temperature	Date	Temperature	Date	Temperature
01/02/2001	10.06	02/02/2001	9.39	03/02/2001	5.67
04/02/2001	3.67	05/02/2001	6.39	06/02/2001	12.28
07/02/2001	9.94	08/02/2001	6	09/02/2001	5.33
10/02/2001	4.72	11/02/2001	5	12/02/2001	4.28
13/02/2001	3.83	14/02/2001	3.33	15/02/2001	4.33
16/02/2001	8.72	17/02/2001	8.39	18/02/2001	5.33
19/02/2001	2.94	20/02/2001	1.83	21/02/2001	3.67
22/02/2001	3.83	23/02/2001	2.89	24/02/2001	1.89
25/02/2001	0.11	26/02/2001	1.56	27/02/2001	2.06
28/02/2001	1.83	01/03/2001	6.78	02/03/2001	11.89
03/03/2001	9	04/03/2001	9.94	05/03/2001	11.56
06/03/2001	11.06	07/03/2001	6.39	08/03/2001	6.72
09/03/2001	7	10/03/2001	7.78	11/03/2001	7.67
12/03/2001	4.28	13/03/2001	3.22	14/03/2001	3.67
15/03/2001	3.22	16/03/2001	4.56	17/03/2001	8.89
18/03/2001	9.61	19/03/2001	8.56	20/03/2001	5.83
21/03/2001	5.06	22/03/2001	6.61	23/03/2001	7.89
24/03/2001	7.67	25/03/2001	8.17	26/03/2001	11.39
27/03/2001	12.17	28/03/2001	13.17	29/03/2001	9.78
30/03/2001	8.39	31/03/2001	8.17	01/04/2001	11
02/04/2001	7.89	03/04/2001	7.83	04/04/2001	11.94
05/04/2001	10.11	06/04/2001	8.78	07/04/2001	9.72
08/04/2001	7.11	09/04/2001	7.22	10/04/2001	9.78
11/04/2001	7.22	12/04/2001	6.72	13/04/2001	5.78
14/04/2001	4.89	15/04/2001	5.67	16/04/2001	6.89
17/04/2001	7.5	18/04/2001	9.22	19/04/2001	8.67
20/04/2001	9.22	21/04/2001	10.06	22/04/2001	10.5
23/04/2001	10.06	24/04/2001	8.61	25/04/2001	10.11
26/04/2001	8.61	27/04/2001	9.5	28/04/2001	11
29/04/2001	9.56	30/04/2001	8.5	01/05/2001	8.39
02/05/2001	10.22	03/05/2001	11.28	04/05/2001	11.83
05/05/2001	16.83	06/05/2001	19.11	07/05/2001	18.17
08/05/2001	17.61	09/05/2001	13.06	10/05/2001	14.22
11/05/2001	12.72	12/05/2001	8.78	13/05/2001	11.61
14/05/2001	12.72	15/05/2001	14.83	16/05/2001	13.83
17/05/2001	14.44	18/05/2001	15.83	19/05/2001	16.72
20/05/2001	14.94	21/05/2001	17.28	22/05/2001	17.22
23/05/2001	19	24/05/2001	17.5	25/05/2001	17.5
26/05/2001	14.83	27/05/2001	14.67	28/05/2001	13.78
29/05/2001	12	30/05/2001	14.56	31/05/2001	15.94
01/06/2001	15.17	02/06/2001	13.11	03/06/2001	11.78
04/06/2001	11.78	05/06/2001	11.5	06/06/2001	13.56
07/06/2001	15.11	08/06/2001	16.61	09/06/2001	15.44
10/06/2001	16.17	11/06/2001	14.89	12/06/2001	13.44
13/06/2001	14.33	14/06/2001	16.83	15/06/2001	17.89
16/06/2001	16.78	17/06/2001	16.44	18/06/2001	17
19/06/2001	20.17	20/06/2001	22.39	21/06/2001	24.28
22/06/2001	19.94	23/06/2001	18.44	24/06/2001	18.56
25/06/2001	19.11	26/06/2001	20.06	27/06/2001	22.72
28/06/2001	23.22	29/06/2001	24.06	30/06/2001	23.56

Date	Temperature	Date	Temperature	Date	Temperature
01/07/2001	21.28	02/07/2001	18.72	03/07/2001	17.83
04/07/2001	16.89	05/07/2001	16.72	06/07/2001	16.61
07/07/2001	16.06	08/07/2001	15.39	09/07/2001	14.61
10/07/2001	15.17	11/07/2001	16.61	12/07/2001	15.44
13/07/2001	16.39	14/07/2001	14.89	15/07/2001	15.61
16/07/2001	18.22	17/07/2001	17.44	18/07/2001	19.5
19/07/2001	18.44	20/07/2001	20.22	21/07/2001	21.44
22/07/2001	23.56	23/07/2001	24.28	24/07/2001	25.33
25/07/2001	23.56	26/07/2001	21.61	27/07/2001	20.56
28/07/2001	17	29/07/2001	17.56	30/07/2001	16.39
31/07/2001	17.56	01/08/2001	18.78	02/08/2001	17.44
03/08/2001	17.06	04/08/2001	14	05/08/2001	15.22
06/08/2001	16.17	07/08/2001	17.94	08/08/2001	20.5
09/08/2001	21.5	10/08/2001	22.94	11/08/2001	18.61
12/08/2001	17.89	13/08/2001	19.06	14/08/2001	18.06
15/08/2001	18.28	16/08/2001	18.22	17/08/2001	20.72
18/08/2001	21.28	19/08/2001	22.78	20/08/2001	23.06
21/08/2001	19.39	22/08/2001	17.67	23/08/2001	17.06
24/08/2001	16.94	25/08/2001	17.22	26/08/2001	14.67
27/08/2001	15.83	28/08/2001	18.28	29/08/2001	16.06
30/08/2001	14.44	31/08/2001	14.67	01/09/2001	16.22
02/09/2001	16.22	03/09/2001	15.61	04/09/2001	12.39
05/09/2001	12.78	06/09/2001	15.39	07/09/2001	15.11
08/09/2001	13	09/09/2001	14.17	10/09/2001	14.22
11/09/2001	13.11	12/09/2001	11.44	13/09/2001	13.11
14/09/2001	13.17	15/09/2001	13.94	16/09/2001	12.72
17/09/2001	12.56	18/09/2001	12.39	19/09/2001	13.22
20/09/2001	12.06	21/09/2001	12.89	22/09/2001	16.44
23/09/2001	17.61	24/09/2001	16.5	25/09/2001	15.5
26/09/2001	16.5	27/09/2001	15.11	28/09/2001	14.72
29/09/2001	14.72	30/09/2001	16.39	01/10/2001	15.22
02/10/2001	13.39	03/10/2001	13	04/10/2001	13.17
05/10/2001	13.33	06/10/2001	15.83	07/10/2001	15.94
08/10/2001	18.06	09/10/2001	16.33	10/10/2001	15.17
11/10/2001	12.56	12/10/2001	14.94	13/10/2001	15.11
14/10/2001	14.17	15/10/2001	15.94	16/10/2001	12
17/10/2001	11.94	18/10/2001	14.94	19/10/2001	13.39
20/10/2001	13.78	21/10/2001	14.67	22/10/2001	13.06
23/10/2001	12.17	24/10/2001	12.06	25/10/2001	15
26/10/2001	11.06	27/10/2001	8.44	28/10/2001	8.78
29/10/2001	7.83	30/10/2001	9.11	31/10/2001	7.89
01/11/2001	11.83	02/11/2001	11.61	03/11/2001	6.28
04/11/2001	3.61	05/11/2001	4.61	06/11/2001	10.17
07/11/2001	9.72	08/11/2001	5.89	09/11/2001	4.17
10/11/2001	4.5	11/11/2001	9.39	12/11/2001	9.5
13/11/2001	8.22	14/11/2001	7.72	15/11/2001	7.56
16/11/2001	10.56	17/11/2001	9.56	18/11/2001	3.89
19/11/2001	10.17	20/11/2001	10.44	21/11/2001	4.72
22/11/2001	5.67	23/11/2001	6.78	24/11/2001	12.44
25/11/2001	13.94	26/11/2001	10.5	27/11/2001	4.89
28/11/2001	7.06	29/11/2001	9.33	30/11/2001	9.44

Date	Temperature	Date	Temperature	Date	Temperature
01/12/2001	6.5	02/12/2001	7.44	03/12/2001	3.94
04/12/2001	4.11	05/12/2001	4.5	06/12/2001	3
07/12/2001	5.5	08/12/2001	6.56	09/12/2001	1.94
10/12/2001	2.56	11/12/2001	4.33	12/12/2001	3.61
13/12/2001	4.39	14/12/2001	2.89	15/12/2001	2.56
16/12/2001	4.33	17/12/2001	0.94	18/12/2001	0.06
19/12/2001	6.5	20/12/2001	4.94	21/12/2001	0.78
22/12/2001	5.94	23/12/2001	6.5	24/12/2001	1.28
25/12/2001	1.44	26/12/2001	0.17	27/12/2001	-1.28
28/12/2001	-0.11	29/12/2001	0.11	30/12/2001	0
31/12/2001	7.22	01/01/2002	7.22	02/01/2002	5.06
03/01/2002	3.83	04/01/2002	3.56	05/01/2002	5.83
06/01/2002	2.56	07/01/2002	6.06	08/01/2002	9.44
09/01/2002	9.78	10/01/2002	7.33	11/01/2002	5.17
12/01/2002	8.39	13/01/2002	5.06	14/01/2002	7.67
15/01/2002	10.61	16/01/2002	11.33	17/01/2002	9.06
18/01/2002	9.83	19/01/2002	8.83	20/01/2002	6.72
21/01/2002	10.56	22/01/2002	10.61	23/01/2002	11.17
24/01/2002	11	25/01/2002	11.11	26/01/2002	8.72
27/01/2002	11.39	28/01/2002	12.5	29/01/2002	9.39
30/01/2002	8.44	31/01/2002	10.17	01/02/2002	6.89
02/02/2002	6.39	03/02/2002	11.67	04/02/2002	10.67
05/02/2002	9.28	06/02/2002	12.78	07/02/2002	11.44
08/02/2002	8	09/02/2002	5.22	10/02/2002	3.94
11/02/2002	5.06	12/02/2002	3.17	13/02/2002	6.39
14/02/2002	9.11	15/02/2002	8.72	16/02/2002	4.67
17/02/2002	10.06	18/02/2002	5.28	19/02/2002	5.28
20/02/2002	10.72	21/02/2002	9.5	22/02/2002	5.28
23/02/2002	6.17	24/02/2002	3.5	25/02/2002	4.39
26/02/2002	7.33	27/02/2002	7.67	28/02/2002	7.56
01/03/2002	9.44	02/03/2002	11.56	03/03/2002	10.39
04/03/2002	7.5	05/03/2002	7.89	06/03/2002	9.78
07/03/2002	9.22	08/03/2002	6.11	09/03/2002	5.17
10/03/2002	6.61	11/03/2002	10.11	12/03/2002	10.5
13/03/2002	9.28	14/03/2002	9.89	15/03/2002	11.67
16/03/2002	12.33	17/03/2002	11.72	18/03/2002	8.89
19/03/2002	7.78	20/03/2002	9.61	21/03/2002	8.89
22/03/2002	7.11	23/03/2002	8.06	24/03/2002	9.83
25/03/2002	10.83	26/03/2002	10.11	27/03/2002	11.72
28/03/2002	13.06	29/03/2002	15.06	30/03/2002	12.44
31/03/2002	11	01/04/2002	8.78	02/04/2002	8.28
03/04/2002	9.06	04/04/2002	7	05/04/2002	8.61
06/04/2002	8.61	07/04/2002	8.17	08/04/2002	7.17
09/04/2002	7.17	10/04/2002	9.22	11/04/2002	9.72
12/04/2002	10.06	13/04/2002	8.78	14/04/2002	9.78
15/04/2002	11.06	16/04/2002	13.67	17/04/2002	14.39
18/04/2002	15.39	19/04/2002	14.67	20/04/2002	13.44
21/04/2002	10.28	22/04/2002	9.72	23/04/2002	10.39
24/04/2002	9.94	25/04/2002	9.67	26/04/2002	10.39
27/04/2002	10	28/04/2002	10.22	29/04/2002	9.44
30/04/2002	8.61	01/05/2002	11.33	02/05/2002	11.83

Date	Temperature	Date	Temperature	Date	Temperature
03/05/2002	10.72	04/05/2002	11	05/05/2002	13.61
06/05/2002	14	07/05/2002	12.56	08/05/2002	12.17
09/05/2002	13.56	10/05/2002	14.56	11/05/2002	17.67
12/05/2002	17.56	13/05/2002	14.72	14/05/2002	15.44
15/05/2002	15.67	16/05/2002	14.83	17/05/2002	14.72
18/05/2002	14.17	19/05/2002	13.17	20/05/2002	12.72
21/05/2002	10.28	22/05/2002	11.89	23/05/2002	12.28
24/05/2002	13.17	25/05/2002	12.89	26/05/2002	14.72
27/05/2002	16.17	28/05/2002	19.56	29/05/2002	15.28
30/05/2002	12.72	31/05/2002	12.61	01/06/2002	15.61
02/06/2002	13.94	03/06/2002	14.56	04/06/2002	13.33
05/06/2002	13.11	06/06/2002	13.39	07/06/2002	14.22
08/06/2002	14.94	09/06/2002	18.5	10/06/2002	16.5
11/06/2002	17.5	12/06/2002	20.72	13/06/2002	16.5
14/06/2002	16.11	15/06/2002	16.44	16/06/2002	16
17/06/2002	17.39	18/06/2002	14.94	19/06/2002	14.39
20/06/2002	14.72	21/06/2002	15.17	22/06/2002	14.61
23/06/2002	13.67	24/06/2002	13.94	25/06/2002	15.11
26/06/2002	15.44	27/06/2002	16.06	28/06/2002	16.28
29/06/2002	16.72	30/06/2002	16.5	01/07/2002	14.72
02/07/2002	15	03/07/2002	14.61	04/07/2002	17.22
05/07/2002	19.11	06/07/2002	20.56	07/07/2002	20.83
08/07/2002	17.56	09/07/2002	18.22	10/07/2002	18.33
11/07/2002	17.83	12/07/2002	15.78	13/07/2002	16.94
14/07/2002	17.78	15/07/2002	17.61	16/07/2002	17.67
17/07/2002	21.11	18/07/2002	20.72	19/07/2002	23.39
20/07/2002	24.17	21/07/2002	21.94	22/07/2002	18.39
23/07/2002	16.78	24/07/2002	17.78	25/07/2002	16.83
26/07/2002	16.17	27/07/2002	16.78	28/07/2002	19.39
29/07/2002	19.94	30/07/2002	16.67	31/07/2002	16.22
01/08/2002	16.83	02/08/2002	16.78	03/08/2002	18.22
04/08/2002	19.17	05/08/2002	20.5	06/08/2002	22.11
07/08/2002	21.11	08/08/2002	22.5	09/08/2002	21.28
10/08/2002	21	11/08/2002	19.11	12/08/2002	18.61
13/08/2002	18.56	14/08/2002	18.44	15/08/2002	19.06
16/08/2002	17.72	17/08/2002	15.17	18/08/2002	17.56
19/08/2002	18.61	20/08/2002	18.33	21/08/2002	19.61
22/08/2002	16.83	23/08/2002	15.22	24/08/2002	16.83
25/08/2002	18.5	26/08/2002	16.89	27/08/2002	17.39
28/08/2002	18.17	29/08/2002	16.17	30/08/2002	14.89
31/08/2002	13.94	01/09/2002	15.5	02/09/2002	16.56
03/09/2002	18.67	04/09/2002	18.72	05/09/2002	16.28
06/09/2002	15.83	07/09/2002	14.61	08/09/2002	15.56
09/09/2002	15.28	10/09/2002	16	11/09/2002	16.17
12/09/2002	15.39	13/09/2002	13.94	14/09/2002	13.94
15/09/2002	12.94	16/09/2002	13.61	17/09/2002	14.06
18/09/2002	13.56	19/09/2002	13.89	20/09/2002	14.83
21/09/2002	15.28	22/09/2002	15.78	23/09/2002	16.61
24/09/2002	15.72	25/09/2002	12.94	26/09/2002	13.94
27/09/2002	14.89	28/09/2002	13.56	29/09/2002	12.72
30/09/2002	11.78	01/10/2002	13.28	02/10/2002	11.78

Date	Temperature	Date	Temperature	Date	Temperature
03/10/2002	11.22	04/10/2002	8.56	05/10/2002	10.83
06/10/2002	11.22	07/10/2002	9.78	08/10/2002	7.33
09/10/2002	6.06	10/10/2002	6.44	11/10/2002	7.39
12/10/2002	13.06	13/10/2002	14.44	14/10/2002	9
15/10/2002	8.22	16/10/2002	12.67	17/10/2002	12.06
18/10/2002	12.67	19/10/2002	9.72	20/10/2002	11.94
21/10/2002	10.72	22/10/2002	12	23/10/2002	13.56
24/10/2002	13.28	25/10/2002	11.72	26/10/2002	10
27/10/2002	12	28/10/2002	11.89	29/10/2002	7.5
30/10/2002	9.94	31/10/2002	9.72	01/11/2002	11.28
02/11/2002	10.22	03/11/2002	10.83	04/11/2002	10.22
05/11/2002	10.44	06/11/2002	10.11	07/11/2002	8.33
08/11/2002	8.11	09/11/2002	5	10/11/2002	7.5
11/11/2002	9.11	12/11/2002	10.17	13/11/2002	9.28
14/11/2002	9.22	15/11/2002	7.72	16/11/2002	6.83
17/11/2002	7.83	18/11/2002	9.61	19/11/2002	10.44
20/11/2002	8.33	21/11/2002	9.22	22/11/2002	10.67
23/11/2002	9.22	24/11/2002	8.17	25/11/2002	7.56
26/11/2002	6.5	27/11/2002	7.06	28/11/2002	5.17
29/11/2002	3.78	30/11/2002	3.61	01/12/2002	2.11
02/12/2002	3.11	03/12/2002	3.83	04/12/2002	6.11
05/12/2002	6.94	06/12/2002	6.72	07/12/2002	6.06
08/12/2002	4.61	09/12/2002	3.61	10/12/2002	3.22
11/12/2002	4.67	12/12/2002	7.33	13/12/2002	11.22
14/12/2002	10.89	15/12/2002	12.06	16/12/2002	10.22
17/12/2002	10.94	18/12/2002	11.39	19/12/2002	8.11
20/12/2002	10.22	21/12/2002	10.06	22/12/2002	4.78
23/12/2002	9.56	24/12/2002	9.22	25/12/2002	5.72
26/12/2002	2	27/12/2002	0.83	28/12/2002	1.28
29/12/2002	-0.39	30/12/2002	-0.78	31/12/2002	0.83
01/01/2003	3.11	02/01/2003	0.28	03/01/2003	-0.06
04/01/2003	8.28	05/01/2003	9.22	06/01/2003	8.56
07/01/2003	6.61	08/01/2003	6.83	09/01/2003	5.67
10/01/2003	7.61	11/01/2003	8.56	12/01/2003	8.06
13/01/2003	7.22	14/01/2003	6.11	15/01/2003	5.5
16/01/2003	9.22	17/01/2003	9.39	18/01/2003	9.94
19/01/2003	6.39	20/01/2003	5.11	21/01/2003	1.5
22/01/2003	0.22	23/01/2003	3.44	24/01/2003	5.39
25/01/2003	4.28	26/01/2003	2.33	27/01/2003	1.78
28/01/2003	2.5	29/01/2003	8.61	30/01/2003	9.44
31/01/2003	7.72	01/02/2003	5.78	02/02/2003	6.06
03/02/2003	6.17	04/02/2003	1.94	05/02/2003	1.33
06/02/2003	1.83	07/02/2003	1.94	08/02/2003	1.22
09/02/2003	0.89	10/02/2003	1.22	11/02/2003	4.39
12/02/2003	5.78	13/02/2003	4.39	14/02/2003	8.67
15/02/2003	8.17	16/02/2003	7.72	17/02/2003	9.11
18/02/2003	9.61	19/02/2003	9.11	20/02/2003	8.56
21/02/2003	7.72	22/02/2003	5.78	23/02/2003	10.11
24/02/2003	10.61	25/02/2003	7.39	26/02/2003	7.11
27/02/2003	8.72	28/02/2003	11	01/03/2003	10.39

Date	Temperature	Date	Temperature	Date	Temperature
02/03/2003	10.28	03/03/2003	7.17	04/03/2003	5.83
05/03/2003	6	06/03/2003	5.94	07/03/2003	7.17
08/03/2003	7.67	09/03/2003	6.94	10/03/2003	7.61
11/03/2003	7.83	12/03/2003	6.61	13/03/2003	6.61
14/03/2003	9.94	15/03/2003	11.33	16/03/2003	11.61
17/03/2003	11.11	18/03/2003	10.61	19/03/2003	9.28
20/03/2003	12.22	21/03/2003	11.67	22/03/2003	9.39
23/03/2003	7.83	24/03/2003	7.44	25/03/2003	8.67
26/03/2003	12.44	27/03/2003	11.33	28/03/2003	8.44
29/03/2003	4.83	30/03/2003	4.33	31/03/2003	3.78
01/04/2003	4.67	02/04/2003	5.44	03/04/2003	8.06
04/04/2003	12.56	05/04/2003	14.83	06/04/2003	16.56
07/04/2003	17.17	08/04/2003	16.28	09/04/2003	14.67
10/04/2003	7.56	11/04/2003	10.06	12/04/2003	11.94
13/04/2003	11.61	14/04/2003	12.28	15/04/2003	11.89
16/04/2003	13.56	17/04/2003	11.28	18/04/2003	13.28
19/04/2003	12.5	20/04/2003	12.89	21/04/2003	12.39
22/04/2003	12.06	23/04/2003	11.06	24/04/2003	11.89
25/04/2003	15.61	26/04/2003	14	27/04/2003	12
28/04/2003	12.89	29/04/2003	12.5	30/04/2003	12.89
01/05/2003	10.67	02/05/2003	10.78	03/05/2003	10.06
04/05/2003	8.11	05/05/2003	10	06/05/2003	11.22
07/05/2003	10.5	08/05/2003	12.78	09/05/2003	13.39
10/05/2003	12.5	11/05/2003	11.06	12/05/2003	13.22
13/05/2003	14.94	14/05/2003	14.06	15/05/2003	12.83
16/05/2003	13.28	17/05/2003	14.28	18/05/2003	14.61
19/05/2003	18.5	20/05/2003	18.94	21/05/2003	20.67
22/05/2003	22.28	23/05/2003	17.83	24/05/2003	17.56
25/05/2003	16.89	26/05/2003	16.39	27/05/2003	16
28/05/2003	15.28	29/05/2003	18.22	30/05/2003	15.22
31/05/2003	15.78	01/06/2003	17.89	02/06/2003	17.44
03/06/2003	17.06	04/06/2003	17.56	05/06/2003	19.94
06/06/2003	20.11	07/06/2003	21.44	08/06/2003	19.78
09/06/2003	17.78	10/06/2003	19.39	11/06/2003	17.39
12/06/2003	18.39	13/06/2003	20.06	14/06/2003	18.72
15/06/2003	17.83	16/06/2003	18	17/06/2003	19.11
18/06/2003	18.28	19/06/2003	16.67	20/06/2003	19.44
21/06/2003	17.5	22/06/2003	16.5	23/06/2003	16.5
24/06/2003	16.17	25/06/2003	17.11	26/06/2003	16.56
27/06/2003	18.39	28/06/2003	17.67	29/06/2003	19.39
30/06/2003	22.39	01/07/2003	22.67	02/07/2003	19.78
03/07/2003	20.06	04/07/2003	21.33	05/07/2003	22.83
06/07/2003	25.28	07/07/2003	21.17	08/07/2003	18.39
09/07/2003	19.67	10/07/2003	21.72	11/07/2003	19.83
12/07/2003	19.39	13/07/2003	19.28	14/07/2003	18.83
15/07/2003	18.5	16/07/2003	17	17/07/2003	16.39
18/07/2003	18.17	19/07/2003	17.94	20/07/2003	18.17
21/07/2003	19.67	22/07/2003	18.22	23/07/2003	17.5
24/07/2003	19.22	25/07/2003	21.67	26/07/2003	24
27/07/2003	24.67	28/07/2003	27.39	29/07/2003	23.72
30/07/2003	24.61	31/07/2003	26.78	01/08/2003	28.33

Date	Temperature	Date	Temperature	Date	Temperature
02/08/2003	26.39	03/08/2003	23.89	04/08/2003	22.83
05/08/2003	20.06	06/08/2003	19.06	07/08/2003	18.39
08/08/2003	20.5	09/08/2003	19.89	10/08/2003	17.44
11/08/2003	17.39	12/08/2003	18.78	13/08/2003	21.28
14/08/2003	22.22	15/08/2003	21.39	16/08/2003	18.56
17/08/2003	19.11	18/08/2003	19.11	19/08/2003	16.06
20/08/2003	14.61	21/08/2003	14.22	22/08/2003	14.33
23/08/2003	15.61	24/08/2003	16.28	25/08/2003	18.22
26/08/2003	17.67	27/08/2003	19.17	28/08/2003	16.72
29/08/2003	14.39	30/08/2003	16.5	31/08/2003	15.78
01/09/2003	16.28	02/09/2003	15.61	03/09/2003	16.78
04/09/2003	16.94	05/09/2003	18.33	06/09/2003	18.39
07/09/2003	19	08/09/2003	19.67	09/09/2003	17.22
10/09/2003	17.28	11/09/2003	18.72	12/09/2003	20
13/09/2003	15.28	14/09/2003	11	15/09/2003	10.94
16/09/2003	13	17/09/2003	13.78	18/09/2003	13.94
19/09/2003	12.5	20/09/2003	12.22	21/09/2003	15.06
22/09/2003	14.56	23/09/2003	14.39	24/09/2003	15.39
25/09/2003	10.5	26/09/2003	8.44	27/09/2003	12.44
28/09/2003	11.5	29/09/2003	13.67	30/09/2003	15.11
01/10/2003	15.94	02/10/2003	12.89	03/10/2003	12.22
04/10/2003	13.11	05/10/2003	13	06/10/2003	11.61
07/10/2003	11.11	08/10/2003	10.06	09/10/2003	9.61
10/10/2003	9.94	11/10/2003	8.22	12/10/2003	6.22
13/10/2003	7.39	14/10/2003	7.22	15/10/2003	5.61
16/10/2003	6.11	17/10/2003	7.33	18/10/2003	6.22
19/10/2003	6.33	20/10/2003	7.94	21/10/2003	7.28
22/10/2003	9.33	23/10/2003	8.72	24/10/2003	11.28
25/10/2003	11.28	26/10/2003	10.67	27/10/2003	12.33
28/10/2003	12.61	29/10/2003	10.28	30/10/2003	8.5
31/10/2003	7.89	01/11/2003	10.94	02/11/2003	9.44
03/11/2003	11.06	04/11/2003	10.17	05/11/2003	11.72
06/11/2003	10	07/11/2003	7.06	08/11/2003	8.83
09/11/2003	13.67	10/11/2003	13.44	11/11/2003	11.94
12/11/2003	9.5	13/11/2003	7.83	14/11/2003	6.89
15/11/2003	6.83	16/11/2003	8.83	17/11/2003	9.11
18/11/2003	4.22	19/11/2003	6.17	20/11/2003	9.5
21/11/2003	8.39	22/11/2003	9.28	23/11/2003	8.72
24/11/2003	8.5	25/11/2003	8.94	26/11/2003	7.83
27/11/2003	6.33	28/11/2003	3.78	29/11/2003	3.22
30/11/2003	6.72	01/12/2003	3.33	02/12/2003	9.33
03/12/2003	8.72	04/12/2003	12.5	05/12/2003	7.94
06/12/2003	3.94	07/12/2003	2.17	08/12/2003	3.89
09/12/2003	4.5	10/12/2003	6	11/12/2003	8.11
12/12/2003	5.28	13/12/2003	1.61	14/12/2003	6.17
15/12/2003	9.61	16/12/2003	10.17	17/12/2003	9.61
18/12/2003	5.89	19/12/2003	3.89	20/12/2003	2.61
21/12/2003	3.28	22/12/2003	2.22	23/12/2003	5.94
24/12/2003	4.28	25/12/2003	1.17	26/12/2003	6.33
27/12/2003	7.94	28/12/2003	10.17	29/12/2003	8.83
30/12/2003	9.06	31/12/2003	6.11	01/01/2004	9.33

Date	Temperature	Date	Temperature	Date	Temperature
02/01/2004	8.78	03/01/2004	6.72	04/01/2004	8.39
05/01/2004	4.78	06/01/2004	5.56	07/01/2004	6.83
08/01/2004	3.28	09/01/2004	3.56	10/01/2004	8.67
11/01/2004	9.78	12/01/2004	8.56	13/01/2004	7.56
14/01/2004	7.5	15/01/2004	6.5	16/01/2004	3.33
17/01/2004	4.22	18/01/2004	3.11	19/01/2004	1.28
20/01/2004	0.61	21/01/2004	4.5	22/01/2004	10.39
23/01/2004	10.78	24/01/2004	12.28	25/01/2004	13.89
26/01/2004	13.78	27/01/2004	12	28/01/2004	9.56
29/01/2004	7.06	30/01/2004	5.83	31/01/2004	2.17
01/02/2004	5.22	02/02/2004	9.89	03/02/2004	9.22
04/02/2004	8.56	05/02/2004	7.39	06/02/2004	7.22
07/02/2004	6.61	08/02/2004	6	09/02/2004	6.11
10/02/2004	4.89	11/02/2004	2.39	12/02/2004	3.5
13/02/2004	4	14/02/2004	2.28	15/02/2004	2.44
16/02/2004	1.5	17/02/2004	0.5	18/02/2004	0.78
19/02/2004	1.39	20/02/2004	1.89	21/02/2004	2
22/02/2004	2.22	23/02/2004	5	24/02/2004	8.22
25/02/2004	7.11	26/02/2004	6.17	27/02/2004	5.17
28/02/2004	5.78	29/02/2004	5.06	01/03/2004	2.89
02/03/2004	3.17	03/03/2004	3.61	04/03/2004	8
05/03/2004	9.78	06/03/2004	11	07/03/2004	13.28
08/03/2004	11.06	09/03/2004	9.78	10/03/2004	9.5
11/03/2004	11.11	12/03/2004	8.78	13/03/2004	6.44
14/03/2004	5.44	15/03/2004	5.67	16/03/2004	4.5
17/03/2004	5.72	18/03/2004	6.89	19/03/2004	8.28
20/03/2004	9.06	21/03/2004	9.67	22/03/2004	12.11
23/03/2004	12.61	24/03/2004	11.61	25/03/2004	10.78
26/03/2004	9.39	27/03/2004	8.28	28/03/2004	6.06
29/03/2004	6.78	30/03/2004	6.39	31/03/2004	7.72
01/04/2004	9.11	02/04/2004	7.44	03/04/2004	10.5
04/04/2004	10.89	05/04/2004	10.61	06/04/2004	10.44
07/04/2004	13.67	08/04/2004	10.72	09/04/2004	7.67
10/04/2004	7.39	11/04/2004	8.67	12/04/2004	12.44
13/04/2004	11.56	14/04/2004	13.33	15/04/2004	15.28
16/04/2004	15	17/04/2004	15.22	18/04/2004	13.78
19/04/2004	11.44	20/04/2004	8.83	21/04/2004	10
22/04/2004	11	23/04/2004	13	24/04/2004	10.61
25/04/2004	8.39	26/04/2004	9.17	27/04/2004	10.89
28/04/2004	12	29/04/2004	11.11	30/04/2004	13.17
01/05/2004	15.28	02/05/2004	12.72	03/05/2004	10.61
04/05/2004	13.11	05/05/2004	14.83	06/05/2004	16.56
07/05/2004	17	08/05/2004	18.33	09/05/2004	18.06
10/05/2004	18.17	11/05/2004	16.83	12/05/2004	11.78
13/05/2004	10.94	14/05/2004	13.06	15/05/2004	15.17
16/05/2004	15.56	17/05/2004	13.89	18/05/2004	12.78
19/05/2004	14.61	20/05/2004	16.5	21/05/2004	14.72
22/05/2004	14.89	23/05/2004	14.56	24/05/2004	15.94
25/05/2004	16.56	26/05/2004	19	27/05/2004	17.67
28/05/2004	19.39	29/05/2004	21.06	30/05/2004	21.94
31/05/2004	19.11	01/06/2004	19	02/06/2004	17.11

Date	Temperature	Date	Temperature	Date	Temperature
03/06/2004	16.67	04/06/2004	19.44	05/06/2004	22.06
06/06/2004	20.78	07/06/2004	19.89	08/06/2004	17
09/06/2004	15.17	10/06/2004	12.5	11/06/2004	12.33
12/06/2004	13.44	13/06/2004	15.28	14/06/2004	14.78
15/06/2004	15.06	16/06/2004	15.56	17/06/2004	15.22
18/06/2004	17.22	19/06/2004	15.61	20/06/2004	17.67
21/06/2004	17.11	22/06/2004	15.61	23/06/2004	14.56
24/06/2004	15.5	25/06/2004	15.06	26/06/2004	16.06
27/06/2004	17.5	28/06/2004	15.72	29/06/2004	15.06
30/06/2004	14.61	01/07/2004	14.22	02/07/2004	14.61
03/07/2004	15.56	04/07/2004	16.06	05/07/2004	17.28
06/07/2004	19.83	07/07/2004	19.28	08/07/2004	19.22
09/07/2004	18.06	10/07/2004	17.22	11/07/2004	19.06
12/07/2004	19.22	13/07/2004	20.44	14/07/2004	20.39
15/07/2004	18.56	16/07/2004	17.33	17/07/2004	18.33
18/07/2004	19.06	19/07/2004	20.78	20/07/2004	22.33
21/07/2004	21.11	22/07/2004	21.83	23/07/2004	21.33
24/07/2004	21.33	25/07/2004	20.72	26/07/2004	22.06
27/07/2004	21.06	28/07/2004	21.39	29/07/2004	21.94
30/07/2004	24.5	31/07/2004	21.06	01/08/2004	20.39
02/08/2004	20.11	03/08/2004	19.39	04/08/2004	18.17
05/08/2004	19.56	06/08/2004	19.28	07/08/2004	18.06
08/08/2004	19.11	09/08/2004	18.78	10/08/2004	17.78
11/08/2004	17.06	12/08/2004	15.61	13/08/2004	17.11
14/08/2004	17.11	15/08/2004	17.22	16/08/2004	16.33
17/08/2004	17.17	18/08/2004	17.22	19/08/2004	16.11
20/08/2004	15.06	21/08/2004	15.61	22/08/2004	15.22
23/08/2004	15.78	24/08/2004	18.22	25/08/2004	19.5
26/08/2004	20	27/08/2004	21.11	28/08/2004	19.89
29/08/2004	19.39	30/08/2004	18.17	31/08/2004	19.61
01/09/2004	18.17	02/09/2004	18.17	03/09/2004	15.17
04/09/2004	15.61	05/09/2004	14.5	06/09/2004	13.56
07/09/2004	13.39	08/09/2004	16.22	09/09/2004	16.67
10/09/2004	13.33	11/09/2004	15.39	12/09/2004	13.17
13/09/2004	15.61	14/09/2004	16.33	15/09/2004	11.61
16/09/2004	11.33	17/09/2004	14.67	18/09/2004	16.61
19/09/2004	15.67	20/09/2004	14.39	21/09/2004	15.56
22/09/2004	13.22	23/09/2004	13	24/09/2004	13.44
25/09/2004	14.39	26/09/2004	12.28	27/09/2004	11.56
28/09/2004	11.22	29/09/2004	11.06	30/09/2004	11.22
01/10/2004	12	02/10/2004	11.44	03/10/2004	12.44
04/10/2004	12.11	05/10/2004	10.44	06/10/2004	9
07/10/2004	8.89	08/10/2004	9.44	09/10/2004	10.17
10/10/2004	10.56	11/10/2004	14.78	12/10/2004	12.33
13/10/2004	14.28	14/10/2004	15.61	15/10/2004	15.11
16/10/2004	11.83	17/10/2004	9.56	18/10/2004	9.5
19/10/2004	13.28	20/10/2004	12.28	21/10/2004	12.89
22/10/2004	11.56	23/10/2004	10.72	24/10/2004	10.67
25/10/2004	11.67	26/10/2004	11	27/10/2004	8
28/10/2004	10.11	29/10/2004	11.28	30/10/2004	10.83
31/10/2004	9.17	01/11/2004	7.89	02/11/2004	8.06

Date	Temperature	Date	Temperature	Date	Temperature
03/11/2004	9.94	04/11/2004	4.72	05/11/2004	4.17
06/11/2004	7.33	07/11/2004	10.78	08/11/2004	12.22
09/11/2004	9.44	10/11/2004	3.28	11/11/2004	2.22
12/11/2004	7.17	13/11/2004	12.11	14/11/2004	11.06
15/11/2004	10.11	16/11/2004	9.06	17/11/2004	10.5
18/11/2004	8.61	19/11/2004	7.33	20/11/2004	6.39
21/11/2004	5.61	22/11/2004	4.72	23/11/2004	4.5
24/11/2004	3.94	25/11/2004	7.5	26/11/2004	9.22
27/11/2004	9.5	28/11/2004	7.11	29/11/2004	8.5
30/11/2004	5.61	01/12/2004	5.22	02/12/2004	3.94
03/12/2004	5.56	04/12/2004	1.94	05/12/2004	7.5
06/12/2004	10.61	07/12/2004	9.39	08/12/2004	6.39
09/12/2004	5.39	10/12/2004	4.17	11/12/2004	2.89
12/12/2004	2.61	13/12/2004	8.33	14/12/2004	11.28
15/12/2004	8.83	16/12/2004	2.61	17/12/2004	0.5
18/12/2004	2.11	19/12/2004	4.94	20/12/2004	5.83
21/12/2004	10.39	22/12/2004	10.22	23/12/2004	8.83
24/12/2004	5.39	25/12/2004	7.83	26/12/2004	9.33
27/12/2004	5.94	28/12/2004	8.33	29/12/2004	12.67
30/12/2004	8.78	31/12/2004	9.33	01/01/2005	11.44
02/01/2005	9.83	03/01/2005	7.28	04/01/2005	5.44
05/01/2005	5.11	06/01/2005	7.5	07/01/2005	7.44
08/01/2005	8.39	09/01/2005	5.06	10/01/2005	7.06
11/01/2005	11.39	12/01/2005	7.39	13/01/2005	3.78
14/01/2005	3.44	15/01/2005	3.11	16/01/2005	3.61
17/01/2005	2.28	18/01/2005	5.78	19/01/2005	6.33
20/01/2005	6.22	21/01/2005	6.94	22/01/2005	7.67
23/01/2005	8.67	24/01/2005	7.22	25/01/2005	7.72
26/01/2005	8.28	27/01/2005	6.22	28/01/2005	6.61
29/01/2005	4.72	30/01/2005	6.06	31/01/2005	8
01/02/2005	10.33	02/02/2005	8.5	03/02/2005	10.56
04/02/2005	5.44	05/02/2005	4.39	06/02/2005	3.94
07/02/2005	3.22	08/02/2005	3.61	09/02/2005	6.39
10/02/2005	4.17	11/02/2005	2	12/02/2005	2.61
13/02/2005	1.83	14/02/2005	1.44	15/02/2005	1.67
16/02/2005	1.17	17/02/2005	2.78	18/02/2005	0.89
19/02/2005	0	20/02/2005	2.94	21/02/2005	2.39
22/02/2005	0.72	23/02/2005	1.39	24/02/2005	3
25/02/2005	1.72	26/02/2005	3.61	27/02/2005	6.28
28/02/2005	6.39	01/03/2005	6.06	02/03/2005	6.94
03/03/2005	5.22	04/03/2005	3.72	05/03/2005	5.44
06/03/2005	9.11	07/03/2005	13.39	08/03/2005	13.78
09/03/2005	13.17	10/03/2005	12.89	11/03/2005	10.61
12/03/2005	11.78	13/03/2005	12.78	14/03/2005	12.33
15/03/2005	12.39	16/03/2005	12	17/03/2005	10.83
18/03/2005	9.11	19/03/2005	10.44	20/03/2005	7.89
21/03/2005	9.89	22/03/2005	9.83	23/03/2005	11.17
24/03/2005	12.78	25/03/2005	13	26/03/2005	10.44
27/03/2005	8.28	28/03/2005	10.06	29/03/2005	8.61
30/03/2005	4.94	31/03/2005	5.72	01/04/2005	10.94

Date	Temperature	Date	Temperature	Date	Temperature
02/04/2005	11.61	03/04/2005	10.83	04/04/2005	9.5
05/04/2005	8.83	06/04/2005	6.67	07/04/2005	6.94
08/04/2005	8	09/04/2005	11.17	10/04/2005	9.22
11/04/2005	8.56	12/04/2005	9.94	13/04/2005	11.39
14/04/2005	11.22	15/04/2005	11.78	16/04/2005	10.22
17/04/2005	11.17	18/04/2005	10.61	19/04/2005	12.28
20/04/2005	14.17	21/04/2005	16.56	22/04/2005	18.61
23/04/2005	16.33	24/04/2005	13.94	25/04/2005	10.56
26/04/2005	11.39	27/04/2005	13.33	28/04/2005	11.56
29/04/2005	9.5	30/04/2005	9	01/05/2005	8.5
02/05/2005	8.33	03/05/2005	10.33	04/05/2005	11.56
05/05/2005	10.17	06/05/2005	11.28	07/05/2005	10.83
08/05/2005	9	09/05/2005	10.61	10/05/2005	12.72
11/05/2005	14.44	12/05/2005	12.5	13/05/2005	13.06
14/05/2005	12.39	15/05/2005	13.22	16/05/2005	16.28
17/05/2005	19.17	18/05/2005	22.72	19/05/2005	17.06
20/05/2005	13.39	21/05/2005	14.61	22/05/2005	14.94
23/05/2005	14.22	24/05/2005	15.5	25/05/2005	14.94
26/05/2005	15.11	27/05/2005	14.89	28/05/2005	13.61
29/05/2005	12.5	30/05/2005	15.06	31/05/2005	16.61
01/06/2005	15.67	02/06/2005	12.5	03/06/2005	14.17
04/06/2005	13.61	05/06/2005	14.83	06/06/2005	15.39
07/06/2005	17.28	08/06/2005	21.5	09/06/2005	23.72
10/06/2005	25.83	11/06/2005	23.11	12/06/2005	20.72
13/06/2005	22.28	14/06/2005	24.56	15/06/2005	21.22
16/06/2005	17.44	17/06/2005	16.17	18/06/2005	19.06
19/06/2005	18.83	20/06/2005	19.22	21/06/2005	16.61
22/06/2005	17	23/06/2005	18.56	24/06/2005	16.89
25/06/2005	14.5	26/06/2005	14.11	27/06/2005	16
28/06/2005	15.39	29/06/2005	16.61	30/06/2005	17.28
01/07/2005	22.17	02/07/2005	22.94	03/07/2005	20.56
04/07/2005	22.61	05/07/2005	24.17	06/07/2005	21.72
07/07/2005	19.94	08/07/2005	21.78	09/07/2005	19.17
10/07/2005	17.83	11/07/2005	19.44	12/07/2005	17.56
13/07/2005	17.11	14/07/2005	19	15/07/2005	17.33
16/07/2005	16	17/07/2005	16.61	18/07/2005	14.33
19/07/2005	19.33	20/07/2005	18.39	21/07/2005	16.61
22/07/2005	16.67	23/07/2005	17.06	24/07/2005	18.61
25/07/2005	18.83	26/07/2005	17.78	27/07/2005	17.44
28/07/2005	15.89	29/07/2005	16.33	30/07/2005	17.33
31/07/2005	19.28	01/08/2005	19.17	02/08/2005	19.94
03/08/2005	17.61	04/08/2005	16.5	05/08/2005	16.06
06/08/2005	17.56	07/08/2005	18.89	08/08/2005	20.17
09/08/2005	21.89	10/08/2005	16.78	11/08/2005	17
12/08/2005	19.11	13/08/2005	16.39	14/08/2005	16.78
15/08/2005	15.06	16/08/2005	14.61	17/08/2005	14.78
18/08/2005	17.11	19/08/2005	18	20/08/2005	19.5
21/08/2005	21.22	22/08/2005	23.78	23/08/2005	20.06
24/08/2005	18.78	25/08/2005	19.5	26/08/2005	22.11
27/08/2005	19.72	28/08/2005	18.67	29/08/2005	19.06
30/08/2005	19.06	31/08/2005	18.67	01/09/2005	19.72

Date	Temperature	Date	Temperature	Date	Temperature
02/09/2005	16.33	03/09/2005	17.28	04/09/2005	17.67
05/09/2005	19.33	06/09/2005	17.33	07/09/2005	12.39
08/09/2005	11.33	09/09/2005	13.28	10/09/2005	15.78
11/09/2005	16.28	12/09/2005	16.83	13/09/2005	15.83
14/09/2005	15.06	15/09/2005	13.33	16/09/2005	16.33
17/09/2005	15.11	18/09/2005	16	19/09/2005	12.61
20/09/2005	12.83	21/09/2005	16.56	22/09/2005	13.06
23/09/2005	11.56	24/09/2005	11.33	25/09/2005	12.78
26/09/2005	13.28	27/09/2005	14.83	28/09/2005	15.83
29/09/2005	15.28	30/09/2005	11.61	01/10/2005	16.11
02/10/2005	18.56	03/10/2005	17.44	04/10/2005	14.17
05/10/2005	14.28	06/10/2005	16.33	07/10/2005	14.22
08/10/2005	13.67	09/10/2005	11.11	10/10/2005	11.94
11/10/2005	11.78	12/10/2005	13.28	13/10/2005	12.33
14/10/2005	10.5	15/10/2005	14.78	16/10/2005	14.78
17/10/2005	15	18/10/2005	16.72	19/10/2005	15.22
20/10/2005	13.94	21/10/2005	16.22	22/10/2005	13.11
23/10/2005	10.83	24/10/2005	14.78	25/10/2005	14.28
26/10/2005	9.83	27/10/2005	9.28	28/10/2005	12.78
29/10/2005	10.39	30/10/2005	13.5	31/10/2005	7.61
01/11/2005	11.17	02/11/2005	12.78	03/11/2005	7.67
04/11/2005	5.5	05/11/2005	4.33	06/11/2005	8.61
07/11/2005	5.5	08/11/2005	2.22	09/11/2005	1.56
10/11/2005	1.17	11/11/2005	0.61	12/11/2005	1.72
13/11/2005	4.28	14/11/2005	2.78	15/11/2005	4.22
16/11/2005	0.33	17/11/2005	3.5	18/11/2005	3.06
19/11/2005	2.83	20/11/2005	2.33	21/11/2005	3.33
22/11/2005	8.06	23/11/2005	7.89	24/11/2005	7.61
25/11/2005	5.72	26/11/2005	6.33	27/11/2005	3.83
28/11/2005	3.22	29/11/2005	5.44	30/11/2005	1.72
01/12/2005	3.11	02/12/2005	1.11	03/12/2005	4.56
04/12/2005	5	05/12/2005	6.56	06/12/2005	8.11
07/12/2005	8.5	08/12/2005	1.56	09/12/2005	0.44
10/12/2005	5.56	11/12/2005	3	12/12/2005	7.83
13/12/2005	8.06	14/12/2005	8.5	15/12/2005	7.22
16/12/2005	3.06	17/12/2005	3.17	18/12/2005	0.33
19/12/2005	-0.78	20/12/2005	-1	21/12/2005	4.11
22/12/2005	5.83	23/12/2005	6.28	24/12/2005	5.83
25/12/2005	7.28	26/12/2005	4.89	27/12/2005	2.39
28/12/2005	2.61	29/12/2005	1.06	30/12/2005	3.5
31/12/2005	4.89	01/01/2006	6.28	02/01/2006	7.39
03/01/2006	2.56	04/01/2006	6.67	05/01/2006	7.56
06/01/2006	7.22	07/01/2006	7	08/01/2006	7.56
09/01/2006	9.33	10/01/2006	9.44	11/01/2006	8.06
12/01/2006	5.56	13/01/2006	2.22	14/01/2006	1.72
15/01/2006	-0.5	16/01/2006	1.11	17/01/2006	2.44
18/01/2006	2.39	19/01/2006	1.89	20/01/2006	2.61
21/01/2006	4.56	22/01/2006	3.28	23/01/2006	0.56
24/01/2006	-1.33	25/01/2006	-0.61	26/01/2006	3.11
27/01/2006	4	28/01/2006	5.39	29/01/2006	7.5
30/01/2006	5.67	31/01/2006	2.56	01/02/2006	1.83

Date	Temperature	Date	Temperature	Date	Temperature
02/02/2006	1.33	03/02/2006	5.94	04/02/2006	8.5
05/02/2006	7.5	06/02/2006	8.78	07/02/2006	6.22
08/02/2006	6.5	09/02/2006	3.94	10/02/2006	4.78
11/02/2006	4.33	12/02/2006	2.72	13/02/2006	2.44
14/02/2006	1.28	15/02/2006	1.44	16/02/2006	3.11
17/02/2006	3	18/02/2006	3.5	19/02/2006	2.5
20/02/2006	-0.11	21/02/2006	0.5	22/02/2006	0.67
23/02/2006	0	24/02/2006	2.72	25/02/2006	3.56
26/02/2006	3.5	27/02/2006	9.33	28/02/2006	8.06
01/03/2006	5.44	02/03/2006	3.06	03/03/2006	0.89
04/03/2006	1.44	05/03/2006	3.61	06/03/2006	4.78
07/03/2006	1.5	08/03/2006	2.33	09/03/2006	2.61
10/03/2006	4.5	11/03/2006	3.72	12/03/2006	3.11
13/03/2006	2.56	14/03/2006	4.33	15/03/2006	9.06
16/03/2006	10.67	17/03/2006	12.11	18/03/2006	10.89
19/03/2006	9.11	20/03/2006	9.06	21/03/2006	11.5
22/03/2006	11.78	23/03/2006	10.33	24/03/2006	9.44
25/03/2006	8	26/03/2006	4.72	27/03/2006	4.89
28/03/2006	6.78	29/03/2006	7.22	30/03/2006	7.67
31/03/2006	4.5	01/04/2006	5.28	02/04/2006	5.28
03/04/2006	8.39	04/04/2006	11.56	05/04/2006	10.33
06/04/2006	10	07/04/2006	11.17	08/04/2006	9.72
09/04/2006	9.67	10/04/2006	10.39	11/04/2006	10.67
12/04/2006	12.5	13/04/2006	11.33	14/04/2006	10.11
15/04/2006	10.39	16/04/2006	10.78	17/04/2006	11.83
18/04/2006	12.61	19/04/2006	10	20/04/2006	9.44
21/04/2006	8.28	22/04/2006	10.39	23/04/2006	10.44
24/04/2006	13.44	25/04/2006	18.94	26/04/2006	15.39
27/04/2006	10.83	28/04/2006	13.11	29/04/2006	11.89
30/04/2006	13.17	01/05/2006	12.72	02/05/2006	15.83
03/05/2006	16.44	04/05/2006	13.5	05/05/2006	12.33
06/05/2006	13.28	07/05/2006	12.78	08/05/2006	12.89
09/05/2006	14	10/05/2006	12.72	11/05/2006	12.56
12/05/2006	11.61	13/05/2006	11.44	14/05/2006	9.83
15/05/2006	10.72	16/05/2006	13.22	17/05/2006	15.33
18/05/2006	14.61	19/05/2006	13.39	20/05/2006	10.44
21/05/2006	9.33	22/05/2006	10.5	23/05/2006	11.39
24/05/2006	14.33	25/05/2006	16.5	26/05/2006	16.44
27/05/2006	15.22	28/05/2006	14.72	29/05/2006	17.89
30/05/2006	19.89	31/05/2006	19.78	01/06/2006	21.67
02/06/2006	22.44	03/06/2006	23.89	04/06/2006	18.28
05/06/2006	15.11	06/06/2006	15.28	07/06/2006	18.06
08/06/2006	21.06	09/06/2006	19.83	10/06/2006	17.28
11/06/2006	17.22	12/06/2006	15.89	13/06/2006	15.28
14/06/2006	16.39	15/06/2006	18.11	16/06/2006	18.11
17/06/2006	13.56	18/06/2006	14.67	19/06/2006	16.83
20/06/2006	17.72	21/06/2006	20.56	22/06/2006	22.56
23/06/2006	24.67	24/06/2006	24.22	25/06/2006	24
26/06/2006	19.78	27/06/2006	19.61	28/06/2006	18.44
29/06/2006	17.67	30/06/2006	17.39	01/07/2006	17.5

Date	Temperature	Date	Temperature	Date	Temperature
02/07/2006	19.56	03/07/2006	19.78	04/07/2006	18.61
05/07/2006	17.22	06/07/2006	18.78	07/07/2006	21.17
08/07/2006	23.89	09/07/2006	24.39	10/07/2006	25.94
11/07/2006	24.72	12/07/2006	24.89	13/07/2006	22.39
14/07/2006	20.83	15/07/2006	22.56	16/07/2006	25.22
17/07/2006	26	18/07/2006	22.5	19/07/2006	21.89
20/07/2006	20.83	21/07/2006	20.78	22/07/2006	19.5
23/07/2006	18.11	24/07/2006	17.33	25/07/2006	16.83
26/07/2006	17.67	27/07/2006	20.89	28/07/2006	22.5
29/07/2006	20.06	30/07/2006	19.39	31/07/2006	18.44
01/08/2006	16.44	02/08/2006	16.33	03/08/2006	16.22
04/08/2006	14.78	05/08/2006	15.39	06/08/2006	16.67
07/08/2006	16.89	08/08/2006	18.56	09/08/2006	16.89
10/08/2006	17.56	11/08/2006	16.78	12/08/2006	17.17
13/08/2006	16.39	14/08/2006	17	15/08/2006	16.78
16/08/2006	16.67	17/08/2006	17.56	18/08/2006	17.61
19/08/2006	16.44	20/08/2006	15.06	21/08/2006	15.67
22/08/2006	19	23/08/2006	18.22	24/08/2006	17.28
25/08/2006	21.22	26/08/2006	19.61	27/08/2006	21.06
28/08/2006	21.17	29/08/2006	17.17	30/08/2006	15
31/08/2006	16.39	01/09/2006	18.5	02/09/2006	21.11
03/09/2006	18.67	04/09/2006	19.33	05/09/2006	18.39
06/09/2006	18.06	07/09/2006	18.72	08/09/2006	19.56
09/09/2006	17.72	10/09/2006	16.56	11/09/2006	17.28
12/09/2006	21.83	13/09/2006	16.72	14/09/2006	17.83
15/09/2006	18.33	16/09/2006	17.11	17/09/2006	16.44
18/09/2006	16.28	19/09/2006	17.89	20/09/2006	16.56
21/09/2006	15.61	22/09/2006	16.61	23/09/2006	15.33
24/09/2006	12.67	25/09/2006	12.67	26/09/2006	12.94
27/09/2006	16.33	28/09/2006	13.22	29/09/2006	13.39
30/09/2006	17.44	01/10/2006	17.5	02/10/2006	16.33
03/10/2006	13.22	04/10/2006	13.72	05/10/2006	14.28
06/10/2006	15	07/10/2006	14.11	08/10/2006	14.17
09/10/2006	15.83	10/10/2006	15.44	11/10/2006	15.11
12/10/2006	14.67	13/10/2006	14.61	14/10/2006	12.44
15/10/2006	12.17	16/10/2006	12.56	17/10/2006	15.44
18/10/2006	10.89	19/10/2006	15.5	20/10/2006	14.44
21/10/2006	13.72	22/10/2006	12.83	23/10/2006	6.67
24/10/2006	5.22	25/10/2006	4.83	26/10/2006	5.39
27/10/2006	7.44	28/10/2006	7.33	29/10/2006	6.67
30/10/2006	10.5	31/10/2006	8	01/11/2006	7.17
02/11/2006	11.06	03/11/2006	10.11	04/11/2006	13.11
05/11/2006	12.78	06/11/2006	13.44	07/11/2006	10.94
08/11/2006	8.89	09/11/2006	6.44	10/11/2006	6.39
11/11/2006	10.28	12/11/2006	6.39	13/11/2006	8.17
14/11/2006	11.33	15/11/2006	10.78	16/11/2006	11.11
17/11/2006	10.5	18/11/2006	12.5	19/11/2006	11.39
20/11/2006	9.17	21/11/2006	9.78	22/11/2006	11.5
23/11/2006	10.22	24/11/2006	9.61	25/11/2006	11.28
26/11/2006	12.44	27/11/2006	8.83	28/11/2006	9.83
29/11/2006	7.5	30/11/2006	4.33	01/12/2006	5.17

Date	Temperature	Date	Temperature	Date	Temperature
02/12/2006	10.22	03/12/2006	8.17	04/12/2006	12
05/12/2006	12.33	06/12/2006	11.72	07/12/2006	6.17
08/12/2006	4.5	09/12/2006	5.67	10/12/2006	1.72
11/12/2006	0.17	12/12/2006	-0.22	13/12/2006	-0.78
14/12/2006	3.06	15/12/2006	6.17	16/12/2006	6.06
17/12/2006	6.28	18/12/2006	5.17	19/12/2006	9.56
20/12/2006	8.5	21/12/2006	11.28	22/12/2006	10
23/12/2006	7.22	24/12/2006	6.61	25/12/2006	9.11
26/12/2006	9.72	27/12/2006	9.61	28/12/2006	6.78
29/12/2006	9.89	30/12/2006	10	31/12/2006	13.28
01/01/2007	9.33	02/01/2007	10	03/01/2007	11.06
04/01/2007	11.06	05/01/2007	6.78	06/01/2007	8.17
07/01/2007	10.83	08/01/2007	9.89	09/01/2007	11.33
10/01/2007	12.17	11/01/2007	9.89	12/01/2007	6.22
13/01/2007	3.94	14/01/2007	1.72	15/01/2007	1.44
16/01/2007	1.61	17/01/2007	3.61	18/01/2007	6.5
19/01/2007	7.11	20/01/2007	8.83	21/01/2007	7.39
22/01/2007	5.89	23/01/2007	9	24/01/2007	8.56
25/01/2007	4.89	26/01/2007	2.56	27/01/2007	3.5
28/01/2007	2.11	29/01/2007	-0.22	30/01/2007	1.61
31/01/2007	2.83	01/02/2007	7.39	02/02/2007	9.33
03/02/2007	8.39	04/02/2007	8.11	05/02/2007	7.39
06/02/2007	6.5	07/02/2007	9.11	08/02/2007	7.44
09/02/2007	7.78	10/02/2007	8.67	11/02/2007	9.78
12/02/2007	9.33	13/02/2007	9.11	14/02/2007	9.67
15/02/2007	9.67	16/02/2007	7.89	17/02/2007	8
18/02/2007	8.89	19/02/2007	9.61	20/02/2007	7.39
21/02/2007	6.39	22/02/2007	7.94	23/02/2007	8.39
24/02/2007	9.33	25/02/2007	10.72	26/02/2007	8.5
27/02/2007	8.44	28/02/2007	9.28	01/03/2007	8.44
02/03/2007	10.11	03/03/2007	10.78	04/03/2007	9.56
05/03/2007	8.5	06/03/2007	8.17	07/03/2007	9.78
08/03/2007	11.17	09/03/2007	7.61	10/03/2007	3.83
11/03/2007	3.72	12/03/2007	3.72	13/03/2007	3.44
14/03/2007	6.56	15/03/2007	6.22	16/03/2007	9.11
17/03/2007	9.39	18/03/2007	10.11	19/03/2007	9.94
20/03/2007	7.39	21/03/2007	7.33	22/03/2007	10.17
23/03/2007	10.78	24/03/2007	11.28	25/03/2007	7.11
26/03/2007	7.39	27/03/2007	10.39	28/03/2007	11.56
29/03/2007	10.5	30/03/2007	11.17	31/03/2007	12.11
01/04/2007	14.44	02/04/2007	13.72	03/04/2007	12.94
04/04/2007	12.94	05/04/2007	15.17	06/04/2007	17.39
07/04/2007	17.11	08/04/2007	14	09/04/2007	11.44
10/04/2007	13.22	11/04/2007	11.72	12/04/2007	12.5
13/04/2007	14.94	14/04/2007	13.89	15/04/2007	16.22
16/04/2007	15.89	17/04/2007	12.5	18/04/2007	12.78
19/04/2007	15.17	20/04/2007	14.33	21/04/2007	14.28
22/04/2007	15.33	23/04/2007	15.28	24/04/2007	10.78
25/04/2007	11.83	26/04/2007	10.83	27/04/2007	14.17
28/04/2007	15.44	29/04/2007	14.22	30/04/2007	12.94

Date	Temperature	Date	Temperature	Date	Temperature
01/05/2007	12.78	02/05/2007	12.11	03/05/2007	13.56
04/05/2007	12.5	05/05/2007	10.94	06/05/2007	11.56
07/05/2007	12.72	08/05/2007	15.94	09/05/2007	16.17
10/05/2007	13.44	11/05/2007	13.5	12/05/2007	13.11
13/05/2007	16.89	14/05/2007	18.72	15/05/2007	20.28
16/05/2007	18.22	17/05/2007	12.17	18/05/2007	10.44
19/05/2007	7.33	20/05/2007	10.06	21/05/2007	11.72
22/05/2007	14.83	23/05/2007	16.61	24/05/2007	18.56
25/05/2007	18.89	26/05/2007	16.06	27/05/2007	15.83
28/05/2007	14.06	29/05/2007	15.39	30/05/2007	16.94
31/05/2007	19.67	01/06/2007	19.67	02/06/2007	18.39
03/06/2007	18.61	04/06/2007	18.28	05/06/2007	18.22
06/06/2007	17.06	07/06/2007	16.06	08/06/2007	16.61
09/06/2007	16.22	10/06/2007	18.83	11/06/2007	18.22
12/06/2007	17.11	13/06/2007	16.39	14/06/2007	16.83
15/06/2007	13.94	16/06/2007	14.06	17/06/2007	13.5
18/06/2007	13.89	19/06/2007	14.5	20/06/2007	17.17
21/06/2007	16.11	22/06/2007	17.06	23/06/2007	16.39
24/06/2007	15.22	25/06/2007	15.78	26/06/2007	16.28
27/06/2007	16.78	28/06/2007	16.94	29/06/2007	16.11
30/06/2007	15.44	01/07/2007	15.5	02/07/2007	16.44
03/07/2007	18.17	04/07/2007	19.33	05/07/2007	19.11
06/07/2007	19.94	07/07/2007	19.33	08/07/2007	17.56
09/07/2007	18.33	10/07/2007	17.94	11/07/2007	16.61
12/07/2007	15.17	13/07/2007	16.11	14/07/2007	15.94
15/07/2007	17.44	16/07/2007	16.5	17/07/2007	16.56
18/07/2007	17.22	19/07/2007	17.67	20/07/2007	15.89
21/07/2007	15.39	22/07/2007	16.33	23/07/2007	18.39
24/07/2007	17.06	25/07/2007	18.44	26/07/2007	20.28
27/07/2007	21.89	28/07/2007	18.94	29/07/2007	16.83
30/07/2007	16.67	31/07/2007	16.78	01/08/2007	18.17
02/08/2007	18.89	03/08/2007	17.22	04/08/2007	16.78
05/08/2007	17.17	06/08/2007	18.11	07/08/2007	15.11
08/08/2007	15.44	09/08/2007	16.06	10/08/2007	15.72
11/08/2007	14.39	12/08/2007	15.28	13/08/2007	15.56
14/08/2007	15.39	15/08/2007	16.56	16/08/2007	19.33
17/08/2007	18.89	18/08/2007	15.78	19/08/2007	16.56
20/08/2007	15.44	21/08/2007	16.44	22/08/2007	17.67
23/08/2007	17.67	24/08/2007	15.89	25/08/2007	13.78
26/08/2007	17.83	27/08/2007	19.11	28/08/2007	19.5
29/08/2007	16.06	30/08/2007	17.56	31/08/2007	17.11
01/09/2007	15.5	02/09/2007	15.72	03/09/2007	16.56
04/09/2007	16.5	05/09/2007	15	06/09/2007	15.72
07/09/2007	13.94	08/09/2007	11.33	09/09/2007	14
10/09/2007	16.94	11/09/2007	17	12/09/2007	16.78
13/09/2007	16.11	14/09/2007	15.22	15/09/2007	12.94
16/09/2007	10.61	17/09/2007	10.89	18/09/2007	12.83
19/09/2007	14.22	20/09/2007	12.5	21/09/2007	13.39
22/09/2007	13.39	23/09/2007	14.39	24/09/2007	14.56
25/09/2007	12.44	26/09/2007	14.22	27/09/2007	12.67
28/09/2007	13.5	29/09/2007	12	30/09/2007	13.67

Date	Temperature	Date	Temperature	Date	Temperature
01/10/2007	11.56	02/10/2007	15.28	03/10/2007	15.67
04/10/2007	14.22	05/10/2007	13.56	06/10/2007	15.28
07/10/2007	12.5	08/10/2007	8.78	09/10/2007	8.17
10/10/2007	8.61	11/10/2007	7.5	12/10/2007	8
13/10/2007	7.22	14/10/2007	8.94	15/10/2007	9.83
16/10/2007	9.94	17/10/2007	12.28	18/10/2007	13.89
19/10/2007	10.5	20/10/2007	9.78	21/10/2007	10.33
22/10/2007	13.06	23/10/2007	12.61	24/10/2007	11.94
25/10/2007	9.72	26/10/2007	7.72	27/10/2007	8.5
28/10/2007	11.06	29/10/2007	11.28	30/10/2007	8.17
31/10/2007	11.5	01/11/2007	10	02/11/2007	3.83
03/11/2007	6.61	04/11/2007	7.06	05/11/2007	4.33
06/11/2007	2.44	07/11/2007	4.89	08/11/2007	5.39
09/11/2007	7.67	10/11/2007	7.67	11/11/2007	9.78
12/11/2007	8.67	13/11/2007	4.72	14/11/2007	3.28
15/11/2007	8.17	16/11/2007	7.89	17/11/2007	9.5
18/11/2007	9.89	19/11/2007	8.56	20/11/2007	11
21/11/2007	8.78	22/11/2007	10.17	23/11/2007	8.33
24/11/2007	10.5	25/11/2007	12.67	26/11/2007	13
27/11/2007	9.44	28/11/2007	7.56	29/11/2007	7.83
30/11/2007	6.28	01/12/2007	2.56	02/12/2007	1.89
03/12/2007	1.72	04/12/2007	3.83	05/12/2007	2.44
06/12/2007	2	07/12/2007	3.22	08/12/2007	3.5
09/12/2007	2.67	10/12/2007	1.06	11/12/2007	1.17
12/12/2007	3.17	13/12/2007	0.89	14/12/2007	7.56
15/12/2007	7.78	16/12/2007	6.56	17/12/2007	11.56
18/12/2007	10.61	19/12/2007	7.94	20/12/2007	7.33
21/12/2007	7.06	22/12/2007	7.67	23/12/2007	4.28
24/12/2007	2.28	25/12/2007	6.44	26/12/2007	7
27/12/2007	5.39	28/12/2007	7.83	29/12/2007	8.39
30/12/2007	6.83	31/12/2007	10.22	01/01/2008	8
02/01/2008	5.56	03/01/2008	10	04/01/2008	9
05/01/2008	9.67	06/01/2008	6.33	07/01/2008	6.89
08/01/2008	10.89	09/01/2008	13.72	10/01/2008	13.56
11/01/2008	11.56	12/01/2008	6.28	13/01/2008	11.22
14/01/2008	9.28	15/01/2008	7.83	16/01/2008	8.17
17/01/2008	7.44	18/01/2008	4.89	19/01/2008	7.89
20/01/2008	5.56	21/01/2008	7.33	22/01/2008	5
23/01/2008	3.5	24/01/2008	6.56	25/01/2008	6.67
26/01/2008	10.89	27/01/2008	7.94	28/01/2008	7.56
29/01/2008	7.39	30/01/2008	7.22	31/01/2008	9.5
01/02/2008	6.39	02/02/2008	5.67	03/02/2008	5.33
04/02/2008	4.61	05/02/2008	4.83	06/02/2008	2.17
07/02/2008	2.22	08/02/2008	3.06	09/02/2008	4.22
10/02/2008	2.67	11/02/2008	8.61	12/02/2008	11.61
13/02/2008	9.5	14/02/2008	10.28	15/02/2008	6.61
16/02/2008	10.44	17/02/2008	7.67	18/02/2008	7.61
19/02/2008	7.44	20/02/2008	10.67	21/02/2008	11.06
22/02/2008	6.11	23/02/2008	4.5	24/02/2008	4.67
25/02/2008	9.44	26/02/2008	9	27/02/2008	8.22
28/02/2008	7.28	29/02/2008	7.11	01/03/2008	9.39

Date	Temperature	Date	Temperature	Date	Temperature
02/03/2008	8.33	03/03/2008	8.33	04/03/2008	9.61
05/03/2008	11.28	06/03/2008	8.17	07/03/2008	6
08/03/2008	5.11	09/03/2008	5.44	10/03/2008	6.33
11/03/2008	7.11	12/03/2008	3.22	13/03/2008	1.72
14/03/2008	2.67	15/03/2008	4.67	16/03/2008	7.72
17/03/2008	7.06	18/03/2008	7.94	19/03/2008	8.61
20/03/2008	10.28	21/03/2008	8.61	22/03/2008	11.28
23/03/2008	10.89	24/03/2008	12.67	25/03/2008	11.72
26/03/2008	7	27/03/2008	2.61	28/03/2008	4.33
29/03/2008	5.44	30/03/2008	6.89	31/03/2008	7.5
01/04/2008	8.28	02/04/2008	8.67	03/04/2008	7.33
04/04/2008	7.78	05/04/2008	7	06/04/2008	7.56
07/04/2008	7.28	08/04/2008	8.11	09/04/2008	8.22
10/04/2008	11.39	11/04/2008	11.5	12/04/2008	11.72
13/04/2008	12	14/04/2008	11.22	15/04/2008	12.94
16/04/2008	15	17/04/2008	14.06	18/04/2008	10.83
19/04/2008	8.67	20/04/2008	7.83	21/04/2008	10.5
22/04/2008	10.67	23/04/2008	14	24/04/2008	17.78
25/04/2008	17.5	26/04/2008	16.72	27/04/2008	18.11
28/04/2008	18.94	29/04/2008	18.78	30/04/2008	19.89
01/05/2008	19.61	02/05/2008	18.56	03/05/2008	16.17
04/05/2008	14.94	05/05/2008	12.28	06/05/2008	11.72
07/05/2008	11.44	08/05/2008	11.72	09/05/2008	9.56
10/05/2008	10.78	11/05/2008	12.83	12/05/2008	15.5
13/05/2008	15.94	14/05/2008	17	15/05/2008	14.06
16/05/2008	12.28	17/05/2008	14.22	18/05/2008	15.17
19/05/2008	14.72	20/05/2008	15.67	21/05/2008	17.83
22/05/2008	15.44	23/05/2008	15.33	24/05/2008	14.72
25/05/2008	15.72	26/05/2008	16.11	27/05/2008	15.17
28/05/2008	15.94	29/05/2008	19.78	30/05/2008	20.94
31/05/2008	19.17	01/06/2008	16.44	02/06/2008	13.22
03/06/2008	13.39	04/06/2008	14.83	05/06/2008	14.78
06/06/2008	14.28	07/06/2008	16.06	08/06/2008	15.5
09/06/2008	16.89	10/06/2008	15.28	11/06/2008	16.17
12/06/2008	18.17	13/06/2008	16.67	14/06/2008	17.56
15/06/2008	17.83	16/06/2008	16.5	17/06/2008	17.5
18/06/2008	19.22	19/06/2008	17.5	20/06/2008	17.33
21/06/2008	20.39	22/06/2008	17.44	23/06/2008	16.33
24/06/2008	16.5	25/06/2008	18.33	26/06/2008	15.5
27/06/2008	15.22	28/06/2008	16.11	29/06/2008	15.11
30/06/2008	17.33	01/07/2008	16	02/07/2008	13.94
03/07/2008	16.17	04/07/2008	18.39	05/07/2008	20.61
06/07/2008	17.67	07/07/2008	16.39	08/07/2008	16.94
09/07/2008	18.11	10/07/2008	15.11	11/07/2008	16
12/07/2008	18.11	13/07/2008	21.44	14/07/2008	21.5
15/07/2008	21.11	16/07/2008	22.06	17/07/2008	23.28
18/07/2008	23.17	19/07/2008	18.83	20/07/2008	20.22
21/07/2008	21.22	22/07/2008	19	23/07/2008	19.11
24/07/2008	17.83	25/07/2008	17.17	26/07/2008	16.94
27/07/2008	21.06	28/07/2008	19.33	29/07/2008	16.89
30/07/2008	16.22	31/07/2008	17.78	01/08/2008	16.83

Date	Temperature	Date	Temperature	Date	Temperature
02/08/2008	16.44	03/08/2008	15.39	04/08/2008	15.67
05/08/2008	15.83	06/08/2008	17.17	07/08/2008	17.22
08/08/2008	17.11	09/08/2008	17.22	10/08/2008	18.11
11/08/2008	16.5	12/08/2008	15.72	13/08/2008	17.06
14/08/2008	17.28	15/08/2008	18.06	16/08/2008	17.94
17/08/2008	18.17	18/08/2008	20.11	19/08/2008	21.28
20/08/2008	17.28	21/08/2008	16.28	22/08/2008	15.44
23/08/2008	15.44	24/08/2008	15.56	25/08/2008	15.17
26/08/2008	15.17	27/08/2008	15.17	28/08/2008	15.22
29/08/2008	15.61	30/08/2008	16.56	31/08/2008	17
01/09/2008	13.94	02/09/2008	14.67	03/09/2008	14.89
04/09/2008	13.83	05/09/2008	13.11	06/09/2008	14.06
07/09/2008	14.06	08/09/2008	13.61	09/09/2008	13.78
10/09/2008	13.5	11/09/2008	14.44	12/09/2008	13.94
13/09/2008	14.17	14/09/2008	15.11	15/09/2008	14.22
16/09/2008	13.67	17/09/2008	13.22	18/09/2008	13.44
19/09/2008	13.67	20/09/2008	13.11	21/09/2008	9.94
22/09/2008	8.83	23/09/2008	9.83	24/09/2008	13.22
25/09/2008	11	26/09/2008	15.28	27/09/2008	11.94
28/09/2008	11.5	29/09/2008	13.78	30/09/2008	13.5
01/10/2008	14.39	02/10/2008	14.33	03/10/2008	12.89
04/10/2008	13.94	05/10/2008	10.83	06/10/2008	9.56
07/10/2008	10.39	08/10/2008	11.83	09/10/2008	13.39
10/10/2008	10.06	11/10/2008	8.33	12/10/2008	12
13/10/2008	11.44	14/10/2008	9.61	15/10/2008	12.78
16/10/2008	7.56	17/10/2008	4.28	18/10/2008	3.28
19/10/2008	4.72	20/10/2008	4.83	21/10/2008	6.11
22/10/2008	9.61	23/10/2008	9.72	24/10/2008	10.67
25/10/2008	10.61	26/10/2008	10	27/10/2008	9.94
28/10/2008	10.89	29/10/2008	9.89	30/10/2008	10.11
31/10/2008	9	01/11/2008	7.72	02/11/2008	8.28
03/11/2008	12.22	04/11/2008	12.83	05/11/2008	11.06
06/11/2008	6.39	07/11/2008	9.72	08/11/2008	9
09/11/2008	11	10/11/2008	8.67	11/11/2008	4.17
12/11/2008	3.06	13/11/2008	4.67	14/11/2008	4.17
15/11/2008	6.06	16/11/2008	9.39	17/11/2008	5.94
18/11/2008	2.89	19/11/2008	4.67	20/11/2008	3.83
21/11/2008	2.94	22/11/2008	1.11	23/11/2008	5.83
24/11/2008	5.17	25/11/2008	5	26/11/2008	1.83
27/11/2008	3.61	28/11/2008	3.78	29/11/2008	1.89
30/11/2008	2.39	01/12/2008	3.44	02/12/2008	5.89
03/12/2008	3.72	04/12/2008	4.89	05/12/2008	3.33
06/12/2008	5.5	07/12/2008	9.5	08/12/2008	6.78
09/12/2008	11.56	10/12/2008	11	11/12/2008	11.11
12/12/2008	9.44	13/12/2008	7.78	14/12/2008	6.5
15/12/2008	3.78	16/12/2008	2.17	17/12/2008	2.5
18/12/2008	1.33	19/12/2008	-0.67	20/12/2008	-0.06
21/12/2008	1.89	22/12/2008	2.78	23/12/2008	-0.67
24/12/2008	-1.83	25/12/2008	0.61	26/12/2008	-1.94
27/12/2008	-0.22	28/12/2008	2.56	29/12/2008	-0.94
30/12/2008	-2.89	31/12/2008	5.44	01/01/2009	8.89

Date	Temperature	Date	Temperature	Date	Temperature
02/01/2009	7.67	03/01/2009	2.33	04/01/2009	5.89
05/01/2009	7.22	06/01/2009	8.67	07/01/2009	5.72
08/01/2009	5.17	09/01/2009	3.78	10/01/2009	3.61
11/01/2009	7.61	12/01/2009	5.17	13/01/2009	2.56
14/01/2009	6.83	15/01/2009	6.22	16/01/2009	4
17/01/2009	6.17	18/01/2009	3.72	19/01/2009	3.67
20/01/2009	3	21/01/2009	0.5	22/01/2009	-0.94
23/01/2009	0.33	24/01/2009	1.44	25/01/2009	1.94
26/01/2009	1.5	27/01/2009	1.22	28/01/2009	2.28
29/01/2009	3.39	30/01/2009	3.44	31/01/2009	2.89
01/02/2009	1.5	02/02/2009	4.17	03/02/2009	2.22
04/02/2009	5.72	05/02/2009	7.5	06/02/2009	8.72
07/02/2009	8.72	08/02/2009	7.5	09/02/2009	7.5
10/02/2009	7.89	11/02/2009	8.72	12/02/2009	9.17
13/02/2009	9.67	14/02/2009	8.89	15/02/2009	7.78
16/02/2009	9.5	17/02/2009	7.89	18/02/2009	7.78
19/02/2009	7.44	20/02/2009	8.11	21/02/2009	4.89
22/02/2009	4.06	23/02/2009	4.72	24/02/2009	8.94
25/02/2009	7.22	26/02/2009	6.72	27/02/2009	9
28/02/2009	7.89	01/03/2009	10.94	02/03/2009	9.11
03/03/2009	9.89	04/03/2009	9.72	05/03/2009	9.83
06/03/2009	8.89	07/03/2009	9.72	08/03/2009	7.83
09/03/2009	7.94	10/03/2009	8.22	11/03/2009	10.44
12/03/2009	8.5	13/03/2009	7.78	14/03/2009	9.39
15/03/2009	9.39	16/03/2009	6.89	17/03/2009	6
18/03/2009	5.33	19/03/2009	7.89	20/03/2009	10.72
21/03/2009	10.39	22/03/2009	10.39	23/03/2009	8.11
24/03/2009	11.56	25/03/2009	10.78	26/03/2009	12.44
27/03/2009	10.67	28/03/2009	11.61	29/03/2009	11.78
30/03/2009	10.22	31/03/2009	10.5	01/04/2009	12.22
02/04/2009	12.78	03/04/2009	14.61	04/04/2009	12.78
05/04/2009	9.94	06/04/2009	10.44	07/04/2009	10.39
08/04/2009	11.78	09/04/2009	13.94	10/04/2009	13.67
11/04/2009	13.17	12/04/2009	13.72	13/04/2009	12.17
14/04/2009	11.39	15/04/2009	8.33	16/04/2009	7.72
17/04/2009	10.67	18/04/2009	12.94	19/04/2009	14.94
20/04/2009	13.39	21/04/2009	11.72	22/04/2009	9.83
23/04/2009	14.17	24/04/2009	15.11	25/04/2009	12.56
26/04/2009	12	27/04/2009	12	28/04/2009	13.28
29/04/2009	12.06	30/04/2009	11.94	01/05/2009	12.44
02/05/2009	15	03/05/2009	12.72	04/05/2009	12.17
05/05/2009	11.61	06/05/2009	13	07/05/2009	13.33
08/05/2009	13.78	09/05/2009	13.94	10/05/2009	14.28
11/05/2009	16.06	12/05/2009	17.83	13/05/2009	17.83
14/05/2009	13.83	15/05/2009	12.44	16/05/2009	18.06
17/05/2009	18.5	18/05/2009	17.56	19/05/2009	18.5
20/05/2009	19.56	21/05/2009	19.17	22/05/2009	16.33
23/05/2009	13.5	24/05/2009	12.06	25/05/2009	11.94
26/05/2009	12.5	27/05/2009	13.06	28/05/2009	13.17
29/05/2009	13.78	30/05/2009	15.56	31/05/2009	15.56

Date	Temperature	Date	Temperature	Date	Temperature
01/06/2009	18.28	02/06/2009	18.78	03/06/2009	17.94
04/06/2009	17.56	05/06/2009	17.11	06/06/2009	15.67
07/06/2009	15.61	08/06/2009	15.22	09/06/2009	16.33
10/06/2009	17.78	11/06/2009	18.67	12/06/2009	18.28
13/06/2009	19.89	14/06/2009	19.72	15/06/2009	20.11
16/06/2009	22	17/06/2009	24.17	18/06/2009	23.72
19/06/2009	23.17	20/06/2009	22.78	21/06/2009	21.39
22/06/2009	20.17	23/06/2009	19.56	24/06/2009	16.89
25/06/2009	16.33	26/06/2009	15.67	27/06/2009	15.89
28/06/2009	16.44	29/06/2009	16.94	30/06/2009	18.61
01/07/2009	17.94	02/07/2009	18.06	03/07/2009	17.94
04/07/2009	18.06	05/07/2009	16.28	06/07/2009	16.33
07/07/2009	16.33	08/07/2009	17	09/07/2009	17.33
10/07/2009	17.89	11/07/2009	17.06	12/07/2009	16.44
13/07/2009	17.89	14/07/2009	16.83	15/07/2009	16.89
16/07/2009	16.94	17/07/2009	17.06	18/07/2009	15.44
19/07/2009	17.06	20/07/2009	17.44	21/07/2009	16.61
22/07/2009	17.5	23/07/2009	19.06	24/07/2009	22.11
25/07/2009	19.06	26/07/2009	17.89	27/07/2009	18.83
28/07/2009	20.44	29/07/2009	18.39	30/07/2009	20.11
31/07/2009	19.33	01/08/2009	19.28	02/08/2009	18.94
03/08/2009	19.17	04/08/2009	19.06	05/08/2009	18.5
06/08/2009	18.67	07/08/2009	20.78	08/08/2009	19.06
09/08/2009	16.11	10/08/2009	17.22	11/08/2009	21.28
12/08/2009	19.06	13/08/2009	16.33	14/08/2009	17.56
15/08/2009	18.56	16/08/2009	15.94	17/08/2009	15.06
18/08/2009	15.33	19/08/2009	20.06	20/08/2009	17.39
21/08/2009	15.56	22/08/2009	15.61	23/08/2009	14.89
24/08/2009	14.89	25/08/2009	16	26/08/2009	17.78
27/08/2009	20.78	28/08/2009	16.67	29/08/2009	14.78
30/08/2009	15.5	31/08/2009	16.78	01/09/2009	14.11
02/09/2009	15.61	03/09/2009	15.11	04/09/2009	15.72
05/09/2009	14.56	06/09/2009	15.44	07/09/2009	18.06
08/09/2009	17.06	09/09/2009	15.06	10/09/2009	16.33
11/09/2009	16.94	12/09/2009	15.39	13/09/2009	14.33
14/09/2009	14.06	15/09/2009	14.72	16/09/2009	15.11
17/09/2009	15.78	18/09/2009	15.67	19/09/2009	14.72
20/09/2009	12.56	21/09/2009	14.5	22/09/2009	13.28
23/09/2009	13.28	24/09/2009	16.78	25/09/2009	13.56
26/09/2009	11.17	27/09/2009	10.78	28/09/2009	14.61
29/09/2009	13.06	30/09/2009	11.5	01/10/2009	10.39
02/10/2009	11.56	03/10/2009	12.06	04/10/2009	12.22
05/10/2009	9.72	06/10/2009	7.39	07/10/2009	8.61
08/10/2009	10.22	09/10/2009	12.56	10/10/2009	12.17
11/10/2009	12.5	12/10/2009	15.17	13/10/2009	13.44
14/10/2009	13	15/10/2009	14.17	16/10/2009	13.78
17/10/2009	12.89	18/10/2009	12.72	19/10/2009	13.5
20/10/2009	13	21/10/2009	9.33	22/10/2009	10.78
23/10/2009	8.67	24/10/2009	10.06	25/10/2009	10
26/10/2009	7.72	27/10/2009	7.83	28/10/2009	5.33
29/10/2009	5.56	30/10/2009	8.44	31/10/2009	11.39

Date	Temperature	Date	Temperature	Date	Temperature
01/11/2009	12.39	02/11/2009	11.72	03/11/2009	10.39
04/11/2009	11.72	05/11/2009	11.06	06/11/2009	13.5
07/11/2009	13.44	08/11/2009	12.94	09/11/2009	12.44
10/11/2009	10.11	11/11/2009	11.11	12/11/2009	12.56
13/11/2009	10.67	14/11/2009	8.39	15/11/2009	6.89
16/11/2009	6.56	17/11/2009	7.44	18/11/2009	5.83
19/11/2009	3.44	20/11/2009	8.44	21/11/2009	6.5
22/11/2009	4.56	23/11/2009	9.89	24/11/2009	10.78
25/11/2009	8.83	26/11/2009	7.89	27/11/2009	10.83
28/11/2009	8.44	29/11/2009	4.5	30/11/2009	5.67
01/12/2009	4.94	02/12/2009	3.39	03/12/2009	2
04/12/2009	0.33	05/12/2009	2.11	06/12/2009	0.44
07/12/2009	-1.11	08/12/2009	0.67	09/12/2009	0.17
10/12/2009	0.61	11/12/2009	-0.33	12/12/2009	4.22
13/12/2009	2.89	14/12/2009	6.89	15/12/2009	5.39
16/12/2009	1.89	17/12/2009	3.94	18/12/2009	4.44
19/12/2009	3.5	20/12/2009	0.78	21/12/2009	1.78
22/12/2009	0.44	23/12/2009	-2.78	24/12/2009	-1.33
25/12/2009	-0.06	26/12/2009	-2.33	27/12/2009	-1.44
28/12/2009	-1.22	29/12/2009	1.44	30/12/2009	0.72
31/12/2009	1.17	01/01/2010	0.56	02/01/2010	2.17
03/01/2010	3.67	04/01/2010	6	05/01/2010	5.06
06/01/2010	4.72	07/01/2010	6.5	08/01/2010	3.39
09/01/2010	4	10/01/2010	7.39	11/01/2010	5.94
12/01/2010	4.28	13/01/2010	3.61	14/01/2010	1.28
15/01/2010	1.89	16/01/2010	5.5	17/01/2010	3.67
18/01/2010	0.5	19/01/2010	0.22	20/01/2010	1.5
21/01/2010	5.83	22/01/2010	4.61	23/01/2010	7.61
24/01/2010	7.22	25/01/2010	5.11	26/01/2010	4.11
27/01/2010	1.72	28/01/2010	2.22	29/01/2010	1.61
30/01/2010	1.28	31/01/2010	2.94	01/02/2010	2.44
02/02/2010	3	03/02/2010	1.83	04/02/2010	4.11
05/02/2010	4.06	06/02/2010	3	07/02/2010	2.5
08/02/2010	1.22	09/02/2010	3.28	10/02/2010	3.33
11/02/2010	3.06	12/02/2010	7.39	13/02/2010	7.72
14/02/2010	6.22	15/02/2010	7.44	16/02/2010	5.61
17/02/2010	4.67	18/02/2010	4.94	19/02/2010	4
20/02/2010	3.89	21/02/2010	3.11	22/02/2010	4.06
23/02/2010	0.89	24/02/2010	2.5	25/02/2010	5.11
26/02/2010	4.06	27/02/2010	4.22	28/02/2010	5.28
01/03/2010	6.5	02/03/2010	8.44	03/03/2010	7.78
04/03/2010	7.11	05/03/2010	8.78	06/03/2010	10.83
07/03/2010	10.67	08/03/2010	11.83	09/03/2010	9.11
10/03/2010	8.56	11/03/2010	7.61	12/03/2010	11.94
13/03/2010	11.44	14/03/2010	9.72	15/03/2010	9.67
16/03/2010	9	17/03/2010	10	18/03/2010	8.44
19/03/2010	4.94	20/03/2010	5.61	21/03/2010	7.44
22/03/2010	7.72	23/03/2010	7.83	24/03/2010	8.94
25/03/2010	11.61	26/03/2010	9.67	27/03/2010	10.72
28/03/2010	12.44	29/03/2010	11.89	30/03/2010	9.44
31/03/2010	9.44	01/04/2010	9.33	02/04/2010	8.67

Date	Temperature	Date	Temperature	Date	Temperature
03/04/2010	8.67	04/04/2010	8.78	05/04/2010	9.78
06/04/2010	11.28	07/04/2010	11.61	08/04/2010	9.78
09/04/2010	7.89	10/04/2010	9	11/04/2010	10.83
12/04/2010	13.11	13/04/2010	13.33	14/04/2010	12.83
15/04/2010	14.22	16/04/2010	14.94	17/04/2010	14.11
18/04/2010	11.72	19/04/2010	12.11	20/04/2010	8.39
21/04/2010	7.78	22/04/2010	7.72	23/04/2010	10.17
24/04/2010	11.06	25/04/2010	9.06	26/04/2010	8.22
27/04/2010	8.94	28/04/2010	9.11	29/04/2010	7.33
30/04/2010	7.33				